Faculty of Science & Engineering

Department of Imaging and Applied Physics

Microstructural Design of High Performance Natural Fibre-Nanoclay-Cement Nanocomposites

Ahmad Magbul Hakamy

This thesis is presented for the degree of
Doctor of Philosophy
of
Curtin University

January 2016

DECLARATION

To the best of my knowledge and belief, this thesis contains no material previously published by any other persons, except where due acknowledgment has been made. This thesis contains no material which has been accepted for the award of any other degree or diploma in any university.

Ahmad Hakamy

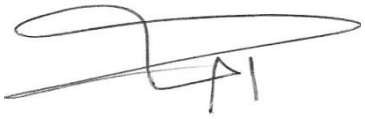

Signature

Date: 13th January 2016

ABSTRACT

Nowadays, in the building industry, natural fibres and nanomaterials have been gaining increasing attention for two reasons: one is to develop 'environmental-friendly materials' through the utilization of natural fibres as an alternative to synthetic fibres in fibre-reinforced concrete and another is to improve the properties of Portland cement matrix with the addition of nanoparticles. Natural and cellulose fibres are used in cement matrix to improve their tensile and flexural strength, as well as fracture resistance properties. They are cheaper, biodegradable and lighter than synthetic fibres. However, the interfacial bonding between the natural fibre and the cement matrix is relatively weak. Also, the degradation of fibres in a high alkaline environment of cement can adversely affect the mechanical and durability properties of natural fibre-reinforced cement composites. Much research is clearly needed to overcome these problems.

In this thesis, a novel approach has been used to overcome the above-mentioned disadvantages of hemp fibres in cementitious composites. This new approach includes the combination of thermal pre-treatment of nanoclay (i.e., producing calcined nanoclay) and chemical pre-treatment of fibre surfaces, to improve the microstructure, mechanical, physical and thermal properties, as well as the durability of hemp fibre-reinforced cement composites. In this thesis, nanoclay-cement nanocomposites, calcined nanoclay-cement nanocomposites, untreated & treated hemp fabric-reinforced cement composites, hemp fabric-reinforced nanoclay-cement nanocomposites and treated hemp fabric-reinforced nanoclay-cement nanocomposites were synthesized. The influence of nanoclay on the properties of the cement paste and hemp fabric-reinforced cement composites was also investigated. In addition, the influence of the sodium hydroxide (NaOH) pre-treatment of fibre surfaces on properties of hemp fabric-reinforced cement composites was studied. The effect of calcined nanoclay (CNC) on the microstructural and mechanical properties, as well as the durability (at 236 days -3 wet/ dry cycles) of cement paste and treated hemp fabric-reinforced cement composites were also looked into.

The microstructures of nanocomposites and untreated and treated-reinforced cement nanocomposites were also investigated using high resolution transmission electron microscopy (HRTEM), quantitative x-ray diffraction Analysis (QXDA) with Rietveld refinement by Bruker DIFFRAC^{plus} TOPAS software, x-ray diffraction, synchrotron radiation diffraction, scanning electron microscopy (SEM), energy dispersive spectroscopy (EDS) and thermogravimetric analysis (TGA).

This study consists of seven sequential parts. In the first part, nanoclay-cement nanocomposites were fabricated and tested at 56 days. Ordinary Portland cement (OPC) was partially substituted by nanoclay with 1, 2 and 3 wt% of OPC. The OPC and nanoclay were first dry mixed for 5 minutes in a Hobart mixer at a low speed and then mixed for another 10 minutes at a high speed, until a uniform mixture was achieved. The cement–nanocomposite paste was prepared by adding water with a water/ binder (nanoclay-cement) ratio of 0.48. The results indicated that an optimum replacement of OPC with 1 wt% nanoclay observed an improved reduced porosity and water absorption as well as increased density, flexural strength and fracture toughness of the nanoclay-cement nanocomposites. The microstructural analyses indicated that the nanoclay behaves not only as a filler to improve the microstructure, but also as an activator to promote the pozzolanic reaction, that led to an obvious consumption of calcium hydroxide ($Ca(OH)_2$) crystals and production of more amorphous calcium silicate hydrate gel (C-S-H).

In the second part, the aim was to investigate the influence of nanoclay on properties of hemp fabric-reinforced cement composites which are small depth specimens -10 mm. Hemp fabric-reinforced nanoclay-cement nanocomposites were fabricated and the samples were tested at 56 days. The cement matrix was the same as in the first part for 1, 2 and 3 wt% of nanoclay. Two layers of hemp fabric were used and the total amount of hemp fabric in each specimen was about 2.5 wt%. For each series, three prismatic plate specimens of 300 × 70 × 10 mm were cast. After 56 days, several rectangular specimens of each series with dimensions of 70 × 20 × 10 mm were cut from the fully cured prismatic plate for mechanical and physical tests. The results indicated that the hemp fabric-reinforced nanocomposites containing 1 wt% of nanoclay had denser microstructure than others. Thus, this improvement led to an enhancement of the hemp fabric-nanomatrix

adhesion. In addition, the incorporation of 1 wt% nanoclay into the hemp fabric-reinforced nanocomposites improved the thermal stability, decreased the porosity and water absorption, as well as increased the density, flexural strength, fracture toughness and impact strength when compared to the hemp fabric-reinforced cement composites.

In the third part, the purpose was to investigate the effect of nanoclay on properties of hemp fabric-reinforced cement composites that have a large dimensional size of 160 × 40 × 40 mm (ASTM C-1365–06 Standard). The cement matrices were the same as in the first part for 1, 2 and 3 wt% of nanoclay. Eight layers of hemp fabric were used and the total amount of hemp fabric in each specimen was about 2.4 wt%. It was found that the incorporation of 1 wt% nanoclay into the hemp fabric-reinforced nanocomposites decreased the porosity and also increased the density, flexural strength and fracture toughness, when compared to the hemp fabric-reinforced cement composite.

In the fourth part, the influence of nanoclay and CNC on the mechanical and thermal properties of cement nano-composites is presented. CNC was prepared by heating nanoclay at 900°C for 2 hours. The OPC was partially replaced by nanoclay or CNC of 1, 2 and 3 wt%. The OPC and sample preparation was the same as per the first part. It was found that CNC was more effective than nanoclay in terms of its high pozzolanic reaction. The optimum content of CNC was also found to be 1 wt%. The cement nanocomposite containing 1 wt% of CNC decreased the porosity, water absorption and increased the density, compressive strength, flexural strength, fracture toughness, impact strength and Rockwell hardness, as well as improved the thermal stability, when compared to the control cement paste and cement nanocomposite containing 1 wt% of nanoclay.

In the fifth part, the influence of the NaOH-treatment on the microstructure and mechanical properties of treated hemp fabric-reinforced cement composites was investigated at 56 days. The surface modification of hemp fibres was treated by immersing the fabric in 1.7m of NaOH solution (pH=14) for 48 hours at 25° C, followed by the processes of neutralization and drying. Samples of untreated hemp fabric-reinforced cement composites were fabricated with various contents of hemp fabric: 4.5 wt% (4 layers of fabric), 5.7 wt% (5 layers of fabric), 6.9 wt% (6 layers of fabric) and 8.1 wt% (8

layers of fabric). For the fabrication of treated hemp fabric-reinforced cement composite (6THFRC) samples, only 6 layers of treated hemp fabric were used because they have been shown to exhibit the best mechanical performance. The results indicated that the optimum content of hemp fabric was found to be 6.9 wt% (6 hemp fabric layers). NaOH-treated hemp fabric-reinforced cement composites exhibit the highest flexural strength and fracture toughness when compared to their non-treated counterparts, due to the efficiency of the NaOH treatment to clean the surface of hemp fibres and to remove amorphous materials such as hemicellulose, pectins and impurities (fatty substances and waxes) from their surface. Thus, NaOH treatment improved the interfacial bonding between the matrix and the hemp fibres, which served to enhance the load transfer process at the interface.

In the sixth part, the influences of CNC and NaOH treatment of hemp fabric on the thermal and mechanical properties of treated hemp fabric-reinforced cement nanocomposites were studied and the respective samples were tested at Day 56. The cement matrix was fabricated in the same manner as in the fourth part with 1, 2 and 3 wt% of CNC. Six layers of treated hemp fabric were used to reinforce the cement nanocomposite matrix and the total amount of treated hemp fabric in each specimen was about 6.9 wt%. The results indicated that the physical, mechanical and thermal properties were enhanced due to the addition of CNC into the cement matrix (the optimum content of CNC was 1 wt%). The treated hemp fabric-reinforced nanocomposites containing 1 wt% CNC had a good fibre-matrix interface and exhibited the highest flexural strength, fracture toughness, impact strength and thermal stability when compared to their counterparts.

In the seventh part, the effect of CNC on the durability of NaOH-treated hemp fabric-reinforced cement nanocomposites was investigated. The treated hemp fabric-reinforced cement composites and nanocomposites were subjected to 3 wetting and drying cycles and then tested at 56 and 236 days. The influences of CNC dispersion on the durability of these composites have been characterized in terms of porosity, flexural strength, stress-midspan deflection curves and microstructural observation of hemp surface by SEM images. The results indicated that CNC effectively mitigated the degradation of hemp fibre. The durability and degradation resistance of hemp fibre were enhanced, due to the addition of CNC into the cement matrix and the optimum content of CNC was 1 wt%.

SEM micrographs indicated that the hemp fibres in treated hemp fabric-reinforced cement composites undergo more degradation than in treated hemp fabric-reinforced cement nanocomposites containing 1 wt% CNC. Based on the results, the addition of CNC has a great potential to improve the durability of treated hemp fabric reinforced cement nanocomposites during wet/ dry cycles, particularly at 1 wt% CNC.

The success in this project could provide new design concepts for developing cementitious composites. The development of long-term durability of treated hemp fabric-reinforced nanocomposites can provide beneficial insights for the development of new 'environmental-friendly nanomaterials', especially for building applications such as the construction of sandwich panels, ceilings and roofs.

Indeed, as particle agglomeration increases, nanoclay and calcined nanoclay contents also follow suit and increase. This adversely reduces the mechanical properties of composites. It can be recommended that much research is required to overcome the problem of nanoclay and calcined nanoclay agglomerations.

ACKNOWLEDGEMENTS

First and foremost, I would like to express my sincere thanks to my supervisor, Prof. It-Meng (Jim) Low, for his guidance, kindness, support, motivation and encouragement during my PhD studies. His positive and optimistic attitude has left a lasting impression on me. Secondly, I would like to thank my associate supervisor, Dr. Faiz Uddin Ahmed Shaikh, for his valuable suggestions and inspiration.

In addition, I would like to thank the staff from the Department of Imaging & Applied Physics at Curtin University, in particular Dr Brendan McGann, for all their help and support.

I wish also to express my sincere appreciation to Ms Elaine Miller from the Department of Imaging & Applied Physics at Curtin University for her valuable assistance with Scanning Electron Microscopy. Moreover, I would like to thank Mr. Mick Elliss, Mr. Ashley Hughes and Andreas Viereckl from the Mechanical Engineering Department at Curtin University for their assistance with the Charpy Impact Test.

Warmest thanks to all my colleagues for their great friendship and emotional support during the compilation of my thesis.

Finally, I would like to take this opportunity to express my gratitude to my family for their prayers, support and encouragement during my studies.

LIST OF PUBLICATION INCLUDED AS PART OF THE THESIS

(Listed in order as found on this thesis)

1. **HAKAMY, A.,** SHAIKH, F.U.A. & LOW, I.M. 2013. Microstructures and mechanical properties of hemp fabric reinforced organoclay–cement nanocomposites. *Construction & Building Materials,* 49, 298–307.
2. **HAKAMY, A.,** SHAIKH, F.U.A. & LOW, I.M. 2014. Thermal and mechanical properties of hemp fabric-reinforced nanoclay–cement nanocomposites. *Journal of Materials Science,* 49, 1684–1694.
3. **HAKAMY, A.,** SHAIKH, F.U.A. & LOW, I.M. 2014. Characteristics of hemp fabric reinforced nanoclay–cement nanocomposites. *Cement & Concrete Composites,* 50, 27–35.
4. **HAKAMY, A.,** SHAIKH, F.U.A. & LOW, I.M. 2015. Characteristics of nanoclay and calcined nanoclay-cement nanocomposites. *Composites Part B: Engineering,* 78, 174-184.
5. **HAKAMY, A.,** SHAIKH, F.U.A. & LOW, I.M. 2015. Effect of calcined nanoclay on microstructural and mechanical properties of chemically treated hemp fabric reinforced cement nanocomposites. *Construction & Building Materials,* 95, 882–891.
6. **HAKAMY, A.,** SHAIKH, F.U.A. & LOW, I.M. 2015. Thermal and mechanical properties of NaOH treated hemp fabric and calcined nanoclay-reinforced cement nanocomposites. *Materials and Design,* 80, 70–81.
7. **HAKAMY, A.,** SHAIKH, F.U.A. & LOW, I.M. 2016. Effect of calcined nanoclay on the durability of NaOH treated hemp fabric-reinforced cement nanocomposites. *Materials and Design*, 92, 659-666.

STATEMENT OF CONTRIBUTION OF OTHERS

Ahmad Hakamy's input into this study and the associated papers include the execution of all experimental work, as well as a dominant contribution to the intellectual input involved in the project. As is always the case in the field of Physical Sciences, other scientists have also made contributions to the current work. These contributions were significant enough to warrant co-authorship on the journal articles, as specified in the next section.

Special mention has to be given to the following people:

Prof. I.M. Low, provided project supervision and manuscript editing.

Dr. F. Shaikh, also provided project supervision and manuscript editing support.

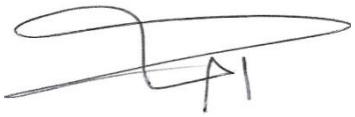

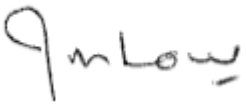

Ahmad Hakamy

Prof. It-Meng (Jim) Low

LIST OF PUBLICATIONS BY THE CANDIDATE RELEVANT TO THE THESIS BUT NOT FORMING PART OF IT

Conference Papers

Oral presentation

Hakamy, A., F.U.A. Shaikh and I.M. Low. 2015. Characteristics of Nanoclay and Calcined Nanoclay-Cement Nanomatrices by the combination of QXDA and TGA techniques. *Proc. 5th International Conference on Civil, Environmental and Medical Engineering (ICEME)*, Melbourne, Australia, 10th April 2015, 6 pages.

Hakamy, A., F.U.A. Shaikh and I.M. Low. 2015. Influence of calcined nanoclay on fracture toughness of NaOH-treated hemp fabric reinforced cement. *8th International Structural Engineering and Construction Conference (ISEC 8)*, Sydney, Australia, November 23-28, 2015, 6 pages.

TABLE OF CONTENTS

LIST OF FIGURES

LIST OF TABLES

LIST OF ABBREVIATIONS

ASTM	American Society of Testing Materials
CH	Calcium Hydroxide
CNC	Calcined Nanoclay
CrI	Crystallinity Index
CSH	Calcium Silicate Hydrate
C_2S	Dicalcium Silicate
C_3S	Tricalcium Silicate
EDS	Energy Dispersive Spectroscopy
HF	Hemp Fabric (Fibre)
HRTEM	High Resolution Transmission Electron Microscopy
NC	Nanoclay
OPC	Ordinary Portland Cement
QXDA	Quantitative X-ray Diffraction Analysis
SCMs	Supplementary Cementitious Materials
SEM	Scanning Electron Microscopy
SRD	Synchrotron Radiation Diffraction
THF	Treated Hemp Fabric
TGA	Thermogravimetric Analysis
UHF	Untreated Hemp Fabric
XRD	X-Ray Diffraction

1. INTRODUCTION

1.1 Background

Concrete is one of the most widely used construction materials in the world. Portland cement is widely utilized in construction materials because it is the most inexpensive binder (Neville, 2011). Concrete, mortar and cement paste have high compressive strength but are characterized by low tensile and flexural strength, as well as flexural and fracture toughness (much weaker in tension than in compression). The brittle concrete, mortar and cement paste matrix can be reinforced by using steel, synthetic (i.e., carbon or glass fibres) or natural fibres in order to produce fibre-reinforced cement composites (FRC) (Balaguru and Shah, 1992, Bentur and Mindess, 2007).

Recently, natural fibres are gaining popularity in the development of 'environmental-friendly construction materials' as an alternative to synthetic fibres in fibre-reinforced concrete (Pacheco-Torgal and Jalali, 2011a, Ardanuy *et al.*, 2015). Moreover, it is worth noting that natural materials have been gaining increasing social acceptance (Hamzaoui *et al.*, 2014). Not only are these fibres cheaper and biodegradable, but they are also lighter than their synthetic counterparts. Some examples of natural fibres are: Sisal, Flax, Hemp, Bamboo and Coir (Li *et al.*, 2000, Elsaid *et al.*, 2011, Santos *et al.*, 2015). Natural and cellulose fibres are commonly used in polymer and cement matrices to improve their tensile and flexural strength, as well as fracture resistance properties (Silva *et al.*, 2009, Islam *et al.*, 2011, Ardanuy *et al.*, 2015).

In particular, the hemp plant is a fast growing annual crop worldwide. The world-leading producer of hemp is China, followed by Australia, Canada and France. According to the Food and Agriculture Organization (FAO), the world production of hemp fibres reaches up to 90,000 tons per year (Shahzad, 2011). Hemp fibres are used in a number of products such as paper, textiles and ropes. In addition, hemp fibre has a high specific tensile strength and specific modulus of elasticity. As such, it is a good candidate for

reinforcement in fibre –reinforced composites (Li *et al.*, 2004c, Misnon *et al.*, 2015). Several studies have shown that using hemp fibres as a reinforcement in concrete improves the tensile and flexural strength, as well as the toughness of hemp fibre-reinforced concrete (Li *et al.*, 2006c, Awwad *et al.*, 2012).

On the other hand, one of the most effective techniques of obtaining a high performance cementitious composite is by reinforcement with textile (i.e., fabrics), which are impregnated with cement paste or mortar. Synthetic fabrics such as polyethylene (PE) and polypropylene (PP) have been used as reinforcement for cement composites (Peled and Bentur, 2000, Peled *et al.*, 2006). This system has a superior filament-matrix bonding, which improves mechanical properties such as tensile and flexural strength better than continuous or short fibres (Mobasher *et al.*, 2006, Soranakom and Mobasher, 2008). In contrast, the use of natural fibre sheets and fabrics is more prevalent in a polymer matrix as compared to a cement-based matrix. For example, the use of cellulose-fibre sheets in an epoxy or a vinyl-ester matrix has resulted in a significantly improved fracture toughness (Alamri *et al.*, 2012, Alhuthali *et al.*, 2012).

However, the long term durability of natural fibres in cement composites has been the major issue. Thus, this has limited their applications in cementitious composites. These issues could be the degradation of fibres in a high alkaline environment of cement composites and relatively weak interfacial bonding between the natural fibres and cement matrix (Mohr *et al.*, 2006, Almeida *et al.*, 2013, Santos *et al.*, 2015). In order to improve the durability of fibre-reinforced cement composites, there are two possible methods: (i) modification of fibre surfaces and (ii) modification of the cement matrix (Toledo Filho *et al.*, 2003, Pacheco-Torgal and Jalali, 2011a, Soroushian *et al.*, 2012).

Concerning the first method, some researchers have shown that pre-treatments of natural fibre surfaces via some chemical agents such as alkalization, Polyethylene Imine (PEI) and $Ca(OH)_2$ have slightly improved the interfacial bonding between the natural fibres and cement matrix. As a result, the mechanical properties of such composites are enhanced (Blankenhorn *et al.*, 2001, Le Troëdec *et al.*, 2009, Rachini *et al.*, 2009). Regarding the second approach, alkalinity (especially calcium hydroxide) in cement can be reduced by

using pozzolanic supplementary cementitious materials (SCMs) such as silica fume, fly ash, metakaolin and amorphous nanomaterials. Thus, this approach could improve the interfacial bond, mechanical properties and durability of natural fibre-reinforced cement composites (de Gutiérrez *et al.*, 2005, Mohr *et al.*, 2007, Pacheco-Torgal and Jalali, 2011a). However, the extent of the substitution is limited, due to the reduction of early strength (Siddique and Klaus, 2009, Flatt *et al.*, 2012, Shaikh, 2013, Juenger and Siddique, 2015).

Nowadays, nanotechnology is one of the most active research areas in the Civil Engineering and construction materials fields (Sanchez and Sobolev, 2010, Singh, 2014). In the construction industry, several types of nanomaterials have been incorporated into concretes such as nano-SiO_2, carbon nanotubes, nano-$CaCO_3$, nano-Al_2O_3 and nano-TiO_2, in order to improve the durability and mechanical properties of the concrete and Portland cement matrix (Pacheco-Torgal and Jalali, 2011b, Hanus and Harris, 2013, Singh *et al.*, 2013). Supit and Shaikh (2014b) reported that the addition of 1 wt% of nano-$CaCO_3$ improved the compressive strength of mortar and concrete significantly. Nanoclay is a new generation of processed clay for a wide range of high-performance cement nanocomposites. Some examples of nanoclay are nano-halloysite, nano-Cloisite 30B and nano-kaolin. As a type of nano-pozzolanic material, nanoclay not only reduces the pore size and porosity of the cement matrix, but also improves the strength of the cement matrix through pozzolanic reactions (Chang *et al.*, 2007, Morsy *et al.*, 2009, Sanchez and Sobolev, 2010, Wei and Meyer, 2014c, Farzadnia *et al.*, 2013). Calcined nanoclay is prepared by heating nanoclay at a certain temperature for a specific period of time, in order to transform the nanoclay to an amorphous state, in which the calcined nanoclay can behave as a highly reactive artificial pozzolan like silica fume, metakaolin, nano-SiO_2, and nano-metakaolin (He *et al.*, 1996, Shebl *et al.*, 2009, Morsy *et al.*, 2010).

The use of nanoclay and calcined nanoclay in natural fibre-reinforced cement composites (especially treated hemp fabric-reinforced cement composites) can be expected to reduce the alkalinity of the cement matrix. This happens as during the pozzolanic reaction, calcium hydroxide is consumed. Hence, the durability of the natural fibre in the composite and the microstructure of the nanoclay-cement matrix can be improved due to the particle

packing (filler effect) of nanoclay. In addition, its bond with the natural fibre is also improved. Thus, a better composite behaviour can be expected in natural fibre reinforced nanoclay-cement composites, particularly treated hemp fabric-reinforced calcined nanoclay-cement composites.

In this project, a novel method for synthesizing hemp fabric-reinforced cement nanocomposites was used and investigated. In order to improve the durability and degradation resistance of hemp fibre for hemp fibre-reinforced cement composites, the combination of both methods (i.e., modification of hemp fibre surfaces and the cement matrix) were used. Nanoparticles, such as nanoclay (Cloisite 30B), were used to partially substitute Portland cement at various ratios. Cloisite 30B was chosen because it is one of nanoclay types that has high specific surface areas (750 m^2 /g) when compare to other nanoclay types such as halloysite nanotubes (HNTs) that has low specific surface areas (20 m^2 /g). Hemp fibres were also utilised to reinforce this nanoclay-cement matrix. Moreover, NaOH pre-treatments of fibre surfaces and thermal pre-treatments of nanoclay were employed in order to enhance the microstructure and mechanical and durability properties. Therefore, this study evaluated the effect of different nanoclay and calcined nanoclay contents on various mechanical and physical properties of cement matrix and untreated and treated hemp fabric reinforced cement composites. The effect of nanoclay and calcined nanoclay on the thermal behaviour of untreated and treated hemp fabric reinforced composites was also evaluated in this study. The effect of calcined nanoclay on the durability properties of treated hemp fabric-reinforced cement composite was studied. The durability of the treated hemp fabric-reinforced cement composites and nanocomposites was discussed based on the porosity and flexural strength obtained at 56 days and 236 days (3 wet/ dry cycles). The microstructures of nanocomposites and untreated and treated-reinforced cement nanocomposites were also investigated using high resolution transmission electron microscopy (HRTEM), Quantitative X-ray Diffraction Analysis (QXDA) with Rietveld refinement by Bruker DIFFRAC^{plus} TOPAS software, x-ray diffraction, synchrotron radiation diffraction, scanning electron microscopy (SEM), energy dispersive spectroscopy (EDS) and thermogravimetric analysis (TGA).

1.2 Project Significance

This project seeks to gain a better understanding of natural fibre-reinforced nanocomposites made from hemp fibres and nanoclay. In this thesis, an innovative method was utilized to synthesize hemp fibre-reinforced cement composite containing nanoclay (which possesses unique mechanical properties for use as building materials). This project also provides new design concepts for developing cementitious composites, which will have a significant impact on the future application of this technology.

To date, little or no research was reported on the use of both chemically treated hemp fabrics and nanoclay (or calcined nanoclay) as hybrid reinforcement in cement-composites. In this project, nanoclay was utilised as a partial replacement of cement at various contents, in order to produce nanocomposites and hemp fabrics (HF) to be used as reinforcements to fabricate HF-reinforced cement nanocomposites. Hemp fibre-reinforced cement based composites are sustainable alternatives to their synthetic fibre-based counterparts, due to their lower cost, bio-degradability, local availability and an extremely little energy-intensive manufacturing process. However, the bond of hemp fibres with the cement matrix is relatively weak and the high alkalinity of the cement matrix adversely affects the durability of hemp fibres in the composites, which ultimately affects the mechanical and durability properties of the composites. The use of nanoclay in hemp fibre-reinforced cement composites could be expected to reduce the alkalinity of cement matrix, via the consumption of calcium hydroxide during the pozzolanic reaction. Hence, this improves the durability of the hemp fibre in the composite and the dense nanoclay-cement matrix, due to the particle packing of nanoclay. Also, it improves its bond with the hemp fibre.

In the future, this novel natural fibre-reinforced nanoclay-cement nanocomposite could be utilised in the construction industry. Moreover, it can also be widely employed in architectural structures, block walls, pavements, bridges, roads and fences. Furthermore, it can be utilised as an alternative to steel or synthetic fibres, which replaces glass fibre-reinforced concrete (GFRC) in some applications, including concrete tiles, roofing sheets,

on-ground floors, window trims, fountains, ceilings, structural laminate and sandwich panels.

1.3 Project Objectives

This project was concerned with studying the cost-effectiveness and optimum design of novel cement nanocomposites that have been reinforced with hemp fibres and nanoclay, so as to achieve optimum mechanical and fracture properties. In addition, this project aimed at building a connection between materials at the nano and macro-scale level, through integrating concepts from natural fibre-reinforced cement composites and nanocomposites for a better understanding of the enhanced physical and mechanical properties brought about by the respective mechanisms.

The specific objectives of this project were as follows:

- To obtain a fundamental understanding of the processing-nanostructure-property relationships of natural fibre-reinforced cement composites.
- To evaluate the mechanical and thermal properties of hemp fabric-reinforced cement composites containing nanoclay.
- To evaluate the effect of nanoclay on the microstructure of the cement matrix and hemp fabric-matrix interface.
- To investigate and determine the effectiveness of chemical pre-treatment of hemp fibre surfaces and thermal pre-treatment of nanoclay (calcined nanoclay) on mechanical and thermal properties of hemp fabric-reinforced cement composites.
- To determine the optimum contents of nanoclay, calcined nanoclay, untreated and treated natural fibres of hemp fabric-reinforced cement composites.
- To investigate the effect of calcined nanoclay on the microstructure of the cement matrix and hemp fabric-matrix interface.

- To study the roles of nanoclay and interfacial properties of the hemp fabric on the efficiency of strengthening and toughening of the composite.

- To identify the underlying mechanisms of enhanced microstructure and mechanical properties of hemp fibre-reinforced cement nanocomposites that contain nanoclay.

- To evaluate the effects of chemical pre-treatment of hemp fibre surfaces and thermal pre-treatment of nanoclay on cyclic wetting-drying durability of hemp fabric-reinforced composites.

1.4 Research Plan

Based on the project significant and objectives as mentioned in the previous section, the following research plan was proposed:

1) Fabrication of nanoclay-cement nanocomposites and hemp fabric-reinforced nanoclay-cement nanocomposites.

2) Carrying out the thermal pre-treatment of nanoclay to produce calcined nanoclay and the chemical pre-treatment (NaOH) of hemp fabric to produce treated hemp fabrics.

3) Fabrication of calcined nanoclay-cement nanocomposites, untreated hemp fabric and treated hemp fabric-reinforced cement composites and treated hemp fabric-reinforced calcined nanoclay-cement nanocomposites.

4) Fabrication of treated hemp fabric-reinforced calcined nanoclay-cement nanocomposites.

5) Characterization of nanoclay and calcined nanoclay dispersion, morphology and micro-structure by High Resolution Transmission Electron Microscopy (HRTEM), Quantitative X-ray Diffraction Analysis (QXDA), Synchrotron

Radiation Diffraction (SRD), Scanning Electron Microscopy (SEM) and Thermogravimetric Analysis (TGA).

6) Investigation of the influence of untreated and treated hemp fabric, nano-fillers (i.e., nanoclay and calcined nanoclay) or treated hemp fabric-calcined nanoclay on durability, mechanical and thermal properties of the produced composites.

7) Determination of the effect of a high alkaline environment of cement (calcium hydroxide) on the mechanical properties, durability, fibre-matrix interface and fibre degradation of the produced composites.

8) Observation of the fracture surfaces and failure mechanisms by Scanning Electron Microscopy (SEM).

2 LITERATURE REVIEW

2.1 Natural Fibres

Natural fibres can be classified according to their sources; they are divided into plant, animal and mineral fibres. The physical, thermal and chemical properties of these fibres are also vastly different (Balaguru and Shah, 1992, Bentur and Mindess, 2007). Plant (vegetable) fibres are usually named based on plant part that fibre is extracted, they can be categorized into seed fibres such as cotton and kapok; bast or stem fibres such as hemp, flax, jute and kenaf; leaf fibres such as sisal and banana; fruit fibres such as coir (coconut); stalk fibres such as bamboo (Figure 2.1) (Akil *et al.*, 2011, Pacheco-Torgal and Jalali, 2011a). Animal fibres are generally made up of proteins examples include hair, wool and silk. These fibres recently use in textile industry. Mineral fibres can be derived from geological materials such as quartz and asbestos, these fibres are tough and highly temperature resistant (Balaguru and Shah, 1992, Bentur and Mindess, 2007).

Regarding plant fibres, several methods that can be used to separate the fibres from the other plant parts include retting, scrapping and pulping. Plant fibres are available all over the world (Coutts, 2005, Razak and Ferdiansyah, 2005, Juárez *et al.*, 2007). They can exhibit high Young's modulus and tensile strength as shown in Table 2.1 (Pacheco-Torgal and Jalali, 2011a). Thus their tensile performance can stand in a favorable manner with synthetic ones (Roma *et al.*, 2008, Ardanuy *et al.*, 2015, Santos *et al.*, 2015).

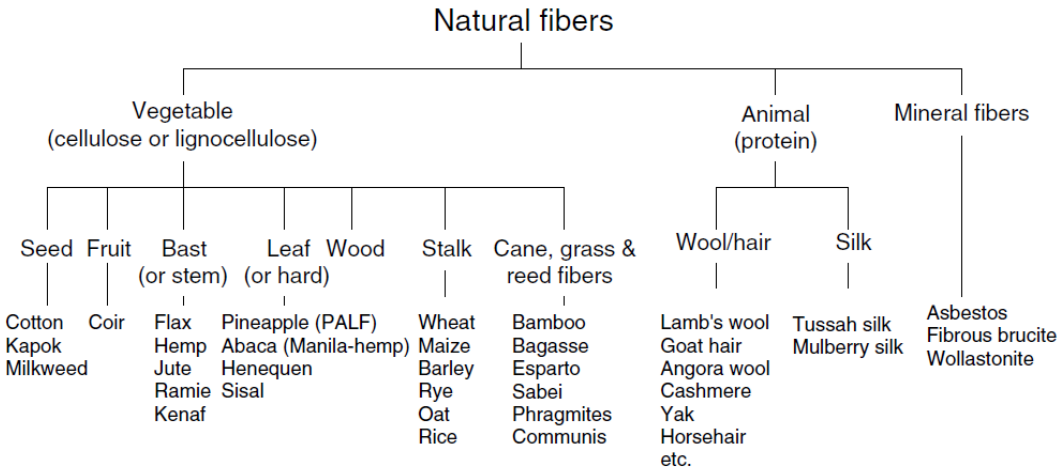

Figure 2.1: Categorization of natural fibres (Akil e*t al.,* 2011).

Table 2.1: Properties of some natural fibres and comparing them with some synthetic fibres (Pacheco-Torgal and Jalali, 2011a).

Properties	Specific gravity (Kg/m^3)	Water absorption (%)	Tensile strength (MPa)	Modulus of elasticity (GPa)
Sisal	1370	110	347-378	15.2
Coconut	1177	93.8	95-118	2.8
Bamboo	1158	145	73-505	10-40
Hemp	1500	85-105	900	34
Banana	1031	407	384	20-51
Polypropylene	913	-	250	2
PVA F45	1300	-	900	23

2.1.1 Chemical Compositions and Structure of Natural Fibres

In fact the chemical composition and structure of natural fibres are quite complex. The most plant fibres are composed of cellulose, hemicelluloses, lignin, pectin, waxes, and a few water-soluble compounds. The physical properties of the fibres are governed by the cellulose, hemicelluloses and lignin that are its basic constituents (John and Thomas, 2008, Le Troedec *et al.*, 2011a, Pacheco-Torgal and Jalali, 2011a). Table 2.2 exhibits the chemical compositions of some plant fibres (De Rosa *et al.*, 2010).

Table 2.2: Chemical compositions of some plant fibres (De Rosa *et al.*, 2010)

Type of fibre	Cellulose (wt%)	Hemicellulose (wt%)	Lignin (wt%)	Pectin (wt%)	Wax (wt%)
Bast Fibre					
Hemp	70.2-74.4	17.9-22.4	3.7-5.7	0.9	0.8
Jute	61-71.5	12-20.4	11.8-13	0.2	0.5
Flax	64.1-71.9	16.7-20.6	2-2.2	1.8-2.3	1.7
Kenaf	31.57	21.5	8-19	3-5	-
Leaf Fibre					
Sisal	65.8-78	8-14	10-14	0.8-10	2
Pineapple	70-82	-	5-12.7	-	-
Banana	63.64	10-19	5	-	-
Seed fibre					
Cotton	82.7-90	5.7	-	0-1	0.6
Fruit fibre					
Coir	32-43	0.15-0.25	40-45	3-4	-

Plant fibres mostly consist of lumen, middle lamella, primary cell wall and secondary cell wall as shown in Figure 2.2. The middle lamella is made up of pectins that hold fibres together. The primary cell wall is composed of disorganized arrangements of cellulose

fibrils in an organic matrix of hemicelluloses, lignin and proteins. The secondary cell wall is made up of three layers (L1, L2 and L3) of cellulose fibrils that are held by lignin (Le Troedec *et al.,* 2011b). The correlation between cellulose chains, hemicelluloses and pectins can be presented as shown in Figure 2.3.

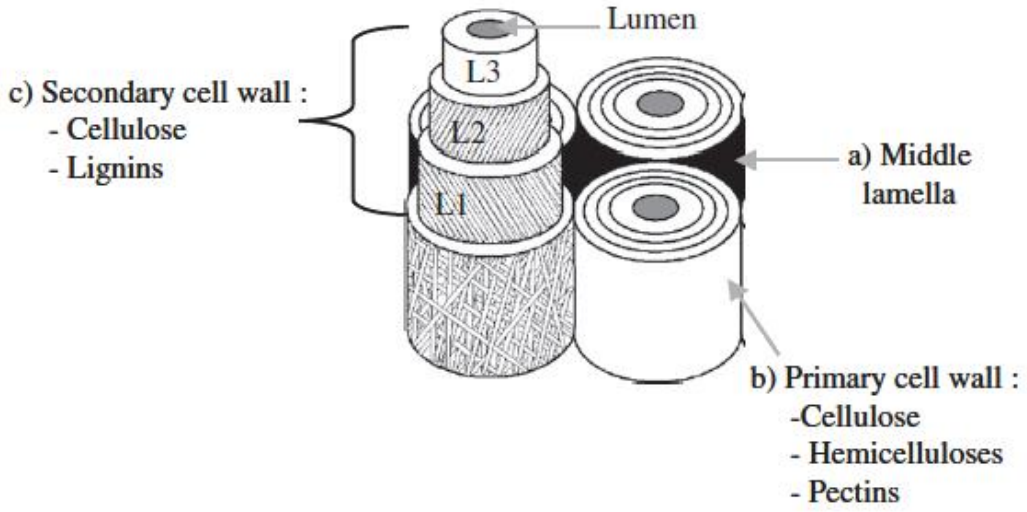

Figure 2.2: Structure of natural fibre (Le Troedec *et al.*, 2011b)

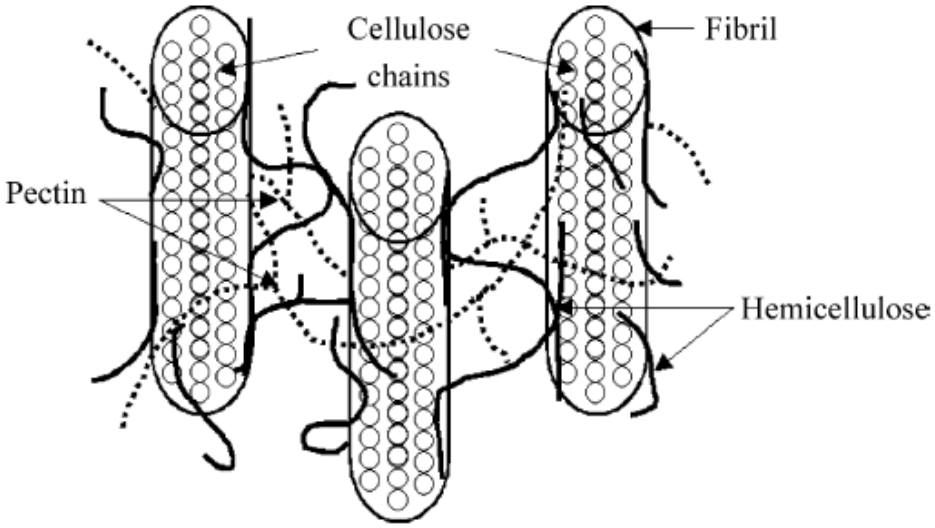

Figure 2.3: Correlation between cellulose chains, hemicelluloses and pectins in natural fibres (Sedan *et al.*, 2008)

(a) Cellulose

Cellulose fibrils (as known Cellulose) are the main part of natural plant fibres. Based on its chemical analysis, cellulose is made up of D-anhydro glucose ($C_6H_{11}O_5$) units. These units are repeating and linked by 1,4-β-D glycosidic bonds as shown in Figure 2.4 (Akil *et al.*, 2011). The degree of polymerization (DP) in the cellulose molecules is about 10,000 and these cellulose molecules are arranged in the microfibrils with diameters ranging from 10 nm to 20 nm (Ouajai and Shanks, 2005, Sedan *et al.*, 2008). Generally, there are four main different forms of cellulose (cellulose I, II, III, IV) (Mittal *et al.*, 2011, Sawpan *et al.*, 2011). Cellulose I (native) is the most abundant crystalline form in plant fibres (Sedan *et al.*, 2007).

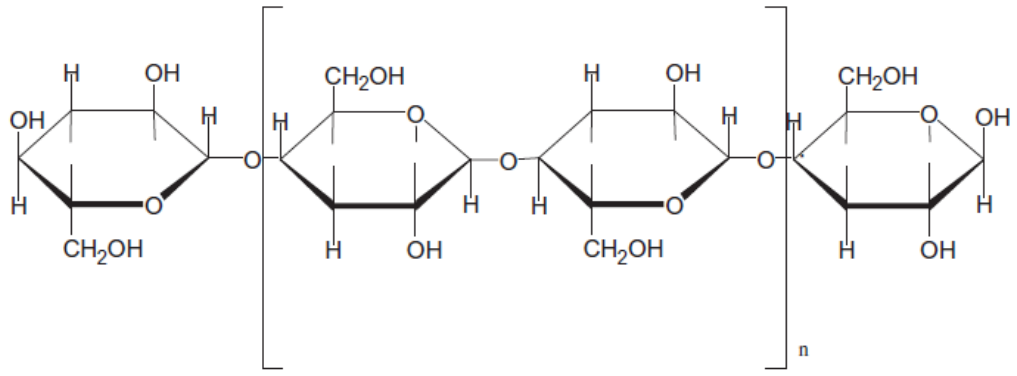

Figure 2.4: The structure of cellulose (Akil *et al.*, 2011).

(b) Hemicelluloses

Hemicellulose is made up of polysaccharides that consist of 5-ring and 6-ring carbon ring sugars. These sugars include glucose and monomers. These sugar monomers include galactose, mannose, arabinose and xylose (Mwaikambo and Ansell, 2002, John

and Thomas, 2008, Akil *et al.*, 2011). The polymer chains are non-crystalline and made up of short and branched chains, with degree of polymerization (DP) ranging 50-300. Therefore, hemicellulose has amorphous structure. Moreover, hemicelluloses are easily hydrolyzed (to break down a compound by chemical reaction with water) in acids and also dissolved by alkali (Demir *et al.,* 2006, John and Thomas, 2008).

(c) Lignin

Lignins are one of essential parts in the formation of cell walls for the plant fibres and also they are basically holding the fibre structure together (Beckermann and Pickering, 2008). Chemically, lignin is a cross-linked phenol polymer and amorphous and it consists of an array of hydroxyl- and methoxy- substituted phenylpropane units. Mostly, lignin is referred as a thermoplastic polymer (Vilay *et al.*, 2008, Akil *et al.*, 2011).

(d) Pectin

Pectin is main component of the middle lamella and plays important role to hold cell walls as shown above in Figure2.3 (Tserki *et al.,* 2005, Sedan *et al.,* 2008). Moreover, pectin is an essential ingredient for non-woods fibres especially bast. Based on chemical structure, pectins are complex polysaccharide acids polymers with chains that comprise of glucuronic acid and rhannose residues (John and Thomas, 2008, Akil *et al.*, 2011). Pectin is amorphous material and can be easily dissolved by alkali such as NaOH (Le Troedec *et al.,* 2011b).

(e) Waxes and fatty substances

Waxes and fatty substances are minor components in the structure of plant fibre and exist normally near the surface of fibre. Natural waxes mostly contain long chain alcohols and ester of carboxylic acids in their structure (John and Thomas, 2008, Le Troëdec *et al.,* 2009, Akil *et al.,* 2011). They are insoluble in water but can be easily removed from the surface of fibres by alkaline and organic solutions (Le Troëdec *et al.,* 2009).

2.1.2 Natural Fibre Surface Modification by Alkaline treatment

Surface treatments of natural fibres can be used to overcome the problem of their incompatibility. Chemical treatments can increase the interfacial adhesion between the fibre and matrix. Some researchers have shown that pre-treatments of natural fibre surfaces via some chemical agents such as alkalization, PEI (polyethylene imine), $Ca(OH)_2$ and $CaCl_2$ have slightly improved the fibre–matrix interface of the eco-composites (Bismarck *et al.,* 2002, Li *et al.,* 2007c, Alix *et al.,* 2009). Alkaline treatment such as NaOH is one of the most used chemical treatments of natural fibres when used to reinforce composites. It is well-known that the un-treated fibres had some impurities on its surface (Ray *et al.,* 2001, Aziz and Ansell, 2004, Mwaikambo, 2009, Yan *et al.,* 2012). Le Troedec *et al.* (2008) reported that these impurities are mostly waxes or fatty substances and also they indicated that NaOH treatment is well-known to bleach and clean the surface of plant fibres and to remove amorphous materials such as hemicelluloses and pectins from their surface and thus surfaces become more homogeneous. Three years later, Le Troedec *et al.* (2011a) reported that the modification of hemp fibres with NaOH has improved the interfacial bonding between the fibres and the lime-based mineral matrix (mortar).

2.2 Cement Matrix

2.2.1 Portland cement and the hydration reactions

Cement is the basic ingredient of cement paste, mortar and concrete. There are various types of cement as cementitious binders including Portland cement, lime, gypsum plaster, pozzolana cement, calcium aluminate cement and others (Neville, 2011). Among these, Ordinary Portland cement (POC) clinker is widely utilized in construction because it is the most inexpensive binder (Flatt *et al.,* 2012). The approximate oxide composition and physical properties of OPC are listed in Table 2.3 (Neville 2011). Generally there are four compounds that consider as the major constituents of Portland cement which are silicate minerals (C_3S and C_2S) and aluminate minerals (C_3A and C_4AF) as shown in Table 2.4 (Taylor, 1990, Scrivener *et al.,* 2004, Neville, 2011, Wei *et al.,* 2012, Soin *et al.,* 2013).

Table 2.3: Physical properties and approximate oxide composition of OPC (Neville, 2011)	
Properties/Compositions	OPC (ASTM Type I)
Physical properties:	
Specific gravity	3.17
Specific surface, Blaine (cm^2/g)	3170
Chemical analysis:	
Oxide	Content (%)
SiO_2	17-25
Al_2O_3	3-8
Fe_2O_3	0.5-6.0
CaO	60-67
MgO	0.5-4.0
SO_3	2-3.5
Alkalis (Na_2O, K_2O)	0.3-1.2

Table 2.4: Four major compounds of Portland cement (Neville, 2011)		
Name of compound	Oxide composition	Abbreviation
Tricalcium silicate	$3CaO.SiO_2$	C_3S
Dicalcium silicate	$2\ CaO.SiO_2$	C_2S
Tricalcium aluminate	$3\ CaO.Al_2O_3$	C_3A
Tetracalcium aluminoferrite	$CaO.Al_2O_3.Fe_2O_3$	C_4AF

The hydration reaction is defined as the chemical reactions that occur between the major compound of OPC and water to produce hydrated cement paste (Balaguru and Shah, 1992). Mainly the hydration reaction can be categorised into two types: hydration of silicates minerals (C_3S and C_2S) that leads to the strength development of cement paste in terms of the formation of calcium silicate hydrates gel ($C_3S_2H_3$ as know C-S-H) and also hydration of aluminate minerals (C_3A and C_4AF) in the present of gypsum that leads to fast stiffening and setting of cement paste (Neville, 2011, Govindarajan and Gopalakrishnan, 2012). Making the approximate assumption that C-S-H is the final product of hydration of both silicates minerals (C_3S and C_2S), the hydration reactions can be written as follows (Neville, 2011, Govindarajan and Gopalakrishnan, 2012):

$$2C_3S + 6H_2O \longrightarrow C\text{-}S\text{-}H + 3Ca(OH)_2 + heat \qquad (2.1)$$

$$2C_2S + 4H_2O \longrightarrow C\text{-}S\text{-}H + Ca(OH)_2 + heat \qquad (2.2)$$

Based on the hydration products, the calcium hydroxide ($Ca(OH)_2$) content in solid volume of the hydrated cement paste is about 20-30 vol.%. The $Ca(OH)_2$ is soluble in water in which this can lead to increase pores in the hydraulic structures of concrete porous, develop micro-cracks, weaken the bond with aggregates and thus affect the durability properties of concrete (Toledo Filho *et al.*, 2009, Neville, 2011). For these reasons, the reduction of calcium hydroxide quantity in concrete can be achieved by using pozzolanic materials.

2.2.2 Supplementary Cementitious Materials (SCMs) and the pozzolanic reaction

Supplementary Cementitious Materials (SCMs) are pozzolanic materials that have high pozzolanic reactivity. Some examples of SCMs include silica fume, metakaolin, ground granulated blast furnace slag, fly ash and others (Schneider *et al.*, 2011, Flatt *et al.*, 2012).

The utilizing of replacement of SCMs in Portland cement has been employed with different ratios (de Gutiérrez *et al.*, 2005, Mohr *et al.*, 2007, Siddique and Klaus, 2009, Juenger and Siddique, 2015). The pozzolanic materials often contain high chemical composition of siliceous (amorphous silica oxide or as know silicates SiO_2) or aluminous (Al_2O_3- SiO_2) (Neville, 2011, Juenger and Siddique, 2015).

Pozzolanic reaction can occur between calcium hydroxide ($Ca(OH)_2$) as hydration product and siliceous (SiO_2) or aluminous (Al_2O_3- SiO_2) to form calcium silicate hydrate (C-S-H), calcium aluminate hydrate (CAH) and calcium aluminate ferrite hydrate (Siddique and Klaus, 2009, Neville, 2011). The pozzolanic reaction that leads to formation additional C-S-H gel is the most important chemical reaction and can be written as follows (Toledo Filho *et al.*, 2009, Bendapudi, 2011):

$$Ca(OH)_2 + SiO_2 + H_2O \longrightarrow C\text{-}S\text{-}H + heat \qquad (2.3)$$

However, the extent of replacements of SCMs is limited due to their problems such as a reduction of early strength and none (or poorly)-reactive (Siddique and Klaus, 2009, Flatt *et al.*, 2012, Shaikh, 2013, Juenger and Siddique, 2015).

2.3 Natural Fibres Reinforced Cement Composites

2.3.1 Introduction

Nowadays, in the building industry, natural fibres have been gaining increasing attention to develop 'environmental-friendly construction materials' as alternative to synthetic fibres in fibre-reinforced concrete (Low *et al.*, 2006, Ahmed *et al.*, 2007, Silva *et al.*, 2010, Jarabo *et al.*, 2012). Natural and cellulose fibres are used in polymer and cement matrices to improve their tensile/flexural strength and fracture resistance properties (Savastano *et al.*, 2003, Snoeck and De Belie, 2012, Soroushian and Hassan, 2012). They

are cheaper, biodegradable and lighter than synthetic fibres. Some examples of natural fibres include sisal, flax, hemp, bamboo, coir, wheat straws and others (Bezerra *et al.*, 2006, Asasutjarit *et al.*, 2007, Sedan *et al.*, 2008).

2.3.2 Mechanical properties of natural fibre reinforced cement composites

The strength and toughness of cement matrix can be improved by using natural and cellulose fibres (Silva *et al.*, 2009, Islam *et al.*, 2011, Ardanuy *et al.*, 2015). Many studies have been carried out on different types of natural fibres such as sisal, flax, hemp, bamboo, coir and others (Savastano *et al.*, 2009, Bentchikou *et al.*, 2012, Santos *et al.*, 2015, Pacheco-Torgal and Jalali, 2011a).

Mansur and Aziz (1982) investigated the effect of fibre volume fraction and length on the tensile strength, flexural strength and flexural toughness of jute fibre reinforced cement mortar. The fibre volume fraction varied from 1 to 4 % and fibre length was 12, 18, 25 and 38 mm. The results indicated that tensile and flexural strength of composite with 2 vol % and 12 mm increased by about 20% and 34% compared to cement mortar. Moreover the highest flexural toughness (1099 N.mm) was achieved for jute fibre reinforced cement mortar composite with 2 vol % and 25 mm.

Ali *et al.* (2012) have studied the mechanical properties of coconut fibre reinforced concrete (CFRC) at 28 days. The fibre contents of 1, 2, 3 and 5 % by mass of cement and fibre length of 2.5, 5 and 7.5 cm were used to fabricate CFRC composites. It was found that CFRC with a fibre length of 5 cm and a fibre content of 5% had the best properties. They reported that MOR of CFRC with 5% fibre content and 5 cm long fibres increased slightly up to 4% compared to plain concrete. The flexural toughness measured as total toughness index (TTI), thus CFRC with 5% fibre content and 5 cm long fibres has the highest toughness index of 10.1.

Abdullah *et al.* (2011) have investigated the mechanical properties of composite cement reinforced with coconut fibres at 28 days. The mix design was based on 1:1 for cement: sand ratio and W/C of 0.55. The coconut fibre contents were 3, 6, 9, 12, and 15 wt. %. They reported that cement composite reinforced with 9 wt% of coconut fibre shown better

properties. Compressive strength of composite increased from 41.19 to 43.84 MPa by 6.4 % increase while modulus of rupture increased from 12.48 to 14.45 MPa. They also indicated that further increased in the fibre content more than 9 wt% decreased the compressive strength and modulus of rupture of composites as shown in Figure 2.5 and 2.6 respectively.

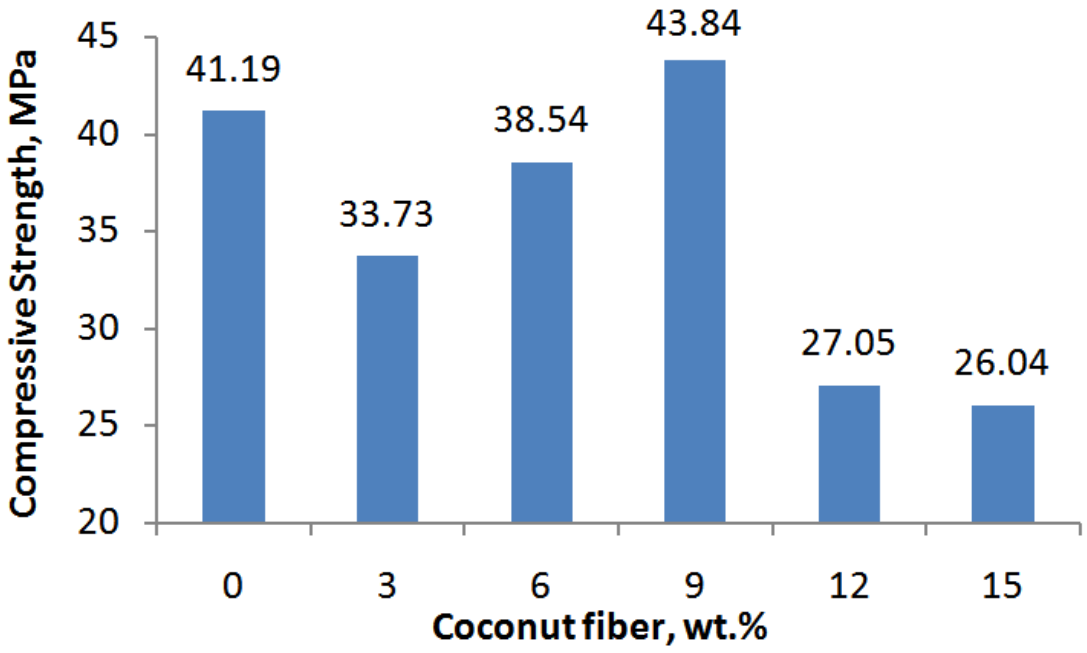

Figure 2.5: Compressive strength of composite for 28 days curing (Abdullah *et al.*, 2011)

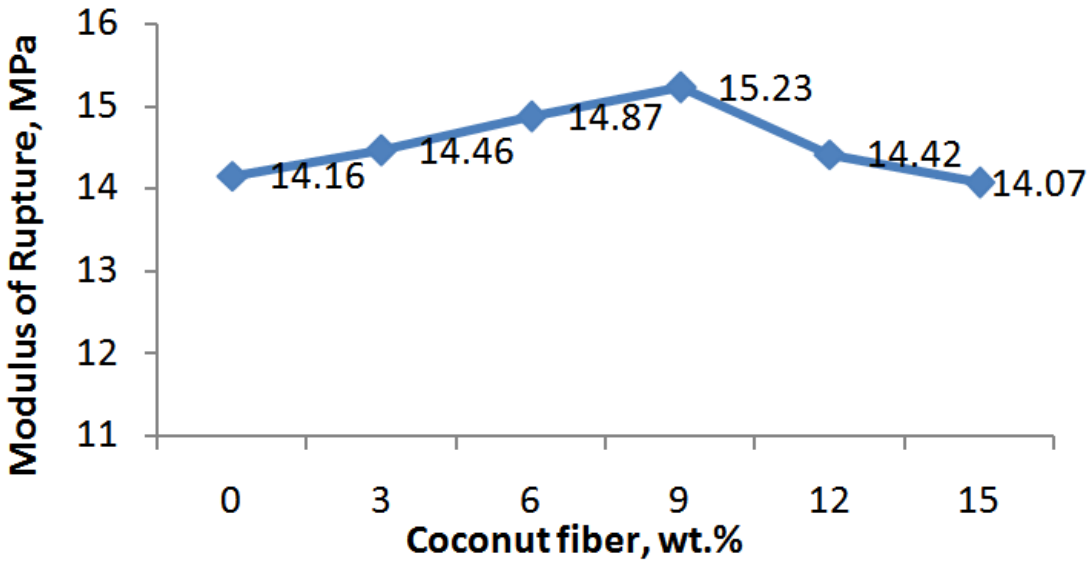

Figure 2.6: Modulus of rupture of composite for 28 days curing (Abdullah *et al.*, 2011)

Elsaid *et al*. (2011) studied the mechanical properties of kenaf fibre-reinforced concrete (KFRC) with fibre volume contents of 1.2% and 2.4% after a curing time of 28 days. They stated that the flexural toughness of KFRC with 2.4 vol % increased from 28.9 to 52.6 joules compared to KFRC with 1.2 vol %.

Li *et al.* (2004c) studied compressive and flexural properties of hemp fiber reinforced concrete. They used different fibre content (0.18, 0.36, 0.60 and 0.84% by weight) and different fibre length (10, 20 and 30 mm). It was found that the optimum fibre content and length was 0.36% and 20mm respectively. They reported that hemp fiber reinforced concrete improved the compressive strength by 4 %, flexural strength by 9 % and flexural toughness by 144 % and toughness index by 214 % compared to plain concrete.

2.3.3 Durability of natural fibre reinforced cement composites

Durability of natural fibre reinforced cement composites is defined as the ability to resist the processes of deterioration either external damage such as chloride attack or internal

damage such as compatibility between fibres and cement matrix (Mohr *et al.*, 2005a, Walker *et al.*, 2014, Santos *et al.*, 2015, Wei and Meyer, 2015). However, the long term durability of natural fibres in cement composites has been the major issue in which it has limited their applications in cementitious composites (Roma *et al.*, 2008, Ramakrishna *et al.*, 2010, Kwan *et al.*, 2014, Wei and Meyer, 2014a). These issues could be the degradation of fibres in a high alkaline environment of cement composites and also the interfacial bonding between the natural fibre and the cement matrix is relatively weak (Mohr *et al.*, 2006, Kriker *et al.*, 2008, Almeida *et al.*, 2013). In order to improve the durability of fibre reinforced cement composites, there are many possible methods; among those methods two basic approaches were selected: (i) modification (treatment) of fibre surfaces, (ii) modification of the cement matrix (Toledo Filho *et al.*, 2003, Ramakrishna and Sundararajan, 2005, Pacheco-Torgal and Jalali, 2011a, Soroushian *et al.*, 2012, Ardanuy *et al.*, 2015).

2.3.3.1 Natural fibre surface modification

Several researches have studied the effect of pre-treatment of natural fibres and different techniques were used. These pre-treatment can be classified into three major techniques; (i) mechanical treatment via pulping processes such as the Kraft process (ii) thermal treatment by the removal of water from cellulosic fibres through many cycles of drying and re-wetting (iii) chemical treatment by some chemical agents or coating (Pacheco-Torgal and Jalali, 2011a, Ardanuy et al., 2015, Santos *et al.*, 2015). The chemical pre-treatment of natural fibres whichever by chemical agents or coating is gaining increasing popularity because the reduction of fibre durability is caused mainly by the alkaline environment of the cement matrix. Several chemical agents were used such as alkalization (NaOH), $Ca(OH)_2$, $CaCl_2$, Na_2CO_3, polyethylene imine (PEI), acid ethylenediaminetetracetic (EDTA) and silane (i.e. Aminopropyltriethoxy silane (APS) and organofunctional trialkoxy silane) (Toledo Filho *et al.*, 2000, Blankenhorn *et al.*, 2001, Wei and Meyer, 2014b, Santos *et al.*, 2015).

Le Troedec *et al.* (2008) investigated the effect of several chemical treatment (NaOH, $Ca(OH)_2$ and $CaCl_2$) on surface structure of hemp fibres. Figure 2.7 shows SEM images of

the surface morphology of untreated, NaOH-treated, $Ca(OH)_2$-treated and $CaCl_2$-treated hemp fibres. The authors found that NaOH treatment was better than other treatment. They reported that NaOH treatment bleached and cleaned the surface of hemp fibres and also removed amorphous materials such as hemicellulose, pectins and impurities (fatty substances and waxes) from their surfaces. The team also supported their results by using X-ray diffraction of fibres and Segal empirical method to calculate the fibre crystallinity index (*CI*) of hemp fibre as follows:

$$CI(\%) = \frac{I_{002} - I_{am}}{I_{002}} \times 100 \qquad (2.4)$$

where I_{002} is the maximum intensity of the (002) crystalline peak and I_{am} is the minimum intensity of the amorphous material in fibre between $I^{c}_{(110)}$ and $I^{c}_{(002)}$ peaks as shown in Figure 2.8. They observed that the cellulose crystallinity index of untreated, NaOH-treated, $Ca(OH)_2$-treated and $CaCl_2$-treated hemp fibres was 80, 86, 78 and 65% respectively. They concluded that the highest crystallinity index of NaOH-treated fibre confirmed that NaOH treatment was more efficient than others.

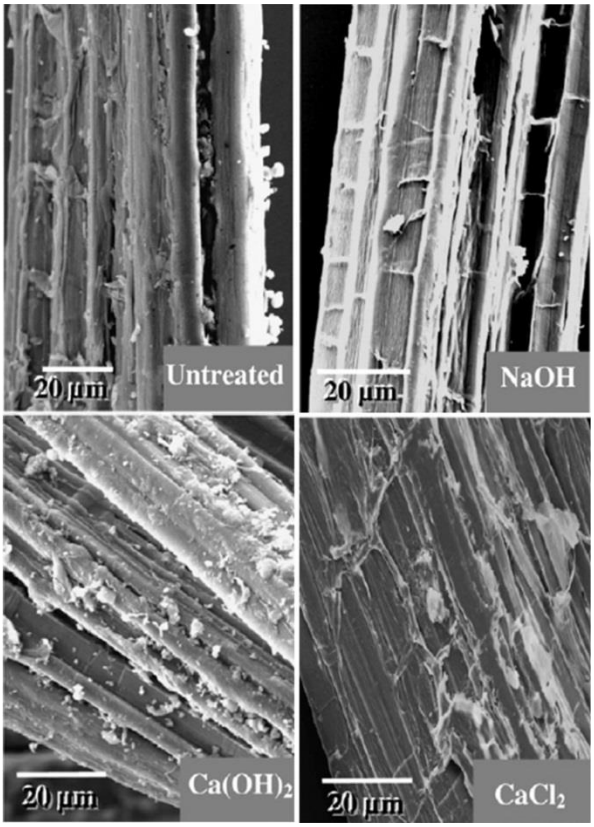

Figure 2.7: SEM images of untreated and treated hemp fibres (Le Troedec *et al.*, 2008).

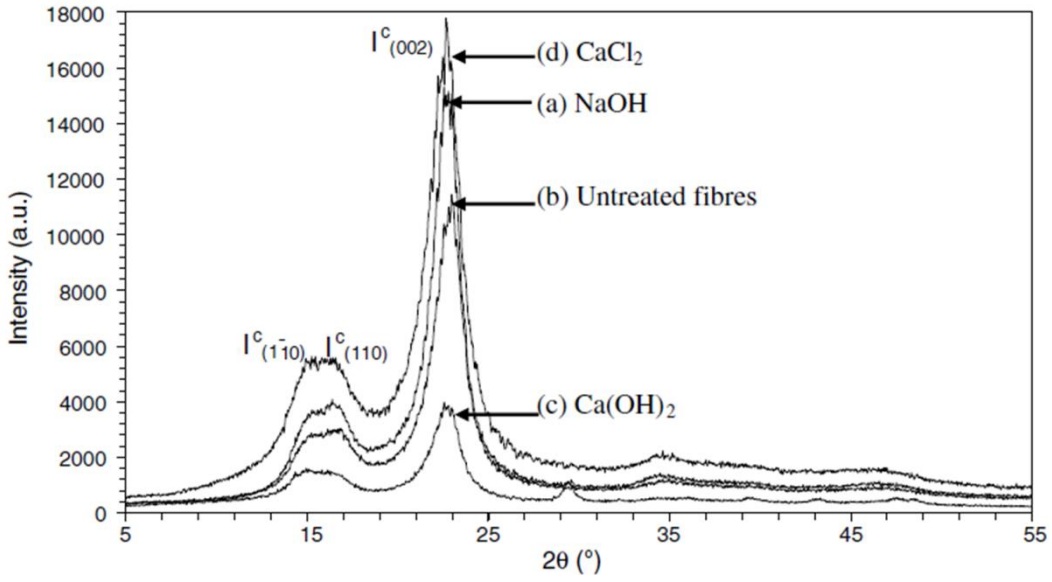

Figure 2.8: X-ray diffraction patterns of (a) NaOH-treated, (b) untreated, (c) $Ca(OH)_2$-treated and (d) $CaCl_2$-treated hemp fibres (Le Troedec *et al.*, 2008).

Sedan *et al*. (2008) studied the untreated and treated hemp fibre reinforced cement composite with different fibre volume fractions of 7, 10, 16 and 20 vol% (w/c=0.5). They reported that the flexural strength of NaOH treated hemp fibre reinforced cement composites with the optimum hemp fibres content of 16 vol% increased by 39% compared to untreated hemp fibre reinforced cement composites.

Tonoli *et al*. (2009) studied the effect of cellulose pulp fibre modification with Aminopropyltri-ethoxy silane on the physical properties of fibre–cement composites with 5 wt% fibre content, and compared the results with un-treated one. They reported that porosity and water absorption slightly decreased by about 7.7% and 12.6%, respectively.

Blankenhorn *et al*. (2001) studied the effect of fibre chemical treatments with 10 vol% alkylalkoxysilane solution on the flexural strength of hardwood fibre-cement composites with 4.24 wt% fibre content. They reported that the flexural strength increased by 11% compared to untreated one.

Asprone *et al*. (2011) where they investigated composite system consisting of a thin pozzolanic mortar slab reinforced with different layers of hemp fiber grids after they coated hemp fibre grids by epoxy resin coating. They observed that the flexural strength of epoxy coated hemp fiber grid-reinforced cement matrix with fibre content of 7 wt% (i.e. 6 layers) increased from 7.0 to 15.0 PMa, by 114% compared to control mortar matrix.

Mohr *et al*. (2005b) investigated the durability of thermomechanical pulp fiber–cement composites that was subjected to wet/dry cycles. Three types of fiber used were: thermomechanical pulp fiber (TMP), bleached kraft pulp fibre and unbleached kraft pulp fibre. Volume fraction of pulp fibres was 4 vol % in each cement paste composite. Samples were placed in a limewater curing tank until wet/dry cycling or testing commenced and duration of one wet/dry cycle was two days. Samples were tested at 78 days as control and after each 1, 2, 5, 10, 15 and 25 wet/dry cycles. Figure 2.9 shows average peak strength and average post-cracking toughness versus number of cycles for all composites. They reported that peak strength and toughness of TMP composite were less than at 78 days and at the first wet/dry cycles but after 25 cycles peak strength and toughness of TMP composite were greater than bleached and unbleached kraft pulp fibre

reinforced composites. These authors concluded that TMP composite exhibited lower progression of degradation than other and the use of TMP fibres can improve the durability of natural fibre reinforced cement composites significantly.

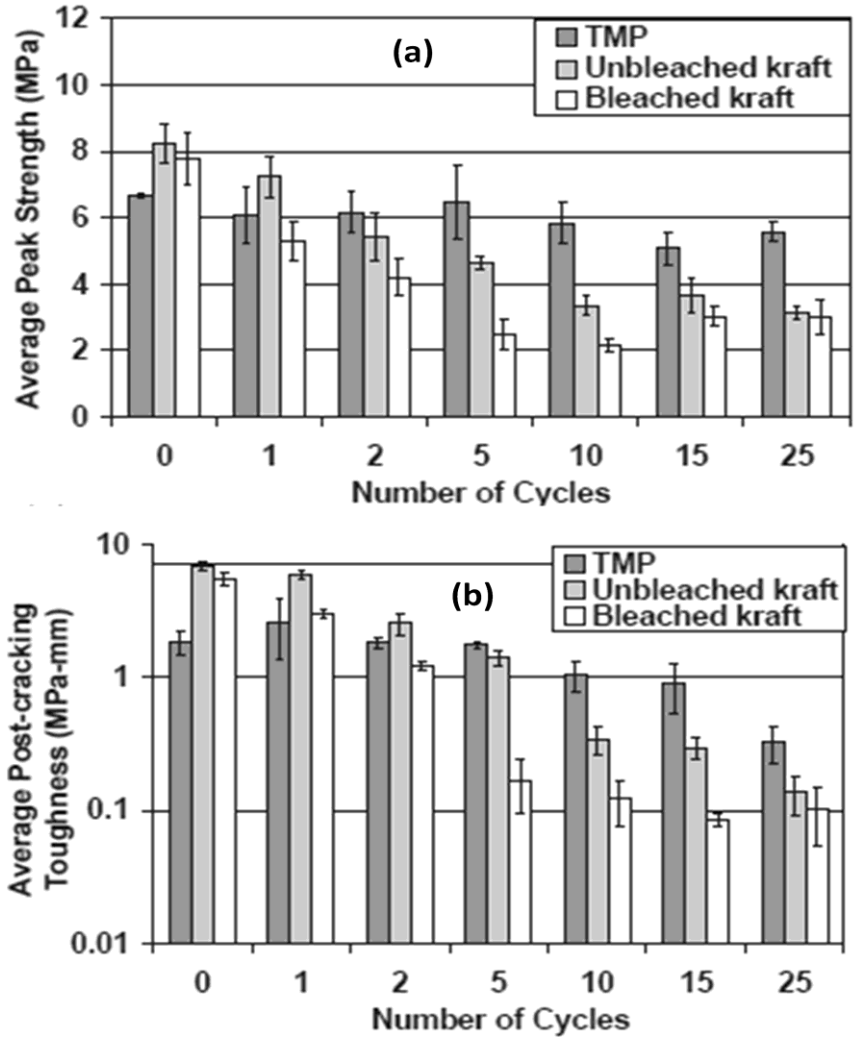

Figure 2.9: (a) Average peak strength (MPa) and (b) Average post-cracking toughness (MPa.mm) versus number of cycles (Mohr *et al.*, 2005b).

2.3.3.2 Cement matrix modification

Calcium hydroxide is a major hydration reaction product that causes degradation of natural fibre in cement matrix composites (Pacheco-Torgal and Jalali, 2011a, Santos *et al.*, 2015). In this second approach, calcium hydroxide in cement matrix can be reduced by using pozzolanic materials such as silica fume and metakaolin. Thus this approach could improve interfacial bond, mechanical properties and durability of natural fiber-reinforced cement composites (Toutanji *et al.*, 2004, Ardanuy *et al.*, 2015).

Khorami and Ganjian (2011) studied the flexural strength of the natural (Sugarcane) bagasse fibre-reinforced cement matrix with fibres content of 4 wt%, and silica fume was replaced for 5% of cement weight. They observed that the flexural strength increased about 20% compared to control bagasse fibre-reinforced cement matrix. They attributed this improvement to the pozzolanic and filler effects of very fine silica fume particles, which led to enhancement of the bonding strength between the matrix and fibres.

de Gutiérrez *et al*. (2005) studied the effect of pozzolans on the performance of fibre-reinforced mortars. They used four different pozzolanic materials which were silica fume (SF), metakaolin (MK) and fly ash (FA) as well as ground granulated blast furnace (GGBS) and also different types of natural fibre (sisal, coir and ique) and synthetic fibre (glass, polypropylene and steel). Silica fume (SF), metakaolin (MK) and fly ash (FA) were added by 15 wt % and ground granulated blast furnace (GGBS) was added by 70 wt % and then samples were tested at 90 days. They reported that although incorporating fibres into control mortar caused a decrease in compressive strength, the addition of pozzolanic materials, especially silica fume, compensated that reduction and improved the strength over that of control mortar. For instance, compressive strength of control mortar and coir fibre-reinforced cement mortar were 50 and 43 MPa respectively. After added SF into mortar the compressive strength of coir fibre-reinforced blended mortar increased from 43 to 52 MPa by 17% increase. Moreover, they also indicated that SF improved the water absorption of composites because of the reduction of permeable voids. For example, addition of SF into sisal fibre-reinforced cement mortar decreased the coefficient of capillary absorption from 0.022 to 0.0103 $kg/m^2s^{1/2}$.

Zhou *et al*. (2013) studied splitting tensile strength and fracture toughness of short discrete jute fibre reinforced concrete composites (JFRCC) at 7, 14 and 28 days. Portland cement was partially replaced by ground granulated blast furnace slag (GGBS) or pulverised fly ash (PFA) with 50 wt% of Portland cement. Total amount of jute fibres in each concrete composite was about 1 vol%. Figure 2.10 shows the splitting tensile strength of JFRCC concrete at various ages. They indicated that jute fibre reinforced concrete composites containing GGBS (FRC-GGBS) exhibited higher strength than jute fibre reinforced concrete composites containing PFA (FRC-PFA) due to high pozzolanic reaction of GGBS than PFA materials. Moreover, Table 2.5 shows the fracture toughness of plain GGBS/PC concrete, jute fibre reinforced GGBS/PC concrete (FRC-GGBS) and jute fibre reinforced PFA /PC concrete (FRC-PFA). They reported that fracture toughness (K^{S}_{IC}) of jute fibre reinforced GGBS/PC concrete (FRC-GGBS) increased from 26.0 to 33.7 MPa.m$^{0.5}$ and this increase was attributed to very strong bond between matrix and jute fibres.

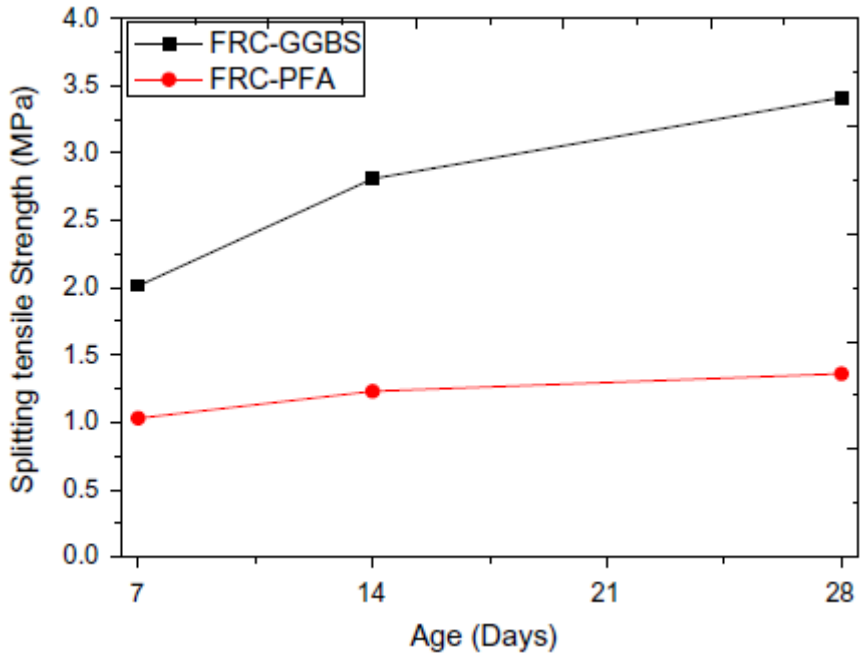

Figure 2.10: Splitting tensile strength of JFRCC concrete at various ages (Zhou *et al.*, 2013).

Table 2.5: Fracture toughness of plain GGBS/PC concrete, jute fibre reinforced GGBS/PC concrete and jute fibre reinforced PFA /PC concrete (Zhou *et al.*, 2013)			
Type of concrete	Ages (days)	Peak load (N)	K^{S}_{IC}
plain GGBS/PC	7	113.8.95	16.897
	14	1814.35	25.462
	28	2075.15	26.019
FRC-GGBS	7	1607.27	20.265
	14	2294.69	28.527
	28	2467.72	33..666
FRC-PFA	7	1170.65	15.707
	14	1238.37	16.717
	28	1480.62	19.964

Toledo Filho *et al*. (2003) conducted a study on the durability of vegetable fibre reinforced mortar composites (VFRMC). Random and aligned sisal and coconut fibres were used with fibre volume content of 3 vol%. They used several approaches to improve the durability of VFRMC including partial replacement of Portland cement by silica fume (10 wt%) or blast furnace slag (40 wt%), immersion of vegetable fibres in slurry of SF before incorporation in cement matrix (fibres were soaked in silica fume slurry for 10 minutes then air dry for 15 minutes) and carbonation of matrix by CO_2. The samples were subjected to three different ageing conditions: immersion in water, wet/dry cycles (7 days for one cycle) and open air weathering (outdoors). Tests carried out after 28 days for control, 180 and 322 days as well as 25 and 46 wet/dry cycles. Table 2.6 shows the flexural strength and Japanese toughness index for the important part of results. These authors concluded that soaking of vegetable fibres in silica fume slurry prior to add them into matrix was effective method to reduce embrittlement of composites in long term use and the partial replacement of Portland cement by silica fume efficient method to improve

durability. However they also stated that replacement of 40 % slag did not significantly improve durability of VFRMC composites and the results of carbonation treatment were promising alternative for improving the durability but more research is needed to confirm the their outcomes.

Table 2.6: Flexural strength and Japanese toughness index for the important part of results (Toledo Filho *et al.*, 2003)

Mix	Ageing condition	Age (days)	σ_b (MPa)	T_{JCI} (KN.mm)
M1S2S1	Control	28	7.51 (4)	0.99 (4)
M1S2S1	Water	322	7.15 (8)	0.82 (9)
M1S2S1	Outdoor	322	5.60 (3)	0.86 (17)
M1S2S1	Wet/dry	46 cycles	3.06 (14)	0.49 (10)
$M1S2S1_i$	Control	28	4.10 (11)	0.59 (7)
$M1S2S1_i$	Water	180	6.16 (13)	0.92 (3)
$M1S2S1_i$	Water	322	5.87 (13)	0.91 (9)
$M1S2S1_i$	Outdoor	180	5.61 (15)	0.71 (10)
$M1S2S1_i$	Outdoor	322	5.81 (4)	0.93 (3)
$M1S2S1_i$	Wet/dry	25 cycles	5.06 (3)	0.62 (7)
$M1S2S1_i$	Wet/dry	46 cycles	5.52 (15)	0.84 (10)
M1msS2S1	Control	28	4.86 (8)	0.72 (6)
M1msS2S1	Water	180	5.51 (13)	0.72 (13)
M1msS2S1	Water	322	5.07 (7)	0.67 (7)
M1msS2S1	Outdoor	180	4.74 (4)	0.82 (4)
M1msS2S1	Outdoor	322	4.32 (13)	0.77 (9)
M1msS2S1	Wet/dry	25 cycles	5.05 (11)	0.73 (13)
M1msS2S1	Wet/dry	46 cycles	4.44 (11)	0.83 (9)

M1S2S1 is untreated VFRMC composites, $M1S2S1_i$ is fibre silica fume slurry of VFRMC composites, M1msS2S1 is VFRMC composites containing silica fume (10 wt%), S is sisal

Mohr *et al.* (2007) investigated the effects of partial Portland cement replacement with various supplementary cementitious materials (SCM) on the degradation of kraft pulp fibre reinforced cement composites. Eight supplementary cementitious materials were used including: silica fume (SF), ground granulated blast furnace slag (SL), Class F fly ash (FA), Class C fly ash (CA), metakaolin (MK235), metakaolin (MK349), diatomaceous earth and volcanic ash (DEVA) raw and DEVA calcined. Binary, ternary, and quaternary blends of SCM were examined. Portland cement partially replaced by different ratios of SCM from 10-90 wt%. The fibre volume fraction was 4 vol% in each composite. The mechanical performance of composites was evaluated in terms of flexural strength and toughness. Tests were carried out at 28 and 78 days for unexposed composites and after 1, 2, 5, 10, 15 and 25 wet/dry cycles in which two days for one cycle was selected. These authors reported that after 25 wet/dry cycles, kraft pulp fibre reinforced cement composites containing 30% or 50% silica fume, 30% metakaolin or 90% slag did not exhibit any signs of degradation in mechanical testing. Ternary blends containing 70% slag/10% metakaolin or 70% slag/10% silica fume were also effective in preventing degradation. For example, after 25 wet/dry cycles the peak strength of control composite reduced from 10.34 to 2.85 MPa whereas for composite containing 30% silica fume the peak strength decreased from 11.62 to 8.57 MPa and for composite containing ternary SCM (70% slag/10% silica fume) the peak strength decreased from 11.91 to 6.47 MPa. It was concluded that the primary mechanism for improved durability was the reduction in calcium hydroxide content due to SCM addition.

Toledo Filho *et al*. (2009) produced cement matrix totally free from calcium hydroxide and studied the durability of sisal fibre reinforced mortar laminates. Portland cement was replaced by different ratios of metakaolin (MK) and calcined waste crushed clay brick (CWCCB) as shown in Table 2.7. They stated that the best partial replacements were 30 wt % of MK and 20 wt % of CWCCB to produce free $Ca(OH)_2$- matrix. After that they used sisal fibres with 400 mm length and fabricated into five layers resulting in a total volume content of 10 vol% in each sisal fibre reinforced mortar composite, the composite moulding procedure is shown in Figure 2.11. The sisal fibre reinforced mortar composites were denominated as M1 (free $Ca(OH)_2$-matrix) and M0. Finally composites tested after

180 days of fog cure and 25, 50, 75 and 100 cycles of wetting and drying (3 days for one wet/dry cycle). Figure 2.12 (a and b) show four point bending curves for (a) non-age and aged M0 composites (b) non-age and aged M1 composites. They reported that flexural strength of M0 composites significantly decreased during wet/dry cycles while the flexural strength of M0 composites increased up to 65% after 100 cycles. They indicated that free $Ca(OH)_2$ cement matrix prevented the sisal fibre from the degradation in the matrix and the durability of sisal fibre reinforced mortar was also maintained.

Table 2.7: Calculation of calcium hydroxide (CH) consume (Toledo Filho *et al.* 2009)

Cement paste mixture number	Compostion of the paste (PC:MK:CWCCB:Water by weight)	CH content at 28 days (%)
1	1.00:0.00:0.00:0.40	14.94
2	0.90:0.10:0.00:0.40	8.02
3	0.70:0.30:0.00:0.40	3.04
4	0.60:0.40:0.00:0.40	1.41
5	0.90:0.00:0.10:0.40	9.57
6	0.70:0.00:0.30:0.40	5.25
7	0.60:0.00:0.40:0.40	4.15
8	0.50:0.25:0.25:0.40	0
9	0.50:0.30:0.20:0.40	0
10	0.45:0.30:0.25:0.40	0

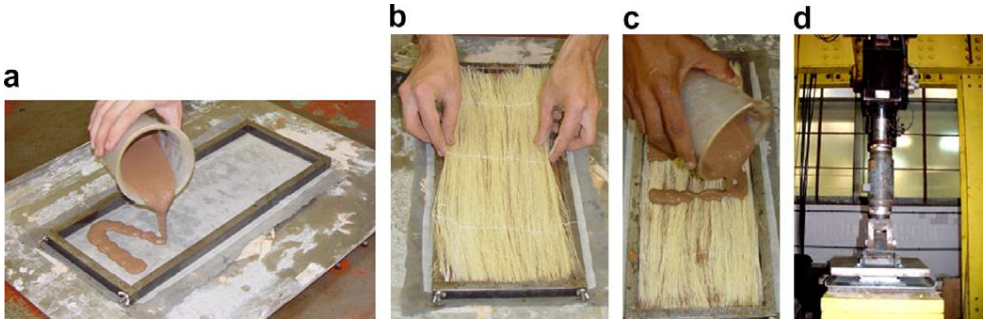

Figure 2.11: The composite molding procedure: (a) the first layer of matrix being poured in the mold, (b) placement of the first fiber layer, (c) placement of the second matrix layer and (d) compression of the laminate (Toledo Filho *et al.*, 2009)

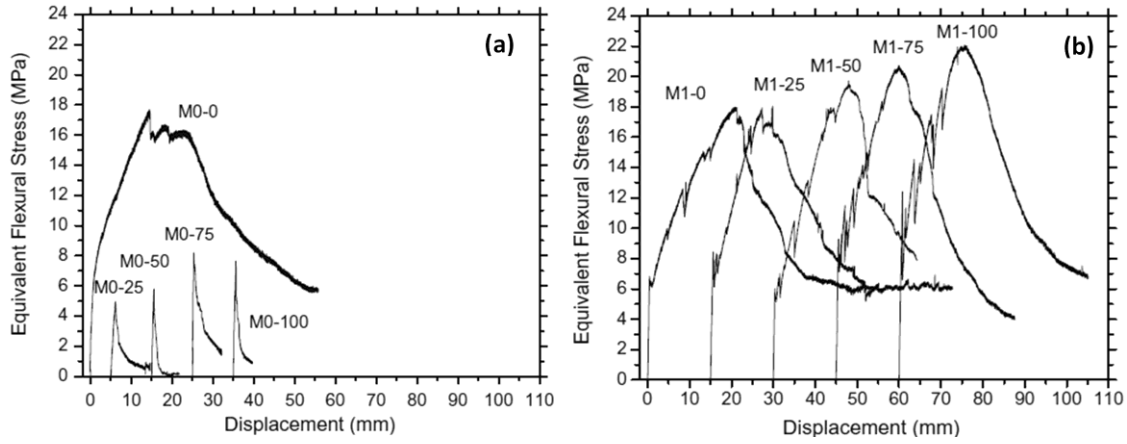

Figure 2.12: Four point bending curves for (a) non-age and aged M0 composites (b) non-age and aged M1 composites (Toledo Filho *et al.*, 2009).

Melo Filho *et al.* (2013) investigated the durability of the sisal fibre-reinforced mortar with 50% metakaolin (PC-MK) and without metakaolin (PC) at 28 days and after 25 wet/dry cycles (75 days after initial curing 28 days). Moreover, some composites was subjected to natural conditions and tested at 180 days, 1 year and 5 years. The total volume content of sisal fibres was 6 vol% in each composite. The effect of wetting and drying cycles on the mechanical behavior under bending load of (a) PC–MK composite and (b) PC composite are shown in Figure 2.13. They observed that after 25 wet/dry

cycles, the flexural strength of PC and PC-MK composites decreased by 63 % and 23 % respectively compared to their control composites at 28 days. Regarding the effect of natural condition on composites, Table 2.8 shows the results of four points bending tests performed in PC–MK composites subjected to natural aging. They concluded that 50% metakaolin replacement significantly prevented the sisal fibres from the degradation in cement matrix. SEM images (Figure 2.14 a-d) compared the degradation of sisal fiber surface between PC–MK composites and control PC composite after 25 wet/dry cycles. The team reported that fiber surface extracted from the PC–MK composites (Figure 2.14b) did not show any signs of calcium hydroxide whereas in that fiber surface extracted from the PC composites, it was observed a high concentration of hydration products (Figure 2.14c) including calcium hydroxide crystals (Figure 2.14d).

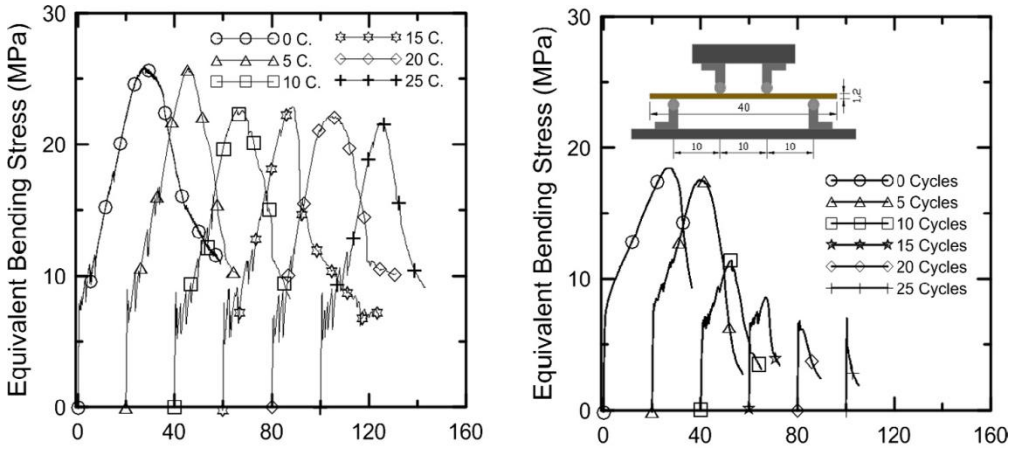

Figure 2.13: Effect of the wetting and drying cycles on the mechanical behavior under bending load of (a) PC–MK composite and (b) PC composite (Melo Filho *et al.*, 2013).

Table 2.8: Results of four points bending tests performed in PC–MK composites subjected to natural aging (Melo Filho *et al.*, 2013).

Natural again time	LOP (MPa)	Displacement at LOP (mm)	Flexural strength (MPa	Displacement at flexural strength (mm)	Toughness (kJ/m2)	Number of cracks	Mean final crack spacing (mm)
28 days	9.66 (0.33)	0.65 (0.09)	32.50 (0.62)	24.77 (0.04)	20.77 (1.03)	17.0	12.0 (2.0)
180 days	10.55 (1.17)	0.59 (0.06)	34.89 (0.78)	22.49 (0.90)	21.43 (0.91)	7.5	18.0 (1.3)
1 year	10.41 (1.46)	0.54 (0.13)	34.07 (1.33)	19.75 (0.46)	17.88 (1.98)	5.0	19.0 (2.2)
5 years	11.33 (1.00)	0.46 (0.01)	33.36 (2.02)	16.70 (1.73)	17.87 (2.30)	5.0	19.0 (2.2)

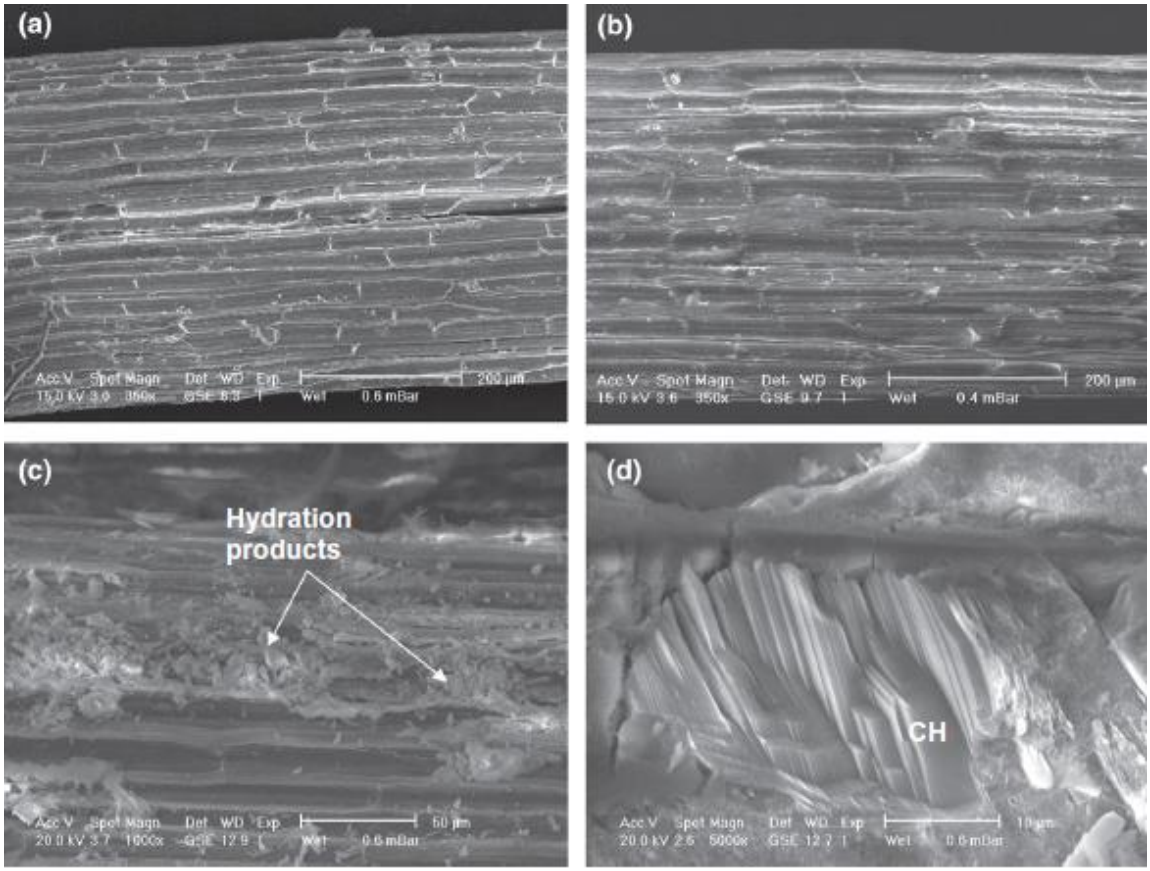

Figure 2.14: Effect of the wetting and drying cycles on the sisal fiber surface: (a) reference, (b) fiber extracted from a PC–MK matrix after 25 cycles, (c and d) fiber extracted from a PC matrix after 25 cycles (Melo Filho *et al.*, 2013).

Recently some research showed interesting approach for cement matrix modification. In this method, $Ca(OH)_2$ can react with carbonate (CO_2) by using accelerated CO_2 curing at early ages in order to produce limestone ($CaCO_3$). Soroushian *et al.* (2012) presented interesting research by fabricating cement thin sheet (board) reinforced with natural fibres as a high performance cementitious composite and using accelerated CO_2 curing. They investigated the effect of accelerated CO_2 curing on the structure and durability of cellulose fiber cement composite. Thin-sheet cellulose fiber reinforced cement composites were manufactured by using softwood kraft pulp (SSK) with fibre mass fraction of 8 wt% and 0.75 wt % of silica fume by weight of Portland (Figure 2.15). In CO_2 chamber, composites exposed to CO_2 environment (10% concentration of carbon dioxide) for 5 hours at room temperature and 95% relative humidity. The samples were subjected to 25

wet/dry cycles according to ASTM C1185 standard. As shown in Figure 2.16, the flexural strength and flexural toughness of CO_2-cement board increased significantly when compared to C and C2 cement board after 25 wet/dry cycles curing.

Figure 2.15: Typical appearance of the cellulose fiber cement board (Soroushian *et al.*, 2012)

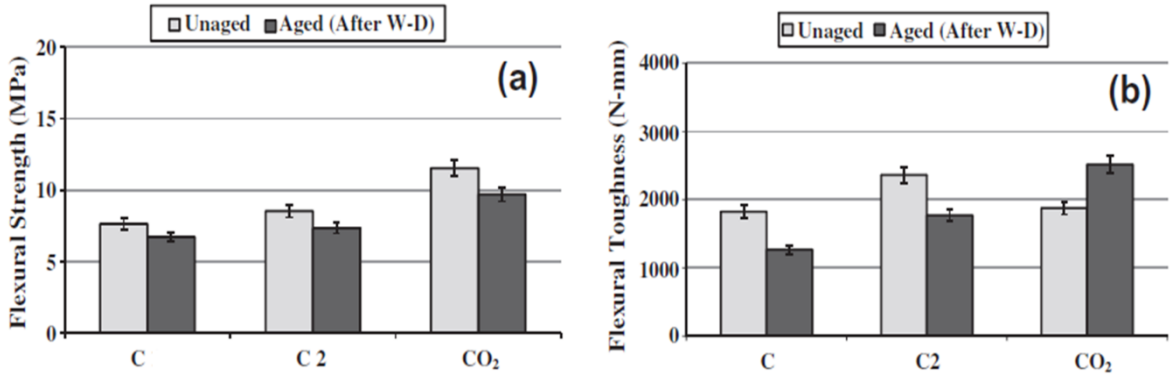

Figure 2.16: Flexural strength (a) and flexural toughness (b) of the cellulose fiber cement board (C1 is control, C2 is the same as C but with longer curing, CO_2 is carbonate curing) (Soroushian *et al.*, 2012).

2.4 Nanotechnology and Cement Nanocomposites

2.4.1 Nanotechnology

The concept of nanotechnology was first mentioned by physicist Richard Feynman in 1959 in his lecture "There's plenty of room at the bottom" (Pacheco-Torgal and Jalali, 2011b). Since then many research have been conducted to establish the concepts and applications of nano-sciences. Nanotechnology can be defined as the science and engineering conducted at the nanoscale ranging 1-100 nano-meters (nm). These extremely small things can be used across all the engineering and science field such as materials science, chemistry, biology, physics, medicine and others (Hanus and Harris, 2013). Today, there is wide research to apply nano-science in industry sectors in order to produce nanomaterials with enhanced physical, mechanical and chemical properties. Generally nanotechnology involves two main approaches: "top-down" or "bottom-up" methods as shown in Figure 2.17. In the "top-down" method, the sizes of bulk materials are reduced to the nano-scales with conserving their original properties. In the "bottom-up" method which is also called "molecular manufacturing", nano-structured materials can be made up of their atoms or molecular components through a process of assembly or self-assembly (Sanchez and Sobolev, 2010).

In the construction industry or sometimes called the nano-engineering, the nanomaterials have been gaining increasing attention to be used in concrete, especially nanoparticles. The nanoparticles have been found to improve the strength of nano-engineered concrete. As the size of nanoparticles decrease, the specific surface area increases and thus this leads to increase the chemical reactivity. As a result of this, nano-engineered concrete demonstrates higher strength than the high performance concrete or conventional concrete as shown in Figure 2.18 (Sanchez and Sobolev, 2010).

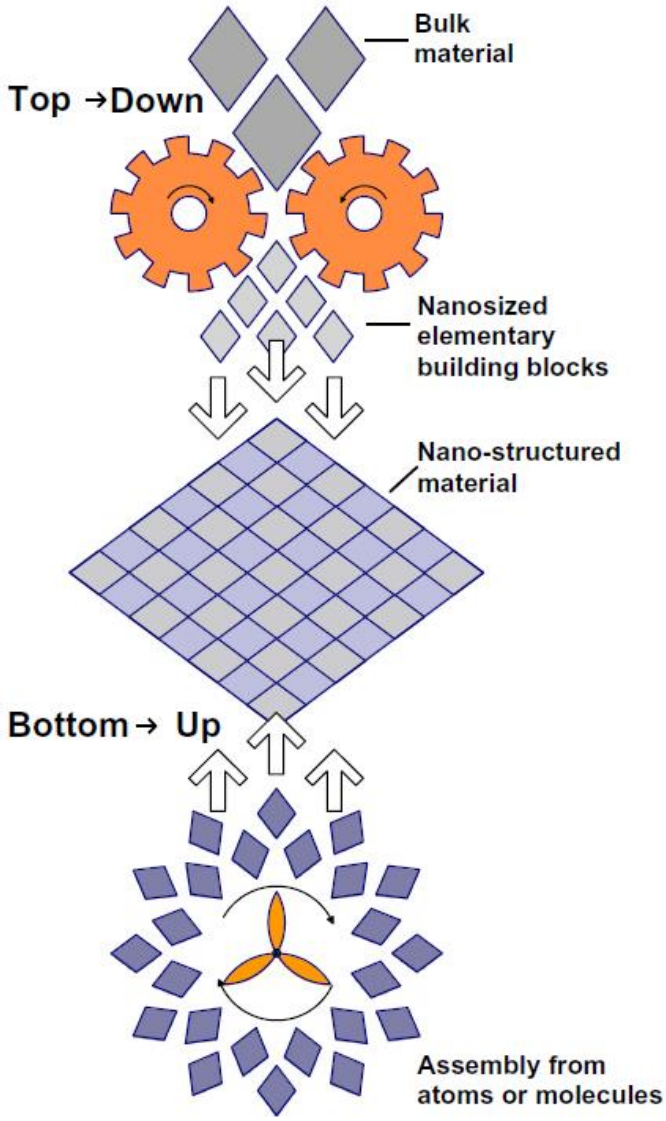

Figure 2.17: Illustrations of the ‘‘top-down” and ‘‘bottom-up” approaches in nanotechnology (Sanchez and Sobolev, 2010).

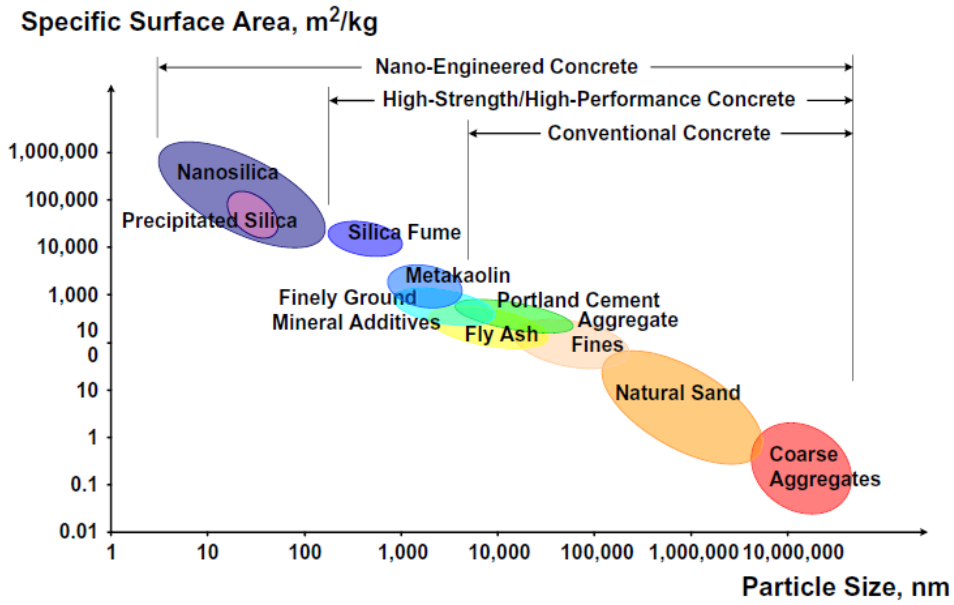

Figure 2.18: Particle size and specific surface area related to concrete materials (Sanchez and Sobolev, 2010).

2.4.2 Cement Nanocomposites

Nowadays, nanotechnology is one of the most active research areas in the civil engineering and construction materials (Sanchez and Sobolev, 2010, Singh, 2014). Nanoparticles are used in polymer, ceramic and construction materials in order to produce nanocomposites that exhibit superior physical and mechanical properties (Pacheco-Torgal and Jalali, 2011b, Alhuthali *et al.*, 2012). In the construction industry, several types of nanomaterials have been incorporated into concretes or cement based materials such as nano-SiO_2, nano-Al_2O_3, nano-Fe_2O_3, nano-ZnO_2, nano-MgO, nano-$CaCO_3$, nano-TiO_2, carbon nanotubes and nano-ZrO_2 in order to improve the durability and mechanical properties of concrete and blended Portland cement matrix (Hanus and Harris, 2013, Singh *et al.*, 2013). These improvements are mainly attributed to two mechanisms either filler effect or pozzolanic reaction or both. But in some cases, nanoparticles can be used to link cement matrix such as carbon nanotubes (Hanus and Harris, 2013). Nanoparticles have extremely high surface area and small particle size, consequently the nanoparticles acted

not only as a filler to improve the microstructure and to fill the micro pores in the matrix, but also as the activator to support the pozzolanic reaction (Sanchez and Sobolev, 2010). Amorphous nanoparticles have recently been introduced as an advanced pozzolan to improve the microstructure and stability of cement based system (Jo *et al.,* 2007, Sanchez and Sobolev, 2010, Kawashima *et al.,* 2013). It has been observed that the amorphous nanoparticles consumed free lime (calcium hydroxide) during cement hydration and formed additional calcium silicate hydrate (CSH) gel due to its high fineness and reactivity (He and Shi, 2008, Maheswaran *et al.,* 2013). In addition, the amorphous nanoparticle is particularly beneficial in acting as a nucleus to make the cement hydrate dense and improves the interfacial transition zone despite of small amount of replacement (Singh *et al.,* 2013, Mendes *et al.,* 2015).

2.4.2.1 Microstructure and Mechanical properties of Cement Nanocomposites

2.4.2.1.1 Effect of nano-silica or nano-SiO_2 (NS)

Nano-silica or nano-SiO_2 (NS) has recently shown promise in improving the microstructure, mechanical performance and durability of cement based system (Hanus and Harris, 2013, Hosseini *et al.,* 2014a, Singh *et al.,* 2015). It has been used with different average particle sizes ranging 5-50 nm and different contents (Jo *et al.,* 2007, Givi *et al.,* 2010, Singh *et al.,* 2013, Supit and Shaikh, 2014a). It is gaining increasing popularity due to its high pozzolanic reactivity and tiny particles. For these reasons it was observed that the NS has both pozzolanic and filler effects (Nazari and Riahi, 2010b, Hanus and Harris, 2013, Hou *et al.,* 2013, Senff *et al.,* 2013, Shaikh *et al.,* 2014).

Qing et al. (2007) studied the effect of as nano-SiO_2 (NS) on the compressive and flexural strength of cement paste and compared the results with silica fume (SF). Portland cement was replaced by 1, 2, 3 and 5 wt% of nano-SiO_2 and by 2, 3 and 5 wt% of silica fume. Dry mixing method was used to mix cement powder with nano-SiO_2 or silica fume. For all the specimens, the ratio of cement, water and superplasticizer was 1:0.22:0.025. It was found that the compressive and flexural strength of nanocomposites increased significantly when compared to composites with the same content of SF. For

example, at 28 days the compressive and flexural strength of nanocomposites with 5 wt% NS increased by about 25%, 88% respectively compared to control cement paste while the value of composites with 5 wt% SF increased by about 20% and 22% respectively. They explained the mechanisms of this improvement as follows: nano-SiO_2 has high surface energy and atoms in the surface have a high activity to contribute in chemical reaction. Thus, the pozzolanic activity of nano-SiO_2 is higher than that of silica fume. Moreover, nano-SiO_2 acts as the micro-filler of the cement particles, which can reduce the amount of water that filled in the void of the composites. Figure 2.19 shows XRD patterns of nanocomposites with 3 wt% NS and composites with 3 wt% SF at 28 days. These authors indicated that the remarkable reduction in the intensities of $Ca(OH)_2$ phases in nanocomposites confirmed that nano-SiO_2 consumed more $Ca(OH)_2$ crystals through pozzolanic reaction than silica fume in which that could lead to improve microstructure of nanocomposites.

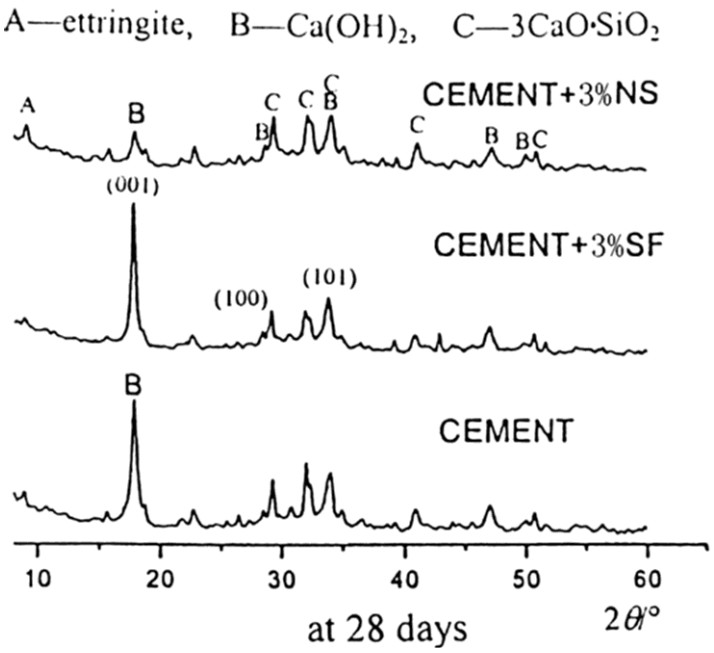

Figure 2.19: XRD patterns of nanocomposites with 3 wt% NS and composites with 3 wt% SF (Qing *et al.*, 2007).

Shih *et al*. (2006) investigated effect of nano-silica on characterization of Portland cement composite. Nano-silica particle in aqueous form with a spherical diameter of about 20 nm was incorporated into the Portland cement paste at four different dosages; 0.2, 0.4, 0.6 and 0.8 wt%. The water/cement ratio was 0.55 and specimens were tested at 7, 14, 28 and 56 days. Results of compressive strengths of cement composite at various contents of NS and ages are shown in Figure 2.20. These authors observed that the compressive strength increased with an increase in NS content until it reaches the optimum content (0.6 wt%) then the value decreased. They indicated that this phenomenon was due to two factors. The first one is the packing effect of NS in which NS filled interstitial spaces in composite thus that led to an increase in its density and strength. The second factor is pozzolanic effect that added more bonding strength and solid volume to microstructure resulting higher strength. These authors also carried out microstructural examination by mercury intrusion porosimetry (MIP) for cement composite with and without the optimum content of NS (0.6 wt%) as shown in Figure 2.21. It was found that the total (cumulative) pore volume decreased from 0.244 ml/g for pure cement paste to 0.238 ml/g for cement nanocomposite with NS by about 2.18% decrease. This decrease indicated that the microstructure of nanocomposite was more consolidated than control cement paste.

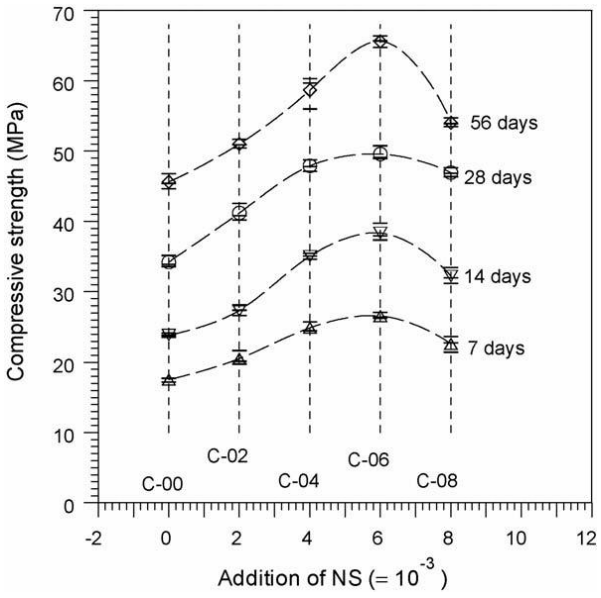

Figure 2.20: Compressive strengths of cement composite at various contents of NS and ages (Shih *et al.*, 2006).

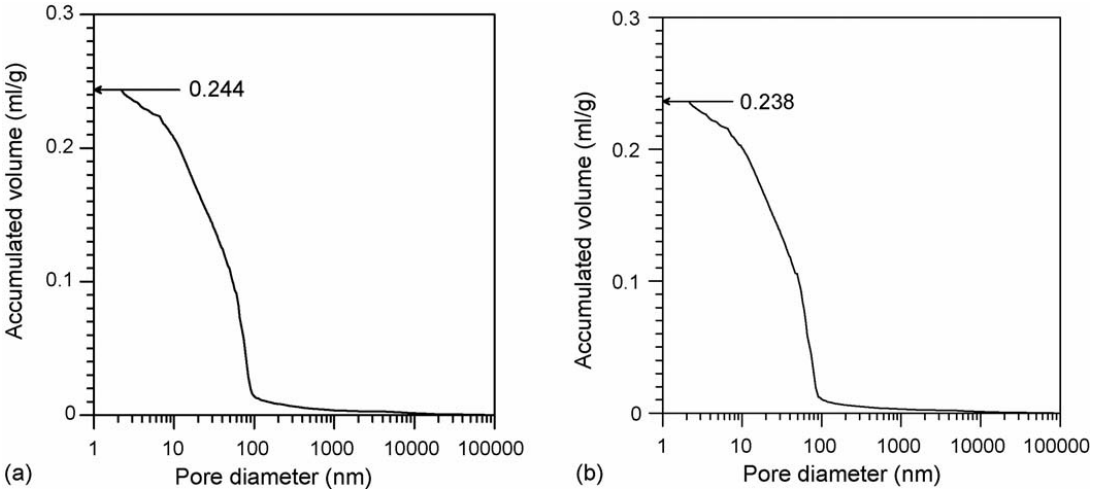

Figure 2.21: Accumulated MIP pore volume of hardened Portland cement composite: (a) without NS and (b) with NS (Shih *et al.*, 2006).

Nazari and Riahi (2011b) studied the split tensile strength and microstructure of concrete containing ground granulated blast furnace slag (GGBFS) and nano-SiO_2 (N). Three types of concrete were prepared; control concrete (C0-GGBFS), concrete containing 15, 30, 45 and 60 wt% GGBFS (labeled as C0-GGBFS15, C0-GGBFS30, C0-GGBFS45 and C0-GGBFS60) as well as concrete containing 45% GGBFS and 1, 2, 3 and 4 wt% of nano-SiO_2 (labeled as N1-GGBFS, N2-GGBFS, N3-GGBFS and N4-GGBFS). Samples were tested at 7, 28 and 90 days. Figure 2.22 shows the split tensile strength for specimens. These authors reported that the optimum content of nano-SiO_2 was 3 wt% in which N3-GGBFS concrete exhibited higher split tensile strength than others. Moreover, it was found that the porosity of N3-GGBFS concrete was lower than other concretes. It was concluded that 3 wt% of nano-SiO_2 consumed rapidly $Ca(OH)_2$ to form more CSH gel and refined microstructure of concrete by increase packing density. However, these authors stated that the addition more than 3 wt% of nano-SiO_2 led to a significant reduction in the split tensile and porosity due to the defects generated in dispersion of nanoparticles that causes weak zones.

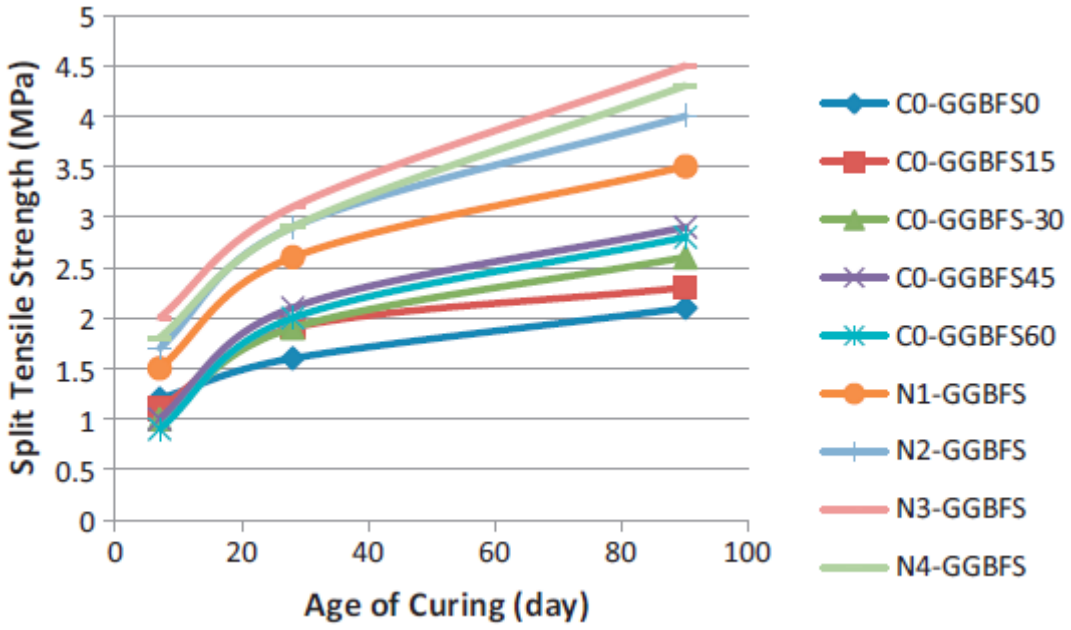

Figure 2.22: Split tensile strength for specimens (Nazari and Riahi, 2011b)

Li (2004) investigated the properties of high-fly ash concrete incorporating nano-SiO_2 (SHFAC) at different ages up to two years. Three types of concrete were prepared which are control Portland cement concrete (PCC), high-volume fly ash high-strength concrete (HFAC) and high-fly ash concrete incorporating nano-SiO_2 (SHFAC). The content of nano-SiO_2 in SHFAC was 4 wt% by binder weight. Samples were tested at 1, 3, 7, 28, 56, 112, 360 and 720 days. The results of the compressive strength versus time are shown in Figure 2.23. It was found that addition of nano-SiO_2 to high-volume high-strength concrete led to increase in the compressive strength of SHFAC concrete at early and later ages. For example, at 720 days the compressive strength of SHFAC, HFAC and PCC was 115.9, 108 and 10.37 MPa respectively. The authors reported that SHFAC can achieve sufficient early compressive strength while maintaining high long term strength. Porosity results at 2 years for SHFAC, HFAC and PCC concretes are shown in Figure 2.24. This team indicated that the porosity of SHFAC concrete was lower than HFAC and PCC

concretes after 2 years. They concluded that the reduction of the pore sizes of SHFAC concrete at long term was attributed to high activity and nucleating site effects of nano-SiO_2.

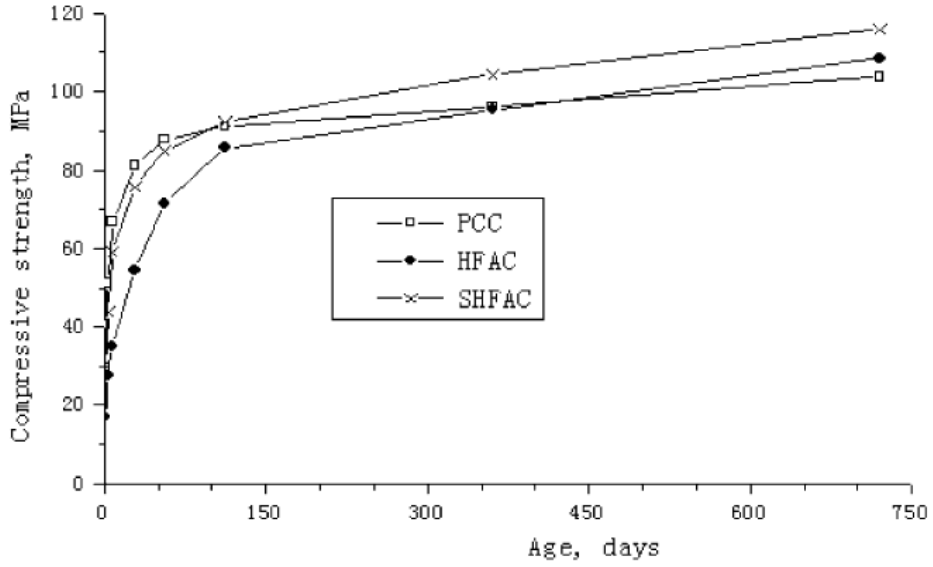

Figure 2.23: Development of the compressive strength versus time (Li, 2004).

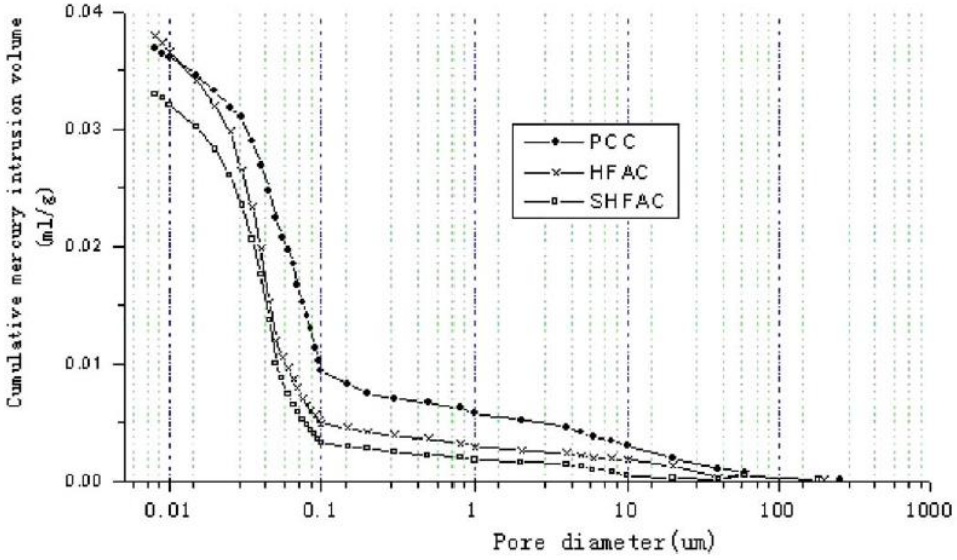

Figure 2.24: Porosity measurements at 2 years for different concretes (Li, 2004)

Rathi and Modhera (2014) studied effect of colloidal nano-SiO_2 (CNS) on compressive strength of cement mortar with and without fly ash at 28 days. The colloidal nano-silica (5-8 nm) was commercially an aqueous dispersion with nano-SiO_2 solid content (by weight) of 16%. The dosage of colloidal nano-SiO_2 (CNS) was from 1 to 6 wt% by mass of binder. Portland cement was replaced by 0, 10, 20 and 30 wt% of FA. As shown in Figure 2.25, the compressive strength of cement mortar increased by increasing CNS content up to the optimum value (4 wt% CNS) and then it decreased considerably for both cement mortar without and with FA. These authors concluded that addition of CNS improved the microstructure and compressive strength of cement mortar due to filler and pozzolanic effects of CNS.

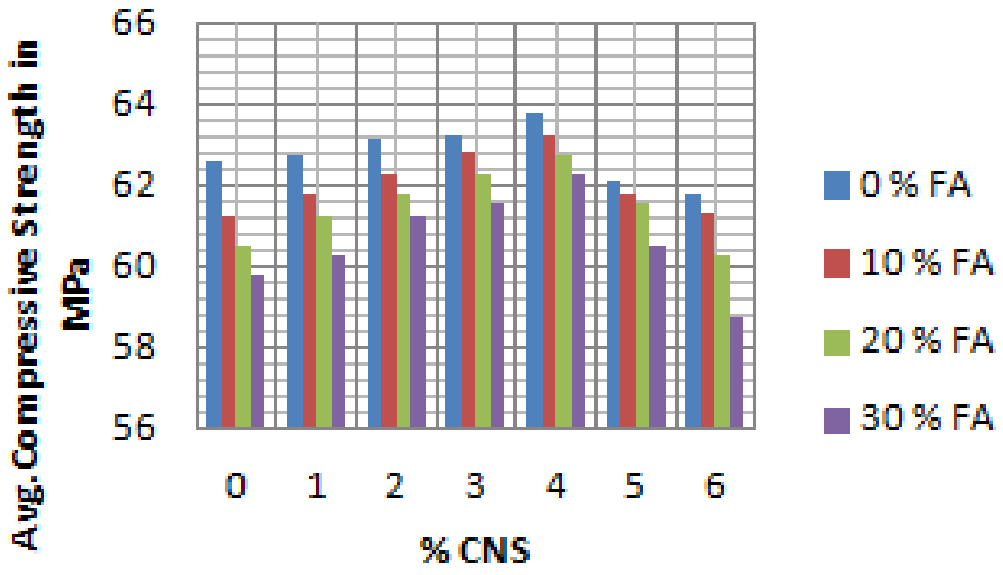

Figure 2.25: Compressive strength of cement mortar containing CNS without and with FA at 28 days (Rathi and Modhera, 2014).

2.4.2.1.2 Effect of nano-ZnO_2, nano-ZrO_2, nano-Al_2O_3 and nano-Fe_2O_3

Besides nano-silica or nano-SiO_2, there are other types of nanoparticles that are used in concrete to enhance its physical and mechanical properties. These nanoparticles include nano-ZnO_2, nano-ZrO_2, nano-Al_2O_3, nano-Fe_2O_3 (Li *et al.*, 2004a, Antonovič *et al.*, 2010, Nazari *et al.*, 2010a, Rashad, 2013, Mendes *et al.*, 2015, Hanus and Harris, 2013). These types of nanoparticles mostly have spherical shape with different sizes and the main effect of them is filler effect (Campillo *et al.*, 2007, He and Shi, 2008, Sanchez and Sobolev, 2010, Pacheco-Torgal and Jalali, 2011b).

Nazari and Riahi (2011a) studied the effects of nano-ZnO_2 nanoparticles on flexural strength of self-compacting concrete. Cement was partially replaced by 1, 2, 3, 4 and 5 wt% of nano-ZnO_2. They reported that the flexural strength of self-compacting concrete containing 4 wt% of nano-ZnO_2 at 28 days increased by 59% compared to of self-compacting concrete containing 1 wt% of nano-ZnO_2. This improvement confirmed that the pore structure of self-compacting concrete containing nano-ZnO_2 nanoparticles was improved.

In another work, Nazari and Riahi (2012) studied the flexural strength of concrete containing ground granulated blast furnace slag (45%GGBFS) and different ratios of nano-ZrO_2. Cement binder was partially replaced by 1, 2, 3 and 4 wt% of nano-ZrO_2. It was found that the optimum content of nano-ZrO_2 was 3 wt%. The authors reported that the flexural strength of concrete containing ground granulated blast furnace slag (45%GGBFS) and 3 wt% of nano-ZrO_2 at 90 days increased by 11% and 45 % compared to concrete containing only 45%GGBFS and control concrete without GGBFS respectively.

Nano-Al_2O_3 is also gaining attention to be used in concrete. Although there are few research about it, it was mentioned that nano-Al_2O_3 could improve the mechanical properties of concrete especially the modulus of elasticity. Li *et al.* (2006b) investigated the effect of nano-Al_2O_3 dispersion on the modulus of elasticity and compressive strength of cement mortar at 28 days. The loading of nano-Al_2O_3 was 3, 5 and 7 wt% as replacement of Portland cement. As shown in Figure 2.26, they reported that the modulus

of elasticity of mortar containing 5 wt% of nano-Al_2O_3 increased by 243% compared to control mortar in which the dosage of 5 wt% of nano-Al_2O_3 considered the ideal content. In contrast, the addition of nano-Al_2O_3 did not show any significant increase in the compressive strength at 28 days.

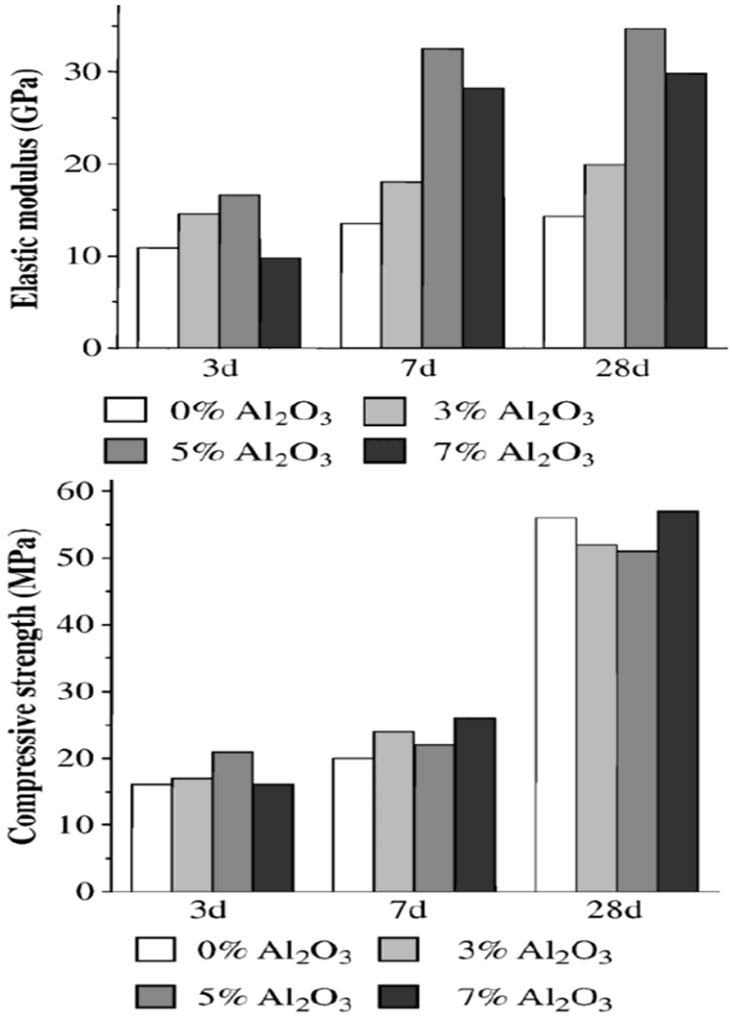

Figure 2.26: Modulus of elasticity and compressive strength of mortars (Li *et al.*, 2006b).

A similar work was done by Nazari *et al*. (2010b) where the influence of nano-Al_2O_3 nanoparticles on compressive strength and workability of concrete at 90 days was investigated. Nano-Al_2O_3 nanoparticles were used with four different loadings of 0.5, 0.1, 1.5 and 2.0 wt % of Portland cement. They reported that compressive strength increased with increase of nano-Al_2O_3 content up to 1 wt% and then it decreased. This was due to efficiency of of nano-Al_2O_3 to fill pores in the microstructure. However, these authors reported that addition of nano-Al_2O_3 adversely reduced the workability of fresh concrete.

Nano-Fe_2O_3 is also an interesting nanomaterial that can be used in construction and building materials (Nazari and Riahi, 2010a, Rashad, 2013). Nano-Fe_2O_3 has been found to enhance the tensile, compressive and flexural strength of concrete as well as provide self-sensing capability of concrete structure. Nazari *et al*. (2010a) investigated the compressive strength of concrete containing nano-Fe_2O_3 at 90 days. Nano-Fe_2O_3 with the average size of 15 nm was used with diverse contents of 0.5, 1, 1.5 and 2 wt% t of cement powder. The results showed that concrete containing 1 wt% nano-Fe_2O_3 exhibited the highest compressive strength when compared to their counterparts. In other words, the compressive strength of concrete containing 1 wt% nano-Fe_2O_3 increased from 42.3 to 46.1 MPa by about 9% increase compared to control concrete. This enhancement was attributed to filling and pozzolanic effects of nano-Fe_2O_3.

Yazdi *et al*. (2011) studied the effect of adding nano-Fe_2O_3 on the tensile and compressive strength of cement mortar at 7 days. Nano-Fe_2O_3 with the average size of 30 nm was used with various contents of 1, 3 and 5 wt% of Portland cement. After sample preparation, control mortar and mortar containing 1, 3 and 5 wt% of nano-Fe_2O_3 was termed as N0, 1NF, 3NF and 5NF. The results of compressive and tensile strength are shown in Figure 2.27. It was found that addition of nano-Fe_2O_3 improved strengths over control cement mortar and the optimum content of nano-Fe_2O_3 was 3 wt%. The compressive and tensile strength of mortar containing 3 wt% nano-Fe_2O_3 increased by about 74% and 49% increase respectively compared to control mortar. The authors stated that this improvement was due to the capacity of nano-Fe_2O_3 to fill micro-voids and consume calcium hydroxide crystals in mortar microstructure.

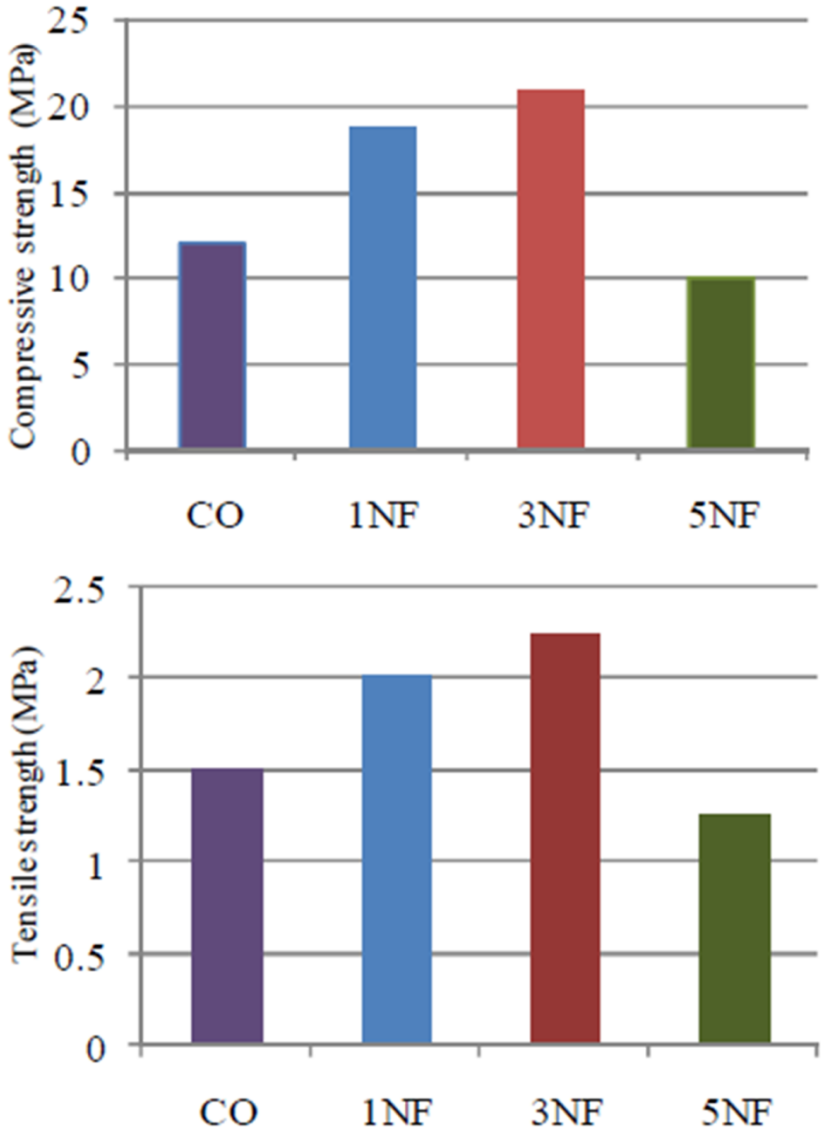

Figure 2.27: Compressive and tensile strength for control mortar (C0) and mortar containing 1, 3 and 5 wt% of nano-Fe_2O_3: namely 1NF, 3NF and 5NF (Yazdi *et al.*, 2011).

Li *et al*. (2004b) investigated the influence of nano-SiO_2 and nano-Fe_2O_3 on the microstructure and mechanical properties of cement mortar. Portland cement (PC) was partially substituted by nano-SiO_2 or nano-Fe_2O_3 of 3, 5 and 10% by weight of PC. The team used wet mixing method, in which water and nanoparticles were mixed by rotary mixer and then cement and sand were added. Water/binder ratio was 0.5 and samples were tested at 7 and 28 days. Table 2.9 shows the compressive and flexural strengths of

mixtures at 28 days. The results showed that the addition of nano-SiO_2 or nano-Fe_2O_3 significantly improved the strengths when compared to control cement mortar. It was also found that as the nano-SiO_2 content increased, the compressive and flexural strengths also increased gradually. Moreover, the optimum content of nano-Fe_2O_3 was found to be 3 wt%, in which the compressive and flexural strengths of nanocomposites increased by 26% and 18% respectively. However it was noticed that the compressive strengths of nanocomposites containing higher content of nano-Fe_2O_3 decreased as nano-Fe_2O_3 content increase. For example the compressive strengths of nanocomposites containing 10 wt% of nano- Fe_2O_3 decreased by 21% compared to nanocomposites containing 3 wt% of nano-Fe_2O_3. These authors concluded that the improvement in mechanical properties was due to the better dispersion of the nano-particles as well as reduction of $Ca(OH)_2$ but the reduction in mechanical properties was attributed to poor dispersion of the nano-particles that created weak zone as in form of voids. They also supported their argument with SEM photographs of mixtures A, C1, B1 and B3 as shown in Figure 2.28(a-d). The microstructure of mixture B3 containing10 wt% of nano- Fe_2O_3 was similar to pure mixture A in terms of the existence of pores, needle of hydrates and $Ca(OH)_2$ crystals that indicated poor filler and pozzolanic effects. In contrast, the microstructure of mixture C1 containing 3 wt% of nano-SiO_2 and B1 containing 3 wt% of nano- Fe_2O_3 were more dense and compact in terms of the increase of CSH gel, few pores and less $Ca(OH)_2$ crystals that revealed good filler and pozzolanic effects occurred in these mixtures.

Table 2.9: Compressive and flexural strengths of mixtures at 28 days (Li *et al.*, 2004b)

Mixture No.	Compressive strength (MPa)	Flexural strength (MPa)
A	28.9	4.9
B1	36.4	5.8
B2	33.1	6.0
B3	30.0	-
C1	32.9	5.8
C2	33.8	6.2
C3	36.4	-

(A) is control cement mortar, (B1, B2,B3) are cement nanocomposites containing 3, 5 and wt% of nano- Fe_2O_3, (C1,C2,C3) are cement nanocomposites containing 3, 5 and wt% of nano-SiO_2

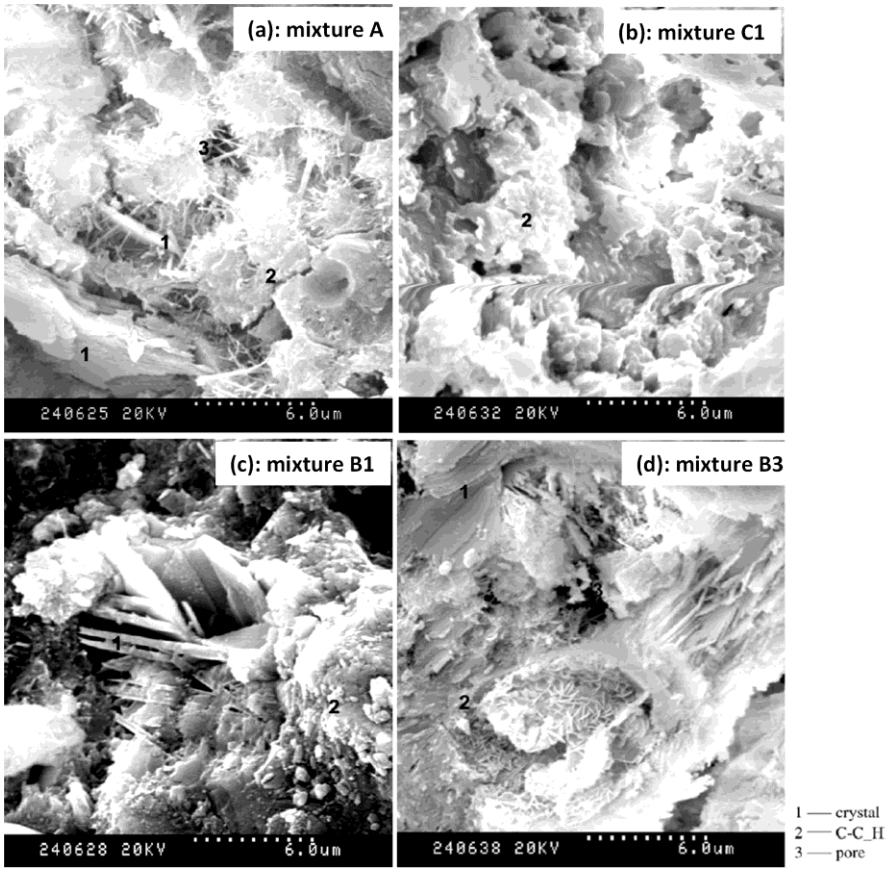

Figure 2.28: SEM photographs of mixtures (a) A, (b) C1, (c) B1 and (d) B3 (Li *et al.*, 2004b).

2.4.2.1.3 Effect of nano-$CaCO_3$

Nano-$CaCO_3$ has been recently introduced in cement composites. Some studies have suggested a potential benefit of the mechanical and physical properties of nano-$CaCO_3$ on the development of cementitious materials particularly for high volume fly ash concrete (Camiletti *et al.*, 2012, Shaikh and Supit, 2014, Mendes *et al.*, 2015). Nano-$CaCO_3$ can accelerate setting time and early development of compressive and flexural strength (Sato and Beaudoin, 2010, Makar *et al.*, 2012).

Li *et al.* (2015a) studied the effect of nano-$CaCO_3$ (NC) on flexural and compressive strength of (UHPC) ultra-high-performance concrete (20% silica fume, 10% fly ash). Portland cement was partially substituted by 1, 2, 3 and 4 wt% of nano-$CaCO_3$ (NC) by

weight of cement. The water/binder ratio of 0.16 was used and the samples were tested at 28 days standard curing. It was found that 3 wt% NC was the optimum content in which the flexural and compressive strength of UHPC nanocomposites increased by 18% and 10% respectively when compared to control UHPC composites. These authors reported that this improvement in strengths can be attributed to filler effect of NC that makes the microstructure more compacted with few micro-pores.

Liu *et al*. (2012) studied the incorporation of nano-$CaCO_3$ (NC) with average diameter of 15 nm in Portland cement paste. In that experiment, Portland cement was replaced by 1, 2, and 3 wt% of nano-$CaCO_3$. The water/binder ratio was 0.45 and the test was done at 7 and 28 days. Figure 2.29 shows the influence of nano-$CaCO_3$ (NC) on the initial and final setting time of cement paste and nanocomposites. It was found that as NC content increased the setting time decreased and then accelerated hydration reaction, this improvement was due to the small sizes and high surface energy of NC that could adsorb Ca^{+2} and OH^- on the surface of NC. For example the final setting time of 3 wt% NC nanocomposite dropped down from 260 to 207 minutes. The flexural and compressive strengths of cement paste and nanocomposites at 7 and 28 days are shown in Figure 2.30. In general, it was observed that addition of NC into cement paste enhanced the strengths. It was noticed that the flexural strength of cement paste reached its maximum when the content of NC was 1 wt%, but the compressive strength reached its maximum when the content of NC was 2 wt%. These authors stated that the compressive strength with 2 wt% NC didn't increase very much compared with 1 wt% and thus it could be considered that 1 wt% was the optimal content of NC. However, they reported that the improvement in flexural and compressive strength was due to the filling effect of NC that making microstructure more dense and also the consuming of $Ca(OH)_2$ grains that led to production of more CSH gel.

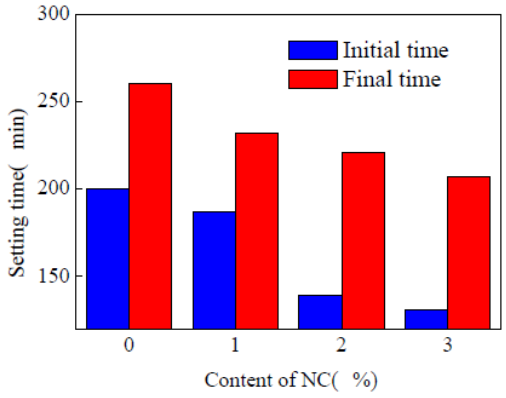

Figure 2.29: Initial and final setting time of cement paste and nanocomposites (Liu *et al.*, 2012)

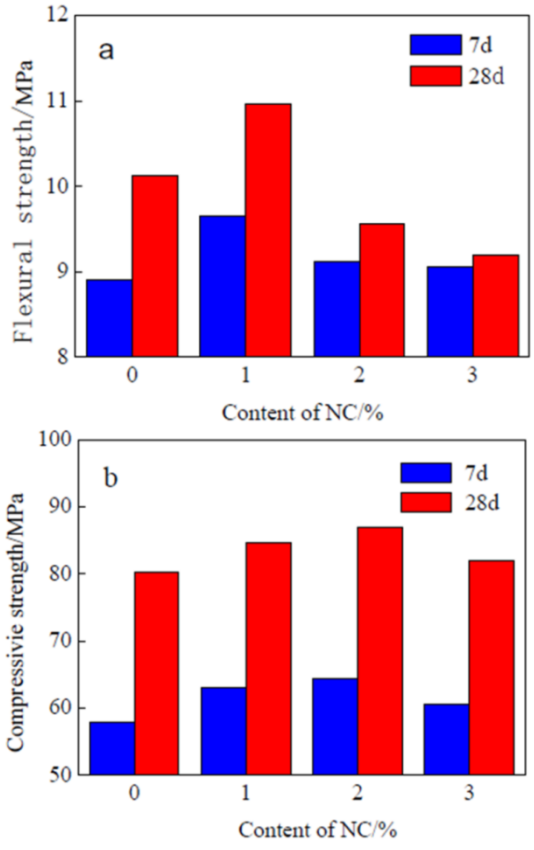

Figure 2.30: The flexural and compressive strength of cement paste and nanocomposites (Liu *et al.*, 2012).

Supit and Shaikh (2014b) presented an experimental study on the effect of nano-$CaCO_3$ content on compressive strength of mortar and high volume fly ash (HVFA) mortar containing 40 wt% and 60 wt% fly ash as partial replacement of cement. Portland cement was partially substituted by 1, 2, 3 and 4 wt% of nano-$CaCO_3$ by weight of cement. The dry mixing method of cement, fly ash, nanoparticles and sand was used and water/binder ratio was 0.4 and finally specimens were cured and tested at 7 and 28 days. The effects of nano-$CaCO_3$ content on compressive strength of control mortar (PC), mortar containing NC (NC1,2,3,4) pure high volume fly ash mortar (FA40, FA60) and high volume fly ash mortar containing 1 wt% NC (FA39NC1, FA59NC1) are shown in Figure 2.31. For cement mortar, it can be seen that 1 wt% NC was the best content in terms of the highest compressive strength of NC1 mortar at 7 and 28 day when compared to other cement mortar. Its strength increased by 22% and 18% compared to control PC mortar. The same trend was seen when the addition of nano-$CaCO_3$ enhanced the strength of high volume fly ash mortar at 7, 28 day. For example the compressive strength of FA59NC1 mortar at 28 days increased from 16 to 33 MPa by about 106 % compared to pure FA40 mortar. The microstructure of control cement paste and 1%NC cement paste was examined by backscatter scanning electron microscope (SEM) images as shown in Figure 2.32. It was found that control cement paste (Figure 2.32 a) had more un-hydrated cement particles (UC) and pores or cracks (black spots) while 1 wt%NC cement paste appeared more uniform and dense (Figure 2.32 b). The authors reported that improvement in early and later compressive strength and compacting microstructure of mortar was attributed to pronounced filler and pozzolanic effects of nano-$CaCO_3$.

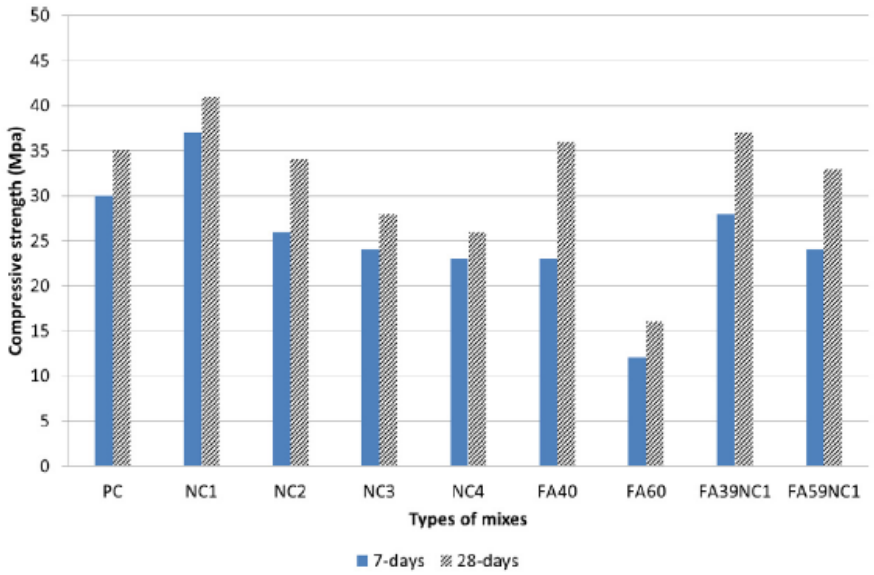

Figure 2.31: Compressive strength of control mortar (PC), mortar containing NC (NC1,2,3,4) pure high volume fly ash mortar (FA40, FA60) and high volume fly ash mortar containing 1 wt% NC (FA39NC1, FA59NC1) (Supit and Shaikh, 2014b).

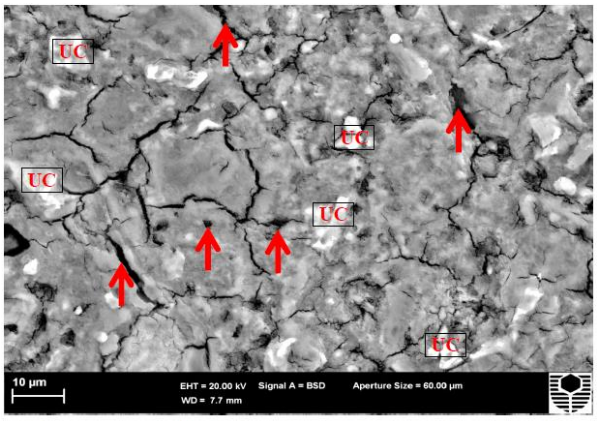

(a) Cement paste (UC represents as unhydrated cement particle, Black spots are represented by arrows as voids)

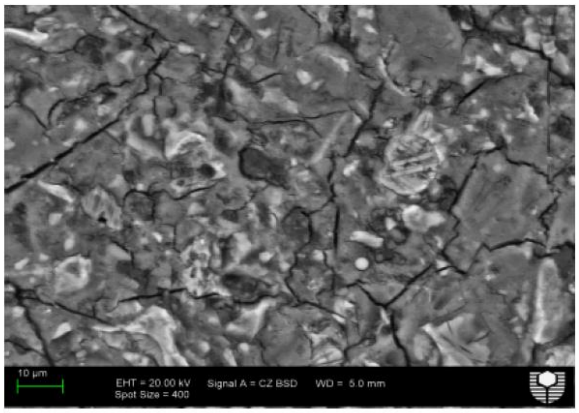

(b) Cement paste containing 1% NC

Figure 2.32: SEM backscattered images of control cement paste and 1 wt%NC cement paste (Supit and Shaikh, 2014b).

Kawashima *et al.* (2013) studied the influence of 5 wt % nano-$CaCO_3$ on setting time and compressive strength of cement paste containing 50% or 30% fly ash at 1, 3, 7 days. During sample preparation, two techniques were used to disperse NC into matrix; dry mix of NC with binder (Blended) and sonication mix where NC was sonicated for 30 minutes in an aqueous solution at 15% concentration. It was found that final setting time/h of plain cement paste (OPC), 50FA, 50FA 5$CaCO_3$ (Blended) and 50FA 5$CaCO_3$ (Sonicated) composites was 5.4, 7.4, 6.1 and 5.4 h. These authors reported that addition of the sonicated nano-$CaCO_3$ overcame the delay of setting time caused by replacement of 50% fly ash and then it increased the setting time better than blended nano-$CaCO_3$. Figure 2.33 shows the compressive strength of the cement paste (OPC), 30FA, 30FA 5$CaCO_3$ (Blended) and 30FA 5$CaCO_3$ (Sonicated) composites at 1, 3 and 7 days. Again, it was found that the compressive strength of 30FA 5$CaCO_3$ (Sonicated) composites increased significantly over typical 30FA.

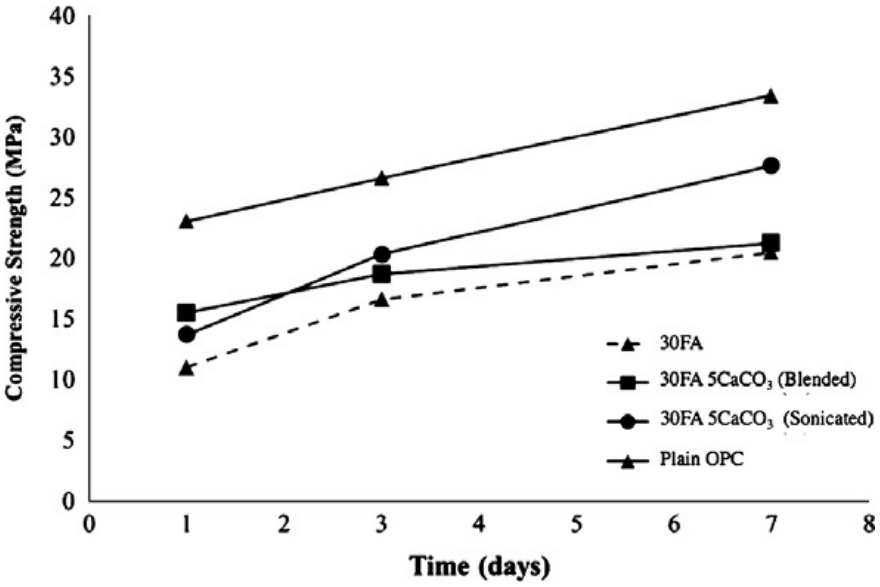

Figure 2.33: Compressive strength of the cement paste (OPC), 30FA, 30FA 5$CaCO_3$ (Blended) and 30FA 5$CaCO_3$ (Sonicated) composites at 1, 3 and 7 days (Kawashima *et al.*, 2013).

2.4.2.1.4 Effect of carbon nanotubes (CNTs)

Carbon nanotubes (CNTs) and nanofibers (CNFs) are gaining widespread attention to be used in cement based materials (Makar *et al.,* 2005, Siddique and Mehta, 2014, Singh, 2014). They are often used as nano-reinforcements in concrete or any building materials in order to improve the resistance to micro-crack propagation in nanocomposites (Figure 2.34) (Sanchez and Sobolev, 2010, Han *et al.,* 2015). The common types of carbon nanotubes that used are single-wall CNT (SWCNT) and multi-wall CNT (MWCNT) that have high aspect ratio and surface areas (Li *et al.,* 2005, Han *et al.,* 2015). The incorporating of CNTs into cement composite can improve the mechanical and physical properties significantly and also interaction zone between CNT and hardened cement products (Nochaiya and Chaipanich, 2011, Hu *et al.,* 2014, Kim *et al.,* 2014). Up to date one of the most challenges that limited the use of CNTs in construction is due to their tendency to agglomerate that leads to poor dispersion in cement paste or mortar when it blends by conventional mixing methods such as dry mixing, wet mixing or normal aqueous form (Cwirzen *et al.,* 2009, Sobolkina *et al.,* 2012). The various methods have been carried out to improve the dispersion of CNTs into cement matrix either by using sonication, pre-treatment or chemical dispersing agent or together (Li *et al.,* 2007a, Siddique and Mehta, 2014, Han *et al.,* 2015).

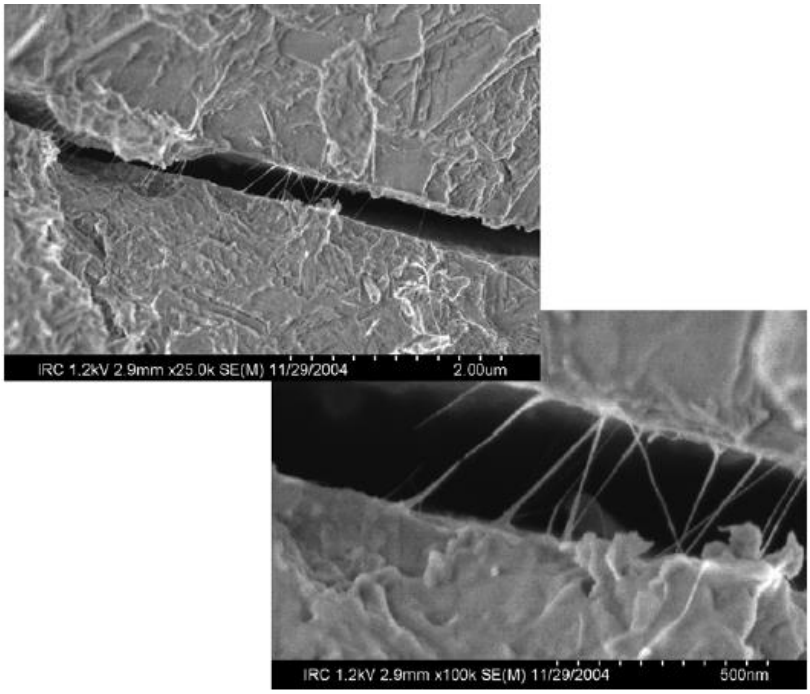

Figure 2.34: Crack bridging observed in SWCNT-cement nanocomposites at age of 3 day (Sanchez and Sobolev, 2010).

Musso *et al*. (2009) studied the effect of adding 0.5 wt% of MWCNT on the flexural strength and compressive resistance of cement mortar at 28 days. Three types of MWCNT were used; p-CNTs (Pristine MWCNTs), a-CNTs (annealed MWCNTs) and f-CNTs (carboxyl-group functionalized MWCNTs). In experimental procedure, the three types were first dispersed using acetone and sonication and then viscosity modifying agent and superplasticizer were added to the mixture during the mixing. As shown in Table 2.10, the results indicated that the flexural strength and compressive resistance of p-CNTs nanocomposites increased by 34% and 10% respectively compared to plain mortar. On the other hand, the flexural strength and compressive resistance of f-CNTs nanocomposites decreased significantly compared to plain mortar. The authors concluded that because of the existence of hydrophilic groups on the f-CNT surface, f-CNTs were very hydrophilic to absorb a lot of the water in the cement mixture consequently the hydration reaction of the cement paste was obstructed.

Table 2.10: Modulus of rupture and compression resistance of the cement with and without addition of MWCNTs (Musso *et al.*, 2009).		
Sample	Modulus of rupture (MPa)	Compression resistance (kN)
Plain cement	7.5	104 ± 20
Cement w 0.5 wt.% of p-CNTs	10.1	115 ± 18
Cement w 0.5 wt.% of a-CNTs	8.2	122 ± 14
Cement w 0.5 wt.% of f-CNTs	2.9	15 ± 3

Konsta-Gdoutos *et al*. (2010) studied mechanical propertied of cement paste reinforced with MWCNTs at 28 days. The short and long MWCNTs with different amount of 0.048, 0.08 and 1 wt% for short and 0.025, 0.048 and 0.08 wt% for long one were used. In order to achieve homogeneous dispersion of MWCNTs in the mixing water, an aqueous surfactant solution and sonication were employed. After sonication, Portland cement was added to MWCNT suspension and mixed in Hobart mixer with the W/C ratio of 0.3. The results showed that the flexural strength of short 0.08 wt% MWCNTs and long 0.048 wt% MWCNTs nanocomposites increased by about 37% and 25% respectively compared to plain cement paste as well as the Young's modulus of both nanocomposites increased by about 35% and 24% respectively.

Hu *et al*. (2014) investigated the influence of carbon nanotube on the fracture toughness of cement-nanocomposites at 28 days. Common MWCNTs and carboxyl group (MWCNTs-COOH) were used and the content of each one was 0.05 and 0.1 wt% of cement. In order to achieve better dispersion of MWCNTs or MWCNTs-COOH, each one was dispersed in water using solution containing Sodium Dodecyl Sulfate (SDS) as surfactant, Gum Arabic Powder (GAP) and Polyethylene glycol (PEG400) after that aqueous solution was subjected to sonication. Later during mixing, superplasticizer and antifoaming agent were used too. Table 2.11 shows the summary of the results. These authors reported that fracture toughness rather than compressive strength of MWCNTs-cement composites

improved significantly, and MWCNTs-COOH could improve the fracture, compression and physical properties of the nanocomposite better than common MWCNTs. In 0.1 wt% MWCNTs-COOH nanocomposites, the fracture toughness and fracture energy increased by 19.2% and 42.9% respectively over the control composite whereas in 0.1 wt% MWCNTs nanocomposites, their values increased by 11.4% and 26.2% respectively.

Table 2.11: Test results of the MWCNT-cement specimens (Hu *et al.*, 2014).

Mixture	%CNTs	Compressive strength (MPa)	Fracture toughness ($MPa.m^{1/2}$)	Fracture energy (N/m)	Porosity (%)
JJ00	0	96.0	0.510	59.5	21.66
JJ50	0.05	96.5	0.542	72.3	-
JJ10	0.1	93.8	0.558	75.5	24.84
CO05	0.05	101.1	0.545	72.9	-
CO10	0.1	100.8	0.608	85.0	15.70

JJ00 is control cement paste, JJ50 and JJ10 represent for MWCNTs-cemen composites, CO05 and CO10 for (MWCNTs-COOH)-cement composites.

Xu *et al.* (2015) studied the mechanical properties and microstructure of MWCNTs-reinforced cement paste at 28 days. Content of MWCNTs was 0.025, 0.05, 0.1 and 0.2 wt% of cement. In that study, MWCNTs dispersed in water by using surfactant solution (TNWDIS) and sonication followed by centrifugation after that MWCNTs were stored stably for over three months. Preparation of the specimens was done as follows; MWCNTs dispersion and water were first mixed in mixer followed by cement as well as W/C ratio was 0.33. These authors reported that when the content of MWCNTs increased the compressive and flexural strength increased and also the porosity decreased (Table 2.12). They stated that the proposed technique for dispersing MWCNTs in water was efficient in terms of improvement in strengths.

Table 2.12: Mechanical and physical properties of nanocomposites at 28 days (Xu *et al.*, 2015).

Sample	MWCNT content (wt%)	Compressive strength (MPa)	Flexural strength (MPa)	Porosity (%)
C0	0	84.8	4.0	21.95
C1	0.025	90.1	4.3	21.62
C2	0.05	95.6	4.6	-
C3	0.1	97.2	5.2	21.10
C4	0.2	-	5.6	20.96

Parveen *et al*. (2015) studied the microstructure and mechanical properties of carbon nanotube reinforced cement mortar developed using Pluronic F-127 as a new dispersion technique. The team obtained CNT aqueous suspensions by mixing and stirring CNTs, 3 vol% Pluronic F-127 surfactant and defoaming agent in water for 10 minutes followed by sonication and centrifuge. Four types of carbon nanotubes were used; SWNT, MWNT, f-SWNT (functionalized SWNT) and f-MWNT (functionalized MWCNT) an also the loadings of each types was 0.08 and 0.1 wt% of cement. The researchers reported that addition of 0.1 wt% SWNT improved flexural and compressive strengths of mortar by 7% and 19% respectively over control mortar at 28 days. Flexural and compressive strengths with 0.08 wt% f-SWNT increased with the hydration period up to 17% and 23% after 56 days. They concluded that Pluronic F-127 surfactant can be successfully employed to disperse carbon nanotubes in cement matrix.

Zou *et al*. (2015) studied the effect of ultrasonication energy (UE in unit J/mL) on mechanical properties of carbon nanotube-cement pastes at 28 days. Multi-walled carbon nanotubes functionalized with COOH groups (CNT) were used with two contents of 0.038 and 0.075 wt% by cement weight. CNT suspensions were prepared by using polycarboxylate Superplasticizer and subjected to five ultra-sonication energy (UE of 25,

75, 150, 250 and 400 J/mL). As shown in Table 2.13, for the nanocomposite containing 0.038 wt% CNT (CNT-1 mix), it was clearly shown that the mixture with a UE of 75 J/mL exhibited the best mechanical performance of all five mixes with UEs from 25 J/mL to 400 J/mL. Moreover, for the nanocomposite containing 0.075 wt% CNT (CNT-2 mix), the mixture with a UE of 150 J/mL indicated the highest mechanical improvement in Young's modulus, flexural strength and fracture energy compared to all other samples. These authors recommended that an optimal UE for achieving good mechanical properties of CNT cement nanocomposites could be 50 J/mL per unit CNTs to suspensions weight ratio.

Table 2.13: Effect of UE on Young's modulus (E), flexural strength (σ_f), and fracture energy (G_F) of reference cement paste (R) and nanocomposites (Zou *et al.*, 2015).

Mix	CNT content (wt%)	UE (J/mL)	E (GPa)	σ_f (MPa)	G_F (N/m)
R	0	0	16.36	4.11	7.28
CNT-1	0.038	25	17.14	4.55	8.39
CNT-1	0.038	75	18.67	5.15	9.75
CNT-1	0.038	150	18.52	5.13	9.54
CNT-1	0.038	250	18.39	4.91	9.04
CNT-1	0.038	400	18.28	4.81	8.78
CNT-2	0.075	25	17.12	4.43	8.38
CNT-2	0.075	75	19.82	5.43	10.26
CNT-2	0.075	150	21.52	6.16	11.83
CNT-2	0.075	250	21.29	6.11	11.29
CNT-2	0.075	400	20.84	5.68	10.84

2.4.2.1.5 Effect of nano-TiO_2

Nano-TiO_2 is gaining consideration to be used in concrete. The main application of nano-TiO_2 in concrete relates to its photocatalytic capacity that including self-cleaning, air-cleaning (air pollution reduction) and anti-bacterial (Mamulova Kutlakova *et al.*, 2011,

Pacheco-Torgal and Jalali, 2011b, Matějka *et al.*, 2012, Meng *et al.*, 2012, Hanus and Harris, 2013) . When nano-TiO_2 is used in concrete, photocatalytic process can help to decompose organic materials (such as grime and oil), biological materials (such as fungi and bacteria) and pollutants (such as volatile organic compounds (VOCs) and tobacco smoke) (Sanchez and Sobolev, 2010, Mendes *et al.*, 2015). Nano-TiO_2 can be amorphous or crystalline phase (Li *et al.*, 2006a, Nazari and Riahi, 2011c). However, a few studies have shown that nano-TiO_2 can speed up the rate of hydration reaction and also enhance compressive strength and flexural strength of concrete (Li *et al.*, 2007b, Zhang and Li, 2011, Chen *et al.*, 2012).

Nazari (2010) investigated the flexural strength of concrete incorporating with nano-TiO_2 at 7, 28 and 90 days. TiO_2 nanoparticle was in the amorphous phase with average size of 15 nm that means TiO_2 nanoparticle has pozzolanic actively effect. Portland cement was replaced by 0.5, 1, 1.5 and 2 wt% of nano-TiO_2. It was found that the optimal level of TiO_2 nanoparticle was 1 wt% at all ages. These authors reported that at age of 90 days the flexural strength of nanocomposite containing 1 wt% nano-TiO_2 increased from 4.7 to 6.0 MPa by about 27% when compared to control concrete due to filler and pozzolanic effects of TiO_2 nanoparticles.

Chen *et al*. (2012) studied the effect of two types of nano-TiO_2 on the hydration and mechanical propertied mortars at 3, 7 and 28 days. The two types of TiO_2 nanoparticles were P25 (75% anatase and 25% rutile) and Anatase (99% anatase) and also both were in the crystalline phase that means TiO_2 nanoparticles are not a pozzolanic material. Portland cement was replaced by 5 and 10 wt% of each types of nano-TiO_2. The results showed that the porosity (%) of nanocomposites decreased with increased content of P25 or Anatase nano-TiO_2. These authors reported that the improvement of pore structure and could only be attributed to the micro-filling effect of TiO_2 nanoparticles. The compressive strengths of reference mortar and nanocomposites are shown in Figure 2.35. It was found that the compressive strength of the nanocomposites was significantly improved at all ages due to the addition of nano-TiO_2. For example nanocomposite containing 10 wt% of P25 nano-TiO_2 increased by 25% and 11% compared to reference mortar and nanocomposite containing 10 wt % of Anatase nano-TiO_2 respectively.

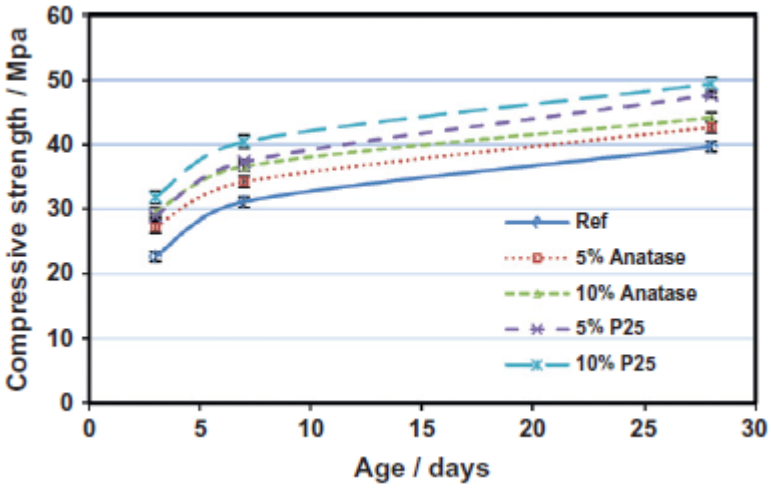

Figure 2.35: Compressive strengths of reference mortar and nanocomposites (Chen *et al.*, 2012).

2.4.2.2 Thermal properties of Cement Nanocomposites

The thermal properties of nanocomposites are intrinsic properties that determine their energy performance and provide information about the structure-property relationship of these materials. The thermal properties often include thermal stability, conductivity, resistance, extension and specific heat capacity (Shaikh and Supit, 2014, Singh *et al.*, 2015). In last decade, lots of studies in cement-nanocomposites have focused on the thermal analysis and thermal stability by using several methods such as thermogravimetric analysis (TGA), differential thermal (DTA) derivative thermogravimetry (DTG) and differential scanning calorimetry (DSC) (Chaipanich *et al.*, 2010, Xu *et al.*, 2011, Heikal *et al.*, 2013).

The measurement of weight loss of the material as a function of temperature under selected atmosphere in each stage can be obtained using TGA. In DTA, the heat changes

within a material are monitored by measuring the difference in temperature between the sample and the inert reference. This differential temperature is then plotted against temperature to get DTA curve. DSC measures the heat flow rate associated with a thermal event as a function of temperature. In DTG method, a DTG curve presents the rate of mass change (*dm*/*dt*) as a function of temperature or time against temperature (Aly *et al.*, 2012, Li *et al.*, 2015b).

Singh *et al*. (2011) studied the effect of nano-SiO_2 on the thermal stability of cement paste at 28 days. Portland cement was replaced by 5 wt% of nano-SiO_2 and also 5 wt% of silica fume was used for comparison. TGA curves of samples (Figure 2.36) showed three stages of decomposition; weight loss up to 200°C due to surface water desorption as well as loss of water from C-S-H gel layer and from the dehydration of ettringite, after that the weight loss about 450-500°C is due to the thermal decomposition of $Ca(OH)_2$ followed by the third decomposition between 670-780°C due to carbonated phases and calcite. It was found that at all stages the weight loss (%) of cement paste containing 5 wt% of nano-SiO_2 was lower than cement paste and cement paste containing 5 wt% of silica fume. These authors reported that the small size and pozzolanic reactivity of nano-SiO_2 led to improving the microstructure of cement-nanocomposites as a result of this cement paste containing 5 wt% of nano-SiO_2 showed better thermal stability than others.

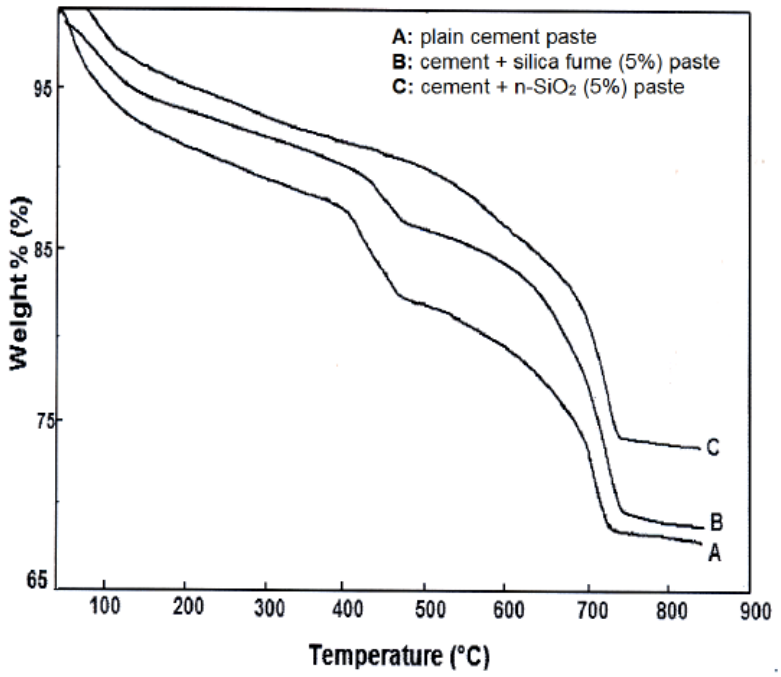

Figure 2.36: TGA curves of samples (Singh *et al.*, 2011).

Chen *et al*. (2012) investigated the thermal stability of cement composites containing 10 wt% of TiO_2 nanoparticles called P25 (75% anatase and 25% rutile) at age of 3, 7 and 28 days. As shown in Figure 2.37 (a & b), it was found that weight loss (%) of cement paste containing 10 wt% of nano-TiO_2 was less than control cement paste. The team reported that the addition of nano-TiO_2 accelerated the hydration reactions at the early ages and improved the microstructure through filler effect and thus the thermal stability of nanocomposites was enhanced.

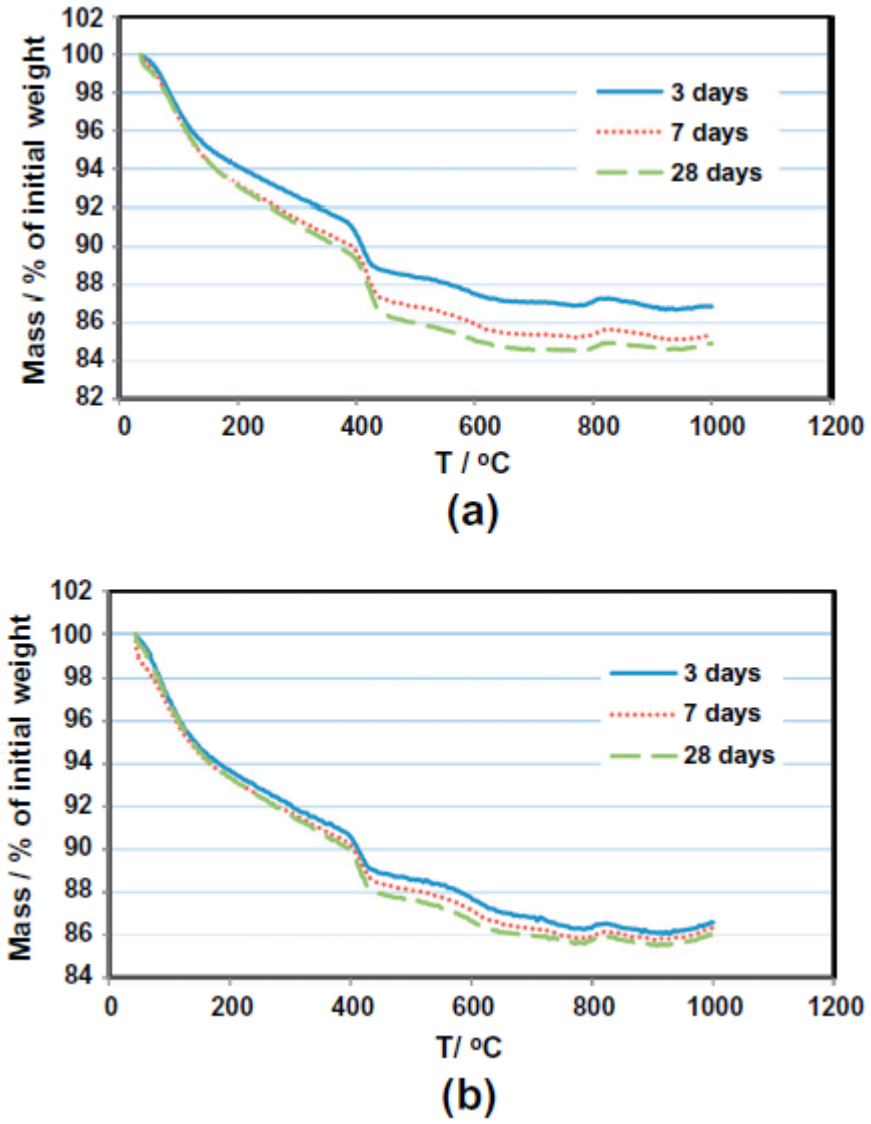

Figure 2.37: TGA curve of; (a) control cement paste and (b) 10 wt% nano-TiO_2 cement paste (Chen *et al.*, 2012).

Rong *et al*. (2015) investigated the influence of nano-SiO_2 particles on the thermal properties of ultra-high performance cementitious composites (containing 33 wt% of fly ash). Portland cement was replaced by 1, 2, 3 and 5 wt% nano-SiO_2 and it was found that the optimum content of nano-SiO_2 was 3 wt% in which nanocomposites (NS3) containing

3 wt% nano-SiO_2 exhibited better mechanical results than others. The thermal stability was investigated by using TGA (TG) and DSC techniques. Figure 2.38 shows the TGA (TG) and DSC results of control cement composite (N0) and NS3 at the curing times of 7 days. The authors found that the peak height (at about 421°C in DSC curves) of the hydrated $Ca(OH)_2$ in NS3 was lower than that in N0. That indicated that the amount of $Ca(OH)_2$ in the sample reduced with the addition of nano-SiO_2. Moreover, the reduction of mass loss value in the temperature interval of 400–500°C implied the consumption of $Ca(OH)_2$ due to the high pozzolanic activity of SiO_2 nanoparticles. The team concluded that addition of SiO_2 nanoparticles improved the thermal stability of nanocomposites.

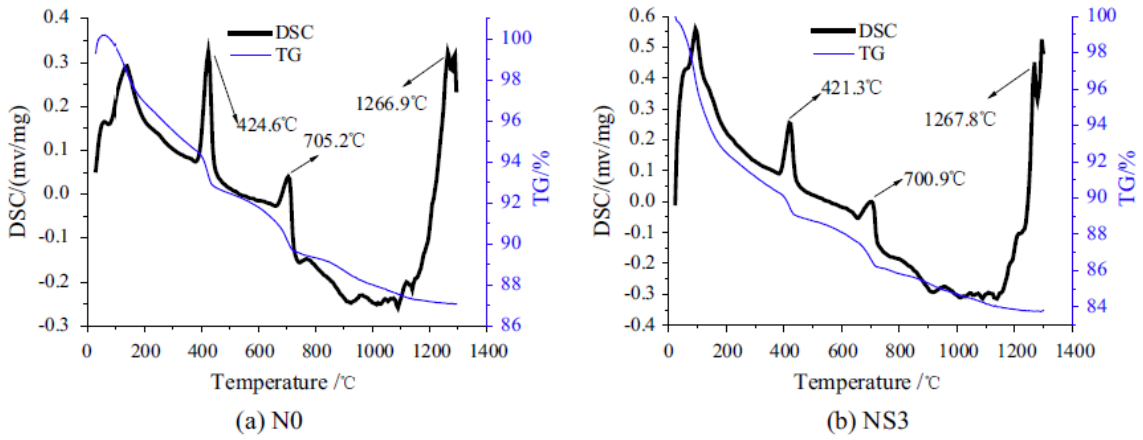

Figure 2.38: TG/DSC results of: (a) control cement composite (N0) and (b) NS3 at the curing times of 7 days (Rong *et al.*, 2015).

Abdel Aleem *et al.* (2014) studied the thermal expansion of cement containing nano-silica at 28 days. The Portland cement was replaced by 1, 2, 3, 4 and 5wt% nano-silica and it was found that the optimum content of nano-silica (NS) was 3 wt% in which nanocomposites (NS3) containing 3 wt% nano-silica exhibited better mechanical results than others. Figure 2.39 shows the thermal expansion coefficient (10^{-6}/K) of cement paste and nanocomposites at 28 days. It was noticed that replacing Portland cement with nano-silica was shown to be efficient for mitigating the thermal expansion coefficient of

cement paste. The nanocomposites containing 2 wt% of nano-silica exhibited lower thermal expansion coefficient than other samples up to 100°C. These authors reported that nano-silica reduced the thermal expansion of cement nanocomposite due to the highly pozzolanic activity of nano-silica to react with of $Ca(OH)_2$, producing the amorphous CSH gel.

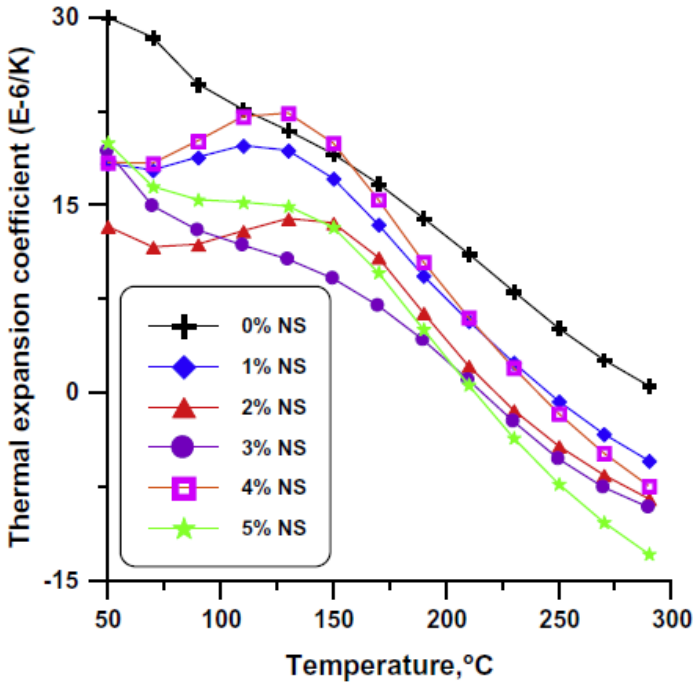

Figure 2.39: Thermal expansion coefficients of cement paste and nanocomposites at 28 days (Abdel Aleem *et al.*, 2014).

2.5 Cement Nanoclay Nanocomposites

2.5.1 Introduction

Nanoclay platelets are clay minerals heightened for use in clay nanocomposites. Nanoclay is a broad class of naturally occurring inorganic minerals, but montmorillonite platelets is the most commonly used in polymer materials applications. In last two decades, polymer-

nanoclay nanocomposites have received much attention in both manufacturing and applications (Hussain *et al.*, 2006, Alhuthali *et al.*, 2012). Polymer-nanoclay nanocomposites have superior physical, mechanical and thermal properties. Several studied have been carried out to investigate the effect of nanoclay addition in the improvement of physical, mechanical and thermal properties of several types of polymer matrices such as polythylene, epoxy, polypropylene, etc. (Alamri *et al.*, 2012). On the other hand, few studies have been carried out on using nanoclay in construction and building materials. Nanoclay is a new processed clay for a wide range of high-performance cement nanocomposite (Chang *et al.*, 2007, Morsy and Aglan, 2007, He and Shi, 2008, Sanchez and Sobolev, 2010, Rashad, 2013, Wei and Meyer, 2014c). As a kind of nano-pozzolanic material, nanoclay not only reduces the pore size and porosity of the cement matrix, but also improves the mechanical and thermal properties of cement nanoclay nanocomposites (Morsy *et al.*, 2009, Farzadnia *et al.*, 2013, Quanji *et al.*, 2014).

2.5.2 Structure of Clay

Clay mineral is hydrous magnesium and aluminium phyllosilicates with small amounts of calcium, sodium, iron or other alkali metals. Chemically, it is layered structure that contains two types of sheets which are tetrahedral or octahedral (Choudalakis and Gotsis, 2009, Kiliaris and Papaspyrides, 2010). These sheets can arrange in two crystal structures; 1:1 or 2:1 form. The 1:1 clay structure can comprise one aluminum octahedron sheet and one silicon tetrahedron sheet. The 2:1 clay structure can consist of an aluminum oxide octahedron sandwiched between two layers of silicon dioxide tetrahedron. The silicate layers in the 2:1 layered structures that are drawn towards each other by the Van de Waals forces .The thickness of each layered sheet is approximately 1 nm whereas the lateral dimensions can range from 30 to 200 nm or even more (Hussain *et al.*, 2006, Kuo *et al.*, 2006, Jo *et al.*, 2008, Pavlidou and Papaspyrides, 2008). An example of 1:1 structure would be kaolin group that includes the minerals such as kaolinite, halloysite, dickite and nacrite. An example of 2:1 structure would be smectite group (such as montmorillonite, hectorite and saponite mineral), illite group (such as illite mineral) and vermiculite group (such as vermiculite mineral) (Hussain *et al.*, 2006, Choudalakis and Gotsis, 2009).

Montmorillonite clay is one of the widespread layered silicates being investigated for its properties (Thostenson *et al.*, 2005, Kuo et al., 2006). It has 2:1 layered silicates structure as shown in Figure 2.40 (Hussain *et al.*, 2006, Jo *et al.*, 2008). Montmorillonite is used widely in polymer matrix due to its high surface area (750 m^2/g), aspect ratio (ranging 10-1000) and surface reactivity (Sinha Ray and Okamoto, 2003, Kiliaris and Papaspyrides, 2010). Consequently, small amounts of montmorillonite clay have extremely high surface areas that can be effectively utilized for interaction with matrix and thus fill the micro-pores and also especially in cement matrix react with free lime through pozzolanic reaction to produce additional C–S–H gel (Chang *et al.*, 2007, Morsy and Aglan, 2007, Wei and Meyer, 2014c).

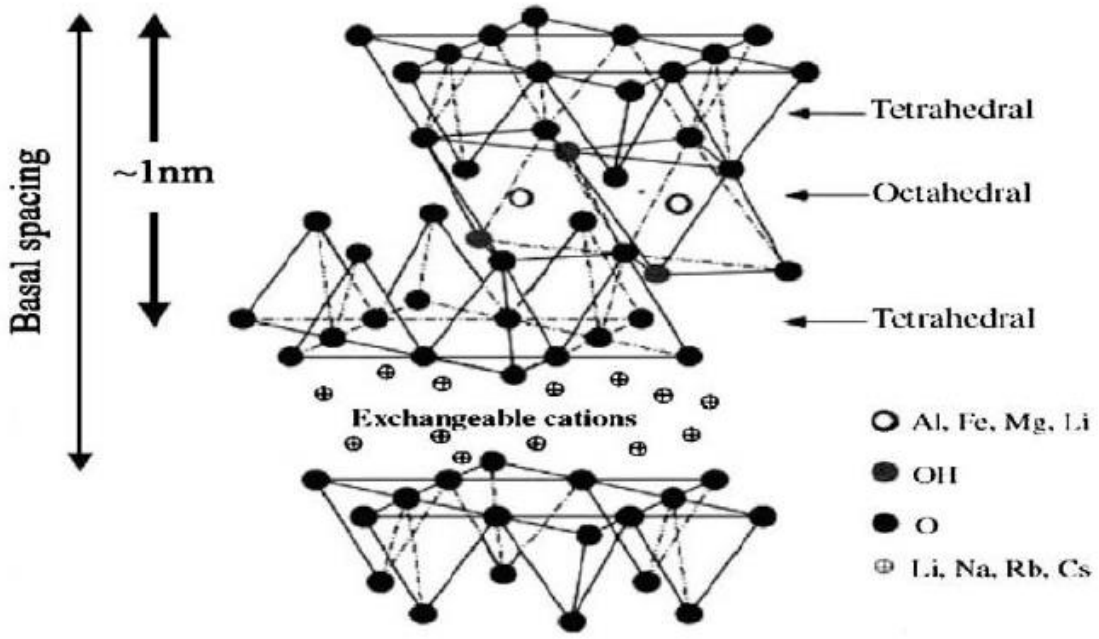

Figure 2.40: 2:1 layered silicates structure of montmorillonite (Hussain *et al.*, 2006)

2.5.3 Synthesis of Cement-Clay Nanocomposites

Nanoclay platelets, i.e. layered silicates, could be used in cement/clay nanocomposites as filler or pozzolanic materials or both due to their extremely high surface area ratio. There are different types of commercial nanoclay platelets. Some of them are chemically synthesized without modification such as nano- montmorillonite and nano-kaolin and others are called organoclay which are chemically synthesized with organically modification such as Cloisite 30B nanoclay (natural montmorillonite modified with an organic quaternary ammonium salt) (Chang *et al.*, 2007, Morsy and Aglan, 2007). The good dispersion of nanomaterials i.e. nanoclay into cement matrix (cement paste, mortar and concrete) is the critical factor in the synthesis of cement nanocomposites. Many different methods are available for the synthesis of cement-nanoclay nanocomposites. For the actual synthesis of cement-nanocomposites, three methods are popularly used: (i) binder dry mixing, (ii) colloidal nanoparticles mixing and (iii) sonication and dispersing agent mixing (Chang *et al.*, 2007, Wei and Meyer, 2014c, Yim *et al.*, 2014).

2.5.3.1 Dry mixing method of the binder

This method is widely used for nanoparticle powders in cement nanocomposite. Portland cement powder is replaced with different content of nanoclay powder and then cement and nanoclay powders are weighed. In the case of cement paste nanocomposites, the cement and nanoclay powders are mixed in concrete mixer (Hobart mixer) for several minutes, in which these powders are considered as binder as shown in Table 2.14 (Morsy and Aglan, 2007). The water/binder ratio in this method is used instead of water/cement ratio. In the case of using high contents of nanoclay, additional water and superplasticizer are required. If supplementary materials (such as silica fume) are used, there are two approaches. First approach, the amount of their replacements from total Portland cement powder previously are determined after that the rest of Portland cement powder is replaced with different content of nanoclay powder as shown in Table 2.15 (Farzadnia *et al.*, 2013). The second approach, the amount of their replacements from total Portland cement powder previously are determined after that the supplementary material powder is replaced with different content of nanoclay powder as shown in Table 2.16 (Wei and Meyer, 2014c). All raw

materials (binder and supplementary materials) are dry mixtures. Finally cement paste (or blended) nanocomposites are prepared by adding certain water amount and superplasticizer to dry mixture in concrete mixer then wet mixed for several minutes. Regarding mortar or concrete nanocomposites, binder/sand or cement/sand ratio is used and raw materials including sand or aggregates are dry mixture followed by adding water for wet mixed.

Table 2.14: The dry mixes composition of blended binder for cement pastes (mass%) (Morsy and Aglan, 2007)

Mixes	PWC	NC
C0	100	0
C1	98	2
C2	97	3
C3	96	4

NC is Cloisite 30B nanoclay and PWC is Portland white cement

Table 2.15: The dry mixes of blended cement (mass%) (Farzadnia *et al.*, 2013)

Mixed	OPC	SF	Nanoclay
Control	95	5	-
NC1	94	5	1
NC2	93	5	2
NC3	92	5	3

Nanoclay (NC) is Halloysite nanoclay, SF is silica fume, OPC is Portland cement

Water/binder was 0.45, cement to sand ratio was 1:2.75

Table 2.16: Composition of blended cement mortars (Wei and Meyer, 2014c)				
Index	Content (wt%)			
	PC	MK	NC	Superplasticizer
PC	100	0	0	0
B10-1	90	10	0	1.5
B10-2	90	9	1	1.5
B30-1	70	29	1	2.0
B30-2	70	27	3	2.0
B50-1	50	49	1	3.0
B50-2	50	47	3	3.0
B50-3	50	45	5	3.0
NC is nanoclay, MK is metakaolin, PC is Portland cement Water/binder was 0.4, binder to sand ratio was 1:1				

2.5.3.2 Colloidal (liquid) nanoparticles mixing method

In this method, nanoparticles i.e. nanoclay are in an aqueous form. Depending on company supplier (synthesis technique), the solid content of nanoparticles or concentration (wt%) in suspension (aqueous solution) can vary in between 15-50 wt% and the average particle sizes can vary from 5-500 nm (Ghasemi *et al.*, 2010, Aly *et al.*, 2012, Singh *et al.*, 2015). The content of colloidal nanoparticles is usually calculated with respect to the weight of cement powder or cementitious materials. In practice, the liquid form (colloid) of nanoclay can facilitate a homogeneous dispersion of nanoclay or any other nanoparticles in cement nanocomposites (Chang *et al.*, 2007, Hou *et al.*, 2013). Water/cement ratio is used and sometimes additions of water and superplasticizer are required. In preparation procedure for cement paste, mortar and concrete, water and colloidal nanoparticles can be mixed and stirred then raw materials are added or raw materials and water are wet mixed in concrete mixer then colloidal nanoparticles are added (Aly *et al.*, 2012). Chang *et al*. (2007) carried out an experiment using nano-montmorillonite (NM) in aqueous form; NM was platy shape with dimension of

100×100×0.1 nm. The contents of nano-montmorillonite in cement nanocomposite were 0.2, 0.4, 0.6 and 0.8 wt% by cement weight and water/cement ratio was 0.55. In that work, the results of mix proportions of cement nanocomposites are shown in Table 2.17.

Table 2.17: Mix proportions of cement nanocomposites (Chang *et al.*, 2007)

Designation	Cement: water: NM
C-00	1: 0.55: 0.000
C-02	1: 0.55: 0.002
C-04	1: 0.55: 0.004
C-06	1: 0.55: 0.006
C-08	1: 0.55: 0.008

2.5.3.3 Sonication and dispersing agent mixing method

Ultrasonic devices or sonication can help to disperse nanoclay into matrix. The dispersion processes of nanoclay such as Cloisite 30B by using sonication are interesting in polymer nanocomposites such as epoxy-nanoclay nanocomposites (Wang and Qin, 2007, Amiri *et al.*, 2009, Thelakkadan *et al.*, 2012). In this third method, suspensions or liquid form from nanoparticles i.e. nanoclay are made by using sonication or chemical dispersing agent or both. This method may help to improve the dispersion of nanomaterials in cement composites. The dispersing agents (surfactants) can be superplasticizer or other chemical agents or together. Some examples of dispersing agents include Polycarboxylate superplasticizer and Sodium Dodecyl Sulfate and Pluronic F-127 (Musso *et al.*, 2009, Parveen *et al.*, 2015). The period time of mixing under sonication, amplitude, frequency and energy power of sonication are important factors in dispersion processes (Zou *et al.*, 2015).

In this method, the Portland cement is replaced by one or more contents of nanoparticles i.e. nanoclay by weight (wt %) and measured. The dispersion processes of this method can

be carried out as follows; water and dispersing agents are mixed, stirring and sonicated if applicable for few minutes after that nanoparticle powders are added and then whole suspensions (aqueous solution) are subjected to sonication for few to several hours (Konsta-Gdoutos *et al.*, 2010, Xu *et al.*, 2015). For fabrication of cement nanocomposites, the raw materials including cement, water, sand or aggregates are wet mixed then nanoparticle suspensions (aqueous solution) are added to the mixture.

2.5.4 Properties of Cement-Clay Nanocomposites

As compared to the conventional composite materials, nanocomposites are more advantageous due to their enhanced properties of mechanical and thermal. In this section, a number of studies on cement-nanoclay nanocomposites have been investigated by various researchers.

2.5.4.1 Microstructure and mechanical properties

Chang *et al.* (2007) presented experimental study on the effect of nano-montmorillonite clay on microstructure and compressive strength of cement paste. Portland cement (PC) was partially substituted by nanoclay (NM) of 0.2, 0.4, 0.6 and 0.8 wt% by weight of PC and water/cement ratio was 0.55. The specimens were cured and tested at 7, 14, 28 and 56 days. The effect of nano-montmorillonite clay (NM) contents on compressive strength of control cement paste, cement nanocomposites are shown in Figure 2.41. It can be seen that 0.6 wt% NM was the best content in terms of the highest compressive strength of C-06 nanocomposites at all ages when compared to other samples. Its strength increased by 13.24 % compared to control cement paste. The same trend was found in the porosity improvement by mercury intrusion porosimetry (MIP) as shown in Figure 2.42. The porosity of cement nanocomposites containing 0.6 wt% NM decreased from 0.244 to 0.34 ml/g by 4.1% when compared to control cement composites. The authors reported that this improvement in compressive strength and porosity clearly indicated the effectiveness of nano-montmorillonite clay (NM) in consuming calcium hydroxide (CH), supporting pozzolanic reaction and filling the micro pores in the matrix. Thus the microstructure of cement nanocomposite was denser than the cement matrix, especially in the case of using 0.6 wt% NM, which was evident from its higher

compressive strength. The team also supported their report by XRD examination of the microstructure of control cement paste and 0.6 wt% NM cement nanocomposite as shown in Figure 2.43. It was found that the major intensities of $Ca(OH)_2$ phases in 0.6 wt% NM cement nanocomposite significantly when compared to control cement paste. The team concluded that the obvious consumption of $Ca(OH)_2$ phases was due to pozzolanic reaction that led to production of more CSH gel which thus improved the microstructure.

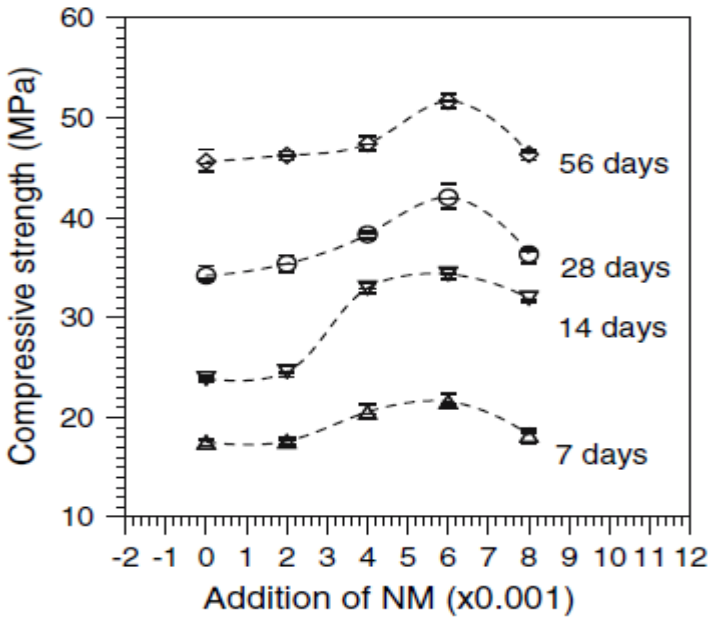

Figure 2.41: Compressive strength of control cement paste, cement nanocomposites are shown in (Chang *et al.*, 2007)

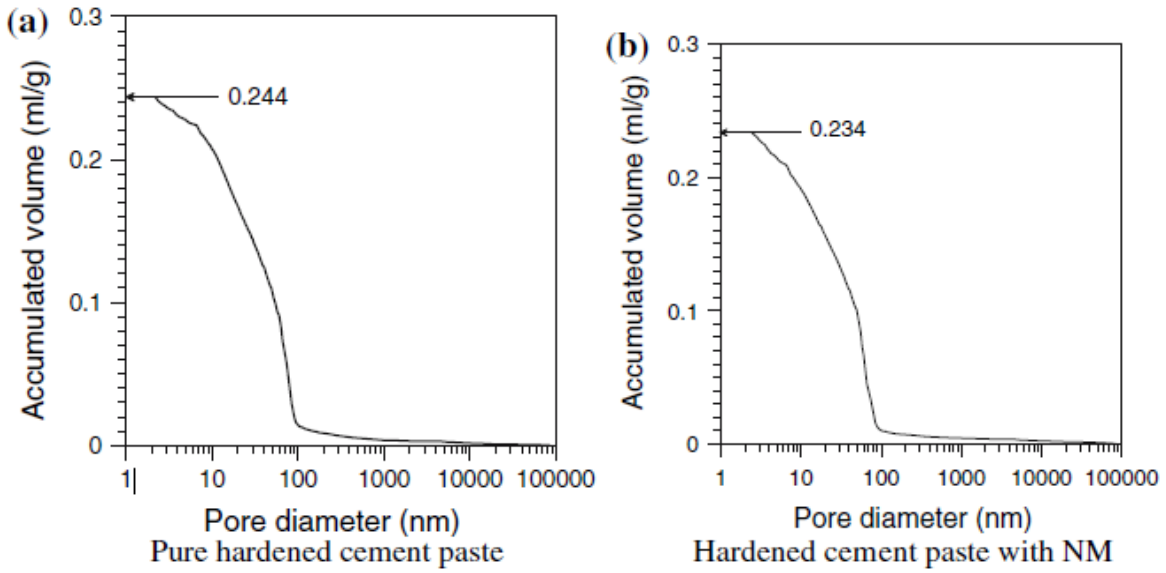

Figure 2.42: Porosity (MIP pore distribution) curves of: (a) control cement paste and 0.6 wt% NM nanocomposites (Chang *et al.*, 2007).

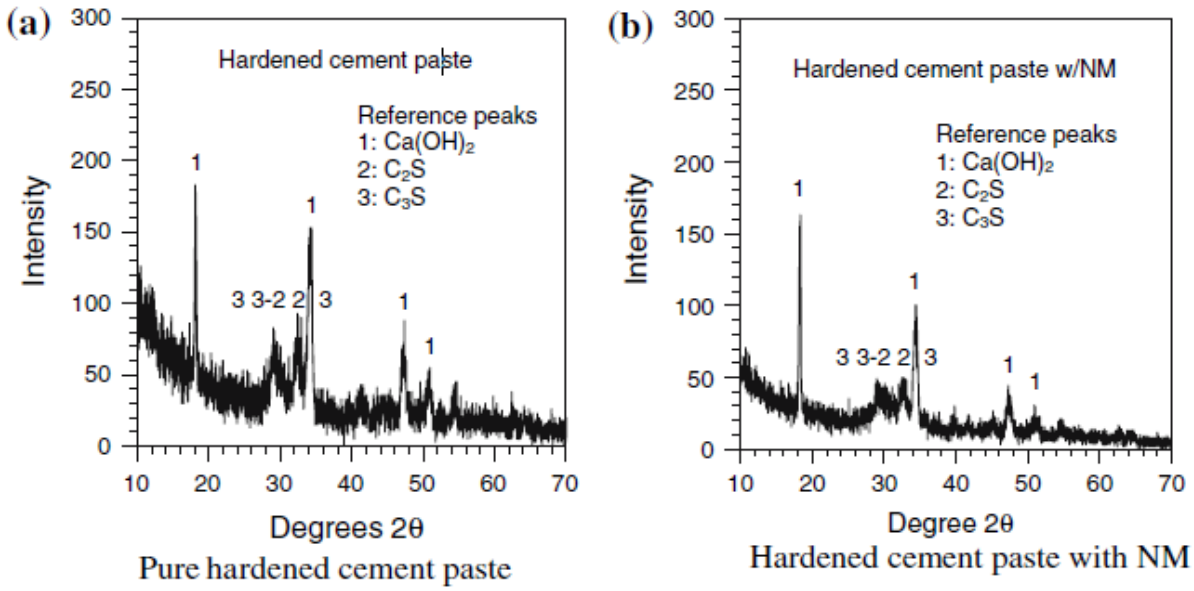

Figure 2.43: XRD patterns of: (a) control cement paste and 0.6 wt% NM nanocomposites (Chang *et al.*, 2007).

Farzadnia *et al.* (2013) studied the effect of halloysite nanoclay (NC) on mechanical properties and microstructure of cement mortars at 7 and 28 days. Portland cement was firstly partially replaced by 5 wt% of silica fume and then the rest of PC was replaced by 1, 2 and 3 wt% of halloysite nanotubes. Figure 2.44 shows the compressive strength of control composites and nanocomposites. It was found that the incorporation of 3 wt% nanoclay increased the compressive strength at 28 days up to 24% compared to the control samples. The authors reported that the enhancement of strength may be attributed to three mechanisms; pore-filler effect, pozzolanic reaction and cross- linking effect that led to denser microstructure than the control sample. As shown in Figure 2.45, halloysite nanotubes might have cross linked the cement hydrates because of their tubular shape which thus improved the potential of crack bridging in cement matrix by bridging the micro-cracks in the matrix.

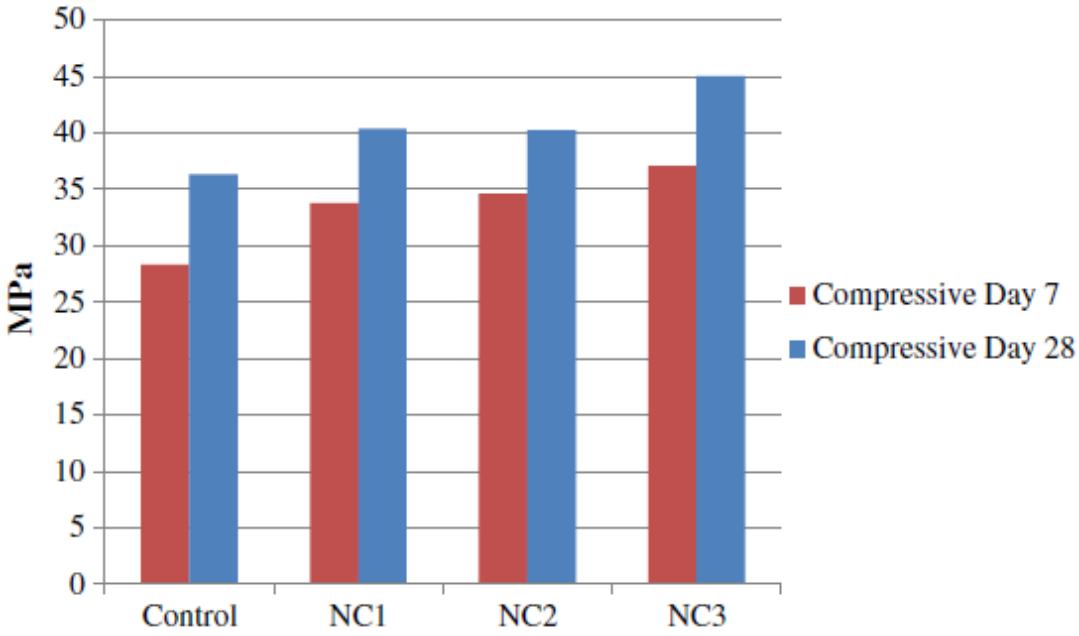

Figure 2.44: Compressive strengths of control composites and nanocomposites (Farzadnia *et al.*, 2013)

Figure 2.45: Cross-linking effect of halloysite nanotube clay in the cement matrix (Farzadnia *et al.*, 2013).

Wei and Meyer (2014c) studied the effect of partial replacement of Portland cement by blending of metakaolin and nanoclay on the microstructure and mechanical properties of cement mortar at different ages. Portland cement (PC) was firstly partially replaced by 10, 30 and 50 wt% of metakaolin (MK) and then each amount of MK was replaced by 1, 2 and 3 wt% of nanoclay (NC). The compressive strength of control mortar and nanocomposites are shown in Figure 2.46. The results showed that addition of NC obviously improved the strength of nanocomposites, and the highest strength at 28 days was achieved by B30-2 nanocomposites (70 wt% PC, 28 wt% MK, 2 wt% NC) that was about 18% increase compared to control mortar. Moreover, the strength of B30-1 nanocomposites (70 wt% PC, 29 wt% MK, 1 wt% NC) increased about 15% compared to control mortar. The authors indicated that this improvement reflected the enhancement in microstructure due to pozzolanic and filler effects. Figure2.47 shows the microstructures of control mortar (a) and B30-1 nanocomposites (b). It can be noticed that control mortar was rich in both ettringite and $Ca(OH)_2$ crystals (CH), while B30-1 nanocomposites had less ettringite and CH and more CSH gel that revealed the compactness of structure due to pozzolanic reactions.

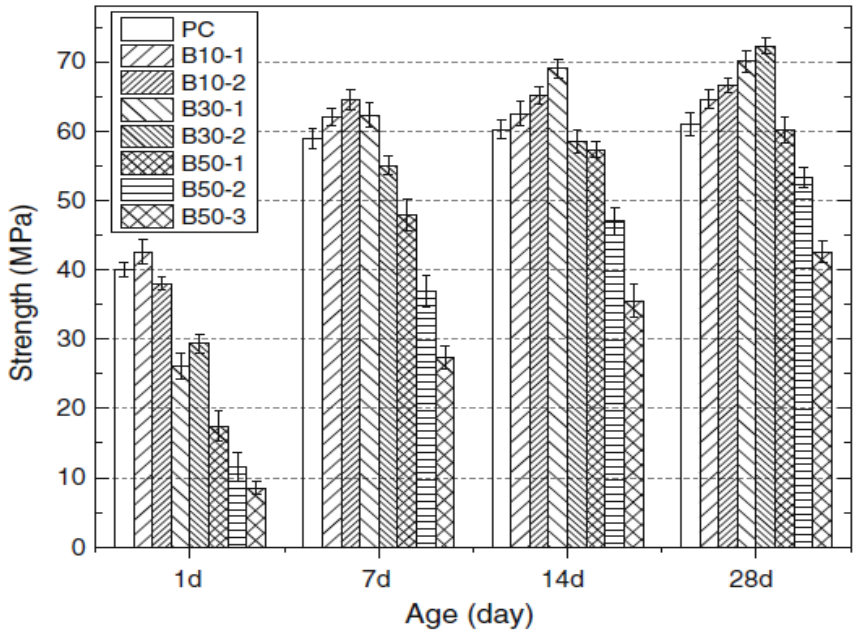

Figure 2.46: Compressive strengths of control mortar and nanocomposites (Wei and Meyer, 2014c).

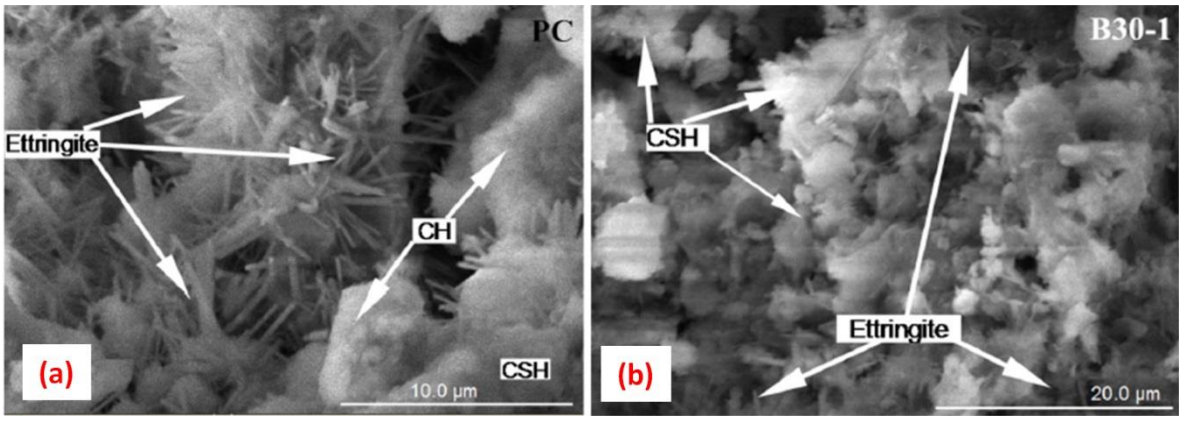

Figure 2.47: SEM micrographs of control mortar (a) and B30-1 nanocomposite (b) (Wei and Meyer, 2014c).

Morsy and Aglan (2007) investigated the effect of nanoclay (Cloisite 30B) on the indirect tensile strength of cement paste at 7 and 28 days. Portland white cement (PWC) was

partially replaced by 2 and 4 wt% (weight %) of nanoclay (NC). As shown in Figure 2.48, the indirect tensile strength of cement nanocomposites containing 2 wt% NC increased by 25% over cement paste at 28 days. The author reported that this improvement was due to filler and pozzolanic effects of NC. However, they stated that addition of more NC beyond the optimum content caused strength reduction due to the poor dispersion and agglomeration of NC.

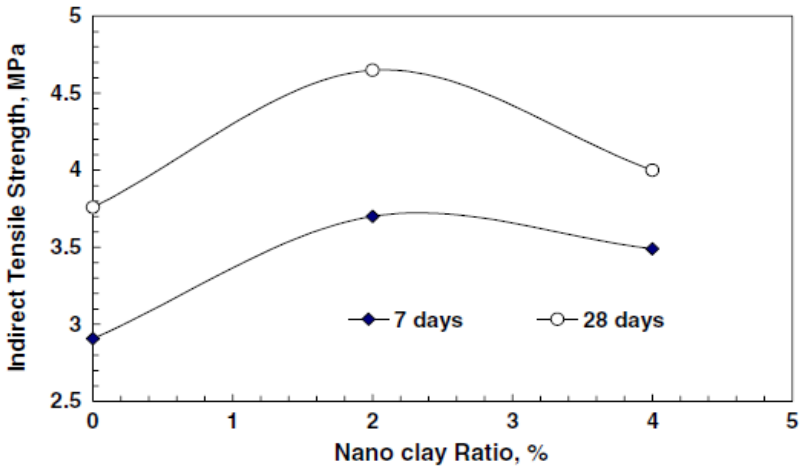

Figure 2.48: Indirect tensile strengths of cement paste and nanocomposites (Morsy and Aglan, 2007).

Hosseini *et al*. (2014a) studied the incorporation of nanoclay (Cloisite 15A) on the microstructure and compressive and flexural strength of cement composite at 7, 28 and 90 days. Portland cement (PC) was partially replaced by 1 wt% of nanoclay (NC) and the water/binder ratio was 0.4. As shown in Table 2.18, the compressive and flexural strength of 1 wt% NC-cement nanocomposite improved significantly at all ages over control composite due to the effective filler and pozzolanic influences of NC. The microstructurew of these samples are shown in Figure 2.49 (a-b). It was seen that the microstructure of control composite (Figure 2.49 a) displayed more CH crystals, Ettringite and pores whereas the microstructure of nanocomposite containing 1 wt% NC (Figure 2.49 b) had more CSH gel with less pores and CH crystals as well as NC sheets formed ordered arrays which introduced a microstructural uniformity in nanocomposite by a more stable bonding framework.

Table 2.18: Compressive and flexural strength of cement composite (C) and 1 wt% NC-cement nanocomposite (NCL) (Hosseini *et al.*, 2014a)					
Mix	Compressive strength (MPa)			Flexural strength (MPa)	
	7 days	28 days	90 days	7 days	28 days
C	39.2	50.1	58.6	5.6	7.0
NCL	44.7	56.4	63.7	6.5	9.1

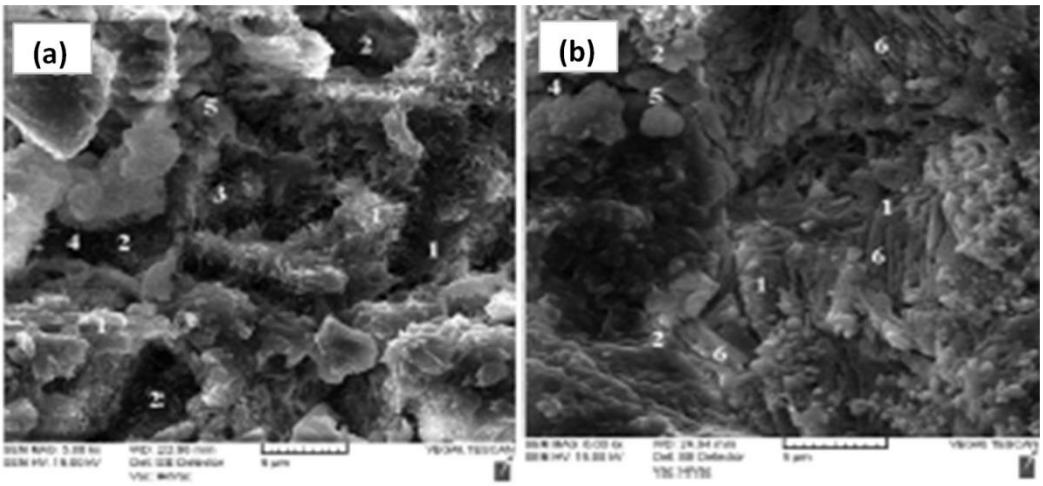

Figure 2.49: SEM micrographs of (a) cement composite and (b) 1 wt% NC-cement nanocomposite (NCL). 1 = CSH gel, 2 = $Ca(OH)_2$, 3 = Ettringite, 4 = pore, 5 = micro-cracks, and 6 = nano-clay sheets (Hosseini *et al.*, 2014a).

Aly *et al*. (2011a) studied the effect of nanoclay (Cloisite 30B) on mechanical properties of waste-glass powder (WGP) cement mortars at 28 days. Portland cement (PC) was partially replaced by 20 wt% of WGP and only 2.5 wt% of nanoclay (NC) and then this nanocomposite termed as NWGP20 while control composite without NC termed as WGP. The authors reported that the compressive and flexural strength of NWGP20 nanocomposite increased by 28% and 14% compared to control WGP mortar. They concluded that this improvement was attributed to pozzolanic and filler effects of NC.

2.5.4.2 Thermal properties

Nanoclay is widely used in polymer nanocomposites hence a lot of studies in literature demonstrated the effect of nanoclay on the thermal properties of polymer nanocomposites. In construction and building materials, nanoclay is still a new filler to be used in cement based composites. However, there are very few studies in literature that have presented the effect of nanoclay on the thermal properties of cement nanocomposites.

Shebl *et al.* (2009) investigated the effect of nanoclay (Cloisite 30B) on the thermal resistivity of cement paste at 7 days. Portland white cement was partially replaced by 2, 5 and 10 wt% of nanoclay (NC). It was found that the thermal resistivity of control cement paste and nanocomposite containing 2 , 5 and 10 wt% NC was 1.5, 1.5, 1.6 and 1.8 (m.K/W) respectively. They reported that addition of NC slightly improved the thermal resistivity of composites due to pozzolanic and its filler effects.

Wei and Meyer (2014c) studied the thermal stability of cement composites containing blending of metakaolin (10, 30 and 50 wt %) and nanoclay (1 and 2 wt %). Figure 2.50 shows TGA (DTG) curves of control (PC), B10-1 composites (90 wt% PC, 10 wt% MK), B30-1 nanocomposites (70 wt% PC, 29 wt% MK, 1 wt% NC) and B50-2 nanocomposites (50 wt% PC, 47 wt% MK, 3 wt% NC). It can be seen that three peaks due to thermal decomposition of ettringite (105° C), CSH gel (175° C) and CH (455° C) were found and the contents of CH and ettringite of PC were higher than those of the nanocomposites. The authors reported that the thermal stability of composites increased due to increase in NC content.

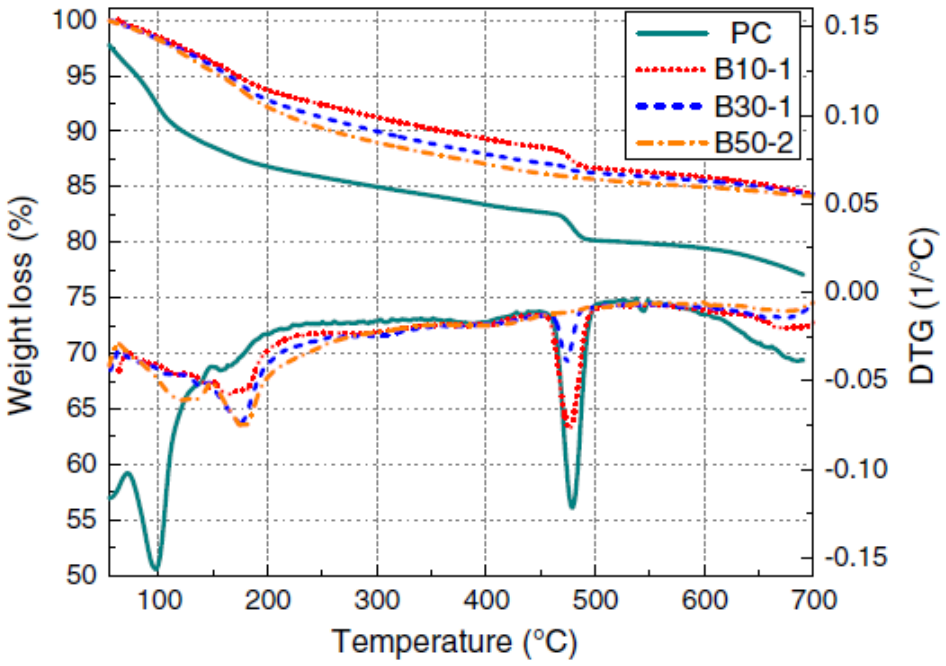

Figure 2.50: TGA (DTG) curves of control (PC), B10-1 composites, B30-1 nanocomposites and B50-2 nanocomposites at 28 days (Wei and Meyer, 2014c).

Aly *et al.* (2011a) compared the thermal stability of mortar containing (NWGP20) 2.5 wt% NC (Cloisite 30B) and 20 wt% waste-glass powder (WGP) with the same mortar (WGP20) without NC. Figure 2.51 shows the TGA (DTA) curves of control WGP20 mortar and NWGP20 nanocomposite at 28 days. The endothermic peaks at 110, 475 and 785° C were corresponding to the mass loss in CSH gel, de-hydration of CH and decomposition of calcium carbonate respectively. The authors reported that the increase in peak at110° C and reduction in peak at 475° C of NWGP20 nanocomposite due to pozzolanic reaction by NC that led to reduced CH amount and produce more CSH gel. They concluded that the thermal stability NWGP20 nanocomposite was better than control WGP20 mortar.

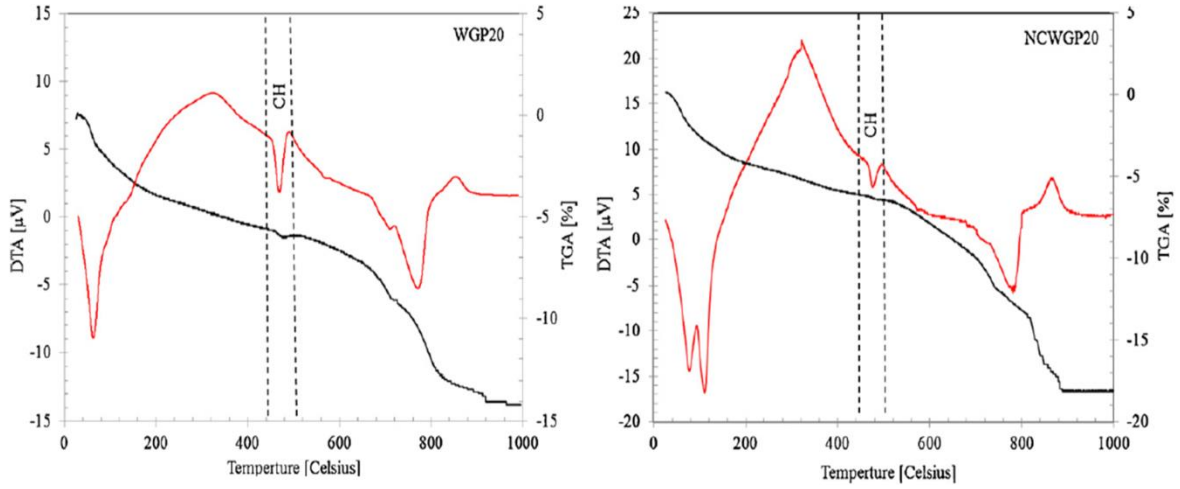

Figure 2.51: TGA (DTA) curves of control WGP20 mortar and NWGP20 nanocomposite at 28 days (Aly *et al.*, 2011a).

Farzadnia *et al.* (2013) studied the thermal stability of cement mortar containing 2 wt% halloysite nanoclay. Differential scanning calorimetry (DSC) was used and samples characterized at 28 days. As shown in Figure 2.52, the thermograms illustrated reduction of the peak area of CH phase and an increase of the peak area of CSH gel, C2ASH8 and C3ASH6 phases for nanocomposites when compared to control. The team reported that incorporation of NC into mortar improved the thermal stability at 28 days.

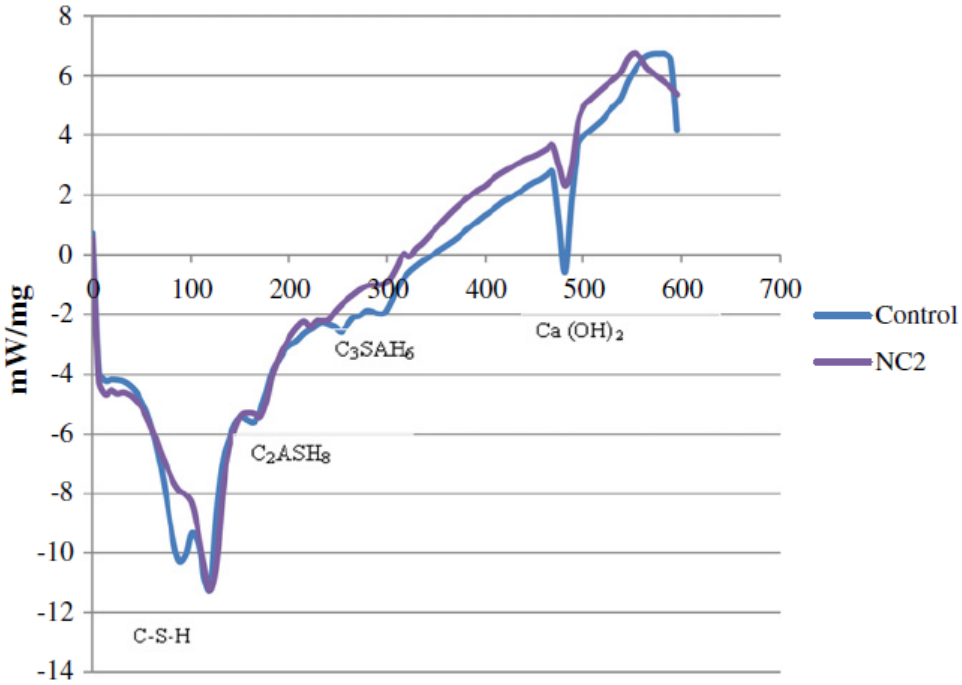

Figure 2.52: DSC of control mortar and NC2 nanocomposites (Farzadnia *et al.*, 2013)

2.6 Cement Calcined Nanoclay Nanocomposites

2.6.1 Introduction

In the last decade, nanoclay based on montmorillonite clay is gaining global interest to use in polymer nanocomposites. In construction and building materials, nanoclay is still a new filler to be used in cement based composites. The new calcined nanoclay could be more acceptable in use in concrete than using nanoclay itself (Shebl *et al.*, 2009). The calcined nanoclay can be prepared by the calcination of nanoclay in order to transform it from semi-crystalline to amorphous state (calcined nanoclay) with high pozzolanic reactivity (Morsy *et al.*, 2010). In this case, calcined nanoclay could be a good competitor to nano-silica or nano-SiO_2 and it can be potential candidate as new pozzolanic materials (Al-Salami *et al.*, 2013).

Historically, metakaolin (MK) is a popular type of calcined clay minerals and classified as one of supplementary cementitious materials. It has been used extensively in cement mortar and concrete due to its high pozzolanic activity (Sabir *et al.*, 2001, Barbhuiya *et al.*, 2015). It can be prepared by heating kaolin clay within the temperature range of 700–850°C (Fernandez *et al.*, 2011, Tironi *et al.*, 2013). Several studies have been carried out on the use of MK in concrete. It has been reported that the replacement of cement by 5–20% MK results in significant increase in compressive strength for high-performance concretes and mortars at 28 days (Siddique and Klaus, 2009, Juenger and Siddique, 2015).

On the other hand, montmorillonite clay is a very common clay mineral but its use in the cement and concrete industry is limited (Fernandez *et al.*, 2011, Garg and Skibsted, 2014). However, calcined montmorillonite clay can be alternative of comment pozzolanic materials (such as metakaolin) for cement and concrete due to its fairly good pozzolanic activity. Calcined montmorillonite clay is produced by heating montmorillonite clay within the temperature range of 800–930°C (He *et al.*, 1996, Garg and Skibsted, 2014). It was found that for the cement mortars with 30 wt% of Portland cement replaced by 830°C calcined montmorillonite at 28 days, compressive strength was 25% higher than control mortar (He *et al.*, 1996). Calcined montmorillonite clay could be potential candidate as a new supplementary cementitious material.

2.6.2 Microstructure and mechanical properties of Cement-Clay Nanocomposites

Recently, the calcined nanoclay is very new nanomaterials that can be employed in concrete. However, there are very few studies in literature that present the effect of calcined nanoclay on the microstructure and mechanical properties of cement composites. In polymer matrix there were few studies about calcined nanoclay (Abdel Gawad *et al.*, 2010, Botana *et al.*, 2010, Filippi *et al.*, 2011).

Morsy *et al.* (2010) studied effect of nano-metakaolin (NMK) on the microstructure and mechanical properties of cement mortar at 28 days. NMK was prepared by heating the nano-kaolin at 750°C for two hours. Ordinary Portland cement (OPC) was partially replaced by nano-metakaolin of 2, 4, 6 and 8 % by weight of OPC. Cement mortar was casted using cement/sand ratio of 1:2 and water/binder ratio was 0.5. As shown in Figure

2.53, the compressive strength of NMK nanocomposite was found to increase with the increase in NMK content from 2 to 8%. The similar trend was found for tensile strength in samples shown in Figure 2.54 where tensile strength increases with an increase in nanoclay contents. The authors reported that improved strength was due to filler effect of NMK to fill the voids in matrix as well as pozzolanic effect that increased CSH gel. The SEM micrographs for control and 10 wt% NMK mortar to support their argument are shown in Figure 2.55a-b. It was found that the microstructure of control mortar (Figure 2.55 a) displayed more CH crystals, Ettringite and pores whereas the microstructure of nanocomposite containing 10 wt% NMK (Figure 2.55 b) had more CSH gel with less pores and CH crystals. Thus indicating that microstructure of nanocomposite was denser and compact that control matrix.

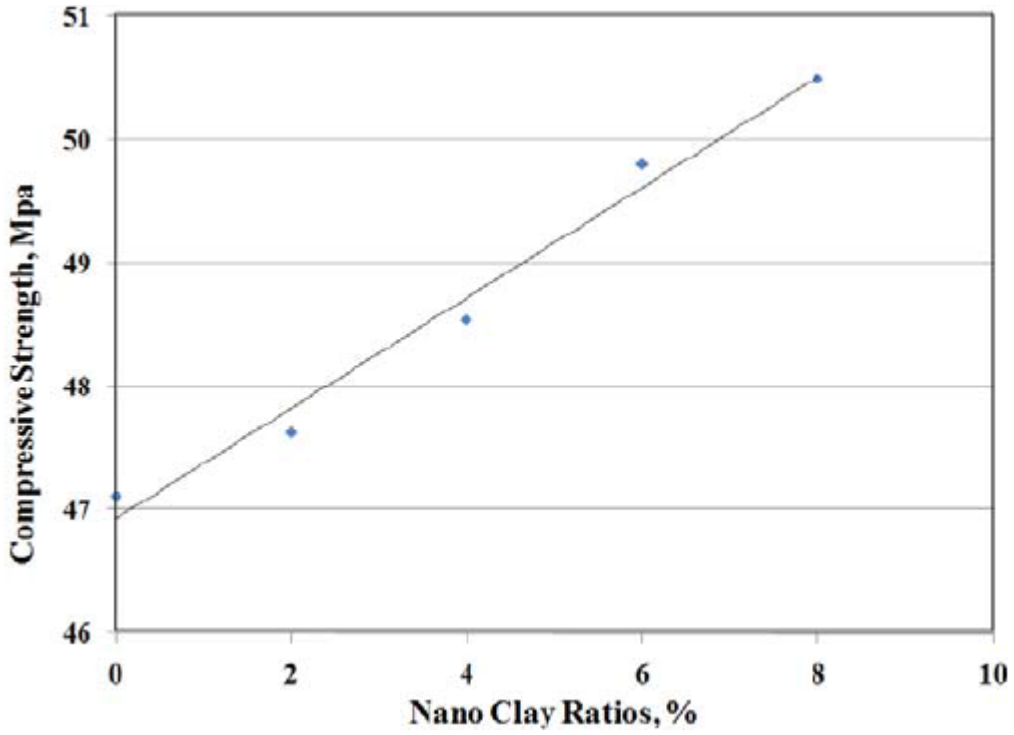

Figure 2.53: Compressive strengths of control mortar and NMK nanocomposites (Morsy *et al.*, 2010).

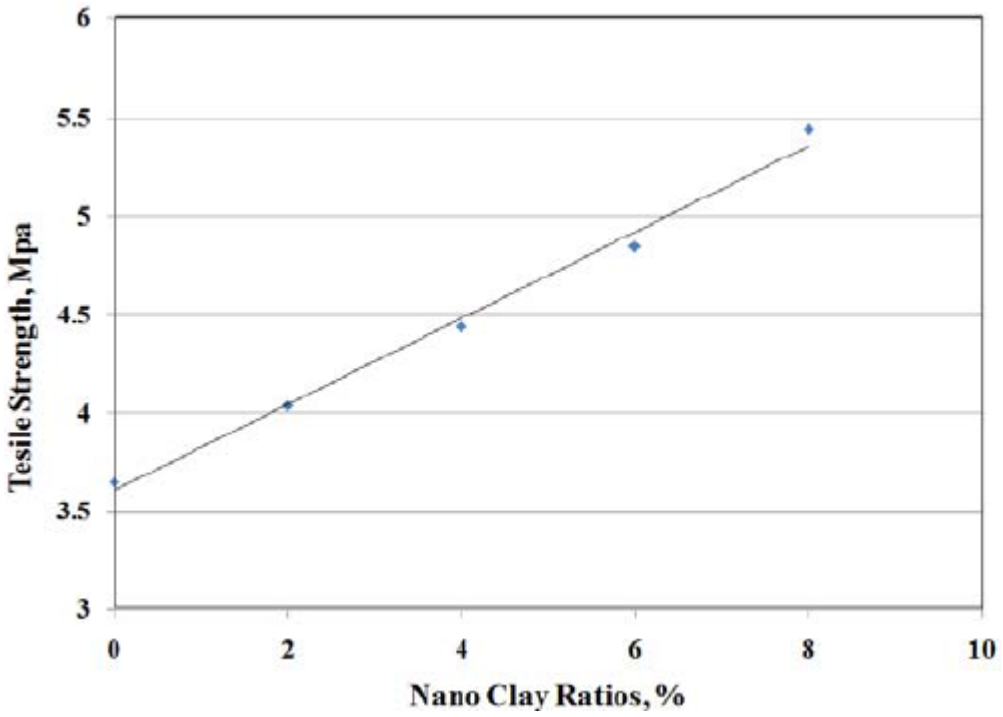

Figure 2.54: Tensile strengths of control mortar and NMK nanocomposites (Morsy *et al.*, 2010).

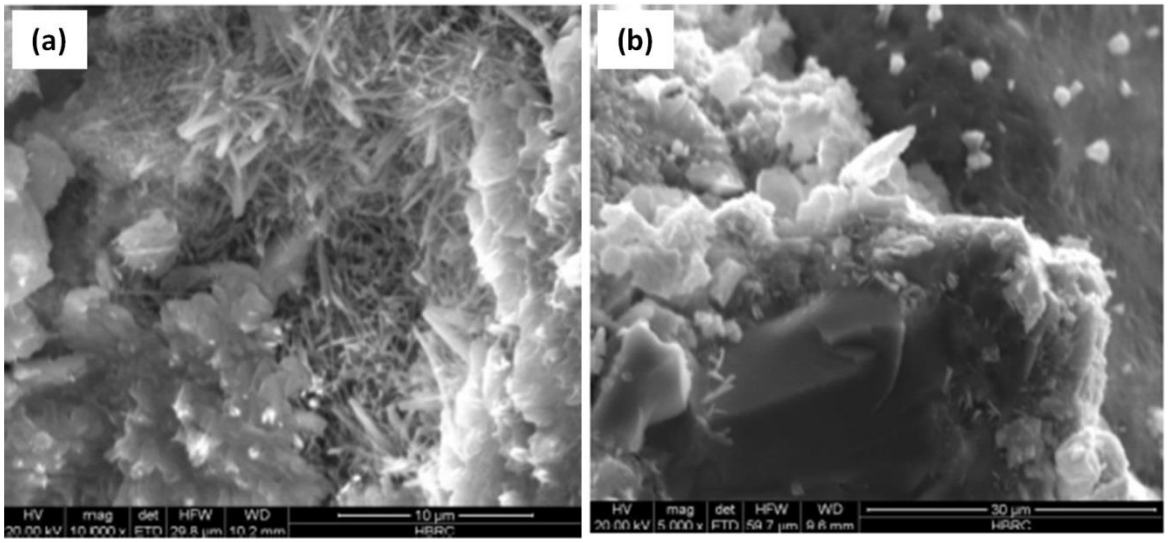

Figure 2.55: SEM micrographs of: (a) control mortar and (b) NMK nanocomposites (Morsy *et al.*, 2010).

Al-Mishhadani *et al*. (2013) investigated effect of calcined nanoclay (nano-metakaolin) on the compressive and splitting tensile strength of concrete. Nano-metakaolin (NMK) was prepared by calcining the nanoclay (nanokaolin) at 750°C for two hours. Portland cement (PC) was partially replaced by NMK of 3, 5 and 10 % by weight of PC. Concrete was cast using water/cement ratio of 0.53 and the samples were tested at 7, 28, 60 and 90 days. Control concrete and concrete nanocomposites were termed as C45, C45+3%NMK, C45+5%NMK and C45+10%NMK respectively. Figure 2.56 shows the results of compressive strengths of control and NMK nanocomposites. It was observed that compressive strength was enhanced atall NMK percentages and at all ages due to micro filling action, better pore refinement and pozzolanic reaction. In addition, as shown in Figure 2.57, splitting tensile strength of C45+5%NMK and C45+10%NMK concrete nanocomposites also increased at all ages (7, 28, 60 and 90 days) when NMK content increased. However, the splitting tensile strength of C45+3%NMK did not show any improvement at all ages.

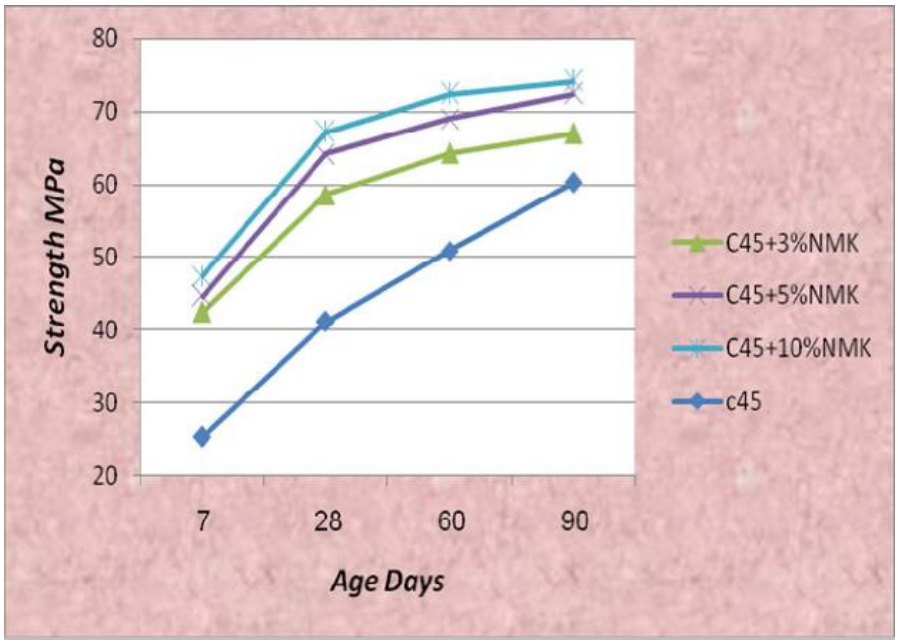

Figure 2.56: Compressive strengths of control and NMK nanocomposites (Al-Mishhadani *et al.*, 2013)

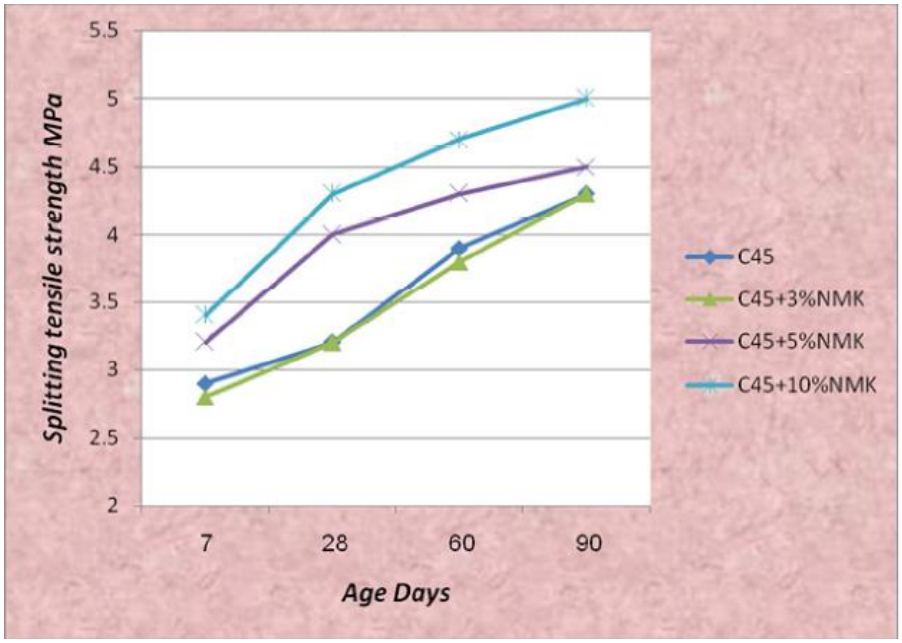

Figure 2.57: Splitting tensile strengths of control and NMK nanocomposites (Al-Mishhadani *et al.*, 2013)

Shebl *et al.* (2009) investigated the effect of nanoclay (inactivated nano-silicate (NS)) and calcined nanoclay (activated nano-silicate) on indirect tensile strength of cement paste at 7 days. Activated nano-silicate was prepared by calcining the nanoclay (Cloisite 30B) at 850°C for two hours. Portland cement (PC) was partially replaced by aactivated nano-silicate of 2, 5 and 10 % by weight of PC and similar replacements for inactivated nano-silicate (NS) which are 2, 5 and 10 wt%. It was found that the indirect tensile strength of nanocomposites containing activated NS were higher than nanocomposites containing inactivated NS as shown in Figure 2.58. The authors reported that this improvement was due to the high pozzolanic reactivity of activated NS (Shebl *et al.*, 2009) than inactivated NS that could lead to consumption of more CH to produce more CSH gel as well as the efficient filler effect. Furthermore, the optimum content of either activated NS or inactivated NS was 2 wt%. For example the indirect tensile strength of cement nanocomposite containing 2 wt% activated NS was increased by 50% compared to nanocomposite containing 2 wt% inactivated NS. However, the team concluded that

further addition of activated NS or inactivated NS beyond the optimum content led to a decrease in the indirect tensile strength due to the poor dispersion and agglomerations of the high NS contents which create more voids in the matrix.

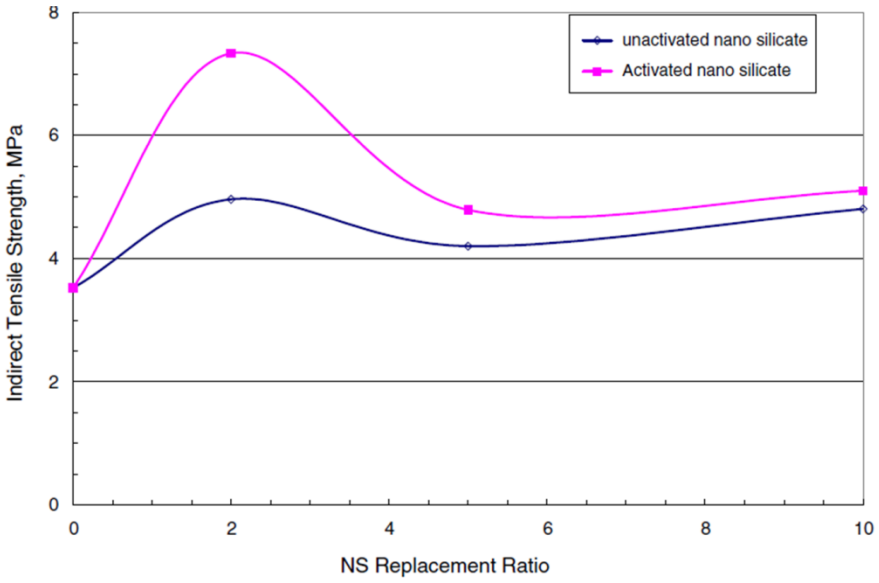

Figure 2.58: Indirect tensile strength of cement paste, nanocomposites containing activated NS and nanocomposites containing inactivated NS (Shebl *et al.*, 2009).

2.7 Natural Fibre-Reinforced Cement Nanocomposites

In last decade, natural fibre-reinforced polymer nanocomposite is gaining global interest for use in polymer manufacturing. The use of nanocomposites filled with nano-particles (carbon nanotube, silicon carbide, nanoclay etc.) as a matrix for natural fibre-reinforced composites has been recently conducted by number of studies (Thelakkadan *et al.*, 2012, Paluvai *et al.*, 2015). Several types of natural fibre or fabric such sisal, hemp were used as reinforcements in fibre-reinforce polymer nanocomposite (Saba *et al.*, 2014). It was found that natural fibre-reinforced polymer nanocomposite have better microstructure, mechanical and thermal properties than conventional natural fibre-reinforced polymer composites in terms of good fibre-matrix adhesion (Alhuthali *et al.*, 2012, Lee and Won, 2015).

Alamri *et al.* (2012) investigated the effect of nanoclay dispersion on the mechanical properties of recycled cellulose fibre (RCF) reinforced epoxy nanocomposites. The epoxy nanocomposite matrices were prepared by mixing the epoxy resin with three different ratios (1, 3 and 5 wt %) of nanoclay (Cloisite 30B) and the amount of recycled cellulose fibres was 52 wt%. It was found that the optimum content of nanoclay (NC) was 1 wt%. The authors reported that the incorporation of 1 wt%NC into RCF reinforced epoxy nanocomposites considerably improved the impact strength and impact toughness by 14.5% and 48.3% respectively when compared to RCF reinforced epoxy composites.

On the other hand, in construction and building materials, the investigation of the reinforcement of cement nanocomposite matrices with natural fibres is yet to be widely explored. However, there are very few studies in literature on the use of nanomaterials (such as carbon nanotubes, nano-silica, nanoclay etc.) as a matrix for synthetic or natural fibre-reinforced cement composites. Some of the published works on the use of nanomaterial matrix for fibre cement composites showed that the addition of nanomaterial improved the mechanical properties of synthetic fibre reinforced cement composites (Bentur *et al.,* 2013, Nik and Omran, 2013, Hosseini *et al.,* 2014b, Wei and Meyer, 2014c, Zhang *et al.,* 2014).

An interesting study on polypropylene (PP) fibre reinforced nanoparticle cement nanocomposites was conducted by Salemi and Behfarnia (2013). They investigated the effect of two different types of nanoparticles (nano-silica and nano-Al_2O_3) on the mechanical properties of PP fibre reinforced concrete at 7, 28 and 120 days. Portland cement (PC) was partially replaced by nano-silica of 3, 5 and 10 wt% by weight of PC and also by nano-Al_2O_3 of 1, 2 and 3 wt%. PP fibres were used with fibre volume content of 0.1 and 0.2 vol% in each concrete mixture. The water/binder ratio was 0.48 and the sand ratio was 0.51. Results of compressive strength at all ages are summarized in Table 2.19. It was found that addition of nano-silica or nano-Al_2O_3 significantly improved 0.1 vol% or 0.2 vol% PP fibre reinforced concrete at all ages and the optimum content was 5 wt% of nano-silica. Moreover, 0.2 vol% PP fibre reinforced concrete containing 5 wt% nano-silica showed the highest compressive strength (69.15 MPa at 120 days) over all samples. The

authors reported that filler and pozzolanic effects (especially nano-silica) reduced the micro-pores and $Ca(OH)_2$ content and also increased CSH gel. Consequently all these factors improved microstructure, fibre-matrix interface and durability of PP fibre reinforced concrete containing nano-silica (especially 5 wt%) or nano-Al_2O_3.

Table 2.19: Compressive strength for samples (Salemi and Behfarnia 2013).

Concrete mixture		Compressive strength (MPa)		
Type	Symbol	7 days	28 days	120 days
Control concrete	C	27.1	42.11	47.15
0.1% PP	C1P	27.69	43.04	49.75
0.2% PP	C2P	28.11	43.52	50.92
3% nano-silica	C3S	29.27	49.13	60.35
0.1% PP+3% nano-silica	C1P3S	29.85	49.87	61.28
0.2% PP+3% nano-silica	C2P3S	30.01	50.12	61.42
5% nano-silica	C5S	31.16	54.8	68.36
0.1% PP+5% nano-silica	C1P5S	31.48	54.89	68.83
0.2% PP+5% nano-silica	C2P5S	31.92	55.07	69.15
7% nano-silica	C7S	30.19	52.04	64.12
0.1% PP+7% nano-silica	C1P7S	30.61	52.37	64.76
0.2% PP+7% nano-silica	C2P7S	30.95	52.06	65.15
1% nano-Al_2O_3	C1A	27.65	43.81	50.45
0.1% PP+1% nano-Al_2O_3	C1P1A	28.34	44.92	51.91
0.2% PP+1% nano-Al_2O_3	C2P1A	29.22	46.21	52.48
2% nano-Al_2O_3	C2A	27.84	44.64	51.39
0.1% PP+2% nano-Al_2O_3	C1P2A	28.31	45.97	52.29
0.2% PP+2% nano-Al_2O_3	C2P2A	29.47	47.15	53.61
3% nano-Al_2O_3	C3A	27.97	45.48	52.34
0.1% PP+3% nano-Al_2O_3	C1P3A	29.1	46.52	53.3
0.2% PP+3% nano-Al_2O_3	C2P3A	30.03	45.91	54.78

Up to date, limited studies have investigated effect of nanomaterials on natural fibre reinforced cement composites. Hamzaoui *et al*. (2014) studied mechanical performance of cement mortar containing hemp fibres and carbon nanotubes at 90 days. The contents of hemp fibres were 1.1 , 2.1 and 3.1 wt% by weight of cement and both wet and dry hemp fibres were used in hemp-mortar composites. Carbon nanotubes (CNT) were in form of liquid solution and CNT concentration in solution was 2 wt%. CNT was used in mortar with various weight concentrations; 0.01, 0.02, 0.03, 0.04, 0.05 and 0.06%. Mortar was prepared with cement/sand ratio of 1:3 and water/cement ratio of 0.5. Based on the compressive and flexural strengths results of hemp-mortar composites, it was found that 2.1 wt% wet hemp fibre was optimum content. Regarding CNT-mortar, it was found that mortar containing 0.01% CNT demonstrated higher compressive and flexural strengths than control mortar and other nanocomposites. The results of the compressive and flexural strengths of hemp-CNT-mortar are shown in Figure 2.59. The authors reported that addition of 0.01% CNT into hemp-CNT-mortar increased the compressive and flexural strengths by 24% and 6% compared to hemp-mortar. They concluded that addition of small amount of (0.01 %) CNT improved the stiffness of cement matrix and then the adhesion between the hemp fibres and the matrix was improved.

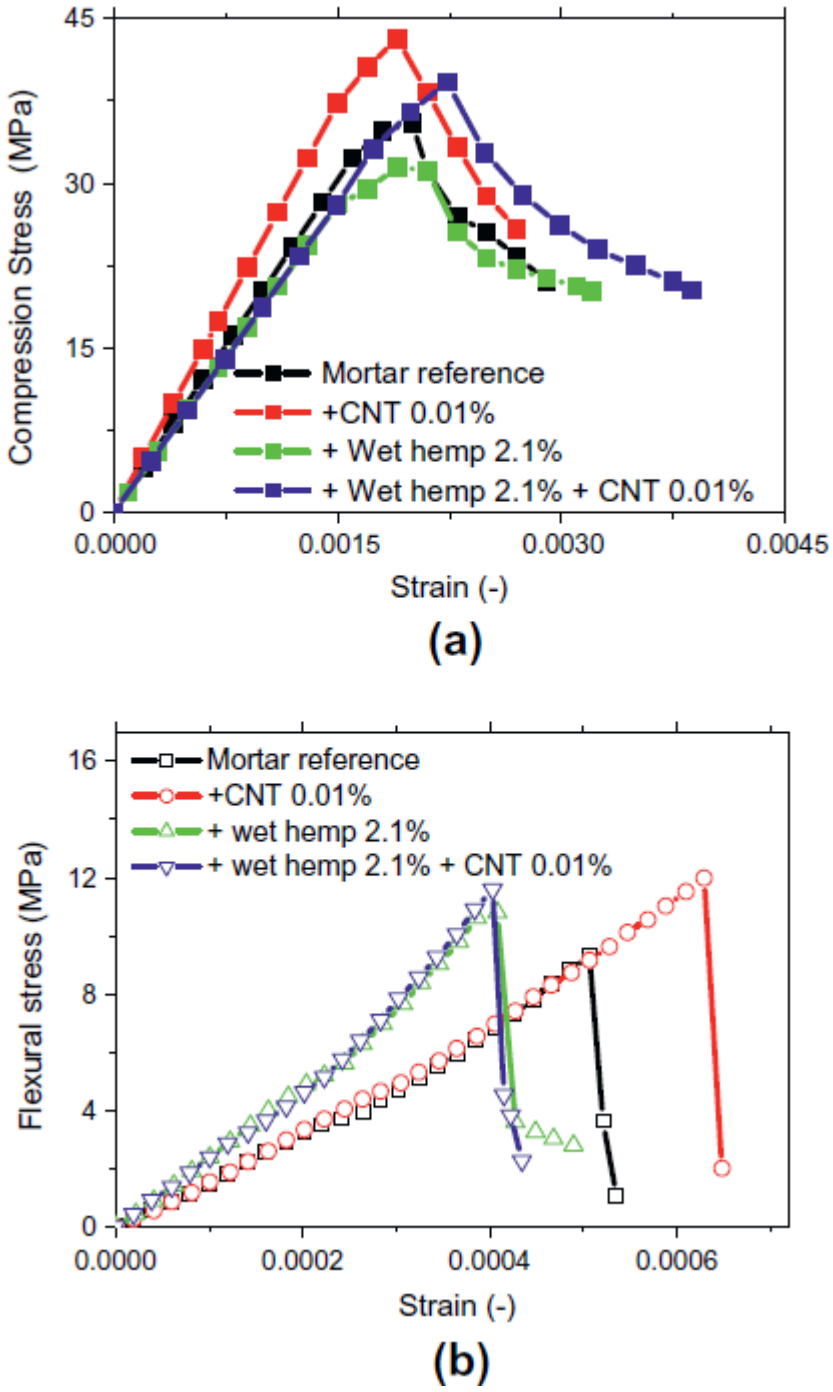

Figure 2.59: (a) Compressive and (b) flexural strengths of hemp-CNT-mortar (Hamzaoui *et al.*, 2014)

An interesting study on using nanoparticles and natural fibres as reinforcements in cement nanocomposites was obtained by Aly *et al*. (2011b). They studied the durability of flax fibre reinforced cement mortar (FRCGN) containing 2.5 wt % nanoclay (N) and 20 wt% ground waste glass powder (G) at 28 days and after 50 wet/dry cycles (378 days). As shown in Figure 2.60, at 28 days the flexural strength of FRCGN containing nanoclay increased by 23% compared to FRCG composites without nanoclay. Moreover, the FRCGN nanocomposites after accelerating ageing cycles (378 days) showed small reduction (19%) in the flexural strength compared to its initial strength at 28 days. The authors reported that pozzolanic and filler effects of nanoclay led to improved microstructure of cement matrix and fibre-matrix interface.

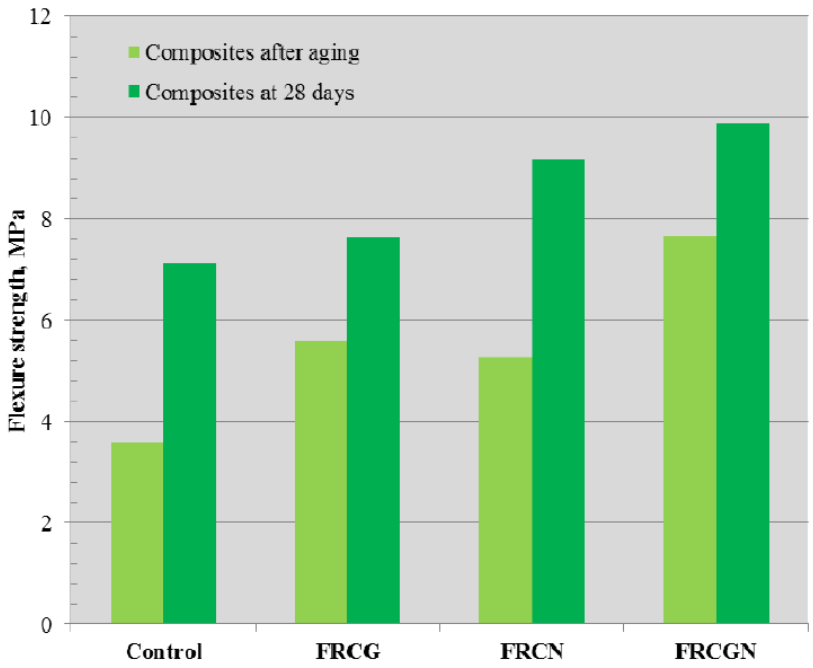

Figure 2.60: Flexural strength of specimens (Aly *et al.*, 2011b).

Wei and Meyer (2014c) investigated the mechanical properties of sisal fiber-reinforced mortar with Portland cement replacement by a combination of metakaolin (MK) and nanoclay (NC) at 28 days. Firstly, Portland cement was replaced by 10, 30 and 50 wt% of MK. After that each amount of MK was replaced by 1, 3 and 5 wt% of NC. The content of sisal fibre in each composites was 2 vol% (volume fraction) and water/binder ratio of 0.4 was used. Figure 2.61 shows the flexural strength and toughness of sisal fiber-reinforced MK-NC mortar beams. It was found that B30-1 (sisal fiber-reinforced mortar containing 29 wt% MK and 1 wt% NC) and B30-2 (sisal fiber-reinforced mortar containing 28 wt% MK and 2 wt% NC) showed better flexural behavior than others. The first-crack strength of B30-1 and B30-2 increased by 36.4 % and 31.57% respectively compared to PC mortar. B30-2 exhibited the highest post-crack flexural strength and post-cracking toughness which was 49.7% and 77.71 % respectively greater than PC mortar. The authors concluded that combined replacement of PC by MK and NC not only enhanced the interface bonding between sisal fibre and cement matrix, but also prevented the fiber degradation from alkaline attack and $Ca(OH)_2$ mineralization.

The team supported their conclusion by SEM examinations (Figure 2.62a-f) of the sisal fiber degradation for the sisal fiber reinforced PC, B30-1, B30-2 and B50-1 composites. In sisal fiber reinforced PC, the signs of fiber deterioration are present on their surface (Figure 2.62a-c) in terms of existence of hydration products in interfacial zone between fibre and cement matrix and $Ca(OH)_2$. The fibre-matrix interface improved in sisal fiber reinforced B30-1, B30-2 and B50-1 (Figure 2.62d-f) when compared PC (Figure 2.62a-c) due to the pozzolanic reaction of MK and NC. But the fibre-matrix adhesion for sisal fiber reinforced B30-2 (Figure 2.62e) was the best one over all samples in which this improvement can delay the fiber deterioration from alkaline environment.

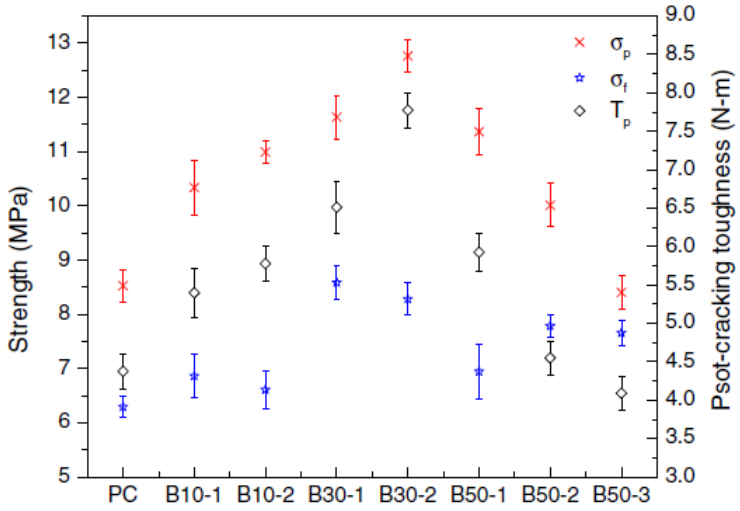

Figure 2.61: Flexural strength and toughness of sisal fiber-reinforced MK-NC mortar beams: σ_f average first-crack strength (MPa), σ_p average post-crack flexural strength (MPa) and T_p average post-cracking toughness (N.m) (Wei and Meyer, 2014c).

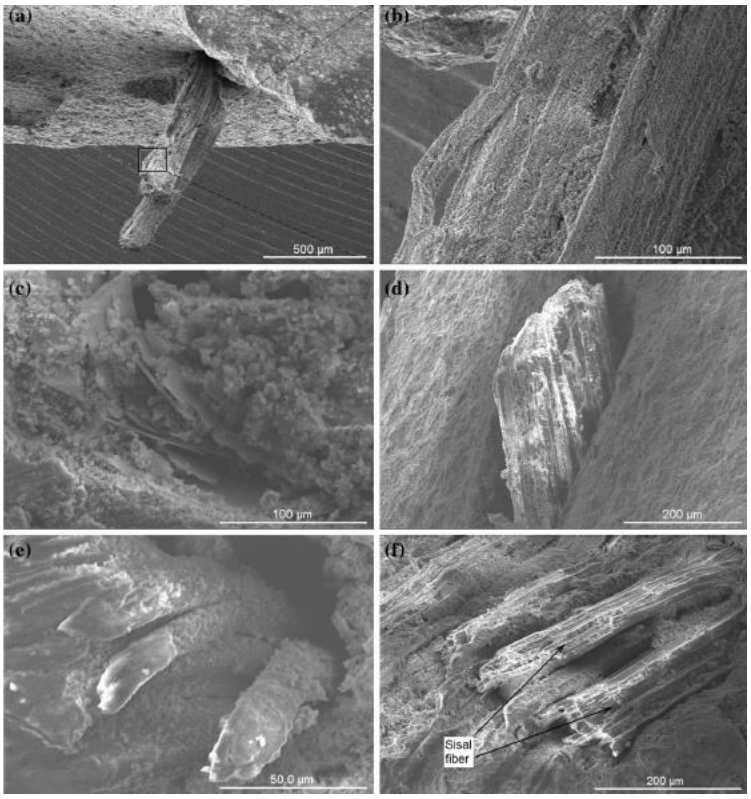

Figure 2.62: SEM micrographs of the fracture surface of the investigated samples at 28 days of curing: (a–c) PC, (d) B30-1, (e) B30-2, (f) B50-1 (Wei and Meyer, 2014c).

2.8 Effect of fibre characters on mechanical properties of natural fibre reinforced cement composites

There are a number of factors that can effect on the mechanical properties of fibre reinforced cement composites. Some examples of these factors including: fibre weight or volume fraction, fibre-matrix adhesion, aspect ratio, fibre orientation and fibre dispersion (Balaguru and Shah, 1992, Bentur and Mindess, 2007, Silva *et al.*, 2011).

(a) Weight or volume fraction

The content of fibres in cement matrix is an important parameter of fibre reinforced cement composites. Generally, mechanical properties such as strength, toughness and modulus increase with an increase in fibre content up to the optimum content and then mechanical performance adversely decrease. At the optimum content of fibre, this maximum improvement in mechanical properties of fibre-reinforced cement composites can be attributed to high fibre-matrix interfacial bounding which increase the maximum load-transfer capacity. However, beyond the optimum content of fibre, fibre-reinforced-cement composites exhibits low mechanical properties due to the increase in porosity which reduces the bond strength between fibres and matrix and thus reduce the load-transfer capacity (Pacheco-Torgal and Jalali, 2011a, Santos *et al.*, 2015).

(b) Fibre-matrix interfacial bounding

The fibre-matrix interfacial bounding is considered as a critical parameter that improves mechanical properties such as flexural and tensile strength in fibre-reinforced composites. Regarding natural fibres, several studies indicate that the interfacial bonding between natural fibre and cement matrix is relatively weak. The presence of hemicellulose, pectins and impurities (waxes and fatty substances) in raw natural fibres reduce fibre-matrix interface. Some researchers have shown that pre-treatments of natural fibres by pulping processes such as the Kraft process, coating of fibre by polymer resin (i.e. epoxy) or using chemical agents (i.e. alkalization, polyethylene imine) have slightly improved the interfacial bond strength between natural fibres and the matrix of the fibre reinforced cement composites. As a result of this pre-treatment, the mechanical properties of such

fibre-reinforced cement composites are enhanced (Sedan *et al.*, 2008, Pacheco-Torgal and Jalali, 2011a).

(c) Aspect ratio

Aspect ratio (l_c/d) is defined as ratio of critical length to diameter of fibre and it is considered as efficient factor for short fibres that are used in fibre-reinforced cement composites. The critical (minimum) length of fibre is required in order that the applied load (stress) can transfer from the matrix to fibre before composite failures. The critical length is calculated by the following equation (Callister, 2007):

$$l_c = \frac{\sigma_f^* d}{2\tau_c} \qquad (2.5)$$

Where d is the fibre diameter, σ_c^* is fibre ultimate (or tensile) strength and τ_c is the fibre-matrix bond strength (interfacial shear stress).

As shown in Figure 2.63 (a-c), when tensile stress is equal to fibre tensile strength, there are three cases. If fibre length (l) is equal to the critical length (Figure 2.63 a), the maximum fibre load is achieved only at the axial center of the fibre. If fibre length increases ($l > l_c$), the fibre reinforcement can be more effective (Figure 2.63 b). If fibre length is less than the critical length ($l > l_c$), virtually no stress can be transferred and there is ineffective reinforcement by fibre (Figure 2.63 c).

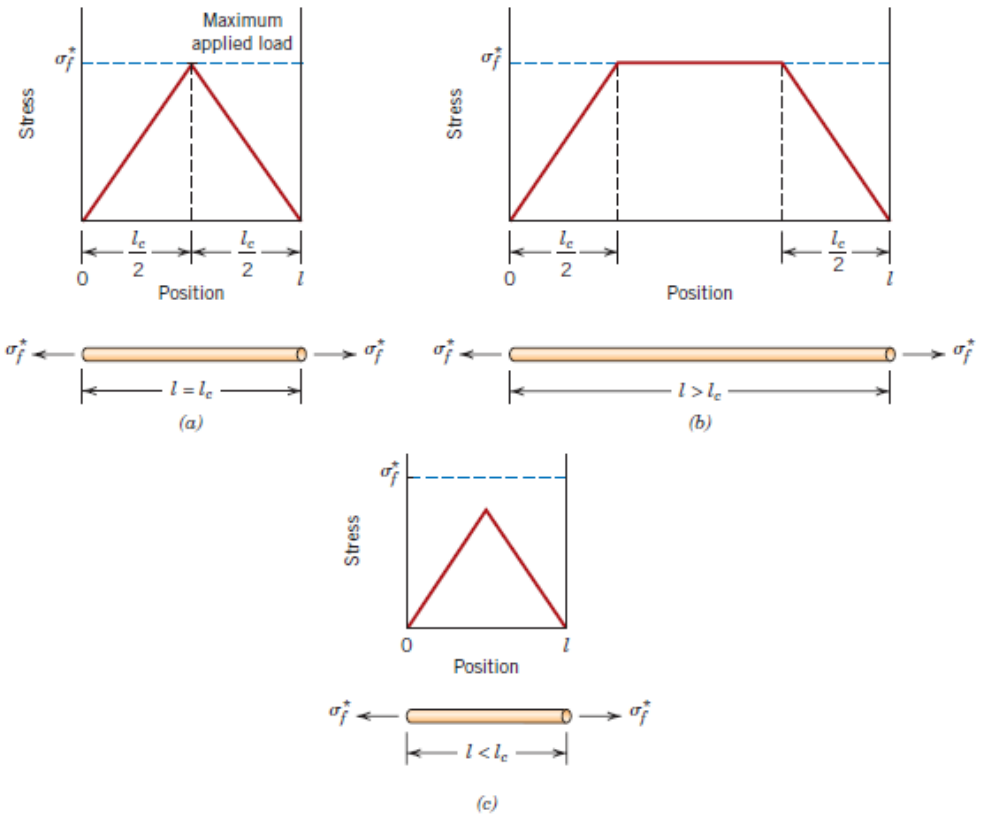

Figure 2.63: Stress–position profiles when fibre length (l) is: (a) equal to the critical length (l_c), (b) greater than the critical length, and (c) less than the critical length for a fibre-reinforced composite that is subjected to a tensile stress equal to the fibre tensile strength (Callister, 2007).

(d) Fibre orientation

Fibre orientation is also an effective parameter that influences on the mechanical performance of fibre-cement composites. The fibres can be divided to continuous fibres and discontinuous fibre (short fibre). Based on orientation, there are two possible arrangements: (i) a parallel alignment of the longitudinal axis of the fibres in a single direction, (ii) a totally random alignment (Callister, 2007). As shown in Figure 2.64 (a-c), continuous fibres are usually aligned orientation (Figure 2.64 a), while short fibres generally could be aligned (Figure 2.64 b) or random oriented (Figure 2.64 c). A better mechanical performance of fibre-cement composites can be achieved when fibre distribution is uniform.

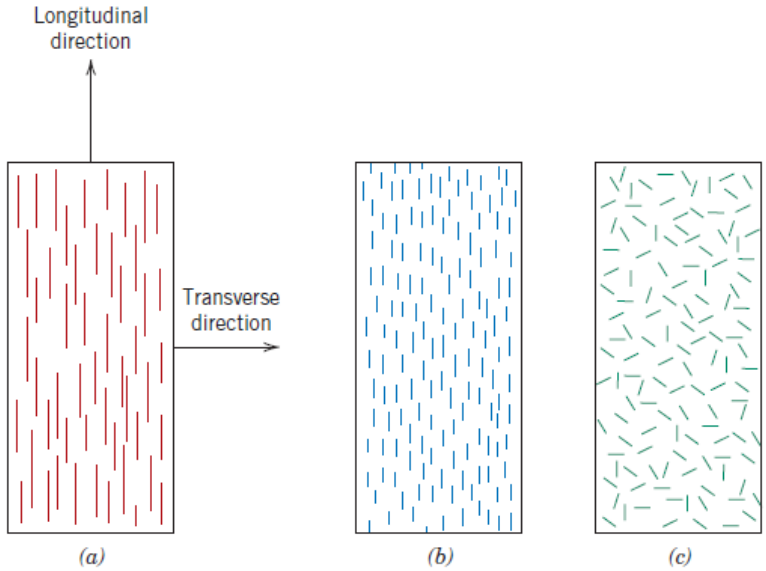

Figure 2.64: Schematic representations of (*a*) continuous and aligned, (*b*) discontinuous and aligned, and (*c*) discontinuous and randomly oriented fibre reinforced composites (Callister, 2007).

Under longitudinal direction (loading), if the continuous fibres and matrix behave elastically, the elastic modulus of composite can determined by rule of mixtures as follows (Callister, 2007):

$$E_{cl} = E_m V_m + E_f \mathrm{V_f} \qquad (2.6a)$$

Or

$$E_{cl} = E_m (1 - V_f) + E_f \mathrm{V_f} \qquad (2.6b)$$

Where E_{cl}, E_m and E_f are moduli of composite, matrix and continuous fibres respectively and also V_m and V_f are volume fractions of matrix and continuous fibres respectively (V_m + V_f = 1).

However, under transverse direction (loading), the elastic modulus of composite can be expressed as:

$$E_{ct} = \frac{E_m E_f}{(1-V_f)E_f + V_f E_m} \qquad (2.7)$$

Regarding discontinuous and randomly orientated fibre composites, the rule of mixtures for the elastic modulus of composite can be written as follows (Callister, 2007):

$$E_{cd} = E_m V_m + K E_f \mathrm{V_f} \qquad (2.8)$$

Where K is a fibre efficiency parameter that depends V_f on and E_f/E_m ratio. As shown in Table 2.20, in case of all fibres parallel, the maximum reinforcement can be achieved only if the fibres are oriented parallel along with the stress direction. In the case of randomly oriented fibres, the reinforcement efficiency can be 3/8 or 1/5 depending on the stress direction and orientation angle.

Table 2.20: Reinforcement efficiency of fibre-reinforced composites for several fibre orientations and at various directions of stress application (Callister, 2007).

Fibre orientation	**Stress direction**	**Reinforcement efficiency**
All fibres parallel	Parallel to fibres	1
	Perpendicular to fibres	0
Fibres randomly and uniformly distributed within a specific plane	Any direction in the plane of the fibres	3/8
Fibres randomly and uniformly distributed within three dimensions in space	Any direction	1/5

(e) Fibre dispersion and mixing procedure

The dispersion of short fibres in cement matrix is a critical factor that can influence the mechanical properties of short fibre-reinforced cement composites. Therefore the primary concern in mixing is the uniform distribution of short fibres throughout the matrix. Poor dispersion of fibres could lead to interlock them to form a mat or a ball during mixing as a

result of this the matrix-rich regions increase and thus the strength of composites decrease (Balaguru and Shah, 1992, Bentur and Mindess, 2007). Good dispersion of fibres in cement matrix usually enhances the strength of composites due to the efficiency of fibre to carry the transferred load from the matrix. Generally, there are two mixing methods to distribute short fibres into cement matrix. The first method is called dry mix, in which short fibres mix with dry materials (cement powder, sand and aggregates) in concrete mixer for several minutes until fibres are dispersed homogenously. After that required water is added to complete casting of short fibre-reinforced cement composites (Balaguru and Shah, 1992, Bentur and Mindess, 2007). The second method is called wet mixing, in which water and dry materials (cement powder, sand and aggregates) are mixed in concrete mixer for several minutes and then fibres can be added manually or automatically into mixture to fabricate short fibre-reinforced cement composites (Balaguru and Shah, 1992, Bentur and Mindess, 2007).

2.9 Effect of nano-materials characters on mechanical properties of cement nanocomposites.

The characters of nano-materials can affect the mechanical properties of nanomaterial-cement nanocomposites. Some examples of these characters including: content, size, geometry and crystalline or amorphous phases. Moreover, these characters play a major role in filler effect and pozzolanic activity in cement nanocomposites.

(a) Effect of content

The content of nanomaterials in cement mixtures is an important factor of cement nanocomposites. Generally, mechanical properties such as strength, toughness and modulus increase with an increase in nanomaterials content up to the optimum content and then mechanical performance adversely decrease (Sanchez and Sobolev, 2010). At the optimum content of nanomaterials, this maximum improvement in mechanical properties of cement nanocomposites can indicate that microstructure become more dense and compact due to filling of micro-pores and densification by a good dispersion of nanomaterials (Stefanidou and Papayianni, 2012). However, beyond the optimum content of nanomaterials, cement nanocomposites exhibits lower mechanical properties due to the

poor dispersion and agglomeration of nanomaterials which create more void in nanocomposites (Shaikh *et al.,* 2014, Mendes *et al.,* 2015).

(b) Effect of particle size

Size of nanomaterial is considered as efficient factor in cement nanocomposites. When nanoparticle size decreases, the filler effect increases and then microstructure of nanocomposites significantly improves (Mendes *et al.*, 2015). In other words, the smaller particle size shows better mechanical and physical properties of nanocomposites than bigger particle size at the fixed filler content. The size usually depends on type of nanomaterial and shape (Sanchez and Sobolev, 2010, Hanus and Harris, 2013). For example, in spherical nanoparticles such as nano-silica, average sizes normally vary between 3-100 nm. Chen et al. (2012) studied two types of nano-TiO_2 with the same content (5 wt%) on compressive strength of cement paste at 28 days. The two types of crystalline nano-TiO_2 were nano-P25 with size of 21 nm and nano-Anatase with size of 350 nm. The authors confirmed that nano-TiO_2 was non-reactive fine filler and had no pozzolanic activity. It was found that the compressive strength of nanocomposite containing nano-P25 was greater than nano-Anatase. They concluded that the change of pore structure and the improvement of compressive strength could only be attributed to the micro-filling effect of fine powders.

(c) Effect of nano-materials geometry

The geometry of nano-materials is also an effective factor that influences on the mechanical and physical properties of cement nanocomposites. Generally, nanomaterials that are used in cement composites have certain shapes. These shapes include: spherical shape such as nano-silica, tube shape such as carbon nanotube and halloysite nanoclay, fibre shape such as carbon nanofibers, platelet shape such as nano-montmorillonite and Cloisite 30B (Sanchez and Sobolev, 2010). Besides the filler effect, recent research showed that tube shape (i.e. carbon nanotube) can link cement matrix hydrates and improve the resistance to micro-crack propagation in nanocomposites (Hanus and Harris, 2013). As a result of this toughness and strength of nanocomposites can improve significantly (Shekari and Razzaghi, 2011, Parveen *et al.*, 2013).

(d) Effect of amorphous phase and specific surface area of nanomaterials

Pozzolanic effect of nanomaterials is usually governed by high chemical constituent (fraction) of silicon dioxide (silica SiO_2 > 50wt %) in nanoparticle, amorphous (sometimes semi-amorphous) nature, specific surface area and size of nanoparticle (Singh *et al.*, 2013). The degree of the pozzolanic reaction of material fundamentally depends on high silica fraction and amorphous state. It is known that the pozzolanic reaction is chemical reaction between $Ca(OH)_2$ crystals in cement matrix and amorphous silica to yield amorphous calcium silicate hydrate (C-S-H) gel (Sanchez and Sobolev, 2010, Pacheco-Torgal and Jalali, 2011b, Maheswaran *et al.*, 2013). In addition, as particle sizes decrease to nanoscale the specific surface areas increase extremely. These high reactive specific surface areas of nanoparticles can contribute to increase the pozzolanic reaction rates better than micro-materials. As a result of this effective pozzolanic reaction, the mechanical and physical properties of nanocomposites will improve significantly (Raki *et al.*, 2010).

2.10 Summary

Recently, natural fibres are gaining increasing popularity to develop 'environmental-friendly construction materials' as alternative to synthetic fibres in fibre-reinforced concrete. Natural and cellulose fibres have been used in cement matrices to improve their tensile and flexural strengths and fracture resistance properties. Some research has shown that pre-treatments of natural fibre surfaces via some chemical agents such as alkalization have slightly improved the interfacial bond strength between natural fibres and the matrix of the fibre reinforced cement composites. However, the interfacial bonding between the natural fibre and the cement matrix is relatively weak and also the degradation of fibres in a high alkaline environment of cement can adversely affect the mechanical and durability properties of natural fibre reinforced cement composites. On the other hand, due to the new potential uses of nanomaterials, there is a growing global interest in the research of their effect in civil engineering and construction materials particularly in short and long-term properties of mortar and concrete. According to the literature, several experimental results on the use of nanoparticles in OPC cement paste, mortar and concrete have been reported.

However, little laboratory data exist on the effects of calcined nanoclay in cement composites as well as the combined use of calcined nanoclay and hemp fabrics as hybrid reinforcement in cement-composites. Therefore, the use of calcined nanoclay in hemp fibre-reinforced cement composite can be an attempt to overcome the above-mentioned disadvantages of hemp fibres in cementitious composites.

3. PUBLICATIONS FORMING PART OF THESIS

(Listed in order as found on this thesis)

1. **HAKAMY, A.,** SHAIKH, F.U.A. & LOW, I.M. 2013. Microstructures and mechanical properties of hemp fabric reinforced organoclay–cement nanocomposites. *Construction & Building Materials,* 49, 298–307.
2. **HAKAMY, A.,** SHAIKH, F.U.A. & LOW, I.M. 2014. Thermal and mechanical properties of hemp fabric-reinforced nanoclay–cement nanocomposites. *Journal of Materials Science,* 49, 1684–1694.
3. **HAKAMY, A.,** SHAIKH, F.U.A. & LOW, I.M. 2014. Characteristics of hemp fabric reinforced nanoclay–cement nanocomposites. *Cement & Concrete Composites,* 50, 27–35.
4. **HAKAMY, A.,** SHAIKH, F.U.A. & LOW, I.M. 2015. Characteristics of nanoclay and calcined nanoclay-cement nanocomposites. *Composites Part B: Engineering,* 78, 174-184.
5. **HAKAMY, A.,** SHAIKH, F.U.A. & LOW, I.M. 2015. Effect of calcined nanoclay on microstructural and mechanical properties of chemically treated hemp fabric reinforced cement nanocomposites. *Construction & Building Materials,* 95, 882–891.
6. **HAKAMY, A.,** SHAIKH, F.U.A. & LOW, I.M. 2015. Thermal and mechanical properties of NaOH treated hemp fabric and calcined nanoclay-reinforced cement nanocomposites. *Materials and Design,* 80, 70–81.
7. **HAKAMY, A.,** SHAIKH, F.U.A. & LOW, I.M. 2016. Effect of calcined nanoclay on the durability of NaOH treated hemp fabric-reinforced cement nanocomposites. *Materials and Design,* 92, 659-666.

3.1 Microstructures and mechanical properties of hemp fabric reinforced organoclay–cement nanocomposites.

HAKAMY, A., SHAIKH, F.U.A. & LOW, I.M. 2013. Microstructures and mechanical properties of hemp fabric reinforced organoclay–cement nanocomposites. *Construction & Building Materials,* 49, 298–307.

Construction and Building Materials 49 (2013) 298–307

Contents lists available at ScienceDirect

Construction and Building Materials

journal homepage: www.elsevier.com/locate/conbuildmat

Microstructures and mechanical properties of hemp fabric reinforced organoclay–cement nanocomposites

A. Hakamy [a], FUA Shaikh [b], I.M. Low [a,*]

[a] Department of Imaging & Applied Physics, Curtin University, GPO Box U1987, Perth, WA 6845, Australia
[b] Department of Civil Engineering, Curtin University, GPO Box U1987, Perth, WA 6845, Australia

HIGHLIGHTS

- Synthesis of hemp fabric reinforced nanoclay–cement nanocomposites.
- Mechanical properties increased with addition of nanoclay and hemp.
- 1 wt% nanoclay was optimum in enhancing strength and toughness.

ARTICLE INFO

Article history:
Received 21 March 2013
Received in revised form 1 June 2013
Accepted 20 August 2013

Keywords:
Cement
Nanoclay
Hemp fabric
Mechanical properties
Microstructure
Fracture toughness

ABSTRACT

Cement eco-nanocomposites reinforced with hemp fabric (HF) and nanoclay platelets (Cloisite30B) are fabricated and investigated in terms of XRD, SEM, physical and mechanical properties. Results indicated that the mechanical properties generally increased as a result of the addition of nanoclay into the cement matrix with and without HF. An optimum replacement of ordinary Portland cement by 1 wt% nanoclay is concluded from the current work. It is found that, 1 wt% nanoclay decreases the porosity and also significantly increases the density, flexural strength and fracture toughness of cement composite and HF reinforced nanocomposite. The microstructural analysis results indicate that the nanoclay behaves not only as a filler to improve microstructure, but also as an activator to promote pozzolanic reaction which modified cement matrix and improved the hemp fabric-matrix adhesion. The failure micromechanisms and energy dissipative processes in HF reinforced cement composite and nanocomposite are discussed in terms of microstructural observations.

1. Introduction

To date, one of the current tendencies in the building industry is to develop 'environmentally friendly materials' through utilizing natural fibres as alternative to synthetic fibres in fibre-reinforced concrete [1–3]. Another one is that some Portland cement is replaced by nanomaterials or supplementary cementitious materials (SCMs) [4]. Currently, nanotechnology has several applications in the polymer, ceramic and construction industries, particularly producing nanocomposites which have superior physical and mechanical properties [5]. In the construction industry, several types of nanoparticles have been incorporated into concrete composites such as nano-SiO_2, nano-Al_2O_3, nano-Fe_2O_3, nano-ZnO_2, nano-TiO_2, carbon nanotubes and nano-metakaolin in order to improve the durability and mechanical properties of concrete [6–9].

Natural and cellulose fibres are used in polymer and cement matrices to improve their strength and fracture resistance properties [10,11]. They are cheaper, biodegradable and lighter than its counterpart synthetic fibres. Some examples of natural fibres are: cotton, sisal, flax, hemp, bamboo, coir, wheat straws and others [12–14]. On the other hand, one of the most effective techniques to obtain a high performance cementitious composite is by reinforcement with textile (fabrics), which are impregnated with cement paste or mortar. Synthesis (textile) fabrics such as polyethylene (PE) and polypropylene (PP) have used as reinforcement for cement composites, in which fabrics are made of multi-filaments. This system has superior filaments–matrix bond which improve mechanical properties such as tensile and flexural strength more than continuous or short fibres [15–19]. In contrast, the use of natural fibre sheets and fabrics in polymer matrix is reported in many studies than that used in cement based matrix. For example, using cellulose sheets in epoxy or viny-ester matrix have improved the fracture toughness significantly [5,20].

Indeed, despite all the advantages of natural fibres and fabrics and also nanoparticles, there are also some obstacles which have limited their applications in the cementitious composites. Firstly, for natural fibres, the interfacial bond between the natural fibre

* Corresponding author. Tel.: +61 8 92667544; fax: +61 8 92662377.
E-mail address: j.low@curtin.edu.au (I.M. Low).

0950-0618/$ - see front matter
http://dx.doi.org/10.1016/j.conbuildmat.2013.08.028

and the cement matrix is relatively weak and also the degradation of fibres in a high alkaline environment of cement adversely affects the mechanical and durability properties of natural fibre reinforced cement composites [21]. Some researchers have recently recommended that much research is needed to overcome these disadvantages [22]. Secondly, for all nanoparticles, one of the major issues is that increasing the content of nanoparticles leads to reduction of some mechanical properties such as the flexural strength of cement paste [23]. However, little or no research is reported on using of natural fabrics and nano particles (e.g. nanoclay) as reinforcement in cement-composites. In this study, a novel material which involves synthesizing cement eco-nanocomposites will be synthesized and investigated. Nanoclay is to be utilised to a partially replace cement at various ratios to produce nanocomposites. Hemp fabrics (HF) are to be utilised to reinforce the nanocomposites. The effects of different amounts of nano-clay on mechanical properties of HF reinforced cement nanocomposites are evaluated. The microstructure of the surface of hemp fabric and eco-nanocomposite has been investigated by XRD and scanning electron microscopy (SEM).

2. Experimental procedure

2.1. Materials

Hemp fabric (HF) and nanoclay platelets (Cloisite 30B) were used as reinforcements for the cement–matrix composites. The hemp fabric was supplied by Hemp Wholesale Australia Pty. Kalamunda, Western Australia as shown in Fig. 1. The chemical composition of and also the physical properties and structure of hemp fabric are shown in Tables 1 and 2 respectively [12,16]. The nanoclay platelets (Cloisite 30B) used in this investigation are based on natural montmorillonite clay (hydrated sodium calcium aluminium magnesium silicate hydroxide $(Na,Ca)_{0.33}(Al,Mg)_2(Si_4O_{10})(OH)_2{\cdot}nH_2O$). Cloisite30B is a natural montmorillonite modified with a quaternary ammonium salt, which was supplied by Southern Clay Products, USA. The specification and physical properties of Cloisite 30B are outlined in Table 3 [5]. Ordinary Portland cement (OPC) was used in all mixes. The chemical composition and physical properties of OPC are listed in Table 4 [2].

2.2. Sample preparation

2.2.1. Nanocomposites

In this study, the OPC is partially substituted by nanoclay with 1%, 2% and 3% by weight of OPC. The OPC and nanoclay were first dry mixed for 5 min in Hobart mixer at a low speed and then mixed for another 10 min at high speed until homogeneity was achieved. The cement–nano-composite paste was prepared through adding water with a water/binder (nanoclay–cement) ratio of 0.48. The cement paste without nanoclay was considered as a control.

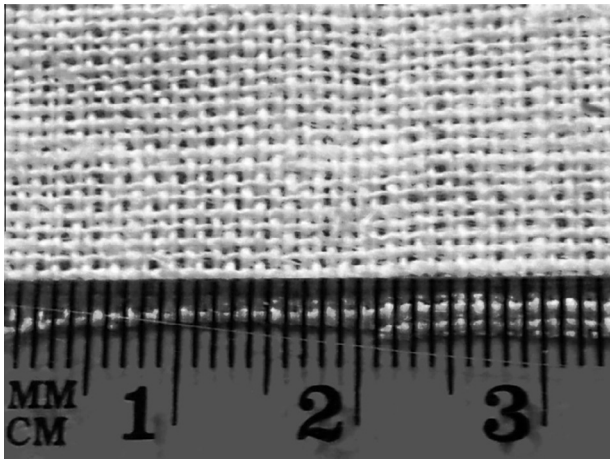

Fig. 1. Hemp fabric.

2.2.2. Hemp fabric reinforced nanocomposites

Two layers of hemp fabrics were used in hemp fabric reinforced nano-composites. The hemp fabrics were first soaked into the matrix in order to achieve a better penetration of the matrix in between the openings of the fabrics. The fabrication of the hemp fabric reinforced nanocomposite specimen was done in five steps. First, a thin layer of matrix was poured into the mould, then the pre-soaked hemp fabric was laid on top of it, then another layer of matrix was poured into the mould followed by the other pre-soaked hemp fabric and the final layer of matrix. The total amount of hemp fabric in each specimen was about 2.5 wt%. The mix proportions are given in Table 5.

2.2.3. Curing and specimens

For each series, three prismatic plate specimens of 300 × 70 × 10 mm in dimension were cast. All specimens were demolded after 24 h of casting and kept under water for approximately 56 days. Five rectangular specimens of each series with dimensions 70 × 20 × 10 mm were cut from the fully cured prismatic plate for each mechanical and physical test [16,23].

2.3. Characterisation

2.3.1. XRD

The samples were measured on a D8 Advance Diffractometer (Bruker-AXS) using copper radiation and a LynxEye position sensitive detector. The diffractometer were scanned from 3° to 70° (2θ) in steps of 0.02° using a scanning rate of 0.5°/min. XRD patterns were obtained by using Cu Ka lines (λ = 1.5406 Å). A knife edge collimator was fitted to reduce air scatter.

2.3.2. Scanning electron microscopy (SEM)

Scanning electron microscopy imaging was obtained using a NEON 40ESB, ZEISS, equipped with energy dispersive spectroscopy (EDS). The SEM investigation was carried out in detail on microstructures and the fractured surfaces of samples. Specimens were coated with a thin layer of platinum before observation by SEM to avoid charging.

2.4. Physical properties

Measurements of bulk density and porosity were conducted to determine the quality of nanocomposites. The thickness, width, length and weight are measured in order to determine the bulk density. The calculation for density was carried out by using the following equation:

$$D = \frac{M}{V} \tag{1}$$

where D is the density in g/cm^3, M the mass of the test specimen (g) and V is the volume of the test specimen (cm^3).The value of apparent porosity P_S was determined using the Archimedes principle in accordance with the ASTM Standard (C-20) and clean water was used as the immersion water. The apparent porosity P_S was calculated using the following equation [25]:

$$P_S\% = \frac{m_s - m_d}{m_s - m_i} \times 100 \tag{2}$$

where m_d is themass of the dried sample, m_i the mass of the sample saturated with and suspended in water, m_s is the mass of the sample saturated in air.

2.5. Mechanical properties

Five specimens of each composition, all 70 × 20 × 10 mm, were used in the mechanical tests. Three-point bend tests were conducted using a LLOYD Material Testing Machine to evaluate the flexural strength, flexural modulus and fracture toughness. The support span used was 40 mm with a displacement rate of 0.5 mm/min. The flexural strength σ_F was evaluated using the following equation:

$$\sigma_F = \frac{3P_mS}{2BW^2} \tag{3}$$

where P_m is the maximum load at crack extension, S is the span of the sample, W is the specimen thickness (depth) and B is the specimen width. Values of the flexural modulus E_F were computed using the initial slope of the load–displacement curve, $\frac{\Delta P}{\Delta X}$ using the formula:

$$E_F = \frac{S^3}{4BW^3}\left(\frac{\Delta P}{\Delta X}\right) \tag{4}$$

In order to determine the fracture toughness, a sharp razor blade was used to initiate a sharp crack in the samples. The ratio of crack length to thickness (depth) ($\frac{a}{W}$) was about (1/3). The fracture toughness was calculated using the following equation [26]:

$$K_{IC} = \frac{p_mS}{BW^{3/2}} f\left(\frac{a}{W}\right) \tag{5}$$

Table 1
Chemical analysis of hemp fibre [12].

	Cellulosic residue (wt%)	Pectin (wt%)	Hemicellulose (wt%)	Lignin (wt%)	(Wax, fat, and protein) (wt%)
Hemp fibre	56.1	20.1	10.9	6	7.9

Table 2
Properties and structure of hemp fabric [12,16].

Fabric thickness (mm)	0.43
Fabric geometry	Woven (plain weave)
Yarn nature	Bundle
Filament size (mm)	0.04253
Number of filaments in a bundle	24
Bundle diameter (mm)	0.21
Opening size (mm)	0.3
Fabric density (gm/cm^3)	0.6
Modulus of elasticity (GPa)	38–58
Tensile strength (MPa)	591–857

Table 3
Physical properties of nanoclay platelets (Cloisite 30B) [5].

Physical properties of the (Cloisite 30B)	
Colour	Off white
Density (g/cm^3)	1.98
d-Spacing (001) (nm)	1.85
Aspect ratio	200–1000
Surface area (m^2/g)	750
Mean particle size (μm)	6

Table 4
Physical properties and chemical compositions of OPC [2].

Properties/Compositions	OPC (ASTM type I)
Physical properties	
Specific gravity	3.17
Specific surface, blaine (cm^2/gm)	3170
Chemical analysis	
SiO_2	21.10
Al_2O_3	5.24
Fe_2O_3	3.10
CaO	64.39
MgO	1.10
SO_3	2.52
Na_2O	0.23
K_2O	0.57
LOI	1.22

where a is the crack length (mm) and $f(\frac{a}{W})$ is the polynomial geometrical correction factor given by following equation:

$$f\left(\frac{a}{W}\right) = \frac{3(a/W)^{1/2}[1.99 - (a/W)(1 - a/W) \times (2.15 - 3.93a/W + 2.7a^2/W^2)]}{2(1 + 2a/W)(1 - a/W)^{3/2}} \quad (6)$$

3. Results and discussion

3.1. Characterisation

3.1.1. XRD analysis

Fig. 2a–d shows the XRD patterns of nanoclay, control cement paste and nanocomposites containing 1 wt% and 3 wt% nanoclay, respectively. International Centre for Diffraction Data (PDF-4 2013) database was used for phase identification. Fig. 2a shows the XRD patterns of nanoclay, it has crystalline phase at 2θ angle of 4.82° which indicates the presence of ammonium salt between the platelets. However, this phase was not detected clearly in nanocomposites. In Fig. 2b–d, three important phases are observed: portlandite [$Ca(OH)_2$] (PDF 00-044-1481), dicalcium sili-

Table 5
Mix proportions of prepared specimens.

Sample name	Hemp fabric (HF) (wt%)	Mix proportions (wt%)		
		Cement	Nanoclay	Water/binder
NCC-0	0	100	0	0.485
NCC-1	0	99	1	0.485
NCC-2	0	98	2	0.485
NCC-3	0	97	3	0.485
NCC-0/HF	2.5	100	0	0.485
NCC-1/HF	2.5	99	1	0.485
NCC-2/HF	2.5	98	2	0.485
NCC-3/HF	2.5	97	3	0.485

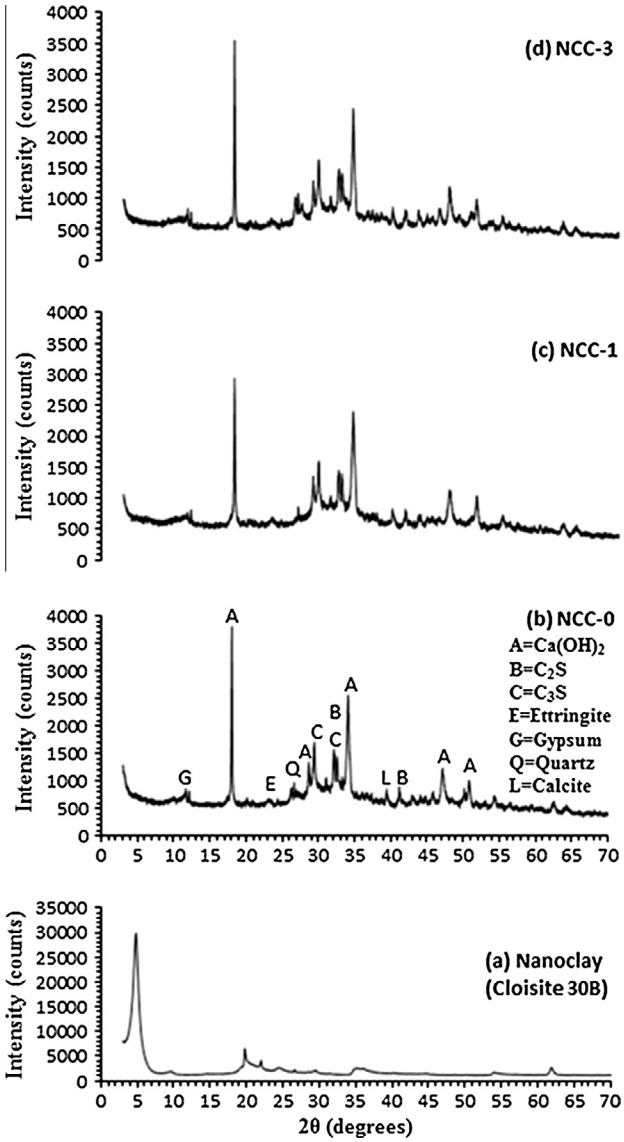

Fig. 2. XRD patterns of: (a) nanoclay, (b) control cement paste, (c) nanocomposites containing 1 wt% nanoclay, and (d) nanocomposites containing 3 wt% nanoclay.

cate [C_2S] (PDF 00-033-0302) and tricalcium silicate [C_3S] (00-049-0442). Moreover, four less important phases are also noticed: Ettringite [$Ca_6Al_2(SO_4)_3(OH)_{12}.26H_2O$] (PDF 000411451), Gypsum [$Ca(SO_4)(H_2O)_2$] (PDF 040154421), Quartz [SiO_2](PDF 000461045) and Calcite [$CaCO_3$](PDF 000050586). The composition of $Ca(OH)_2$ has a well-defined crystallized structure, it has five major peaks in the XRD pattern that corresponds to 2θ of 18.01°, 28.67°, 34.10°, 47.12° and 50.81°, and crystal planes of Miller indices ($h\ k\ l$) of (0 0 1), (1 0 0), (1 0 1), and (1 0 2) and (1 1 0), respectively. Although there are some overlaps of peaks and they have small intensities, dicalcium silicate (C_2S) has four major peaks that correspond to 2θ of 32.05°, 32.14°, 32.59° and 41.21° as well as tricalcium silicate (C_3S) has four major peaks that correspond to 2θ of 29.29°, 32.12°, 32.46° and 51.75°.

Table 6 shows the Quantitative X-ray Diffraction Analysis (QXDA) with Rietveld refinement of cement paste and nanocomposites containing 1 and 3 wt% nanoclay, respectively. Corundum [Al_2O_3] was chosen to serve as an internal standard. It was selected because it does not overlap with important cement peaks up to 2θ of 60° as well as it does not react with water and has no influence on the hydration reaction. However, generally, the addition of 1 and 3 wt% nanoclay into the cement matrix has resulted in apparent change to the crystalline components of the samples. As can be seen from Table 6 and Fig. 2c, the addition of 1 wt% nanoclay reduced the amount of $Ca(OH)_2$ from 19.5% to 15.7%, about 19.5% reduction compared to cement paste. The intensity $Ca(OH)_2$ at 2θ angle of 18.01° also decrease from 3817 to 2940, about 23% reduction compared to cement paste and also other major peaks of $Ca(OH)_2$ crystals were significantly reduced (Fig. 2b and c). Furthermore, the amorphous content was increased slightly from 67.4% to 70%, about 3.7% increase. This result indicates that an obvious consumption of $Ca(OH)_2$ crystals mainly due to the effect of pozzolanic reaction in the presence of nanoclay and good dispersion of nanoclay in the matrix leads to produce more amorphous calcium silicate hydrate gel (C–S–H). This explanation is also confirmed by the inspection of amount of unreacted C_3S (2.1%) and C_2S (8.5), in which the amount of unreacted C_3S and C_2S are slightly higher than the cement paste. Wei et al. [27] reported that pozzolanic reaction decelerates the hydration reaction of C_3S and C_2S during the curing time of 28–112 days. In this study, these unreacted phases could react with water later to produce more C–S–H gel after 56 days.

On the other hand, as can be seen from Table 6 and Fig. 2d for nanocomposites containing 3 wt% nanoclay, there is insignificant effect of nanoclay in the hydration reaction. For example, the amount of $Ca(OH)_2$ was reduced from 19.5% to 18.6%, about 4.6% reduction compared to cement paste. The intensity of $Ca(OH)_2$ at 2θ angle of 18.01° was also slightly reduced from 3817 to 3549, about 7% reduction compared to cement paste (Fig. 2b and d). This may be attributed to agglomerations of nanoclay at high contents which lead to poor dispersion of nanoclay and hence poor pozzolanic reaction. Moreover, the amount of C_3S (1.6%) is similar to the cement paste, and the amount of C_2S (7.4%) is slightly higher than the cement paste by about 4.2%; this also confirms that hydration reaction has occurred more than pozzolanic reaction. Table 6 shows that Ettringite is slightly less in nanocomposites than cement paste. For example, it decreased from 1.8% to 1.1% in nanocomposite containing 1% nanoclay. Overall, the results indicate than 1 wt% nanoclay can consume more $Ca(OH)_2$ crystals and can improve the structure more effectively than 3 wt% nanoclay. The mechanical and physical properties also confirm this phenomenon, which is discussed in the following sections.

Table 6
QXDA results showing the phase abundances in cement paste and nanocomposites containing 1 and 3 wt% nanoclay.

Weight%			
Phase	NCC-0	NCC-1	NCC-3
Portlandite [$Ca(OH)_2$]	19.5	15.7	18.6
Ettringite [$Ca_6Al_2(SO_4)_3(OH)_{12}.26H_2O$]	1.8	1.1	1.2
Gypsum [$Ca(SO_4)(H_2O)_2$]	0.4	0.4	0.6
Tricalcium silicate [C_3S]	1.5	2.1	1.6
Dicalcium silicate [C_2S]	7.1	8.5	7.4
Quartz [SiO_2]	0.4	0.6	0.6
Calcite [$CaCO_3$]	1.1	0.8	1.2
Amorphous content	67.4	70.0	68.0

3.2. Porosity and density

The porosity and density values of cement paste, nano-composites, HF reinforced cement paste and HF reinforced nanocomposites are shown in Fig. 3. Generally the composites containing HF exhibited higher porosity than these without HF. This could be attributed to the formation of voids at the interfacial areas between HF and matrices. However, Fig. 3 shows that the addition of nanoclay decreases the porosity of these composites when compared to control cement paste and HF composites. For nanocomposites with 1 wt% of nanoclay, the porosity decreases by 20.6%. Moreover, in HF reinforced nanocomposites with 1 wt% of nanoclay, it decreases by 16%. This indicates that nanoclay has filling effect in the porosity of cement paste composites with and without HF. This result is in agreement with the work done by Byung-Wan et al. [28] where the porosity of cement mortar is decreased by the addition of nano-SiO_2 particles. In Fig. 3, the addition of 1 wt% of nanoclay increased the density of control cement paste and HF nano-composites by 4% and 3.4% respectively. That improvement demonstrated that cement composites with 1 wt% nanoclay yields more consolidated microstructure. However, the addition of more nanoclay leads to increase in porosity and decrease in density [29]. These results are also supported by the SEM examinations for the microstructure of cement paste, nanocomposites containing 1 wt% and 3 wt% nanoclay. Fig. 4a shows the deposits of $Ca(OH)_2$ crystals are distributed in the cement paste and also in Fig. 4b (at 5 kv), the C–S–H gel connected with many ettringite (needle like hydration products), as well as the pores were extremely existed, in which that revealed weak structure. Fig. 4c shows the SEM micrograph for nanocomposites containing 1 wt% nanoclay, it is different from that of cement paste, the structure is denser and compact with few pores. On the other hand, in Fig. 4d, the nanocomposites containing 3 wt% nanoclay shows more pores and microcracks which weaken the structure.

3.3. Mechanical properties

In general, the addition of nanoclay improved the mechanical properties of the cement matrix. In addition, the pre-soaking of hemp fabric in cement paste during sample preparation leads to good penetration of the cement matrix in between the reinforced filaments of the bundle as shown in Fig. 5, which also improved the mechanical properties of samples [24].

3.3.1. Flexural strength

Figs. 6 and 7 show flexural strength and load-midspan deflection curves for control cement paste, nanocomposites, HF reinforced cement paste and HF reinforced nanocomposites. In general, the incorporation of nanoclay platelets into cement matrix led to a modest enhancement in flexural strength for all nanocomposite samples as shown in Fig. 6. The addition of 1% nanoclay resulted in the highest flexural strength of all nanocomposites. The flexural strength of nanocomposites containing 1 wt% nanoclay is increased from 5.18 to 7.12 MPa, about 37% increase compared to control one. Basically, the improvement in mechanical proper-

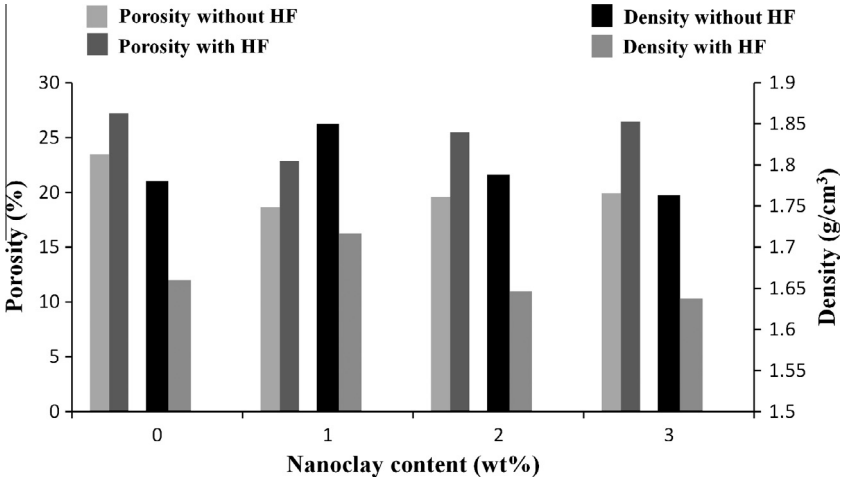

Fig. 3. Porosity and density as a function of nanoclay content for control cement and its nanocomposites with and without HF.

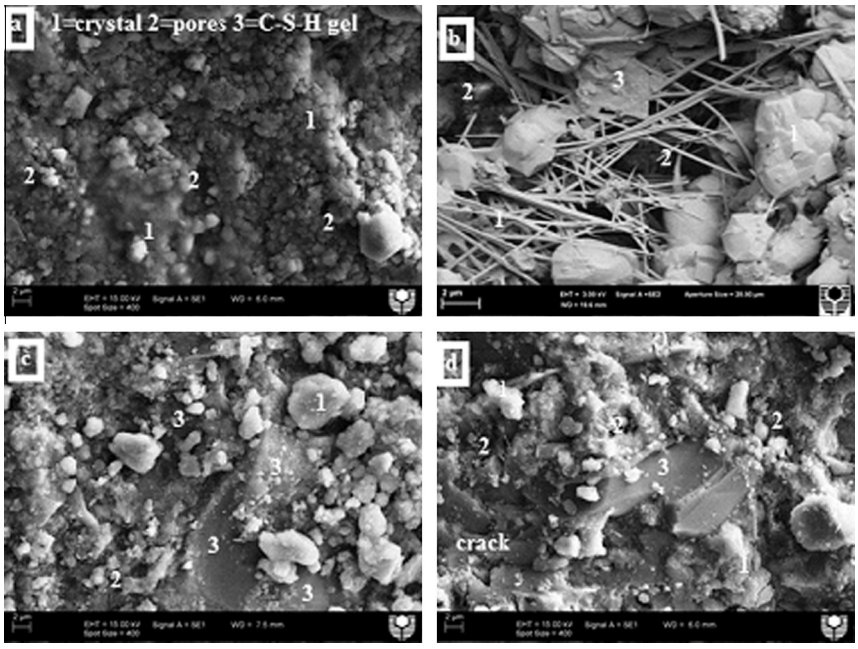

Fig. 4. SEM micrographs of: (a) and (b) cement paste, (c) nanocomposites containing 1 wt% nanoclay and (d) nanocomposites containing 3 wt% nanoclay.

Fig. 5. Penetration of the cement matrix in between the reinforced fibres of hemp fabric.

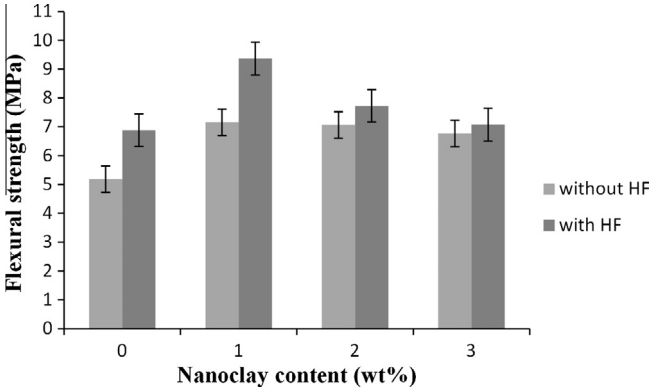

Fig. 6. Flexural strength as a function of nanoclay content for control cement paste and its nanocomposites with and without HF.

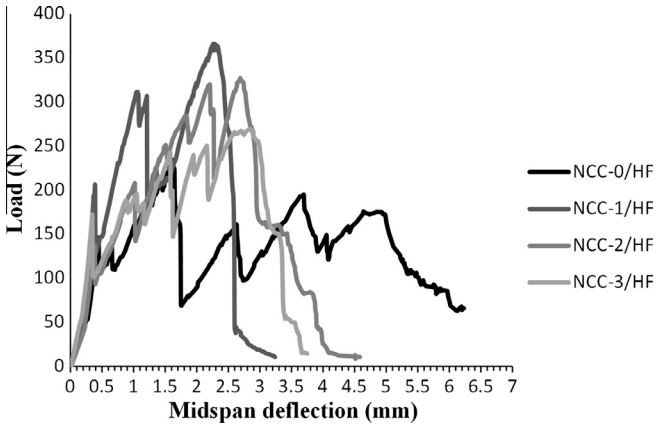

Fig. 7. Load versus mid-span deflection curves for curves for HF reinforced cement composite and HF reinforced nanocomposites from flexural test.

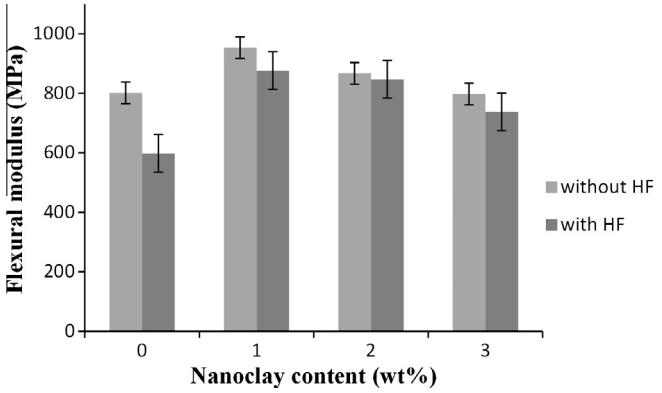

Fig. 8. Flexural modulus as a function of nanoclay content for control cement paste and its nanocomposites with and without HF.

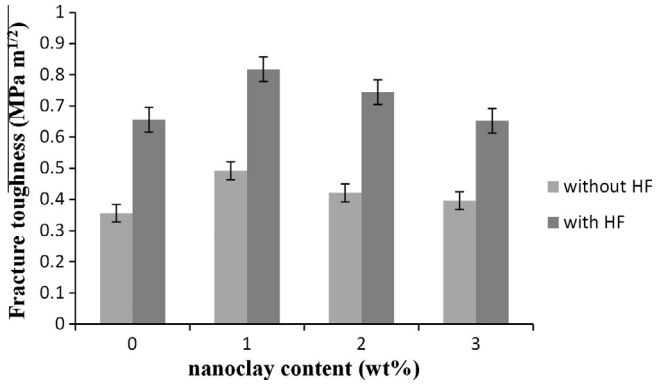

Fig. 9. Fracture toughness as a function of nanoclay content for control cement paste and its nanocomposites with and without HF.

ties of nanocomposites can be attributed to two mechanisms. First is the filling effect where the nanoclay filled the voids or pores in cement paste in which the nano-particles were uniformly dispersed in the matrix thus making the microstructure of nanocomposites denser than the control cement paste [7,30]. Another mechanism is the pozzolanic reaction, in which nanoclay react with free calcium-hydroxide (CH) in cement matrix to produce more calcium silicate hydrate (C–S–H) that also deposited in pore system. However, the addition of more nanoclay than 1 wt% caused a marked decrease in flexural strength. This can be due to the poor

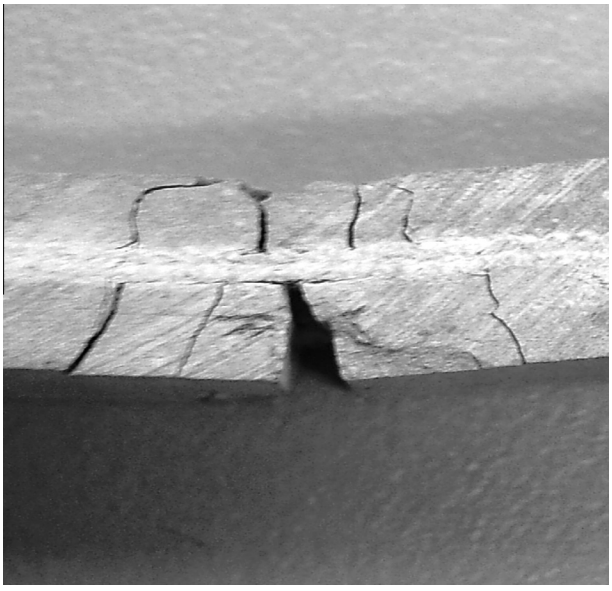

Fig. 10. Multiple cracking behaviour of HF reinforced nanocomposites.

dispersion and agglomerations of the nanoclay in the cement matrix at higher clay contents, which create weak zones, in form of micro-voids as stress concentrators [7,31].

The effect of nanoclay on the flexural strength of HF reinforced cement composite can also be seen in Fig. 6. The flexural strength of HF reinforced nanocomposites containing 1 wt% nanoclay is increased from 6.88 to 9.37 MPa, about 36% increase compared to HF reinforced cement composite. This improvement is explained as follows: in order to improve the interfacial bond between natural fibre and cement paste, the matrix could be modified in which calcium-hydroxide (CH) must be mostly consumed or reduced [32]. In this study, the nanoclay effectively modified the matrix through pozzolanic reaction as described above. Thus, the hemp fabric-nanocomposite matrix adhesion is mostly improved, especially in the case of using 1 wt% nanoclay, which is evident from the higher flexural strength value. Sedan et al. [12] studied the hemp fibre reinforced cement matrix with W/C of 0.5 and optimum hemp fibres content of 16 vol%, with fibre length ranged between 1 and 10 mm. They reported that the flexural strength for untreated hemp fibre reinforced cement matrix was increased from 4.9 to 6.8 MPa, about 38.8% increase compared to cement matrix. Moreover, the flexural strength of NaOH treated hemp fibre reinforced cement matrix was increased to 9.5 MPa, about 93.9% increase compared to cement matrix and also about 39.7% increase compared to untreated fibre reinforced cement matrix. Hence, the improvement in flexural strength of HF reinforced nanocomposites containing 1 wt% nanoclay observed in this study is similar to that observed in Sedan et al. study where hemp fibres is treated by NaOH. However, the addition of more nanoclay (i.e. 3 wt%) led to a slight reduction in flexural strength due to increase in porosity.

The load–midspan deflection curves for HF reinforced cement composite and HF reinforced nanocomposites are shown in Fig. 7. The HF reinforced nanocomposites containing 1 wt% nanoclay shows highest flexural load but smaller deflection capacity at peak load. This is due to high fibre–matrix interface bond, which increases the maximum load capacity. On the other hand, the HF reinforced nanocomposites containing 2 and 3 wt% nanoclay and HF reinforced cement composite show low flexural load but large deflection capacity at peak load, thereby higher ductility. This

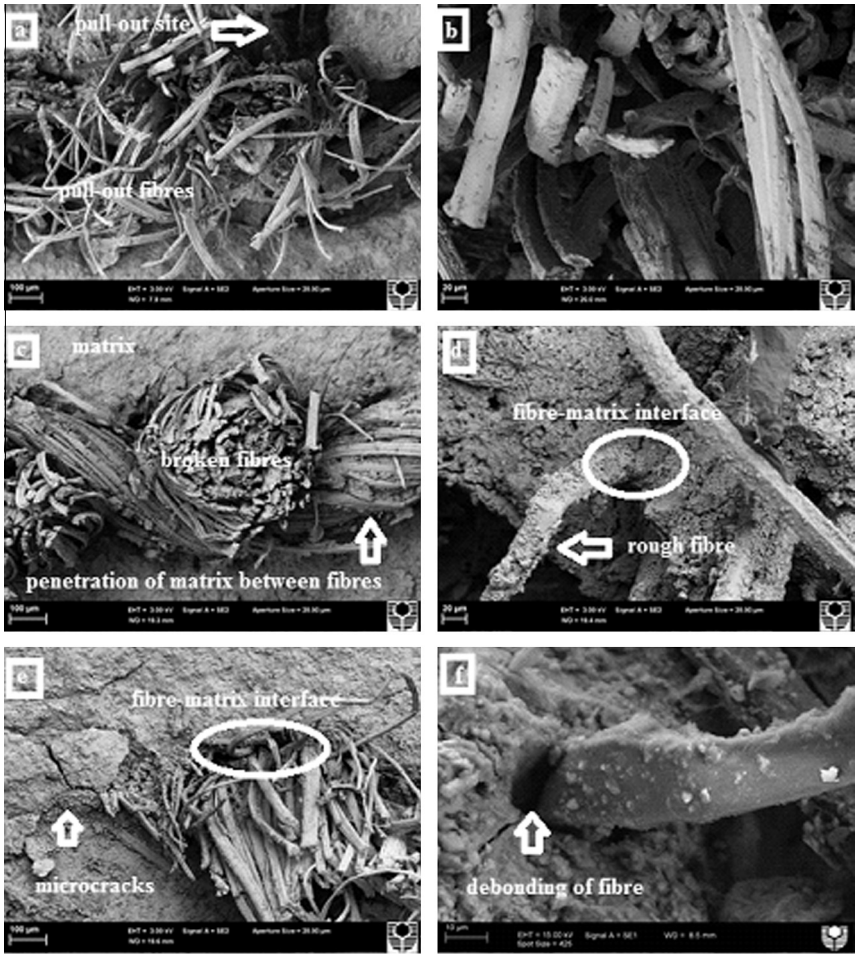

Fig. 11. SEM images of the fracture surface at low and high magnification: (a and b) HF reinforced cement composite, (c and d) HF reinforced nanocomposite containing 1%wt nanoclay, and (e and f) HF reinforced nanocomposite containing 3 wt% nanoclay.

could be attributed to the increase in porosity which decreases the bond strength of fibre–matrix adhesion.

3.3.2. Flexural modulus

The calculated flexural modulus of all composites is shown in Fig. 8. Fig. 8. shows that the addition of 1 wt% nanoclay in cement matrix increased the flexural modulus by 18.9% over control. The addition of HF fabrics adversely affected the flexural modulus for control cement composite and nanocomposites. For example, flexural modulus of control cement paste was decrease from 802.04 to 598.42 MPa, about 25.4% decrease, after the addition of HF fabrics. Similarly, Elsaid et al. [14] reported that as the length of the natural fibres used in a concrete mixture increase, the flexural modulus decrease. However, in HF reinforced nanocomposites the flexural modulus was slightly enhanced. For instance, flexural modulus of HF reinforced nanocomposites containing 1 wt% nanoclay was increase from 802.04 to 876.93 MPa, about 8.5% increase compared to control cement paste.

3.3.3. Fracture toughness

The effect of nanoclay on fracture toughness of control and nanocomposites without and with HF is shown in Fig. 9. In general, all composites containing HF showed significantly improvement in fracture toughness as well as multiple-cracking behaviour as shown in Fig. 10 [33]. In case of nanocomposites, the fracture toughness of control and nanocomposites with 1, 2 and 3 wt% nanoclay was 0.356, 0.492, 0.421 and 0.396 MPa.$m^{1/2}$, respectively. It can be seen clearly that, the nanocomposites with 1 wt% of nanoclay achieve better fracture properties with improvement reaching up to 38.2%. In similar study, Alamri and Low [34] reported that addition of 1 wt% nano-SiC into epoxy matrix significantly increased the fracture toughness by a maximum 89.4% compared to neat epoxy. However, Fig. 10 also shows that facture toughness of nanocomposites decreased slightly when more nanoclay was added .because the poor dispersion of high content of nanoclay leads to agglomeration which increased the porosity as observed in this study. Moreover, agglomeration acts as a stress concentration that can initiate tiny cracks, which leads to crack propagation [7,34].

The influence of HF on fracture toughness is also shown in Fig. 9. As expected, the composites reinforced with HF showed a significant increase in fracture toughness. This extraordinary enhancement is due to fracture resistance by hemp fabrics which resulted in increased energy dissipation from crack-deflection at the fibre–matrix interface, fibre-debonding, fibre-bridging, fibre pull-out and fibre-fracture [2,14,33,35].

The addition of nanoclay, in HF reinforced nanocomposites also increased the fracture toughness. The fracture toughness for HF reinforced nanocomposites containing 1, 2 and 3 wt% nanoclay is 0.818, 0.744, and 0.652 MPa $m^{1/2}$, respectively. This is attributed to the fact that the nanoclay improves the adhesion between hemp fabric and nanocomposite matrix through pozzolanic reaction and reduction of CH, especially in the case of 1 wt% nanoclay in which the increase in fracture toughness was 129.8% comparing to control cement matrix. However, the inclusion of high content of nanoclay increases the porosity which adversely affected the

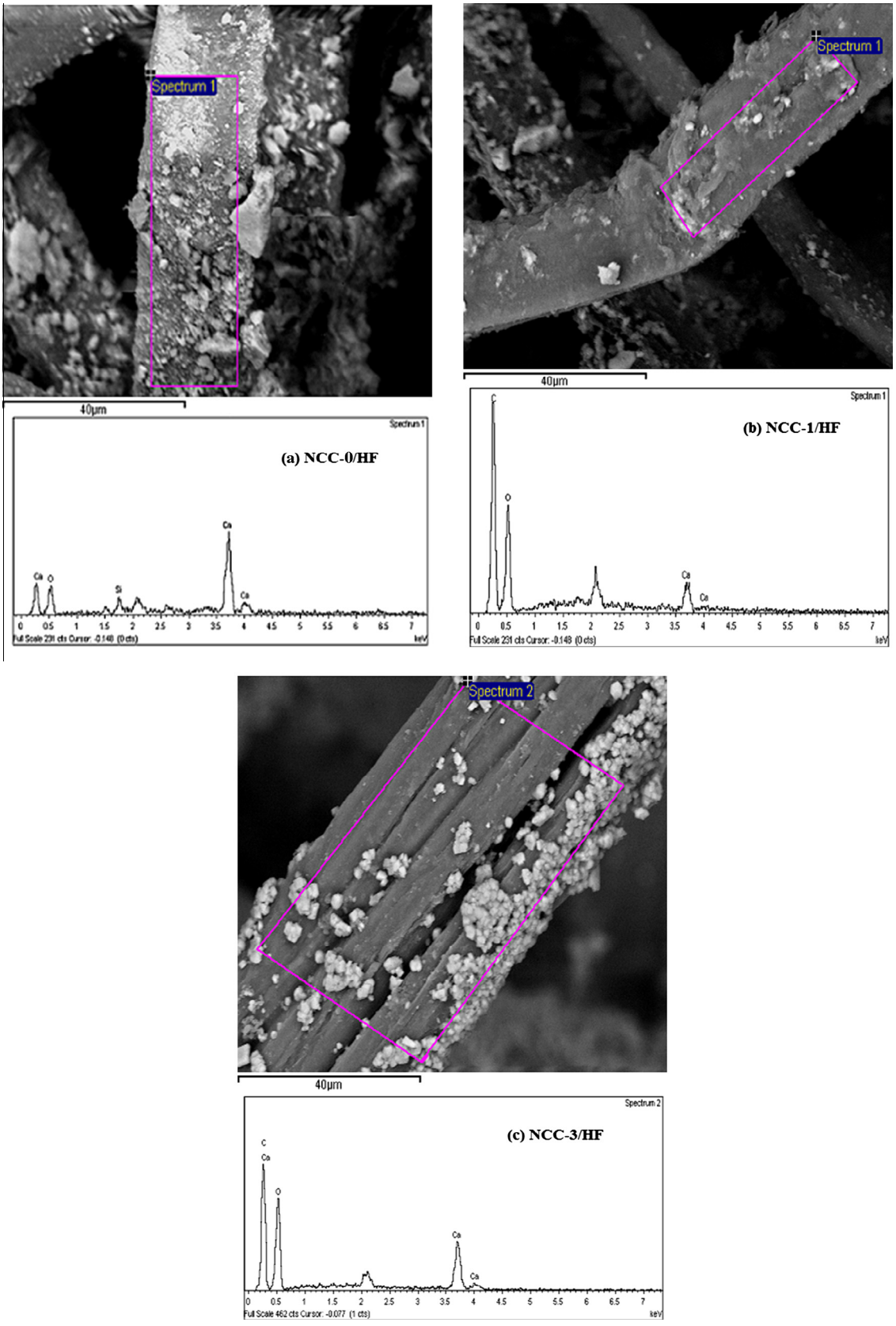

Fig. 12. EDS analysis with SEM images of hemp fabric surface: (a) HF reinforced cement composite, (b) HF reinforced nanocomposite containing 1 wt% nanoclay, and (c) HF reinforced nanocomposite containing 3 wt% nanoclay.

interfacial bond between the matrix and the fabric thus decreased the fracture toughness [36].

3.3.4. SEM micrographs of Failure mechanisms

Fig. 11 shows the SEM micrographs of the fracture surface and HF/matrix interface of HF reinforced cement composite and HF reinforced nanocomposite containing 1 and 3 wt% nanoclay after fracture toughness test. A variety of toughness mechanisms such as shear deformation, crack bridging, fibre pull-out and rupture and matrix fracture can be clearly seen. The examination of fracture surface of HF reinforced nanocomposites containing 1 wt% nanoclay shows good penetration of matrix between hemp filaments (Fig. 11c) as well as rough hemp fibre surface (Fig. 11d). However, poor adhesion between fibres and matrix is observed in HF reinforced cement composite (Fig. 11a and b). In HF reinforced nanocomposite containing 3 wt% nanoclay, macro-crack is observed which revealed relativity weak matrix as shown in Fig. 11e, and also debonding of fibre was occurred (Fig. 11f).

3.3.5. EDS analysis of hemp fabric surface in a cementitous environment

Fig. 12 shows the comparison of Ca^{2+} obtained from EDS analysis on hemp fabric surfaces in different samples. EDS analysis supports that the nanoclay effectively reduced Ca^{2+} ions on the hemp fabric surface. In previous study, Sedan et al. [37] studied a deleterious effect of Ca^{2+} element on hemp fibre degradation. They reported that hemp fibre surface can interact with Ca^{2+} ions to form $Ca(OH)_2$ nodules on it, and this lead to decrease the durability of hemp fibre in alkaline environment. Fig. 12a shows the EDS analysis of hemp fibre surface in cement paste, ratio of Ca^{2+} ions at 37 keV is considered high, this reveal that hemp fibres trapped and fixed Ca^{2+} ions on their surfaces. On contrast, in HF reinforced nanocomposite contain 1 wt%, Fig. 12b, this ratio is significantly decreased. This result could confirm that durability of hemp fibre increased by good consumption of Ca^{2+} ions. On the other hand, HF reinforced nanocomposite containing 3 wt% nanoclay behaves very similar to that of HF reinforced cement composite. In Fig. 12c, it is clearly seen that the ratio of Ca^{2+} ions at 37 keV again increased which could lead to decrease the durability of hemp fibres. This could be attributed to the agglomeration of nanoclay at high content which leads to poor consumption of Ca^{2+} ions.

4. Conclusions

This paper presents the mechanical properties and microstructural characterization of hemp fabric reinforced cement composite and nanocomposites. The optimum content of nanoclay is found to be 1 wt%. In the case of nanocomposite, reduction in porosity (20.6%) and enhancement in density (4%), flexural strength (37%) and fracture toughness (38.2%) are achieved by the addition of 1 wt% nanoclay. However, adding more nanoclay (2 and 3 wt%) adversely affected the above properties due the increased voids and poor dispersion with high clay contents. In the case of the HF reinforced cement composite, it is found that the presence of HF significantly increased the flexural strength (32.6%) and fracture toughness (84.3%) compared to control cement paste. In HF reinforced nanocomposites, the inclusion of nanoclay significantly increased the above mechanical properties compared to control cement paste and HF reinforced cement composite and nanocomposites. It is found that HF reinforced nanocomposites containing 1 wt% nanoclay increased the flexural strength (36%) and fracture toughness (129.8%) compared to cement composite. However, the addition of more nanoclay (more than 1 wt%) into cement or HF reinforced cement composites adversely affected the flexural strength and the fracture toughness. SEM micrographs of HF reinforced nanocomposite containing 1 wt% nanoclay also support the above phenomenon in terms of presence of hydration products on the fibre surface indicating better fibre/matrix interface. The XRD analysis showed that the addition of 1 wt% nanoclay in cement paste reduced the amount of $Ca(OH)_2$ by about 19.5%. However, no such significant reduction is observed when nanoclay content is increased. The SEM micrographs also supported the above, where pores and cracks are observed in the composite containing 3 wt% nanoclay. The EDS analysis also showed less Ca^{2+} ions on the hemp fabric surface in nanocomposites containing 1 wt% nanoclay compared to that containing 3 wt% nanoclay and pure cement composite.

Acknowledgments

The authors would like to thank Mr. Mick Elliss, Mr. Ashley Hughes, Mr. Mark Whittaker, Mr. Andreas Viereckl, Mr. Carl Lewis, Mr. Luke English and Craig Gwyther from Civil Engineering at Curtin University for the assistance with mechanical tests. Authors are also grateful to Mr. Glen Lawson and Mrs. E. Miller from Applied Physics for assistance with SEM.

References

[1] Low IM, Somers J, Kho H, Davies I, Latella B. Fabrication and properties of recycled cellulose fibre-reinforced epoxy composites. Compos Interface 2009;16(1):659–69.
[2] Ahmed SFU, Maalej M, Paramasivam P. Flexural responses of hybrid steel-polyethylene fiber reinforced cement composites containing high volume fly ash. Constr Build Mater 2007;21(1):1088–97.
[3] Jarabo R, Fuente E, Monte MC, Savastano H, Mutjé P, Negro C. Use of cellulose fibers from hemp core in fiber-cement production. Effect on flocculation, retention, drainage and product properties. Ind Crops Prod 2012;39(1):89–96.
[4] Schneider M, Romer M, Tschudin M, Bolio H. Sustainable cement production–present and future. Cem Concr Res 2011;41(1):642–50.
[5] Alhuthali A, Low IM, Dong C. Characterization of the water absorption, mechanical and thermal properties of recycled cellulose fibre reinforced vinyl-ester eco-nanocomposites. Composites Part B 2012;43(7):2772–81.
[6] Nazari A, Riahi S. The effects of zinc oxide nanoparticles on flexural strength of self-compacting concrete. Composites Part B 2011;42(2):167–75.
[7] Morsy MS, Alsayed SH, Aqel M. Hybrid effect of carbon nanotube and nano-clay on physico-mechanical properties of cement mortar. Constr Build Mater 2011;25(1):145–9.
[8] Givi A, Rashid S, Aziz F, Salleh M. Investigations on the development of the permeability properties of binary blended concrete with nano-SiO_2 particles. J Compos Mater 2011;45(19):1931–8.
[9] Qing Y, Zenan Z, Deyu K, Rongshen C. Influence of Nano-SiO_2 addition on properties of hardened cement paste as compared with silica fume. Constr Build Mater 2007;21(1):539–45.
[10] Silva F, Mobasher B. Cracking mechanisms in durable sisal fiber reinforced cement composites. Cem Concr Compos 2009;31(1):721–30.
[11] Islam S, Hussain R, Morshed M. Fiber-reinforced concrete incorporating locally available natural fibers in normal-and high-strength concrete and a performance analysis with steel fiber-reinforced composite concrete. J Compos Mater 2012;46(1):111–22.
[12] Sedan D, Pagnoux C, Smith A, Chotard T. Mechanical properties of hemp fibre reinforced cement: influence of the fibre/matrix interaction. J Eur Ceram Soc 2008;28(1):183–92.
[13] Ali M, Liu A, Sou H, Chouw N. Mechanical and dynamic properties of coconut fibre reinforced concrete. Constr Build Mater 2012;30(1):814–25.
[14] Elsaid A, Dawood M, Seracino R, Bobko C. Mechanical properties of kenaf fiber reinforced concrete. Constr Build Mater 2011;25(4):1991–2001.
[15] Peled A, Bentur A. Geometrical characteristics and efficiency of textile fabrics for reinforcing cement composites. Cem Concr Res 2000;30(1):781–90.
[16] Peled A, Sueki S, Mobasher B. Bonding in fabric-cement systems: effects of fabrication methods. Cem Concr Res 2006;36(1):1661–71.
[17] Peled A, Mobasher B. Tensile behavior of fabric cement-based composites: pultruded and cast. J Mater Civ Eng 2007;19(4):340–8.
[18] Mobasher B, Peled A, Pahilajani J. Distributed cracking and stiffness degradation in fabric-cement composites. Mater Struct 2006;39(1):317–31.
[19] Soranakom C, Mobasher B. Geometrical and mechanical aspects of fabric bonding and pull out in cement composites. Mater Struct 2009;42(1):765–77.
[20] Alamri H, Low IM, Alothman Z. Mechanical, thermal and microstructural characteristics of cellulose fibre reinforced epoxy/organoclay nanocomposites. Composites Part B 2012;43(1):2762–71.
[21] Snoeck D, De Belie N. Mechanical and self-healing properties of cementitious composites reinforced with flax and cottonised flax, and compared with polyvinyl alcohol fibres. Biosyst Eng 2012;111(4):325–35.

[22] Pacheco-Torgal F, Jalali S. Cementitious building materials reinforced with vegetable fibres: a review. Constr Build Mater 2011;25(2):575–81.
[23] Nazari A, Riahi S. The effects of ZrO_2 nanoparticles on properties of concrete using ground granulated blast furnace slag as binder. J Compos Mater 2012;46(9):1079–90.
[24] Peled A, Bentur A. Fabric structure and its reinforcing efficiency in textile reinforced cement composites. Composites Part A 2003;34(1):107–18.
[25] ASTM C-20. Standard test methods for apparent porosity, water absorption, apparent specific gravity, and bulk density of burned refractory brick and shapes by boiling water. ASTM international, 2010.
[26] ASTM E-399. Standard fracture toughness specimens. ASTM international, 2013.
[27] Wei Y, Yao W, Xing X, Wu M. Quantitative evaluation of hydrated cement modified by silica fume using QXRD, Al MAS NMR, TG–DSC and selective dissolution techniques. Constr Build Mater 2012;36(1):925–32.
[28] Jo B, Kim C, Tae G, Park J. Characteristics of cement mortar with nano-SiO_2 particles. Constr Build Mater 2007;21(1):1351–5.
[29] Shebl S, Allie L, Morsy M, Aglan H. Mechanical behavior of activated nano silicate filled cement binders. J Mater Sci 2009;44(6):1600–6.
[30] Chang T, Shih J, Yang K, Hsiao T. Material properties of portland cement paste with nano-montmorillonite. J Mater Sci 2007;42(1):7478–87.
[31] Li H, Xiao H, Yuan J, Ou J. Microstructure of cement mortar with nano-particles. Composites Part B 2004;35(1):185–9.
[32] DeGutiérrez R, Dıaz L, Delvasto S. Effect of pozzolans on the performance of fiber-reinforced mortars. Cem Concr Compos 2005;27(1):593–8.
[33] Ahmed SFU, Mihashi H. Strain hardening behavior of lightweight hybrid polyvinyl alcohol (PVA) fiber reinforced cement composites. Mater Struct 2011;44(1):1179–91.
[34] Alamri H, Low IM. Characterization of epoxy hybrid composites filled with cellulose fibres and nano-SiC. J Appl Polym Sci 2012;126(1):222–32.
[35] Banthia N, Shengb J. Fracture toughness of micro-fiber reinforced cement composites. Cem Concr Compos 1996;18(1):251–69.
[36] Alamri H, Low IM. Microstructural, mechanical, and thermal characteristics of recycled cellulose fiber-halloysite-epoxy hybrid nanocomposites. Polym Compos 2012;33(4):589–600.
[37] Sedan D, Pagnoux C, Chotard T, Smith A, Lejolly D, Gloaguen V. Effect of calcium rich and alkaline solutions on the chemical behaviour of hemp fibres. J Mater Sci 2007;42(1):9336–42.

Corrigendum sheet

This corrigendum sheet shows the error bars for Figure 3 for **"HAKAMY, A.,** SHAIKH, F.U.A. & LOW, I.M. 2013. Microstructures and mechanical properties of hemp fabric reinforced organoclay–cement nanocomposites. *Construction & Building Materials,* 49, 298–307".

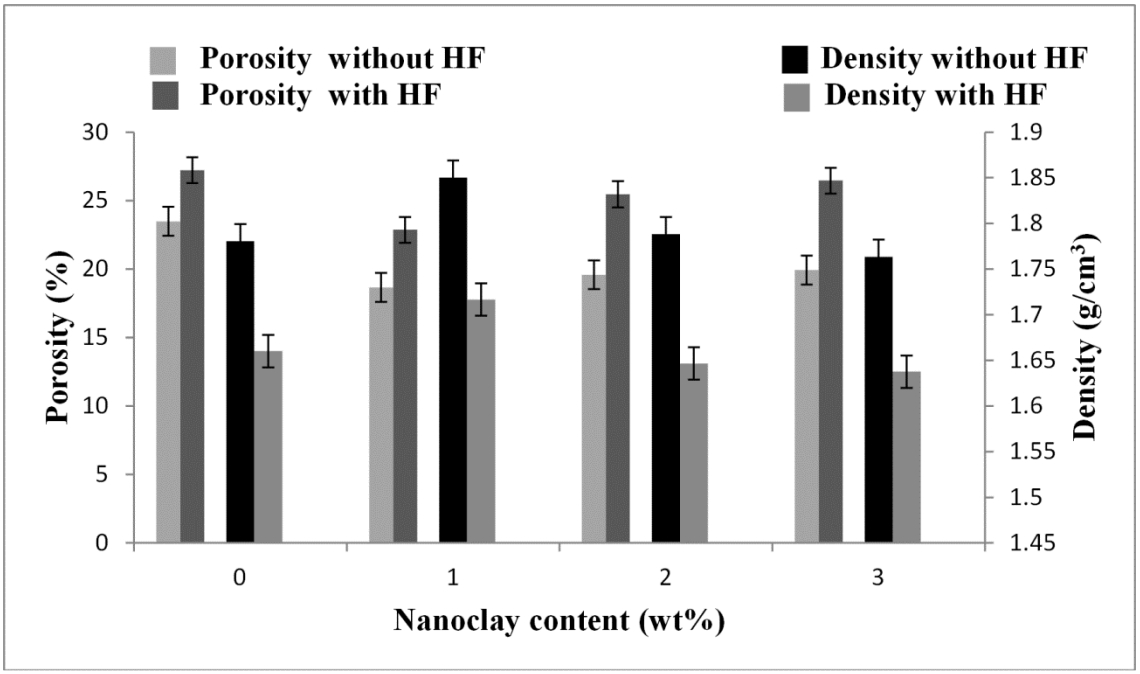

3.2 Thermal and mechanical properties of hemp fabric-reinforced nanoclay–cement nanocomposites.

HAKAMY, A., SHAIKH, F.U.A. & LOW, I.M. 2014. Thermal and mechanical properties of hemp fabric-reinforced nanoclay–cement nanocomposites. *Journal of Materials Science,* 49, 1684–1694.

J Mater Sci (2014) 49:1684–1694
DOI 10.1007/s10853-013-7853-0

Thermal and mechanical properties of hemp fabric-reinforced nanoclay–cement nanocomposites

A. Hakamy · F. U. A. Shaikh · I. M. Low

Received: 22 August 2013 / Accepted: 29 October 2013 / Published online: 14 November 2013

Abstract The influence of nanoclay on thermal and mechanical properties of hemp fabric-reinforced cement composite is presented in this paper. Results indicate that these properties are improved as a result of nanoclay addition. An optimum replacement of ordinary Portland cement with 1 wt% nanoclay is observed through improved thermal stability, reduced porosity and water absorption as well as increased density, flexural strength, fracture toughness and impact strength of hemp fabric-reinforced nanocomposite. The microstructural analyses indicate that the nanoclay behaves not only as a filler to improve the microstructure but also as an activator to promote the pozzolanic reaction and thus improve the adhesion between hemp fabric and nanomatrix.

Introduction

Nowadays, in the building industry, natural fibres and nanomaterials have been gaining increasing attention for two reasons: one is to develop 'environmental-friendly materials' through utilising natural fibres as alternatives to synthetic fibres in fibre-reinforced concrete [1–3] and the other is to 'improve the properties' of Portland cement matrix by adding nanoparticles [4]. Recently, nanoparticles were used in polymer, ceramic and construction materials in order to produce nanocomposites that have superior physical and mechanical properties [5]. In the construction industry, several types of nanoparticles have been incorporated into concretes such as nano-SiO_2, nano-Al_2O_3, nano-Fe_2O_3, nano-ZnO_2, nano-$CaCO_3$, nano-TiO_2, carbon nanotubes and nano-metakaolin in order to improve the durability and mechanical properties of concrete [6–9].

Natural and cellulose fibres are used in polymer and cement matrices to improve their tensile/flexural strength and fracture resistance properties [10, 11]. They are cheaper, biodegradable and lighter than synthetic fibres. Some examples of natural fibres are cotton, sisal, flax, hemp, bamboo, coir, wheat straws and others [12–14]. On the other hand, one of the most effective techniques to obtain a high performance cementitious composite is by reinforcement with textiles (fabrics), which are impregnated with cement paste or mortar. Synthetic (textile) fabrics such as polyethylene (PE) and polypropylene (PP) have been used as reinforcement for cement composites in which fabrics are made of multi-filaments. This system has superior filament–matrix bonding which improves mechanical properties such as tensile and flexural strength better than continuous or short fibres [15–20]. In contrast, the use of natural fibre sheets and fabrics is more prevalent in polymer matrix when compared to a cement-based matrix. For example, using cellulose fibre sheets in epoxy or vinyl–ester matrix has resulted in significantly improved fracture toughness [5, 21].

Despite the advantages of natural fibres and fabrics and also nanoparticles, there are still obstacles which limit their applications in the cementitious composites. Firstly, for natural fibres, the interfacial bond between the natural fibre and the cement matrix is relatively weak and also the degradation of fibres in a high alkaline environment of cement matrix adversely affects the mechanical and durability properties of natural fibre-reinforced cement

A. Hakamy · I. M. Low (✉)
Department of Imaging & Applied Physics, Curtin University, GPO Box U1987, Perth, WA 6845, Australia
e-mail: j.low@curtin.edu.au

F. U. A. Shaikh
Department of Civil Engineering, Curtin University, GPO Box U1987, Perth, WA 6845, Australia

composites [22]. Some researchers have recently recommended that much research is needed to overcome these disadvantages [23]. Secondly, for all nanoparticles, one of the major issues is that increasing the content of nanoparticles leads to reduction of some mechanical properties such as the flexural strength of cement paste [24].

However, little or no research is reported on using of natural fabrics and nanoparticles (e.g. nanoclay) as reinforcement in cement composites. In this paper, nanoclay was utilised as partial replacement for cement at various contents to produce the nanocomposites, and hemp fabrics (HF) were used as reinforcement to fabricate HF-reinforced cement nanocomposites. Natural fibre-reinforced cement-based composites are sustainable alternative to their synthetic fibre-based counterparts, due to their low cost, biodegradability, local availability and extremely low energy-intensive manufacturing process. However, the bond of natural fibres with the cement matrix is relatively weak and high alkalinity of cement matrix can adversely affect the durability of natural fibres in the composites, which ultimately affects the mechanical and durability properties of the composites. The use of nanoclay in natural fibre-reinforced cement composites is expected to reduce the alkalinity of cement matrix by consuming calcium hydroxide during the pozzolanic reaction, hence improving the durability of natural fibres in the composite. The densely packed nanoclay–cement matrix can also improve its bonding with natural fibres, thus imparting better stress transfer and improved mechanical properties. Therefore, this study evaluated the effect of different nanoclay contents on various mechanical and physical properties of cement matrix and hemp fabric-reinforced cement composites. The effect of nanoclay on thermal behaviour of hemp fabric-reinforced composites was also evaluated in this study. The microstructures of nanocomposites and HF-reinforced cement nanocomposites were also investigated using synchrotron radiation diffraction and scanning electron microscopy.

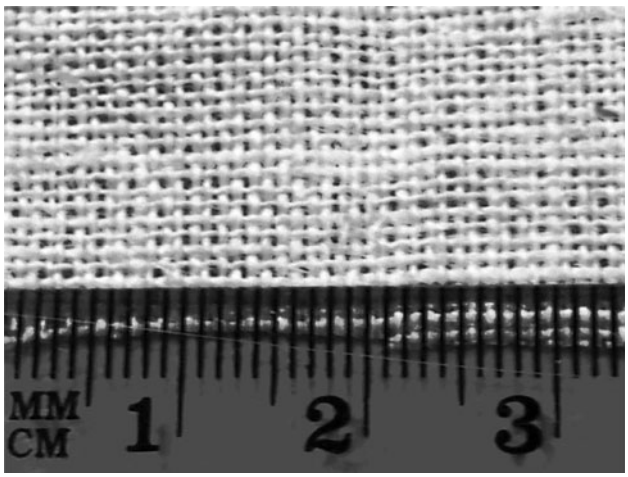

Fig. 1 Structure of hemp fabric

Table 1 Chemical analysis of hemp [12]

	Cellulosic residue (wt%)	Pectin (wt%)	Hemicellulose (wt%)	Lignin (wt%)	Wax, fat, protein (wt%)
Hemp fibre	56.1	20.1	10.9	6	7.9

Table 2 Properties and structure of hemp fabric [12]

Fabric thickness (mm)	0.43
Fabric geometry	Woven (plain weave)
Yarn nature	Bundle
Filament size (mm)	0.04253
Number of filaments in a bundle	24
Bundle diameter (mm)	0.21
Opening size (mm)	0.3
Fabric density (g/cm^3)	0.6
Modulus of elasticity (GPa)	38–58
Tensile strength (MPa)	591–857

Experimental procedure

Materials

Hemp fabric (HF) and nanoclay platelets (Cloisite 30B) were used as reinforcements for the cement-matrix composites. The hemp fabric, as shown in Fig. 1, was supplied by Hemp Wholesale Australia Pty. Kalamunda, Western Australia. The chemical composition, and the physical properties and structure of hemp fabric are shown in Tables 1 and 2, respectively [12, 16]. The nanoclay platelets (Cloisite 30B) used in this investigation are based on natural montmorillonite clay (hydrated sodium calcium aluminium magnesium silicate hydroxide $(Na,Ca)_{0.33}(Al,Mg)_2(Si_4O_{10})(OH)_2{\cdot}nH_2O$). Cloisite 30B is a natural montmorillonite modified with a quaternary ammonium salt, which was supplied by Southern Clay Products, USA. The specifications and physical properties of Cloisite 30B are outlined in Table 3 [5]. Ordinary Portland cement (OPC) was used in all mixes. The chemical composition and physical properties of OPC are listed in Table 4 [2].

Sample preparation

Nanocomposites

In this study, the OPC is partially substituted by nanoclay with 1, 2 and 3 wt% of OPC. The OPC and nanoclay were

Table 3 Physical properties of the nanoclay platelets (Cloisite 30B) [5]

Physical properties	
Colour	Off white
Density (g/cm^3)	1.98
d-spacing (001) (nm)	1.85
Aspect ratio	200–1000
Surface area (m^2/g)	750
Mean particle size (μm)	6

Table 4 Physical properties and chemical composition of OPC [2]

Properties/compositions	OPC (ASTM Type I)
Physical properties	
Specific gravity	3.17
Specific surface, blaine (cm^2/g)	3170
Chemical analysis	
SiO_2	21.10
Al_2O_3	5.24
Fe_2O_3	3.10
CaO	64.39
MgO	1.10
SO_3	2.52
Na_2O	0.23
K_2O	0.57
LOI	1.22

first dry mixed for 5 min in a Hobart mixer at a low speed and then mixed for another 10 min at high speed until homogeneity was achieved. The cement–nanocomposite paste was prepared by adding water with a water/binder (nanoclay–cement) ratio of 0.48. The cement paste without nanoclay was considered as the control.

Hemp fabric-reinforced nanocomposites

Two layers of hemp fabric were used in hemp fabric-reinforced nanocomposites. The hemp fabrics were first soaked into the matrix in order to achieve a better penetration of the matrix in the openings of the fabrics. The fabrication of the hemp fabric-reinforced nanocomposite specimens was done in five steps. First, a thin layer of matrix was poured into the mould, then the pre-soaked hemp fabric was laid on top of it, then another layer of matrix was poured into the mould followed by another pre-soaked hemp fabric and the final layer of matrix. The total amount of hemp fabric in each specimen was about 2.5 wt%. The mix proportions are given in Table 5.

Table 5 Mix proportions of specimens

Sample name	Hemp fabric (HF) (wt%)	Mix proportions (wt%)		
		Cement	Nanoclay	Water/binder
NCC-0	0	100	0	0.485
NCC-1	0	99	1	0.485
NCC-2	0	98	2	0.485
NCC-3	0	97	3	0.485
NCC-0/HF	2.5	100	0	0.485
NCC-1/HF	2.5	99	1	0.485
NCC-2/HF	2.5	98	2	0.485
NCC-3/HF	2.5	97	3	0.485

Curing and specimens

For each series, three prismatic plate specimens of 300 × 70 × 10 mm dimensions were cast. All specimens were demolded after 24 h of casting and kept under water for approximately 56 days. Five rectangular specimens of each series with dimensions 70 × 20 × 10 mm were cut from the fully cured prismatic plate for each mechanical and physical test [16].

Characterisation

High-resolution transmission electron microscopy (HRTEM)

High-resolution transmission electron microscopy imaging was done using 3000F (JEOL company) operating at 300 kV equipped with a 4 × 4 k CCD camera (Gatan). HRTEM is an imaging technique that creates images with atomic resolution. 3000F has excellent HRTEM performance including 0.195-nm point resolution and 0.104-nm lattice resolution. HRTEM was carried out at the University of Western Australia. Nanoclay (Cloisite 30B) powder was dispersed in ethanol inside a small glass container by using an ultrasonic device for 15 min. After that, few drops of suspension were mounted onto a copper grid and kept to dry.

Synchrotron radiation diffraction (SRD)

Synchrotron radiation diffraction (SRD) measurement was carried out on the powder diffraction beamline at the Australian Synchrotron. The diffraction patterns of each sample were collected using a wavelength of 0.825 Å in the 2θ range of 8°–52°.

Scanning electron microscopy (SEM)

Scanning electron microscopy imaging was obtained using a NEON 40ESB, ZEISS. The SEM investigation was

carried out in detail on microstructures and the fractured surfaces of samples. Specimens were coated with a thin layer of platinum before observation by SEM to avoid charging.

Thermogravimetric analysis (TGA)

The thermal stability of samples was studied by thermogravimetric analysis (TGA). A Mettler Toledo TGA 1 star system analyser was used for all these measurements. Samples of 25 mg were placed in an alumina crucible and tests were carried out in Argon atmosphere with a heating rate of 10 °C/min from 25 to 1000 °C.

Physical properties

Measurements of bulk density and porosity were conducted to determine the quality of nanocomposites. The thickness, width, length and weight were measured in order to determine the bulk density. The calculation for density was carried out by using the following equation:

$$\rho = \frac{m_d}{V} \tag{1}$$

where ρ = density in (g/cm^3), m_d = mass of the dried sample (g) and V = volume of the test specimen (cm^3).

The value of apparent porosity P_S was determined using the Archimedes principle in accordance with the ASTM Standard (C-20) and clean water was used as the immersion water. The apparent porosity P_S was calculated using the following equation [25]:

$$P_S = \frac{m_s - m_d}{m_s - m_i} \times 100 \tag{2}$$

where m_i = mass of the sample saturated with and suspended in water and m_s = mass of the sample saturated in air.

For the water absorption test, the produced specimens were dried at a temperature of 80 °C until their mass became constant and then the mass was weighed (W_0). The specimens were then immersed in clean water at a temperature of 20 °C for 48 h. After the desired immersion period, the specimens were taken out, wiped quickly with a wet cloth and then the mass was weighed (W_1) immediately. The rate of water absorption (W_A) was calculated using the formula

$$W_A = \frac{W_1 - W_0}{W_0} \times 100 \tag{3}$$

Mechanical properties

Five specimens, measuring 70 × 20 × 10 mm, in each composition were used to measure the mechanical properties. Three-point bend tests were conducted using a LLOYD material testing machine to evaluate the flexural strength and fracture toughness of the composites. The support span used was 40 mm with a displacement rate of 0.5 mm/min. The flexural strength σ_F was evaluated using the following equation:

$$\sigma_F = \frac{3P_m S}{2BW^2} \tag{4}$$

where P_m is the maximum load at crack extension, S is the span of the sample, W is the specimen thickness (depth) and B is the specimen width.

In order to determine the fracture toughness, a sharp razor blade was used to initiate a sharp crack in the samples. The ratio of the crack length to thickness (depth) ($\frac{a}{W}$) was about 1/3. The fracture toughness was calculated using the following equation [26, 27]:

$$K_{IC} = \frac{p_m S}{BW^{3/2}} f\left(\frac{a}{W}\right) \tag{5a}$$

where a is the crack length (mm) and $f\left(\frac{a}{W}\right)$is the polynomial geometrical correction factor given by

$$f\left(\frac{a}{W}\right) = \frac{3(a/W)^{1/2}[1.99 - (a/W)(1 - a/W) \times (2.15 - 3.93a/W + 2.7a^2/W^2)]}{2(1 + 2a/W)(1 - a/W)^{3/2}} \tag{5b}$$

The impact strength of the composite was determined using a Zwick Charpy impact tester with 1.0 J pendulum hammer. Unnotched sampled were used to compute the impact strength using the following formula:

$$\sigma_I = \frac{E}{A} \tag{6}$$

where E is the impact energy to break a sample with a ligament of area A.

Results and discussion

Characterisation

High-resolution transmission electron microscopy (HRTEM)

HRTEM images for nanoclay (Cloisite 30B) are shown in Fig. 2a, b. The lower magnification image in Fig. 2a gives a general view of the nanoclay platelets. The high magnification image in Fig. 2b shows the layer structure of nanoclay platelets. It can be seen clearly that the distances between the nanoclay platelets were about 1.85 nm, and thus this is evidence that the d-spacing of (0 0 1) planes in nanoclay layers were 1.85 nm as shown in Table 3 [21].

Synchrotron radiation powder diffraction (SRD)

The synchrotron radiation powder diffraction (SRD) patterns of nanoclay, cement paste and nanocomposites containing 1, 2 and 3 wt% nanoclay, respectively, are shown in Fig. 3a–e. The database of the International Centre for Diffraction Data (PDF-4 2013) was used for phase identification. It is common that PDF is calculated according to Cu Ka wavelength ($\lambda = 1.5406$ Å), but because synchrotron wavelength ($\lambda = 0.825$ Å) was used in this study, the PDF database was adjusted according to synchrotron wavelength. However, the serial number of PDF and d-spacing which identify phases did not change, but the two-theta was shifted. Figure 3a shows the SRD pattern of nanoclay. It has a crystalline phase which refers to Montmorillonite-18A [$Na_{0.3}(Al,Mg)_2Si_4O_{10}OH_2{\cdot}6H_2O$] (PDF000120219). However, this phase was not detected clearly in nanocomposites. In Fig. 3b–e, three important phases can be seen: portlandite [$Ca(OH)_2$] (PDF 00-044-1481), dicalcium silicate [C_2S] (PDF 00-033-0302) and tricalcium silicate [C_3S] (00-049-0442). Moreover, there are two less important phases: Quartz [SiO_2] (PDF 000461045) and Calcite [$CaCO_3$] (PDF 000050586) [28, 29].

The composition of $Ca(OH)_2$ has a well-defined crystallized structure; it has five major peaks in the SRD pattern, which correspond to 2θ angles of 9.61°, 15.23°, 18.06°, 24.71° and 26.56°. Although there are some overlaps of peaks and they have small intensities, dicalcium silicate (C_2S) has four major peaks that correspond to 2θ angles of 16.48°, 17.04°, 17.28° and 21.72°, and tricalcium silicate (C_3S) has four major peaks that correspond to 2θ angles of 15.61°, 17.05°, 17.23° and 26.98°. However, generally, the addition of nanoclay reduced the intensities of $Ca(OH)_2$ crystals compared to the control cement paste. In the nanocomposite containing 1 wt% nanoclay, the intensities of $Ca(OH)_2$ crystals significantly reduced compared with the control. This result indicates that an obvious consumption of $Ca(OH)_2$ crystals happens in the cement–nanocomposite mainly due to the effect of pozzolanic reaction in the

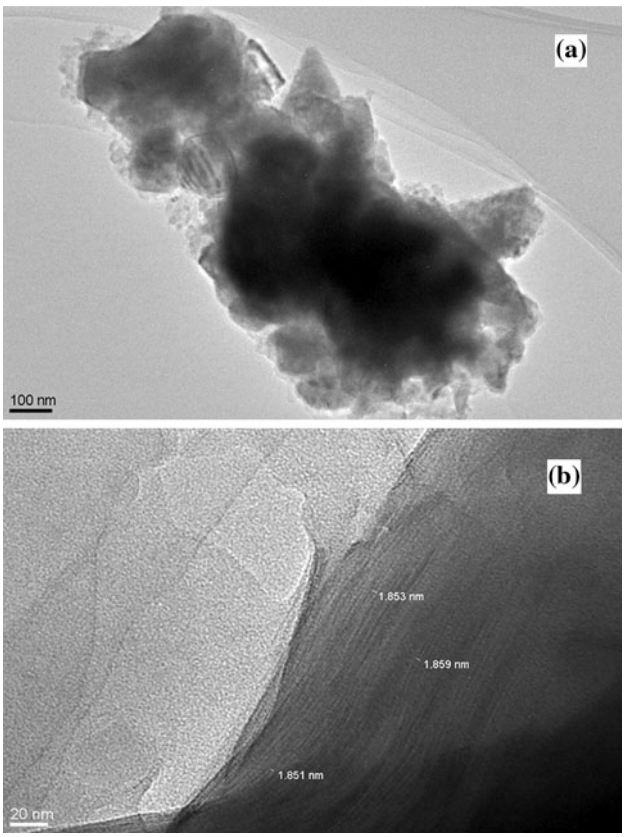

Fig. 2 TEM images of nanoclay (Cloisite 30B) at **a** low magnification, **b** high magnification

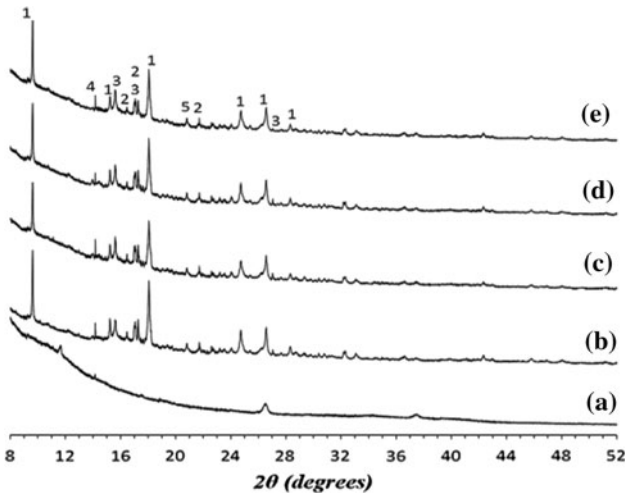

Fig. 3 Synchrotron radiation diffraction (SRD) patterns of **a** nanoclay, **b** cement paste, **c** nanocomposites containing 1wt % nanoclay, **d** nanocomposites containing 2 wt% nanoclay and **e** nanocomposites containing 3 wt% nanoclay. *Numbers* indicate: *1* = Portlandite [$Ca(OH)_2$] phase, *2* = Dicalcium silicate [C_2S] phase, *3* = Tricalcium silicate [C_3S] phase, *4* = Quartz [SiO_2] phase and *5* = Calcite [$CaCO_3$] phase

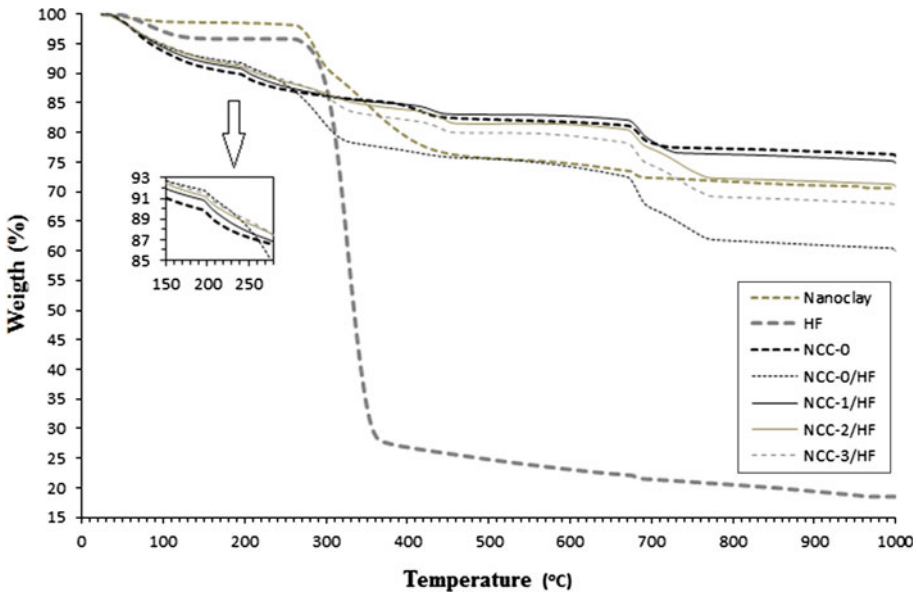

Fig. 4 TGA curves of nanoclay, hemp fabric (HF), cement paste, HF-reinforced cement composite and HF-reinforced nanocomposites

Table 6 Thermal properties of nanoclay, hemp fabric (HF), cement paste, HF-reinforced cement composite and HF-reinforced nanocomposites

Sample	Char yield at different temperatures (%)									
	100 °C	200 °C	300 °C	400 °C	500 °C	600 °C	700 °C	800 °C	900 °C	1000 °C
Nanoclay	98.76	98.52	90.81	79.02	75.64	74.75	72.35	71.68	71.01	70.64
HF	97.01	95.85	86.89	26.79	24.75	23.06	21.40	20.48	19.36	18.48
NCC-0	93.63	89.38	86.14	84.35	82.21	81.77	78.19	77.25	76.81	76.08
NCC-0/HF	94.61	91.41	81.02	76.85	75.58	74.21	67.08	61.69	61.02	59.99
NCC-1/HF	94.27	90.32	86.23	84.70	83.03	82.76	78.46	76.30	75.81	74.85
NCC-2/HF	94.77	90.80	86.52	83.82	81.47	81.34	77.15	72.18	71.76	70.86
NCC-3/HF	94.89	91.14	85.93	82.10	79.94	79.43	74.39	69.04	68.55	67.62

presence of nanoclay and good dispersion of nanoclay in the matrix which lead to the production of more amorphous calcium silicate hydrate gel (C–S–H). This result is in agreement with the work done by Chang et al. [29] where the intensities of $Ca(OH)_2$ crystals were decreased by the addition of 0.6 wt% nano-montmorillonite into cement paste. On the other hand, for nanocomposites containing 3 wt%, there are insignificant effects. This may be attributed to agglomerations of nanoclay at high contents which lead to poor pozzolanic reaction. Overall, the results indicate that nanomatrix with 1 wt% nanoclay can consume more $Ca(OH)_2$ crystals and can improve the structure more effectively than 3 wt% nanoclay.

Thermal stability and properties

The thermal stability of samples was determined using thermogravimetric analysis (TGA). In this test, the thermal stability was studied in terms of the weight loss as a function of temperature in Argon atmosphere. The thermograms (TGA) of nanoclay, hemp fabric, cement paste, HF-reinforced cement composite and HF-reinforced nanocomposites are shown in Fig. 4. The char yields at different temperatures are summarized in Table 6. For hemp fabric, it can be seen from the TGA curve that the weight loss (%) between 285 and 375 °C is due to the decomposition of cellulose. This result is in agreement with Rachini et al. [30] where the weight loss (%) of hemp fibres under Argon in the range of 280–380 °C is due to cellulose decomposition. Concerning nanoclay, it can be seen from the TGA curve that the weight loss (%) between 300 and 400 °C is due to decomposition of the ammonium salts on montmorillonite.

The TGA analysis shows three distinct stages of decomposition in cement paste, HF-reinforced cement composite and HF-reinforced nanocomposites. The first stage of decomposition is between room temperature and 230 °C, which may be related to the decomposition of Ettringite and dehydration of C–S–H gel. The second stage of decomposition is between 420 and 500 °C, which corresponds to $Ca(OH)_2$ decomposition. The last stage of decomposition is between 670 and 780 °C, which corresponds to $CaCO_3$ decomposition [31, 32]. In the first stage,

HF-reinforced nanocomposites show slightly better thermal stability than cement paste due to resistance of nanoclay to the decomposition. In the second stage, the HF-reinforced nanocomposites containing 1 wt% show better thermal stability than all samples due to dense and compact nanomatrix through consumption of CH and formation of secondary CSH gels during pozzolanic reaction [33]. On the other hand, HF-reinforced nanocomposites containing 3 wt% show lower thermal stability than all cement pastes and other HF-reinforced nanocomposites, in which this result confirms that a slightly poor pozzolanic reaction has occurred and hence nanomatrix is less compacted. Moreover, HF-reinforced cement composites and pure nanoclay show lower thermal stability than others. At 800–1000 °C, HF-reinforced nanocomposites containing 1 wt% show thermal stability slightly less than cement paste, but better than other samples. From Table 6 at 1000 °C, the char residue of cement paste and HF-reinforced cement composite was about 76.08 and 59.99 wt%, respectively. The char residue of HF-reinforced nanocomposites containing 1, 2 and 3 wt% was about 74.85, 70.86 and 67.62 wt%, respectively. It can be seen that HF-reinforced nanocomposites containing 1 wt% performed better in thermal stability with higher char residue of 74.85 wt% than other samples. In a similar study, Chen et al. [34] reported that the addition of 10 wt% nano-TiO_2 into cement paste improved the thermal stability of nanocomposite, in which it was a non-reactive filler.

Porosity and density

The porosity, density and water absorption values of cement paste, nanocomposites, HF-reinforced cement paste and HF-reinforced nanocomposites are shown in Table 7. Generally, the composites containing HF exhibited higher porosity and water absorption that those without HF. This could be attributed to the formation of voids at the interfacial areas between HF and matrices. However, Table 7 shows that the addition of nanoclay decreases the porosity and water absorption of these composites when compared to control cement paste and HF composites. For nanocomposites with 1 wt% of nanoclay, the porosity decreases by 20.6 % and water absorption decreases by 23.5 % compared to cement paste. Moreover, in HF-reinforced nanocomposites containing 1 wt% of nanoclay, the porosity and water absorption decrease by 16 and 18.8 %, respectively, compared to HF-reinforced cement composite. This indicates that nanoclay has a filling effect in the porosity of cement paste composites with and without HF. This result is in agreement with the work done by Jo et al. [35] where the porosity of cement mortar is decreased by the addition of nano-SiO_2 particles. In Table 7, the addition of 1 wt% of nanoclay increased the density of control cement paste and HF-reinforced composites by 4 and 3 %, respectively. This improvement demonstrated that cement composites with 1 wt% nanoclay yield more consolidated microstructure. However, the addition of more nanoclay leads to an increase in porosity and a decrease in density [36]. SEM examinations for the microstructure of nanocomposites containing 1 and 3 wt% nanoclay are shown in Fig. 5a, b. The SEM micrograph for nanocomposites containing 1 wt% of nanoclay (Fig. 5a) shows that the structure is denser and compact with few pores. On the other hand, in Fig. 5b, the nanocomposites containing 3 wt% nanoclay shows more pores and microcracks which weaken the structure.

Table 7 Density, porosity and water absorption values for cement paste and its nanocomposites with and without HF

Samples	Density (g/cm^3)	Porosity (%)	Water absorption (%)
NCC-0	1.78	23.48	13.18
NCC-1	1.85	18.64	10.08
NCC-2	1.78	19.57	10.96
NCC-3	1.76	19.91	11.30
NCC-0/HF	1.66	27.21	16.40
NCC-1/HF	1.71	22.86	13.32
NCC-2/HF	1.64	25.45	15.45
NCC-3/HF	1.63	26.45	16.15

Mechanical properties

Flexural strength

Flexural strength of control cement paste, nanocomposites, HF-reinforced cement paste and HF-reinforced nanocomposites is shown in Table 8. In general, the incorporation of nanoclay in cement matrix led to a modest enhancement in flexural strength of all nanocomposites and HF-reinforced nanocomposites. The flexural strength of nanocomposites containing 1 wt% nanoclay is increased by 31.9 % compared to the control one. This improvement can be attributed to pozzolanic and filler effect of 1 wt% nanoclay which led to a denser nanomatrix than the control cement matrix [7, 29]. The effect of nanoclay on the flexural strength of HF-reinforced cement composite can also be seen in Table 8. The flexural strength of HF-reinforced nanocomposites containing 1 wt% nanoclay is increased from 6.9 to 8.8 MPa, about 28.5 % increase compared to HF-reinforced cement composite. This could be attributed to good hemp fabric–nanocomposite matrix adhesion. An analogous study was done by Khorami and Ganjian [37] where cement matrix was reinforced with 4 wt% bagasse fibres, and cement was replaced by 5 % silica fume by weight. The flexural strength was increased by about 20 %

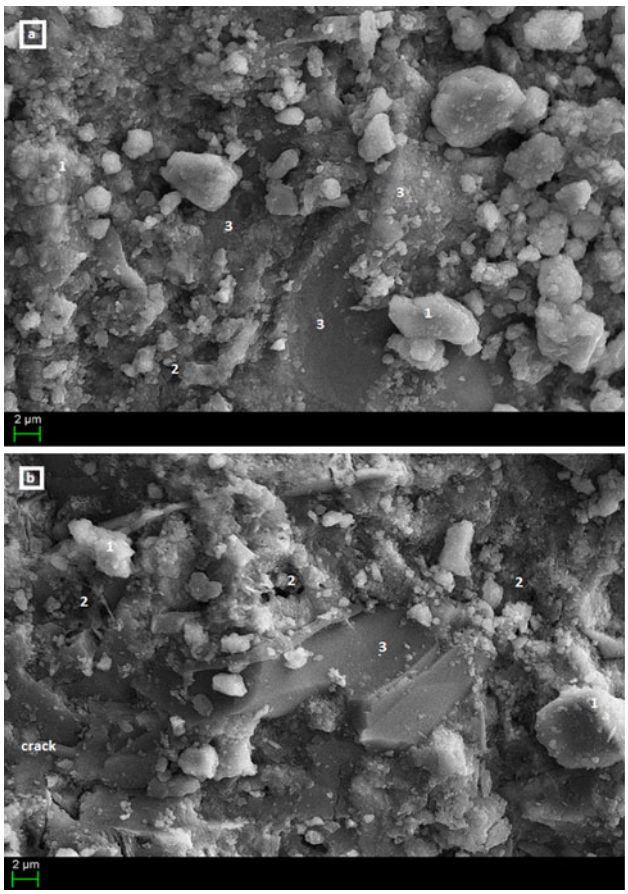

Fig. 5 SEM micrographs of **a** nanocomposites containing 1 wt% nanoclay and **b** nanocomposites containing 3 wt% nanoclay. *Numbers* indicate: *1* = [$Ca(OH)_2$] crystals, *2* = pores and *3* = C–S–H gel

Table 8 Flexural strength and fracture toughness of cement paste and its nanocomposites with and without HF

Samples	Flexural strength (MPa)	Fracture toughness (MPa $m^{1/2}$)
NCC-0	5.43 ± 0.51	0.35 ± 0.02
NCC-1	7.16 ± 0.53	0.46 ± 0.03
NCC-2	7.06 ± 0.11	0.42 ± 0.05
NCC-3	6.76 ± 0.44	0.39 ± 0.02
NCC-0/HF	6.88 ± 0.52	0.65 ± 0.05
NCC-1/HF	8.84 ± 0.40	0.81 ± 0.08
NCC-2/HF	7.72 ± 0.26	0.74 ± 0.02
NCC-3/HF	7.07 ± 0.57	0.66 ± 0.09

compared to the control bagasse fibre-reinforced cement matrix in that study. They attributed this improvement to the pozzolanic and filler effects of very fine silica fume particles, which led to enhancement of the bond strength between the matrix and the fibres. However, the addition of more nanoclay than 1 wt% caused a marked decrease in flexural strength of nanocomposites and HF-reinforced

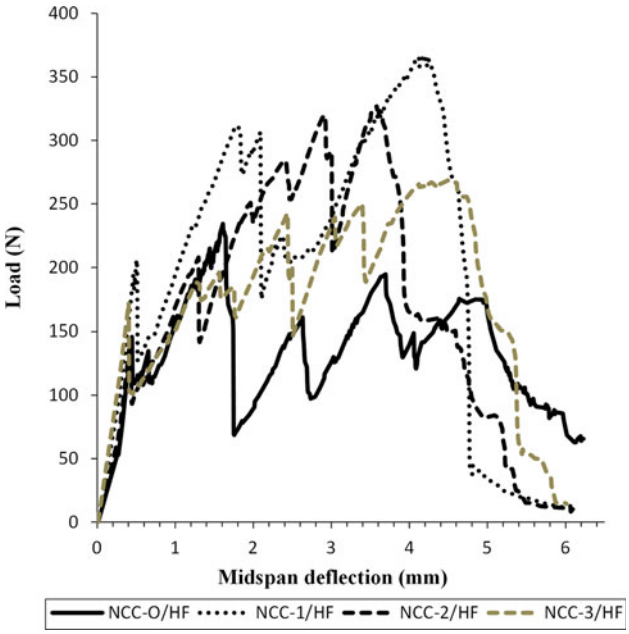

Fig. 6 Load–midspan deflection curves for HF-reinforced cement composite and HF-reinforced nanocomposites from flexural test

nanocomposites containing 2 and 3 wt% nanoclay in this study. This was due to the poor dispersion and agglomerations of the nanoclay in the cement matrix at higher clay contents, which led to an increase in porosity and decreased the bond between the fibres and the nanomatrix [7, 38].

The load–midspan deflection curves for HF-reinforced cement composite and HF-reinforced nanocomposites are shown in Fig. 6. The HF-reinforced nanocomposites containing 1 wt% nanoclay show the highest flexural load. This is due to a high fibre–matrix interface bond, which increases the maximum load capacity. On the other hand, the HF-reinforced nanocomposites containing 2 and 3 wt% nanoclay and HF-reinforced cement composite show a low flexural load. This could be attributed to the increase in porosity which decreases the bond strength of fibre–nanomatrix adhesion.

Fracture toughness

The fracture toughness of the control and nanocomposites with and without HF is shown in Table 8. In general, all composites containing HF showed significant improvement in fracture toughness. This enhancement is due to fracture resistance by hemp fabrics which resulted in increased energy dissipation from crack deflection at the fibre–matrix interface, fibre debonding, fibre bridging, fibre pull-out and fibre fracture [2, 14, 39, 40]. In the case of nanocomposites, the fracture toughness of control cement paste and nanocomposites with 1, 2 and 3 wt% nanoclay was 0.35, 0.46,

0.42 and 0.39 MPa $m^{1/2}$, respectively. It can be seen clearly that the nanocomposites with 1 wt% of nanoclay achieved the highest fracture properties with improvement reaching up to 31.4 %. The addition of nanoclay into HF-reinforced nanocomposites also increased the fracture toughness. The fracture toughness of HF-reinforced composites and HF-reinforced nanocomposites containing 1, 2 and 3 wt% nanoclay were 0.65, 0.81, 0.74 and 0.66 MPa $m^{1/2}$, respectively. It can again be seen that the fracture toughness of HF-reinforced nanocomposites containing 1 wt% nanoclay is increased by 24.6 % compared to HF-reinforced cement matrix. This is attributed to the fact that the nanoclay modified the matrix through pozzolanic reaction and reduced the $Ca(OH)_2$ content. Thus, a good interfacial bond between the nanomatrix and the hemp fibres was achieved. In a similar study, Alamri and Low [41] reported that the addition of 1 wt% halloysite nanotubes (HNTs) into recycled cellulose fibres (RCF)/epoxy matrix significantly increased the fracture toughness by 38.8 % compared to RCF-reinforced epoxy composites. However, facture toughness of nanocomposites and HF-reinforced nanocomposites decreased slightly with more nanoclay addition. This is attributed to the poor dispersion of a high content of nanoclay into the matrix, which leads to an increase in porosity and weakens the interfacial bond between the fibres and the nanomatrix [40]. Figure 7 shows the SEM micrographs of HF/matrix interface of HF-reinforced nanocomposite containing 1 and 3 wt% nanoclay after the fracture toughness test. The examination of the fracture surface of HF-reinforced nanocomposites containing 1 wt% nanoclay shows a good fibre–matrix interface as well as the presence of hydration products on the fibre surface indicating a better fibre/matrix interface bond (Fig. 7a). On the other hand, poor fibre–matrix interface, debonding of fibre and microcracks are observed in HF-reinforced nanocomposite containing 3 wt% nanoclay (Fig. 7b), which revealed a relatively weak matrix.

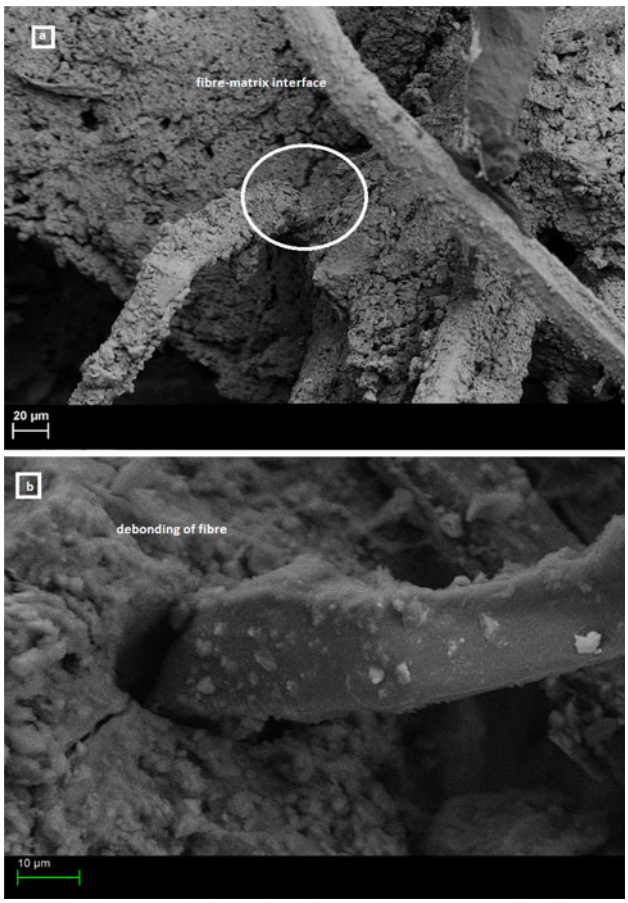

Fig. 7 SEM images of the fracture surface after fracture toughness test: **a** HF-reinforced nanocomposite containing 1 wt% nanoclay and **b** HF-reinforced nanocomposite containing 3 wt% nanoclay

Impact strength

The impact strength can be defined as the ability of the material to withstand impact loading [27, 42]. As shown in Fig. 8, the presence of nanoclay enhanced the impact strength for HF-reinforced nanocomposites. The impact strength of HF-reinforced nanocomposites containing 1 wt% nanoclay was 2.45 kJ/m^2, about 23 % increase compared to HF-reinforced cement composite. This is due to good interfacial bonding between the fibres and the nanomatrix. But, as clay loading increased, the impact strength decreased. For example, the impact strength of HF-reinforced nanocomposites containing 3 wt% nanoclay was 2.25 kJ/m^2, about 13 % increase compared to HF-reinforced cement composite. This reduction in impact strength at higher clay loading was due to the formation of clay agglomerates and voids which led to reduced fibre–nanomatrix adhesion. Alhuthali and Low [5] reported that

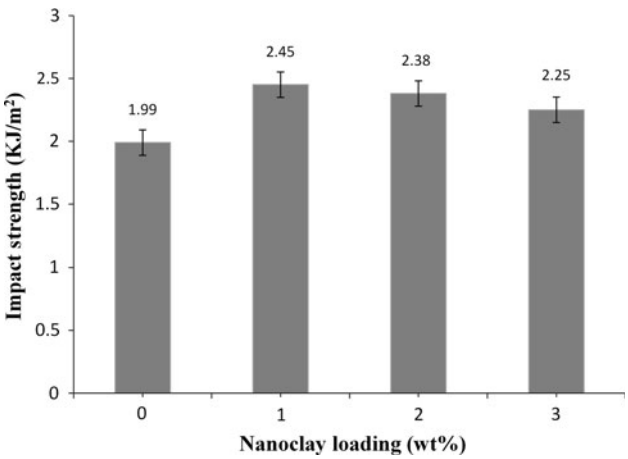

Fig. 8 Impact strength as a function of nanoclay content for HF-reinforced composite and HF-reinforced nanocomposites

the addition of 3 wt% nanoclay into RCF/vinyl ester matrix increased the impact strength by 27 % compared to RCF-reinforced vinyl ester composites.

Conclusions

The effect of nanoclay on thermal, physical and mechanical properties of hemp fabric-reinforced cement nanocomposite has been investigated. The optimum content of nanoclay is found to be 1 wt%. SRD analysis and SEM micrographs showed that HF-reinforced nanocomposite containing 1 wt% nanoclay has a denser microstructure than others, and thus this improvement led to enhancement of the hemp fabric–nanomatrix adhesion. In addition, the incorporation of 1 wt% nanoclay into the HF-reinforced nanocomposites improved the thermal stability, decreased the porosity and water absorption and increased the density, flexural strength, fracture toughness and impact strength when compared to the HF-reinforced cement composite. However, the addition of more nanoclay (>1 wt%) into the HF-reinforced cement composites adversely affected the thermal, physical and mechanical properties.

Acknowledgements The authors are grateful to Mrs. E. Miller and Mr. T. Wang from Applied Physics for assistance with the SEM and TEM. We also acknowledge the facilities, and the scientific and technical assistance of the Australian Microscopy & Microanalysis Research Facility at the Centre for Microscopy, Characterisation & Analysis, The University of Western Australia, a facility funded by the University, State and Commonwealth Governments.

References

1. Low IM, Somers J, Kho H, Davies I, Latella B (2009) Fabrication and properties of recycled cellulose fibre-reinforced epoxy composites. Compos Interface 16:659–669
2. Ahmed SFU, Maalej M, Paramasivam P (2007) Flexural responses of hybrid steel–polyethylene fiber reinforced cement composites containing high volume fly ash. Constr Build Mater 21:1088–1097
3. Jarabo R, Fuente E, Monte MC, Savastano H, Mutjé P, Negro C (2012) Use of cellulose fibers from hemp core in fiber–cement production. Effect on flocculation, retention, drainage and product properties. Ind Crops Prod 39:89–96
4. Schneider M, Romer M, Tschudin M, Bolio H (2011) Sustainable cement production—present and future. Cem Concr Res 41:642–650
5. Alhuthali A, Low IM, Dong C (2012) Characterization of the water absorption, mechanical and thermal properties of recycled cellulose fibre reinforced vinyl-ester eco-nanocomposites. Compos Part B 43:2772–2781
6. Nazari A, Riahi S (2011) The effects of zinc oxide nanoparticles on flexural strength of self-compacting concrete. Compos Part B 42:167–175
7. Morsy MS, Alsayed SH, Aqel M (2011) Hybrid effect of carbon nanotube and nano-clay on physico-mechanical properties of cement mortar. Constr Build Mater 25:145–149
8. Givi A, Rashid S, Aziz F, Salleh M (2011) Investigations on the development of the permeability properties of binary blended concrete with nano-SiO_2 particles. J Compos Mater 45:1931–1938
9. Qing Y, Zenan Z, Deyu K, Rongshen C (2007) Influence of nano-SiO_2 addition on properties of hardened cement paste as compared with silica fume. Constr Build Mater 21:539–545
10. Silva F, Mobasher B (2009) Cracking mechanisms in durable sisal fiber reinforced cement composites. Cem Concr Compos 31:721–730
11. Islam S, Hussain R, Morshed M (2012) Fiber-reinforced concrete incorporating locally available natural fibers in normal- and high-strength concrete and a performance analysis with steel fiber-reinforced composite concrete. J Compos Mater 46:111–122
12. Sedan D, Pagnoux C, Smith A, Chotard T (2008) Mechanical properties of hemp fibre reinforced cement: influence of the fibre/matrix interaction. J Eur Ceram Soc 28:183–192
13. Ali M, Liu A, Sou H, Chouw N (2012) Mechanical and dynamic properties of coconut fibre reinforced concrete. Constr Build Mater 30:814–825
14. Elsaid A, Dawood M, Seracino R, Bobko C (2011) Mechanical properties of kenaf fiber reinforced concrete. Constr Build Mater 25:1991–2001
15. Peled A, Bentur A (2000) Geometrical characteristics and efficiency of textile fabrics for reinforcing cement composites. Cem Concr Res 30:781–790
16. Peled A, Sueki S, Mobasher B (2006) Bonding in fabric–cement systems: effects of fabrication methods. Cem Concr Res 36:1661–1671
17. Peled A, Mobasher B (2007) Tensile behavior of fabric cement-based composites: pultruded and cast. J Mater Civ Eng 19:340–348
18. Mobasher B, Peled A, Pahilajani J (2006) Distributed cracking and stiffness degradation in fabric–cement composites. Mater Struct 39:317–331
19. Soranakom C, Mobasher B (2009) Geometrical and mechanical aspects of fabric bonding and pull out in cement composites. Mater Struct 42:765–777
20. Peled A, Bentur A (2003) Fabric structure and its reinforcing efficiency in textile reinforced cement composites. Compos Part A 34:107–118
21. Alamri H, Low IM, Alothman Z (2012) Mechanical, thermal and microstructural characteristics of cellulose fibre reinforced epoxy/organoclay nanocomposites. Compos Part B 43:2762–2771
22. Snoeck D, De Belie N (2012) Mechanical and self-healing properties of cementitious composites reinforced with flax and cottonised flax, and compared with polyvinyl alcohol fibres. Biosyst Eng 111:325–335
23. Pacheco-Torgal F, Jalali S (2011) Cementitious building materials reinforced with vegetable fibres: a review. Constr Build Mater 25:575–581
24. Nazari A, Riahi S (2012) The effects of ZrO_2 nanoparticles on properties of concrete using ground granulated blast furnace slag as binder. J Compos Mater 46:1079–1090
25. ASTM C-20 (2010) Standard test methods for apparent porosity, water absorption, apparent specific gravity, and bulk density of burned refractory brick and shapes by boiling water
26. ASTM E-399 (2013) Standard fracture toughness specimens
27. Toutanji H, Xu B, Gilbert J, Lavin T (2010) Properties of poly (vinyl alcohol) fiber reinforced high-performance organic aggregate cementitious material: converting brittle to plastic. Constr Build Mater 24:1–10
28. ASTM C-1365–06 (2011) Standard test method for determination of the proportion of phases in Portland cement and Portland-cement clinker using X ray powder diffraction analysis
29. Chang T, Shih J, Yang K, Hsiao T (2007) Material properties of portland cement paste with nano-montmorillonite. J Mater Sci 42:7478–7487

30. Rachini A, Le Troedec M, Peyratout C, Smith A (2009) Comparison of the thermal degradation of natural, alkali-treated and silane-treated hemp fibers under air and an inert atmosphere. J Appl Polym Sci 112:226–234
31. Lothenbach B, Winnefeld F, Alder C, Wieland E, Lunk P (2007) Effect of temperature on the pore solution, microstructure and hydration products of Portland cement pastes. Cem Concr Res 37:483–491
32. Djaknoun S, Ouedraogo E, Benyahia A (2012) Characterisation of the behaviour of high performance mortar subjected to high temperatures. Constr Build Mater 28:176–186
33. Wei Y, Yao W, Xing X, Wu M (2012) Quantitative evaluation of hydrated cement modified by silica fume using QXRD, Al MAS NMR, TG–DSC and selective dissolution techniques. Constr Build Mater 36:925–932
34. Chen J, Kou S, Poon C (2012) Hydration and properties of nano-TiO2 blended cement composites. Cem Concr Compos 34:642–649
35. Jo B, Kim C, Tae G, Park J (2007) Characteristics of cement mortar with nano-SiO_2 particles. Constr Build Mater 21:1351–1355
36. Shebl S, Allie L, Morsy M, Aglan H (2009) Mechanical behavior of activated nano silicate filled cement binders. J Mater Sci 44:1600–1606
37. Khorami M, Ganjian E (2011) Comparing flexural behaviour of fibre–cement composites reinforced bagasse: wheat and eucalyptus. Constr Build Mater 25:3661–3667
38. Li H, Xiao H, Yuan J, Ou J (2004) Microstructure of cement mortar with nano-particles. Compos Part B 35:185–189
39. Ahmed SFU, Mihashi H (2011) Strain hardening behavior of lightweight hybrid polyvinyl alcohol (PVA) fiber reinforced cement composites. Mater Struct 44:1179–1191
40. Alamri H, Low IM (2012) Characterization of epoxy hybrid composites filled with cellulose fibres and nano-SiC. J Appl Polym Sci 126:222–232
41. Alamri H, Low IM (2012) Microstructural, mechanical, and thermal characteristics of recycled cellulose fiber–halloysite–epoxy hybrid nanocomposites. Polym Compos 33:589–600
42. Zhou X, Ghaffar S, Dong W, Oladiran O, Fan M (2013) Fracture and impact properties of short discrete jute fibre-reinforced cementitious composites. Mater Des 49:35–47

3.3 Characteristics of hemp fabric reinforced nanoclay–cement nanocomposites.

HAKAMY, A., SHAIKH, F.U.A. & LOW, I.M. 2014. Characteristics of hemp fabric reinforced nanoclay–cement nanocomposites. *Cement & Concrete Composites,* 50, 27–35.

Cement & Concrete Composites 50 (2014) 27–35

Contents lists available at ScienceDirect

Cement & Concrete Composites

journal homepage: www.elsevier.com/locate/cemconcomp

Characteristics of hemp fabric reinforced nanoclay–cement nanocomposites

A. Hakamy [a,b], F.U.A. Shaikh [c], I.M. Low [a,*]

[a] Department of Imaging & Applied Physics, Curtin University, GPO Box U1987, Perth, WA 6845, Australia
[b] Department of Physics, Umm Al-Qura University, P.O. Box 715, Makkah, Saudi Arabia
[c] Department of Civil Engineering, Curtin University, GPO Box U1987, Perth, WA 6845, Australia

ARTICLE INFO

Article history:
Received 25 June 2013
Received in revised form 4 February 2014
Accepted 9 March 2014
Available online 28 March 2014

Keywords:
Cement
Nanoclay
Hemp fabric
Mechanical properties
Microstructure

ABSTRACT

Cement eco-nanocomposites reinforced with hemp fabric (HF) and nanoclay platelets (Cloisite 30B) are fabricated and investigated in terms of X-ray diffraction, scanning electron microscopy, physical and mechanical properties. Results indicated that the mechanical properties generally increased as a result of the addition of nanoclay into the cement matrix with HF. An optimum replacement of ordinary Portland cement with 1 wt% nanoclay decreased the porosity and also significantly increased the density, flexural strength and fracture toughness of HF-reinforced nanocomposite. The microstructural results indicate that the nanoclay behaves not only as a filler to improve the microstructure, but also as an activator to promote the pozzolanic reaction and thus improved the adhesion with hemp fabric. The failure micromechanisms and energy dissipative processes in HF-reinforced cement composite and HF-reinforced nanocomposite are discussed in terms of microstructural observations. These cement eco-nanocomposites can provide new insights for the development of new 'environmental-friendly nanomaterials' for building applications such as the construction of sandwich panels, ceilings and roofs.

1. Introduction

Nowadays, in the building industry, natural fibres and nanomaterials have been gaining increasing attention due to two reasons. One is to develop 'environmentally friendly materials' through utilizing natural fibres as alternative to synthetic fibres in fibre-reinforced concrete [1–3]. Another is to improve the properties of Portland cement matrix by adding nanoparticles [4]. Recently, nanoparticles are used in polymer, ceramic and construction materials, particularly producing nanocomposites which have superior physical and mechanical properties [5]. In the construction industry, several types of nanoparticles have been incorporated into concretes such as nano-SiO_2, nano-Al_2O_3, nano-Fe_2O_3, nano-ZnO_2, nano-$CaCO_3$, nano-TiO_2, carbon nanotubes and nano-metakaolin in order to improve the durability and mechanical properties of concrete [6–9].

Natural and cellulose fibres are used in polymer and cement matrices to improve their tensile/flexural strength and fracture resistance properties [10,11]. They are cheaper, biodegradable and lighter than synthetic fibres. Some examples of natural fibres are: cotton, sisal, flax, hemp, bamboo, coir, wheat straws and others [12–14]. On the other hand, one of the most effective techniques to obtain a high performance cementitious composite is by reinforcement with textile (fabrics), which are impregnated with cement paste or mortar. Synthetic (textile) fabrics such as polyethylene (PE) and polypropylene (PP) have been used as reinforcement for cement composites, in which fabrics are made of multi-filaments. This system has superior filament-matrix bonding which improve mechanical properties such as tensile and flexural strength more than continuous or short fibres [15–20]. In contrast, the use of natural fibre sheets and fabrics is more prevalent in polymer matrix when compared to cement-based matrix. For example, using cellulose sheets in epoxy or viny-ester matrix have improved the fracture toughness significantly [5,21].

Despite the advantages of natural fibres and fabrics and also nanoparticles, there are still obstacles which limit their applications in the cementitious composites. Firstly, for natural fibres, the interfacial bond between the natural fibre and the cement matrix is relatively weak and also the degradation of fibres in a high alkaline environment of cement matrix adversely affects the mechanical and durability properties of natural fibre reinforced cement composites [22]. Some researchers have recently recommended that much research is needed to overcome these disadvantages [23]. Secondly, for all nanoparticles, one of the major issues is that increasing the content of nanoparticles leads to

* Corresponding author. Tel.: +61 892667544; fax: +61 892662377.
E-mail address: j.low@curtin.edu.au (I.M. Low).

http://dx.doi.org/10.1016/j.cemconcomp.2014.03.002
0958-9465/

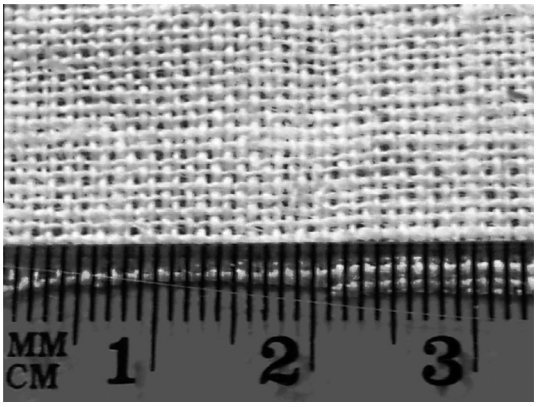

Fig. 1. Optical micrograph of hemp fabric.

reduction of some mechanical properties such as the flexural strength of cement paste [24]. However, little or no research is reported on using of natural fabrics and nanoparticles (e.g. nanoclay) as reinforcement in cement-composites.

In this paper, a novel material which involves synthesizing cement eco-nanocomposites has been investigated. Nanoclay was utilised as partial replacement of cement at various contents to produce the nanocomposites and hemp fabrics (HF) were used to reinforce these nanocomposites. The effects of different amounts of nanoclay on mechanical properties of HF-reinforced cement nanocomposites have been evaluated. The microstructures of hemp fabrics and eco-nanocomposite were investigated using X-ray diffraction and scanning electron microscopy.

2. Experimental procedure

2.1. Materials

Hemp fabric (HF) and nanoclay (Cloisite 30B) were used as reinforcements for the cement-matrix composites. The HF was supplied by Hemp Wholesale Australia Pty. Kalamunda, Western Australia as shown in Fig. 1. The chemical composition and physical properties of hemp fabric are shown in Tables 1 and 2, respectively [12,16]. The nanoclay (Cloisite 30B) used in this investigation are based on natural montmorillonite clay (hydrated sodium calcium aluminium magnesium silicate hydroxide $(Na,Ca)_{0.33}(Al,Mg)_2(Si_4O_{10})(OH)_2{\cdot}nH_2O$). Cloisite 30B is a natural montmorillonite modified with a quaternary ammonium salt, which was supplied by Southern Clay Products, USA. The specification and physical properties of Cloisite 30B are outlined in Table 3 [5]. Ordinary Portland cement (OPC) was used in all mixes. The chemical composition and physical properties of OPC are listed in Table 4 [2].

2.2. Sample preparation

2.2.1. Nanocomposites

In this study, the OPC was partially substituted with nanoclay of 1%, 2% and 3% by weight of OPC. The OPC and nanoclay were first dry mixed for 5 min in Hobart mixer at a low speed and then mixed for another 10 min at high speed until homogeneity was achieved.

Table 2
Properties and structure of hemp fabric [12,16].

Fabric thickness (mm)	0.43
Fabric geometry	Woven (plain weave)
Yarn nature	Bundle
Filament size (mm)	0.04253
Number of filaments in a bundle	24
Bundle diameter (mm)	0.21
Opening size (mm)	0.3
Fabric Density (g/cm^3)	0.6
Modulus of elasticity (GPa)	38–58
Tensile strength (MPa)	591–857

The cement–nanocomposite paste (matrix) was prepared through adding water with a water/binder (nanoclay–cement) ratio of 0.48.

2.2.2. Hemp fabric reinforced nanocomposites

Firstly, hemp fabrics were washed with water and dried for 4 h at room temperature before beginning the casting, in order to reduce the effect of water absorption (hydrophilic effect) by hemp fabrics. Pacheco-Torgal and Jalali [23] indicated that hemp fibre has the lower water absorption (about 85–105%) compared to other natural fibres, such as, bamboo (145%), sisal (110%) and banana (407%). Secondly, eight layers of hemp fabrics were used in hemp fabric reinforced nanocomposites, in which their positions were placed above and below the centre of the nanocomposite sample over the depth of the specimen. Before each hemp fabric was laid into the mould, the hemp fabric was initially soaked into the nanocomposites matrix for 5 min, and then it was laid on polished timber slab and left under heavy weight 20 kg for about 3–4 min, this step is very critical in order to achieve a better penetration of the matrix in between the openings of the fabrics and to reduce air bubbles and voids inside the fabric. The fabrication of the hemp fabric reinforced nanocomposite specimen was done in sequential steps. First, a thick layer of matrix (about 12 mm depth) was poured into the mould, then the fresh pre-soaked hemp fabric (about 0.7 mm depth) was laid on top of it. After that another thin layer of matrix (about 1.5 mm depth) was poured into the mould followed by the other fresh pre-soaked hemp fabric and then the final thick layer of the matrix (about 12 mm depth). Finally, the mould was placed on a concrete vibrating table for several seconds to reduce the air bubbles and voids inside the specimens. The total amount of hemp fabric in each specimen was about 2.4 wt%. The mix proportions are given in Table 5.

2.2.3. Sample curing

For each series, four prismatic plate specimens of $40 \times 40 \times 160$ mm^3 in dimension were cast. All specimens were demolded after 24 h of casting and kept under water for approximately 56 days [25].

2.3. Characterisation

2.3.1. X-ray diffraction

The samples were measured on a D8 Advance Diffractometer (Bruker-AXS) using copper radiation and a LynxEye position sensitive detector. The diffractometer were scanned from 7° to 70° (2θ) in steps of 0.015° using a scanning rate of 0.5°/min. XRD patterns

Table 1
Chemical analysis of hemp [12].

	Cellulosic residue (wt%)	Pectin (wt%)	Hemicellulose (wt%)	Lignin (wt%)	(Wax, fat, protein) (wt%)
Hemp fibre	56.1	20.1	10.9	6	7.9

Table 3
Physical properties of the nanoclay platelets (Cloisite 30B) [5].

Physical properties of the (Cloisite 30B)	
Colour	Off white
Density (g/cm^3)	1.98
d-spacing (001) (nm)	1.85
Aspect ratio	200–1000
Surface area (m^2/g)	750
Mean particle size (μm)	6

Table 4
Physical properties and chemical composition of OPC [2].

Properties/compositions	OPC (ASTM Type I)
Physical properties	
Specific gravity	3.17
Specific surface, Blaine (cm^2/g)	3170
Chemical analysis (weight%)	
SiO_2	21.10
Al_2O_3	5.24
Fe_2O_3	3.10
CaO	64.39
MgO	1.10
SO_3	2.52
Na_2O	0.23
K_2O	0.57
LOI	1.22

Table 5
Mix proportions of specimens.

Sample name	Hemp fabric (HF) (wt%)	Mix proportions (wt%)		
		Cement	Nanoclay	Water/binder
NCC-0	0	100	0	0.485
NCC-1	0	99	1	0.485
NCC-2	0	98	2	0.485
NCC-3	0	97	3	0.485
NCC-0/HF	2.4	100	0	0.485
NCC-1/HF	2.4	99	1	0.485
NCC-2/HF	2.4	98	2	0.485
NCC-3/HF	2.4	97	3	0.485

were obtained by using Cu Kα lines (λ = 1.5406 Å). A knife edge collimator was fitted to reduce air scatter.

The Quantitative X-ray Diffraction Analysis (QXDA) with Rietveld refinement was done with Bruker *DIFFRAC^{plus}* EVA software associated with the International Centre for Diffraction Data PDF-4 2013 database. Corundum [Al_2O_3] was chosen to serve as an internal standard. It was selected because it does not overlap with important cement peaks up to 2θ of 60° as well as it does not react with water and has no influence on the hydration reaction [26–31]. By using an internal standard the concentration of the crystalline phase can be determined on an absolute basis enabling the amorphous fraction to also be determined. The samples for QXDA were prepared by mixing a dry weight of 3.0 g of cement paste or nano-composite with 0.33 g of Corundum [Al_2O_3] as the internal standard. This powder was then added to a McCrone micronising canister with 7 ml of laboratory grade ethanol and sintered alumina milling media and milled for 5.0 min. The suspension was then poured into a polypropylene dish and dried at 105 °C for 24 h. The dried powder was then brushed into a polypropylene vial, and sealed until analysis [32].

2.3.2. Scanning electron microscopy

Scanning electron microscopy imaging was obtained using a NEON 40ESB, ZEISS. The SEM investigation was carried out in detail on microstructures and the fractured surfaces of samples. Specimens were coated with a thin layer of platinum before observation by SEM to avoid charging.

2.4. Physical properties

Measurements of bulk density and porosity were conducted to determine the quality of nanocomposites and HF-reinforced nanocomposites accordance with the ASTM Standard (C-20) [33]. The thickness, width, length and weight are measured in order to determine the bulk density. The calculation for density was carried out by using the following equation:

$$\rho = \frac{m_d}{V} \tag{1}$$

where ρ = density in (g/cm^3), m_d = mass of the dried sample (g) and V = volume of the test specimen (cm^3).

The apparent porosity (P_s) was calculated using the following equation:

$$P_S = \frac{m_s - m_d}{V\rho_w} \times 100 \tag{2}$$

where m_s = mass of the sample saturated with water in air, ρ_w = density of water (g/cm^3) and clean water was used as the immersion water.

2.5. Mechanical properties

Four specimens of each HF-reinforced nanocomposite were used in the mechanical tests. Three-point bend tests were conducted using an Instron Testing Machine to evaluate the flexural strength and fracture toughness of the composites. The support span used was 140 mm with a displacement rate of 0.5 mm/min. The flexural strength σ_F was evaluated using the following equation:

$$\sigma_F = \frac{3P_m S}{2BW^2} \tag{3}$$

where P_m is the maximum load, S is the span of the sample, W is the specimen thickness (depth) and B is the specimen width.To determine the fracture toughness notch specimen was used. A sharp razor blade was used to initiate a sharp notch in the samples. The ratio of notch depth to specimen depth ($\frac{a}{W}$) was about (1/3). The fracture toughness was calculated using the following equation [34,35]:

$$K_{IC} = \frac{p_m S}{BW^{3/2}} f\left(\frac{a}{W}\right) \tag{4a}$$

where a is the crack length (mm) and $f(\frac{a}{W})$ is the polynomial geometrical correction factor given by:

$$f\left(\frac{a}{W}\right) = \frac{3(a/W)^{1/2}[1.99 - (a/W)(1 - a/W) \times (2.15 - 3.93a/W + 2.7a^2/W^2)]}{2(1 + 2a/W)(1 - a/W)^{3/2}} \tag{4b}$$

3. Results and discussion

3.1. Quantitative X-ray Diffraction Analysis (QXDA)

The XRD patterns of nanoclay, cement paste and nanocomposites containing 1–3 wt% nanoclay are shown in Fig. 2a–e), including Corundum [Al_2O_3] phase as the internal standard. Table 6 shows the quantitative analysis with Rietveld refinement of cement paste and nanocomposites containing 1–3 wt% nanoclay, respectively. In Fig. 2, the Corundum phase (PDF 000461212) identified as crystallized structure, and its eight major peaks

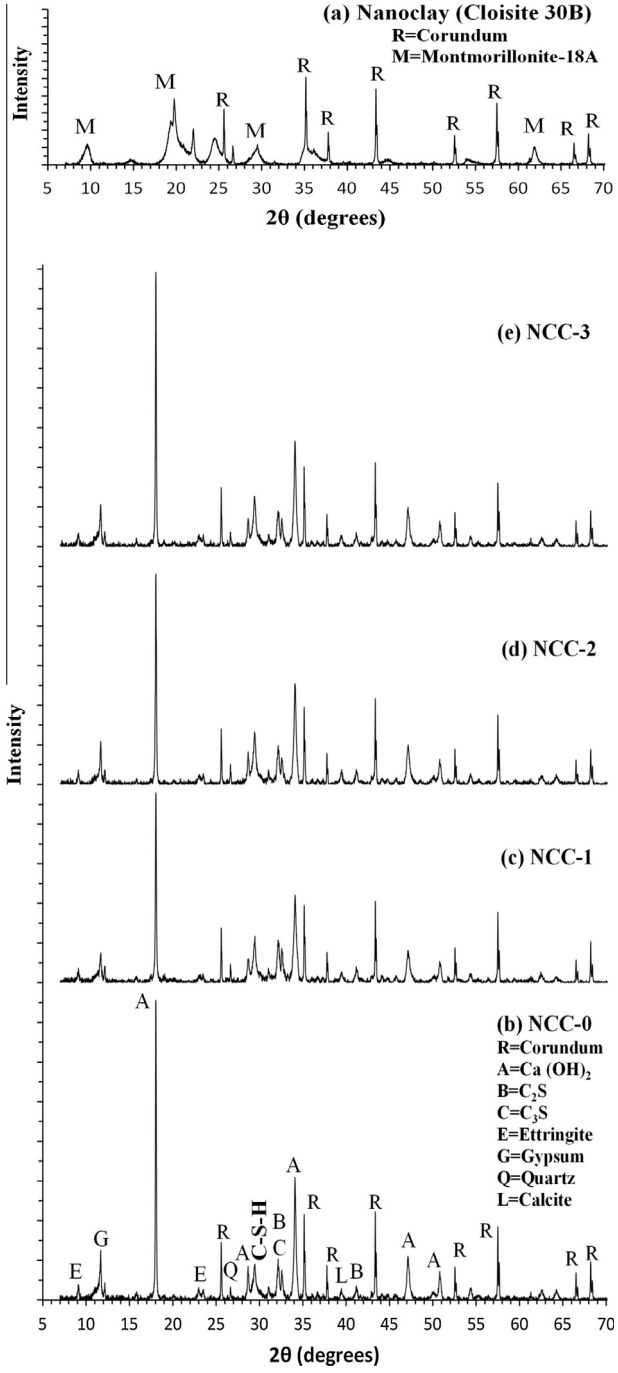

Fig. 2. XRD patterns of: (a) nanoclay, (b) cement paste, and nanocomposites containing various amounts of nanoclay: (c) 1 wt%, (d) 2 wt%, (e) 3 wt%.

correspond to 2θ angle of 25.57°, 35.14°, 37.77°, 43.34°, 52.54°, 57.49°, 66.5°, and 68.19° are shown. Fig. 2a shows the XRD pattern of nanoclay with wide diffraction peaks. It has crystalline phase at 2θ of 9.82°, 19.75°, 29.85° and 61.61° which refers to Montmorillonite-18A [$Na_{0.3}(Al,Mg)_2Si_4O_{10}OH_2{\cdot}6H_2O$] (PDF000120219). However, this phase was not detected clearly in nanocomposites.

The XRD patterns of cement paste and nanocomposites containing 1–3 wt% nanoclay are shown in Fig. 2b–e. Three important phases are noticed in this study: portlandite [$Ca(OH)_2$] (PDF 00-044-1481), dicalcium silicate [C_2S] (PDF 00-033-0302) and tricalcium silicate [C_3S] (00-049-0442). Moreover, four less important phases are also noticed: Ettringite [$Ca_6Al_2(SO_4)_3(OH)_{12}.26H_2O$]

Table 6
QXDA results (phase abundance) for cement paste and nanocomposites containing 1–3 wt% nanoclay.

Phase	Weight%			
	NCC-0	NCC-1	NCC-2	NCC-3
Amorphous content	67.4	70.0	69.4	68.0
Portlandite [$Ca(OH)_2$]	19.5	15.7	17.5	18.6
Ettringite [$Ca_6Al_2(SO_4)_3(OH)_{12}{\cdot}26H_2O$]	1.8	1.1	1.5	1.2
Gypsum [$Ca(SO_4)(H_2O)_2$]	0.4	0.4	0.5	0.6
Tricalcium silicate [C_3S]	1.5	2.1	1.2	1.6
Dicalcium silicate [C_2S]	7.1	8.5	7.7	7.4
Quartz [SiO_2]	0.4	0.6	0.5	0.4
Calcite [$CaCO_3$]	1.1	0.8	0.9	1.2

(PDF 000411451), Gypsum [$Ca(SO_4)(H_2O)_2$] (PDF 040154421), Quartz [SiO_2](PDF 000461045) and Calcite [$CaCO_3$](PDF 000050586). And also unobserved peaks of Vaterite phase [$CaCO_3$] (PDF 000600483). The composition of $Ca(OH)_2$ has a well-defined crystallized structure, it has five major peaks in the XRD pattern that corresponds to 2θ angle of 18.01°, 28.67°, 34.10°, 47.12° and 50.81°, and also crystal planes of Miller indices (hkl) of (001), (100), (101), (102) and (110), respectively. Although there are some overlaps of peaks and they have small intensities, dicalcium silicate (C_2S) has four major peaks that correspond to 2θ of 32.05°, 32.14°, 32.59° and 41.21° as well as tricalcium silicate (C_3S) has three major peaks that correspond to 2θ of 32.12°, 32.46° and 51.75° [26–30].

Table 6 indicates the phase abundance of such phases, but the Corundum phase as the internal standard has not been included in the phase abundance calculation. However, generally, the addition of 1–3 wt% nanoclay into the cement matrix has resulted in apparent change to the crystalline components of the samples. As can be seen from Table 6 and Fig. 2c, the addition of 1 wt% nanoclay reduced the amount of $Ca(OH)_2$ from 19.5 wt% to 15.7 wt%, about 19.5% reduction compared to cement paste. Also the intensities of major peaks of $Ca(OH)_2$ were significantly reduced compared to cement paste (Fig. 2b and c). Furthermore, the amorphous content was increased slightly from 67.4 wt% to 70 wt%, about 3.7% increase. This indicates that an obvious consumption of $Ca(OH)_2$ crystals mainly due to the effect of pozzolanic reaction in the presence of nanoclay and good dispersion of nanoclay in the matrix leads to produce more amorphous calcium silicate hydrate gel (C–S–H). This explanation is also confirmed by the inspection of amount of unreacted C_3S (2.1 wt%) and C_2S (8.5 wt%), in which the amount of unreacted C_3S and C_2S are slightly higher than the cement paste. Wei et al. [36] reported that pozzolanic reaction decelerates the hydration reaction of C_3S and C_2S during the curing time of 28–112 days. In this study, these unreacted phases could react with water later to produce more C–S–H gel after 56 days [30,37].

On the other hand, as can be seen from Table 6 and Fig. 2e for nanocomposites containing 3 wt% nanoclay, there is insignificant effect of nanoclay in the hydration reaction. For example, the amount of $Ca(OH)_2$ was reduced from 19.5 wt% to 18.6 wt%, about 4.6% reduction compared to cement paste. Also the intensities of major peaks of $Ca(OH)_2$ were slightly decreased compared to cement paste (Fig. 2b and e). This may be attributed to agglomerations of nanoclay at high contents which lead to poor dispersion of nanoclay and hence poor pozzolanic reaction. Moreover, the amount of C_3S (1.6 wt%) is similar to the cement paste, and the amount of C_2S (7.4 wt%) is slightly higher than the cement paste by about 4.2% increase; this also confirms that hydration reaction has occurred more than pozzolanic reaction.

Several authors [27,37–39] reported that although the C–S–H gel is mostly amorphous, it has some semicrystalline phase (e.g. tobermorite) which notably occurs at 2θ angle of 29.48°, in which

the intensity of this phase increases with increasing hydration time. In Fig. 2c–e, the intensity of this peak has slightly increased in nanocomposites containing 1–3 wt% nanoclay compared to cement paste (Fig. 2b). This may indicate that more C–S–H gel is deposited in the nanocomposites than the cement paste. Table 6 shows that the calcite varies in all samples. For example, calcite decreased from 1.1% to 0.8% in nanocomposite containing 1% nanoclay. This indicates that little carbonation occurred over the 56 day curing period [38]. Table 6 shows that Ettringite is slightly less in nanocomposites than cement paste. For example, it decreased from 1.8% to 1.1% in nanocomposite containing 1% nanoclay. Overall, the results indicate than 1 wt% nanoclay can consume more $Ca(OH)_2$ crystals and can improve the structure more effectively than 3 wt% nanoclay. The mechanical and physical properties also confirm this phenomenon, which is discussed in the following sections.

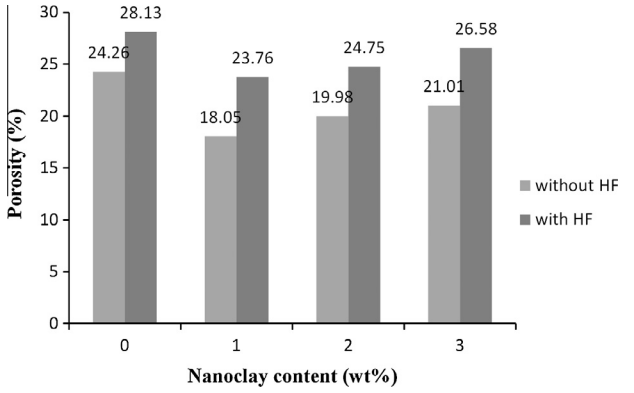

Fig. 3. Variation of porosity as a function of nanoclay content for cement paste and its nanocomposites with and without HF.

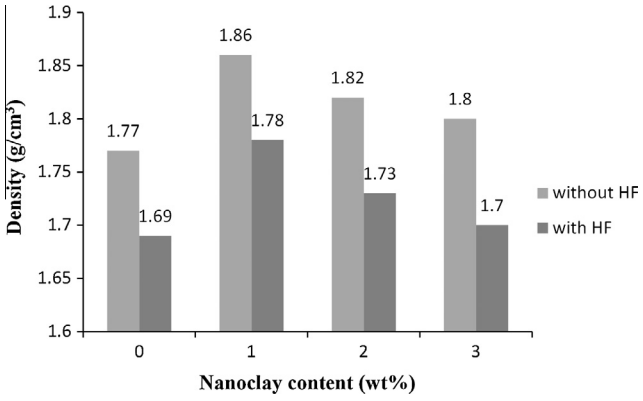

Fig. 4. Variation of density as a function of nanoclay content for cement pastes paste and its nanocomposites with and without HF.

3.2. Porosity and density

The porosity and density of cement matrix, nanocomposites, HF-reinforced cement paste and HF-reinforced nanocomposites are shown in Figs. 3 and 4, respectively. Generally the composites containing HF exhibited higher porosity than those without HF. This could be attributed to the formation of voids at the interfacial areas between the HF and the matrix. However, Fig. 3 shows that the addition of nanoclay decreases the porosity of these composites when compared to cement paste and HF composites. For nanocomposites with 1 wt% of nanoclay, the porosity decreases by 25.6%. Moreover, in HF-reinforced nanocomposites with 1 wt% of nanoclay, it decreases by 15.5%. This indicates that the nanoclay has filling effect in the porosity of cement paste composites with and without HF. This result is in agreement with the work done by Jo et al. [40] where the porosity of cement mortar is decreased by the addition of nano-SiO_2 particles. In Fig. 4, the addition of 1 wt% of nanoclay increased the density of cement paste and HF-reinforced cement composites by 5.1% and 5.3%, respectively. This improvement demonstrated that the cement composites with 1 wt% nanoclay yields more consolidated microstructure. However, the addition of more nanoclay leads to increase in porosity and decrease in density. This could be attributed to the poor dispersion and agglomerations of the nanoclay which create more voids in the matrix [41].

These results are also supported by SEM examinations of microstructure of cement paste and nanocomposites containing 1 wt% and 3 wt% nanoclay. Fig. 5a and b show SEM images of cement

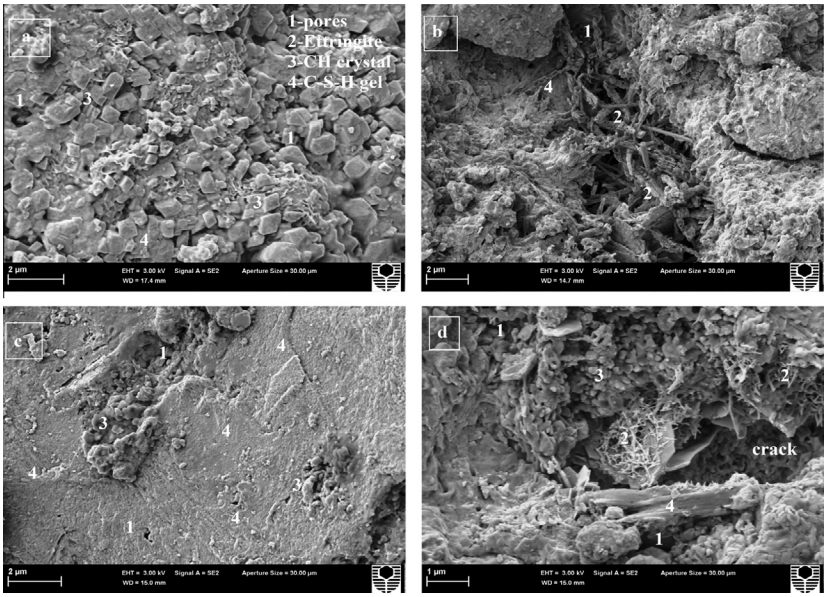

Fig. 5. SEM micrographs of: (a) and (b) cement paste, (c) nanocomposites containing 1 wt% nanoclay and (d) nanocomposites containing 3 wt% nanoclay.

paste. The existence of more ($Ca(OH)_2$) crystals, ettringite and pores revealed weak structure of the matrix. Fig. 5c shows the SEM image of nanocomposites containing 1 wt% nanoclay which is different from that of cement paste, the structure is denser and more compact with few pores. On the other hand, in Fig. 5d, the nanocomposites containing 3 wt% nanoclay shows more pores, ($Ca(OH)_2$) crystals, ettringite and microcracks which weaken the structure.

3.3. Mechanical properties

In general, the addition of nanoclay improved the mechanical properties of the cement matrix. In addition, the pre-soaking of hemp fabric in cement paste during sample preparation leads to good penetration of the nanocomposite matrix in between the reinforced filaments of the bundle as shown in Fig. 6, which also improved the mechanical properties of composites [20].

3.3.1. Flexural strength

The flexural strength and load-midspan deflection curves for HF-reinforced cement paste and HF-reinforced nanocomposites are shown in Figs. 7 and 8, respectively. In general, the incorporation of nanoclay platelets into the cement matrix led to a modest enhancement in the flexural strength of all HF-reinforced nanocomposites as shown in Fig. 7. The flexural strength of HF-reinforced nanocomposites containing 1wt% nanoclay is increased from 4.9 to 6.2 MPa, about 26.2% increase compared to HF-reinforced cement composite. This improvement in mechanical

Fig. 6. SEM micrograph showing the penetration of cement matrix in between the reinforced fibres of hemp fabric.

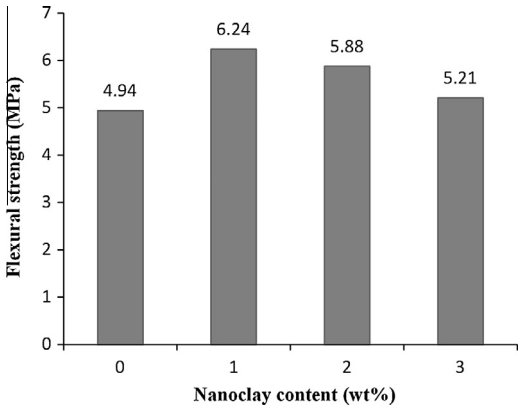

Fig. 7. Variation of flexural strength as a function of nanoclay content for HF-reinforced cement composite and HF-reinforced nanocomposites.

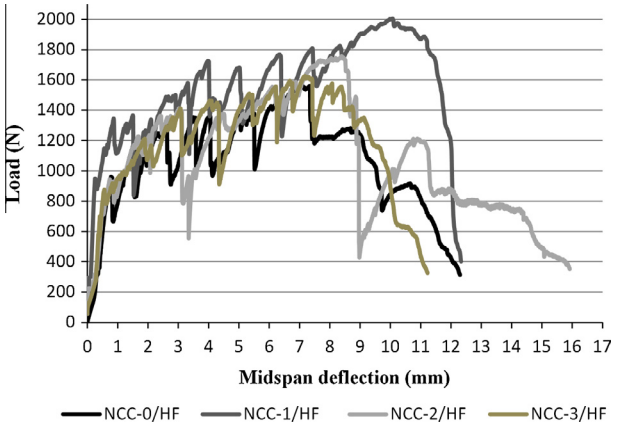

Fig. 8. Load versus mid-span deflection curves for for HF-reinforced cement composite and HF-reinforced nanocomposites from flexural test.

properties can be attributed due to two mechanisms. First is the filling effect where the nanoclay filled the voids or pores in the cement paste in which the nano-particles are uniformly dispersed in the matrix thus making the microstructure of nanocomposites denser than the cement paste. The second mechanism is the pozzolanic reaction, in which the nanoclay reacts with free calcium-hydroxide (CH) in the cement matrix to produce more calcium silicate hydrate (C–S–H) that also deposited in pore system [7,42]. Thus, the hemp fabric- nanocomposite matrix adhesion is mostly improved through consumption of CH by nanoclay, especially in the case of using 1 wt% nanoclay, which is evident from the higher flexural strength value. An analogous research was done by Khorami and Ganjian [43] where they studied the bagasse fibre-reinforced cement matrix with fibres content of 4 wt%, and silica fume was replaced for 5% of cement weight. They observed that the flexural strength increased about 20% compared to control bagasse fibre-reinforced cement matrix. They attributed this improvement to the Pozzolanic and filler effects of very fine silica fume particles, which led to enhancement of the bonding strength between the matrix and fibres. Hence, the improvement in flexural strength of HF-reinforced nanocomposites containing 1 wt% nanoclay observed in this study (26.2%) is slightly better than that observed by Khorami and Ganjian.

However, the addition of nanoclay more than 1 wt% caused a marked decrease in flexural strength. This could be attributed to the poor dispersion and agglomerations of the nanoclay in the cement matrix at higher clay contents, which create weak zones, in the form of micro-voids as stress concentrators [7,44]. Moreover, the addition of more nanoclay (i.e. 3 wt%) led to a significant reduction in flexural strength due to an increase in porosity. Nevertheless the addition of nanoclay improved the flexural strength of HF-reinforced cement composites. The load-midspan deflection

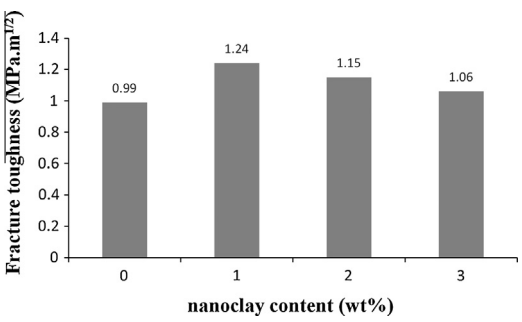

Fig. 9. Variation of fracture toughness as a function of nanoclay content for HF-reinforced cement composite and HF-reinforced nanocomposites.

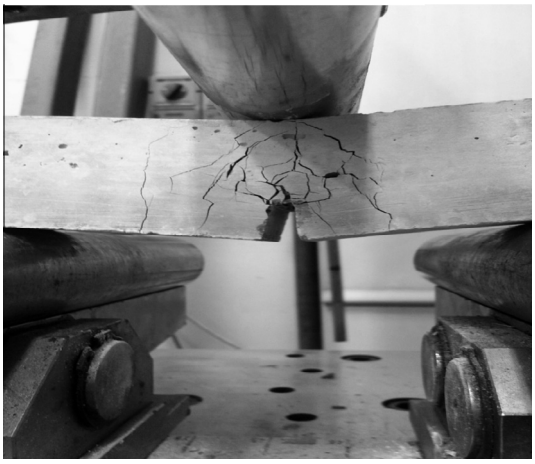

Fig. 10. Optical image showing the multiple-cracking behaviour of HF-reinforced nanocomposites.

curves for HF-reinforced cement composite and HF-reinforced nanocomposites are shown in Fig. 8. The HF-reinforced nanocomposite containing 1 wt% nanoclay shows the highest flexural load. This is due to high fibre–matrix interface bonding, which increases the maximum load-transfer capacity. On the other hand, the HF-reinforced nanocomposites containing 2 and 3 wt% nanoclay and HF-reinforced cement composite show low flexural load. This could be attributed to the increase in porosity which decreases the bonding between fibres and matrix, and thus the load-transfer.

3.3.2. Fracture toughness

The fracture toughness of HF-reinforced cement and nanocomposites are shown in Fig. 9. In general, all HF-reinforced composites and HF-reinforced nanocomposites showed multiple-cracking behaviour, as shown in Fig. 10 [45]. This is due to fracture resistance by hemp fabrics which resulted in increased energy dissipation from crack-deflection at the fibre–matrix interface, fibre-debonding, fibre-bridging, fibre pull-out and fibre-fracture [2,14,45,46]. The addition of nanoclay increased the fracture toughness of HF-reinforced nanocomposites. The fracture toughness for HF-reinforced nanocomposites containing 1–3 wt% nanoclay is 1.24, 1.15, and 1.06 MPa $m^{1/2}$, respectively. This is attributed to the fact that the nanoclay modified the matrix through pozzolanic reaction and reduced the CH content. Thus, good interfacial bonding between the matrix and the hemp fibres was achieved, especially in the case of 1 wt% nanoclay, in which the increase in fracture toughness was 24.9% comparing to HF-reinforced cement matrix. In a similar study, Alamri and Low [47] reported that the addition of 1 wt% halloysite nanotubes (HNTs) into recycled cellulose fibres (RCF)/epoxy matrix significantly increased the fracture toughness by 38.8% compared to RCF-reinforced epoxy composites.

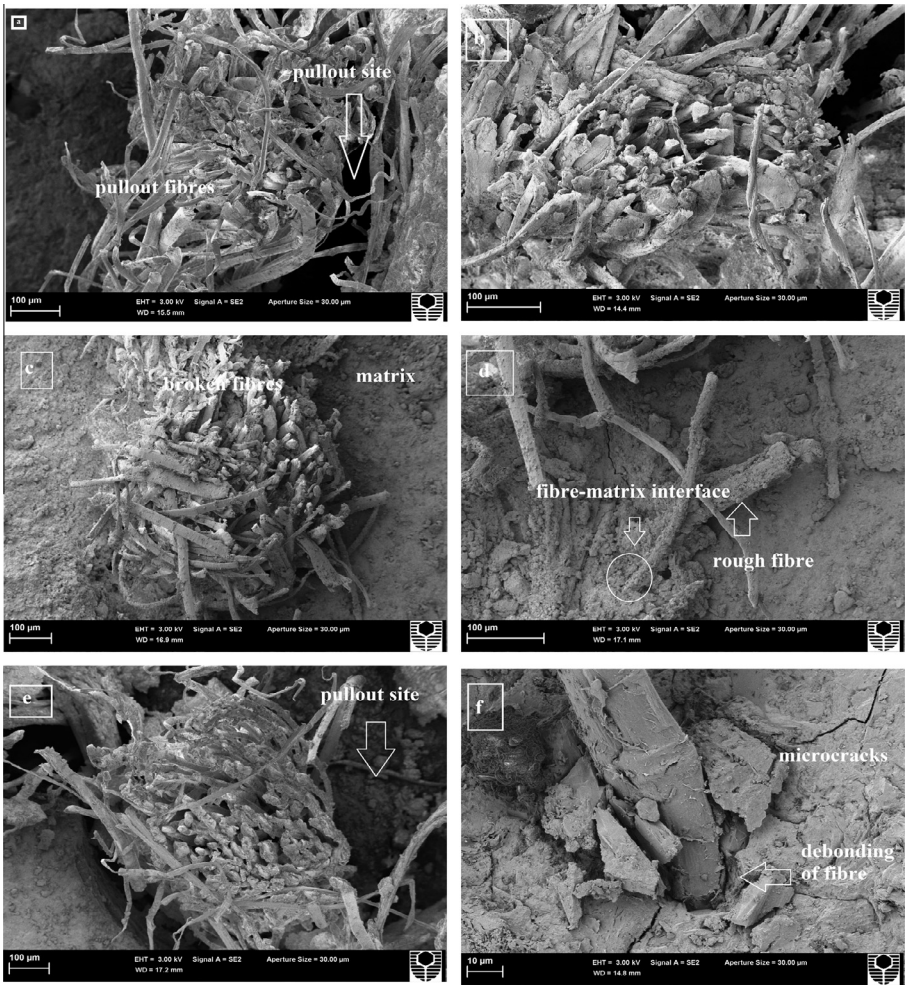

Fig. 11. SEM images showing the fracture surfaces of samples at low and high magnification: (a) and (b) HF-reinforced cement composite, (c) and (d) HF-reinforced nanocomposite containing 1 wt% nanoclay, (e) and (f) HF-reinforced nanocomposite containing 3 wt% nanoclay.

However, the inclusion of high content of nanoclay increases the porosity which adversely affected the interfacial bond between the matrix and the fibres thus decreased the fracture toughness [47].

3.3.3. Failure mechanisms

Fig. 11 shows the SEM images of the fracture surface and HF/matrix interface for HF-reinforced cement composite and HF-reinforced nanocomposite containing 1 and 3 wt% nanoclay after fracture toughness test. A variety of toughness mechanisms such as shear deformation, crack bridging, fibre pull-out and rupture and matrix fracture are observed. The examination of fracture surface of HF-reinforced nanocomposites containing 1 wt% nanoclay shows good fibre–matrix interface (Fig. 11c) as well as rough hemp fibre surface (Fig. 11d). However, poor adhesion between the fibre and the matrix is observed in HF-reinforced cement composite (Fig. 11a and b). In HF-reinforced nanocomposite containing 3 wt% nanoclay, macro-crack is observed which revealed relativity weak matrix and also debonding of fibre was occurred as shown in Fig. 11e and f.

4. Cost-benefit analysis, manufacturing and applications of this composite

Natural fibres/fabrics are increasingly being utilized due to their low density, low cost, renewability, recyclability and availability [1,5,10–14,21–23]. However, the problem is that nanoparticles are expensive and could limit their applications [48]. However, they are used in very small amount in concrete or other cementitious composites. For example, in this study, 1 wt% nanoclay in hemp fabric reinforced cement composites led to significant improvement in mechanical properties. From economic point of view, the addition of 1 wt% nanoclay in hemp fabric reinforced cement composite will not add any significant cost but will improve the mechanical properties by about 26%.

Manufacturing of synthetic or natural fibre-reinforced cement composites or cement board/sheet generally use mixing and casting methods [12,49], pultrusion method or hand lay-up technique [17,50,51]. In this study, the hemp fabric reinforced cement-eco-nanocomposites was manufactured using hand lay-up technique, where nanoclay–cement matrix (paste) and hemp fabrics are placed in alternating layers manually. Woven fabrics are easy to handle and easy to place using both manual and automated manufacturing techniques, so it is easy to made cement-eco-nanocomposites by using both hand lay-up method and automated manufacturing techniques. Thus they can be replicated at an industrial level and/or on site. The environmental benefit of this cement eco-nanocomposite will overcome the cost and manufacturing process. The developed hemp fabric reinforced composite can also be widely employed as an alternative to synthetic fibres in some applications including concrete tiles, roofing sheets, sandwich panels, on-ground floors, ceilings and structural laminate.

5. Conclusions

The physical and mechanical properties of hemp fabric reinforced cement composite and nanocomposites were investigated. The optimum content of nanoclay was found to be 1 wt%. The HF-reinforced nanocomposites containing 1 wt% nanoclay decreased the porosity (15.5%) and also increased the density (5.3%), flexural strength (26.2%) and fracture toughness (24.9%) compared to the HF-reinforced cement composite. However, the addition of more nanoclay (more than 1 wt%) into the HF-reinforced cement composites adversely affected the flexural strength and the fracture toughness. SEM micrographs of HF-reinforced nanocomposite containing 1 wt% nanoclay also support its improvement as compared to other samples in terms of presence of hydration products on the fibre surface indicating better fibre/matrix interface. The QXDA analysis showed that the addition of 1 wt% nanoclay in cement paste reduced the amount of $Ca(OH)_2$ and increased the amount of C–S–H gel. However, no such significant improvement was observed when nanoclay content increased. The SEM micrographs also supported the above observations, where pores and cracks are observed in the nanocomposite containing 3 wt% nanoclay. This hemp fibre reinforced cement eco-nanocomposite could be an interesting alternative to conventional polymeric fibre reinforced cementitious composites in the construction industry. Potential applications include structural laminate, sandwich panels, ceilings, roofing sheets, on-ground floors and concrete tiles. However, much research is still needed to overcome the agglomerations of nanoclay and to discover the best method of mixing which can lead to good dispersion of nanoclay in matrix and thus to increase its content in manufacturing new nanomaterials.

Acknowledgments

The authors thank Mr. Mick Elliss, Mr. Ashley Hughes and Mr. Andreas Viereckl from Civil Engineering at Curtin University for assistance with mechanical tests. We are also grateful to Mrs. E. Miller and Dr. Catherine Kealley from Applied Physics for assistance with SEM and XRD.

References

[1] Low IM, Somers J, Kho H, Davies I, Latella B. Fabrication and properties of recycled cellulose fibre-reinforced epoxy composites. Compos Interface 2009;16(7):659–69.
[2] Ahmed SFU, Maalej M, Paramasivam P. Flexural responses of hybrid steel-polyethylene fiber reinforced cement composites containing high volume fly ash. Constr Build Mater 2007;21(5):1088–97.
[3] Jarabo R, Fuente E, Monte MC, Savastano H, Mutjé P, Negro C. Use of cellulose fibers from hemp core in fiber–cement production: effect on flocculation, retention, drainage and product properties. Ind Crops Prod 2012;39:89–96.
[4] Schneider M, Romer M, Tschudin M, Bolio H. Sustainable cement production-present and future. Cem Concr Res 2011;41(7):642–50.
[5] Alhuthali A, Low IM, Dong C. Characterization of the water absorption, mechanical and thermal properties of recycled cellulose fibre reinforced vinyl-ester eco-nanocomposites. Composites Part B 2012;43(7):2772–81.
[6] Nazari A, Riahi S. The effects of Zinc Oxide nanoparticles on flexural strength of self-compacting concrete. Composites Part B 2011;42(2):167–75.
[7] Morsy MS, Alsayed SH, Aqel M. Hybrid effect of carbon nanotube and nano-clay on physico-mechanical properties of cement mortar. Constr Build Mater 2011;25(1):145–9.
[8] Givi A, Rashid S, Aziz F, Salleh M. Investigations on the development of the permeability properties of binary blended concrete with nano-SiO_2 particles. J Compos Mater 2011;45(19):1931–8.
[9] Qing Y, Zenan Z, Deyu K, Rongshen C. Influence of nano-SiO_2 addition on properties of hardened cement paste as compared with silica fume. Constr Build Mater 2007;21(3):539–45.
[10] Silva F, Mobasher B. Cracking mechanisms in durable sisal fiber reinforced cement composites. Cem Concr Compos 2009;31(10):721–30.
[11] Islam S, Hussain R, Morshed M. Fiber-reinforced concrete incorporating locally available natural fibers in normal-and high-strength concrete and a performance analysis with steel fiber-reinforced composite concrete. J Compos Mater 2012;46(1):111–22.
[12] Sedan D, Pagnoux C, Smith A, Chotard T. Mechanical properties of hemp fibre reinforced cement: influence of the fibre/matrix interaction. J Eur Ceram Soc 2008;28(1):183–92.
[13] Ali M, Liu A, Sou H, Chouw N. Mechanical and dynamic properties of coconut fibre reinforced concrete. Constr Build Mater 2012;30:814–25.
[14] Elsaid A, Dawood M, Seracino R, Bobko C. Mechanical properties of kenaf fiber reinforced concrete. Constr Build Mater 2011;25(4):1991–2001.
[15] Peled A, Bentur A. Geometrical characteristics and efficiency of textile fabrics for reinforcing cement composites. Cem Concr Res 2000;30(5):781–90.
[16] Peled A, Sueki S, Mobasher B. Bonding in fabric–cement systems: effects of fabrication methods. Cem Concr Res 2006;36(9):1661–71.
[17] Peled A, Mobasher B. Tensile behavior of fabric cement-based composites: pultruded and cast. J Mater Civ Eng 2007;19(4):340–8.

[18] Mobasher B, Peled A, Pahilajani J. Distributed cracking and stiffness degradation in fabric–cement composites. Mater Struct 2006;39(3):317–31.
[19] Soranakom C, Mobasher B. Geometrical and mechanical aspects of fabric bonding and pull out in cement composites. Mater Struct 2009;42(6):765–77.
[20] Peled A, Bentur A. Fabric structure and its reinforcing efficiency in textile reinforced cement composites. Composites Part A 2003;34(2):107–18.
[21] Alamri H, Low IM, Alothman Z. Mechanical, thermal and microstructural characteristics of cellulose fibre reinforced epoxy/organoclay nanocomposites. Composites Part B 2012;43(7):2762–71.
[22] Snoeck D, De Belie N. Mechanical and self-healing properties of cementitious composites reinforced with flax and cottonised flax, and compared with polyvinyl alcohol fibres. Biosyst Eng 2012;111(4):325–35.
[23] Pacheco-Torgal F, Jalali S. Cementitious building materials reinforced with vegetable fibres: a review. Constr Build Mater 2011;25(2):575–81.
[24] Nazari A, Riahi S. The effects of ZrO_2 nanoparticles on properties of concrete using ground granulated blast furnace slag as binder. J Compos Mater 2012;46(9):1079–90.
[25] ASTM C348-08. Standard test method for flexural strength of hydraulic cement mortars. ASTM International; 2012.
[26] ASTM C-1365 – 06. Standard test method for determination of the proportion of phases in Portland cement and Portland-cement clinker using X-ray powder diffraction analysis. ASTM International; 2011.
[27] Taylor HFW. Cement chemistry. London: Academic press limited; 1990.
[28] Aldridge A. Accuracy and precision of phase analysis in Portland cement by Bogue, microscopic and x-ray diffraction methods. Cem Concr Res 1982;12(3):381–98.
[29] Suherman P, Riessen A, O'Connor B, Li D, Bolton D, Fairhurst H. Determination of amorphous phase levels in Portland cement clinker. Powder Diffr 2002;17(3):178–85.
[30] Scrivenera K, Fullmanna T, Galluccia E, Walentab G, Bermejob E. Quantitative study of Portland cement hydration by X-ray diffraction/Rietveld analysis and independent methods. Cem Concr Res 2004;34(9):1541–7.
[31] Torre G, Bruque S, Aranda M. Rietveld quantitative amorphous content analysis. J Appl Crystallogr 2001;34(2):196–202.
[32] Williams R, Riessen A. Determination of the reactive component of fly ashes for geopolymer production using XRF and XRD. Fuel 2010;89(12):3683–92.
[33] ASTM C-20. Standard test methods for apparent porosity, water absorption, apparent specific gravity, and bulk density of burned refractory brick and shapes by boiling water. ASTM International; 2010.
[34] ASTM E-399. Standard fracture toughness specimens. ASTM International; 2013.
[35] Mihashi H, João P, de Barros L, Yamakoshi S, Kawamata A. Controlling fracture toughness of matrix with mica flake inclusions to design pseudo-ductile fibre reinforced cementitious composites. Eng Fract Mech 2007;74(1):210–22.
[36] Wei Y, Yao W, Xing X, Wu M. Quantitative evaluation of hydrated cement modified by silica fume using QXRD, 27Al MAS NMR, TG–DSC and selective dissolution techniques. Constr Build Mater 2012;36:925–32.
[37] Govindarajan D, Gopalakrishnan R. Spectroscopic studies on Indian Portland cement hydrated with distilled water and sea water. Front in Sci 2011;1(1):21–7.
[38] Soin A, Catalan L, Kinrade S. A combined QXRD/TG method to quantify the phase composition of hydrated Portland cements. Cem Concr Res 2013;48:17–24.
[39] Battocchio F, Monteiro P, Wenk H. Rietveld refinement of the structures of 1.0 C–S–H and 1.5 C–S–H. Cem Concr Res 2012;42(11):1534–48.
[40] Jo B, Kim C, Tae G, Park J. Characteristics of cement mortar with nano-SiO_2 particles. Constr Build Mater 2007;21(6):1351–5.
[41] Shebl S, Allie L, Morsy M, Aglan H. Mechanical behavior of activated nano silicate filled cement binders. J Mater Sci 2009;44(6):1600–6.
[42] Chang T, Shih J, Yang K, Hsiao T. Material properties of portland cement paste with nano-montmorillonite. J Mater Sci 2007;42(17):7478–87.
[43] Khorami M, Ganjian E. Comparing flexural behaviour of fibre–cement composites reinforced bagasse: wheat and eucalyptus. Constr Build Mater 2011;25(9):3661–7.
[44] Li H, Xiao H, Yuan J, Ou J. Microstructure of cement mortar with nano-particles. Composites Part B 2004;35(2):185–9.
[45] Ahmed SFU, Mihashi H. Strain hardening behavior of lightweight hybrid polyvinyl alcohol (PVA) fiber reinforced cement composites. Mater Struct 2011;44(6):1179–91.
[46] Banthia N, Shengb J. Fracture toughness of micro-fiber reinforced cement composites. Cem Concr Compos 1996;18(4):251–69.
[47] Alamri H, Low IM. Microstructural, mechanical, and thermal characteristics of recycled cellulose fiber-Halloysite-epoxy hybrid nanocomposites. Polym Compos 2012;33(4):589–600.
[48] Sanchez F, Sobolev K. Nanotechnology in concrete – a review. Constr Build Mater 2010;24:2060–71.
[49] Soroushian P, Hassan M. Evaluation of cement-bonded strawboard against alternative cement-based siding products. Constr Build Mater 2012;34:77–82.
[50] Asprone D, Durante M, Prota A, Manfredi G. Potential of structural pozzolanic matrix–hemp fiber grid composites. Constr Build Mater 2011;25(6):2867–74.
[51] Olivito R, Cevallos O, Carrozzini A. Development of durable cementitious composites using sisal and flax fabrics for reinforcement of masonry structures. Mater Des 2014;57:258–68.

Corrigendum sheet

This corrigendum sheet shows the error bars for Figures 3, 4, 7 and 9 for "**HAKAMY, A.,** SHAIKH, F.U.A. & LOW, I.M. 2014. Characteristics of hemp fabric reinforced nanoclay–cement nanocomposites. *Cement & Concrete Composites*, 50, 27–35".

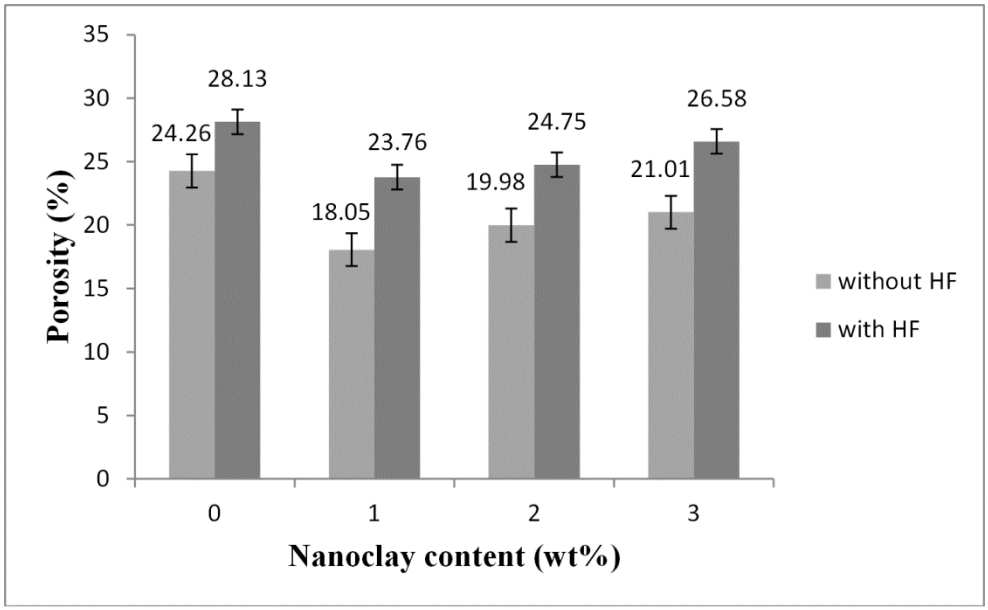

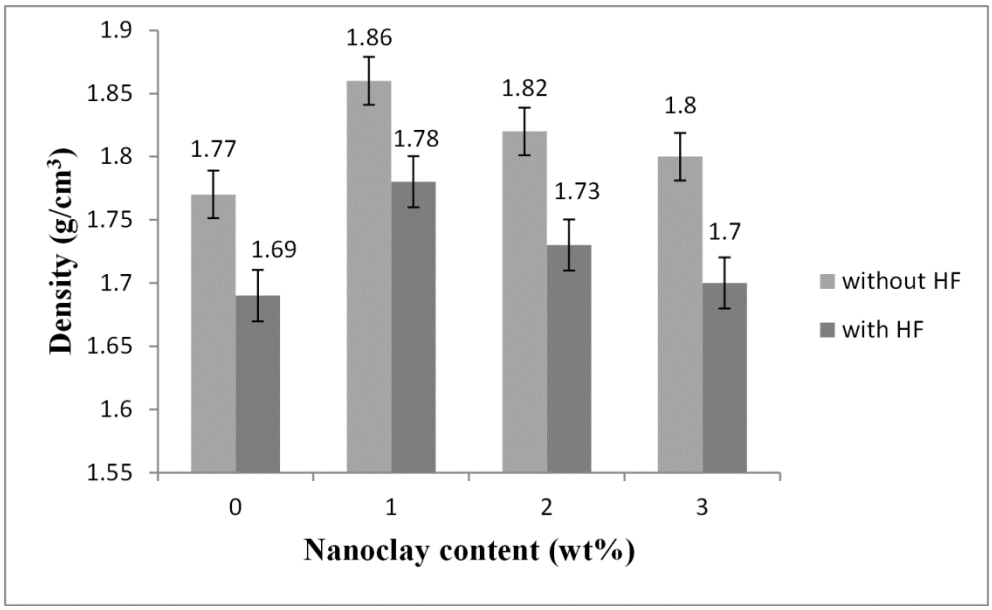

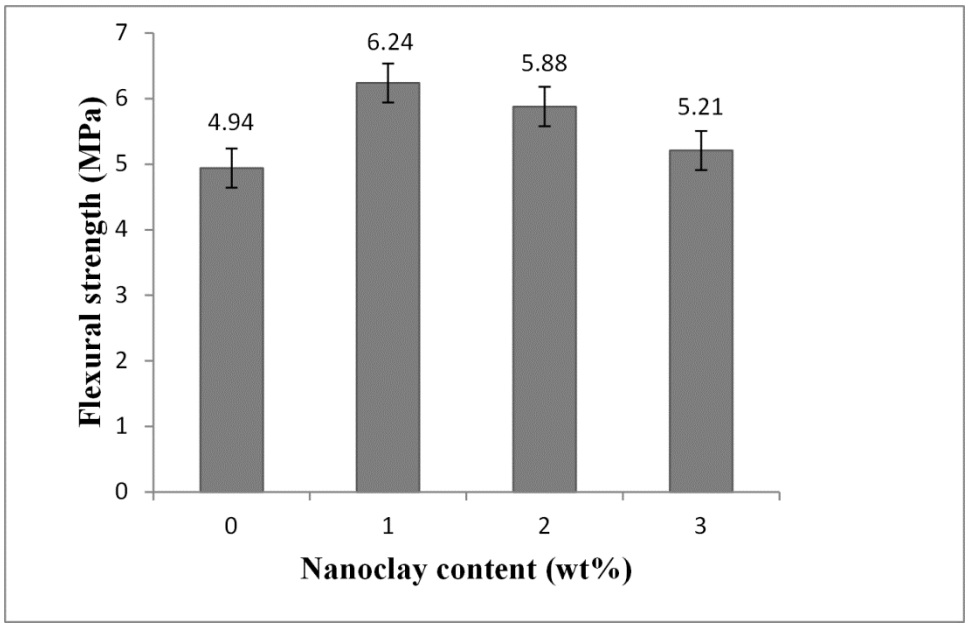
Flexural strength (MPa)
7
6
5
4
3
2
1
0
4.94
6.24
5.88
5.21
0
1
2
3
Nanoclay content (wt%)

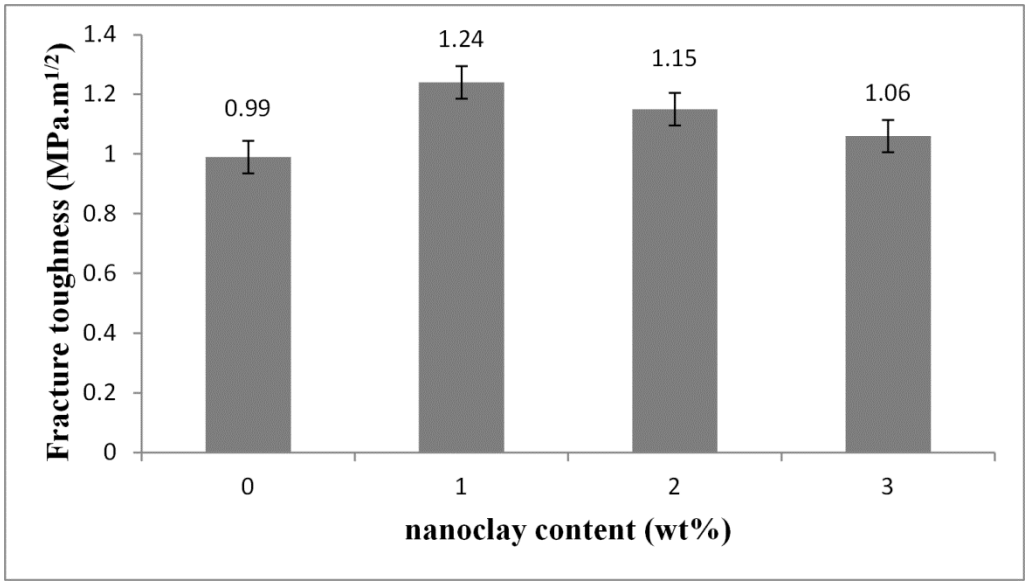
Fracture toughness (MPa.m1/2)
1.4
1.2
1
0.8
0.6
0.4
0.2
0
0.99
1.24
1.15
1.06
0
1
2
3
nanoclay content (wt%)

3.4 Characteristics of nanoclay and calcined nanoclay-cement nanocomposites.

HAKAMY, A., SHAIKH, F.U.A. & LOW, I.M. 2015. Characteristics of nanoclay and calcined nanoclay-cement nanocomposites. *Composites Part B: Engineering*, 78, 174-184.

Composites Part B 78 (2015) 174–184

Contents lists available at ScienceDirect

Composites Part B

journal homepage: www.elsevier.com/locate/compositesb

Characteristics of nanoclay and calcined nanoclay-cement nanocomposites

A. Hakamy [a, b], F.U.A. Shaikh [c], I.M. Low [a, *]

[a] Department of Imaging & Applied Physics, Curtin University, GPO Box U1987, Perth, WA 6845, Australia
[b] Department of Physics, Umm Al-Qura University, P.O. Box 715, Makkah, Saudi Arabia
[c] Department of Civil Engineering, Curtin University, GPO Box U1987, Perth, WA 6845, Australia

ARTICLE INFO

Article history:
Received 6 February 2015
Received in revised form
23 March 2015
Accepted 24 March 2015
Available online 1 April 2015

Keywords:
A. Nano-structures
B. Mechanical properties
B. Thermal properties
D. Mechanical testing
E. Thermal analysis

ABSTRACT

The influence of nanoclay (NC) and calcined nanoclay (CNC) on the mechanical and thermal properties of cement nano-composites presented. Calcined nanoclay is prepared by heating nanoclay (Cloisite 30B) at 900 °C for 2 h. Characterisation of microstructure is investigated using Quantitative X-ray Diffraction Analysis (QXDA) and High Resolution Transmission Electron Microscopy (HRTEM). Estimation of $Ca(OH)_2$ content in the cement nanocomposite is studied by the combination of QXDA and thermogravimetry analysis (TGA) techniques. Results showed that the mechanical and thermal properties of the cement nanocomposites are improved as a result of NC and CNC addition. An optimum replacement of ordinary Portland cement with 1 wt% CNC is observed through reduced porosity and water absorption as well as increased density, compressive strength, flexural strength, fracture toughness, impact strength, hardness and thermal stability of cement nanocomposites. The microstructural analyses from QXRA and SEM indicate that the CNC acted not only as a filler to improve the microstructure, but also as the activator to support the pozzolanic reaction. Cost-benefit analysis indicates that nanoparticles are expensive but from economic point of view nanoclay is used in very small amount (i.e. 1 wt. %) in cementitious materials. As a result nanoclay does not add any significant cost but improves the mechanical properties significantly.

1. Introduction

Nowadays, nanotechnology is one of the most active research areas in the civil engineering and construction materials [1–3]. Nanoparticles are used in polymer, ceramic and construction materials in order to produce cement nanocomposites that exhibit superior physical and mechanical properties [4,5]. In the construction industry, several types of nanomaterials have been incorporated into concretes or cement based materials such as nano-SiO_2, nano-Al_2O_3, nano-Fe_2O_3, nano-ZnO_2, nano-MgO, nano-$CaCO_3$, nano-TiO_2, carbon nanotubes, nano-metakaolin and nano-ZrO_2 in order to improve the durability and mechanical properties of concrete and Portland cement matrix [6–10]. Supit and Shaikh [11] reported that the addition of 1% nano-$CaCO_3$ increased the compressive strength of mortar and concrete significantly. Nano-silica (NS) has recently been introduced as an advanced pozzolan to improve the microstructure and stability of cement based system [12]. It has been observed that the NS consumed free lime (calcium hydroxide) during cement hydration and formed calcium silicate hydrate (CSH) gel due to its high fineness and reactivity [13]. In addition, the NS is particularly beneficial in acting as a nucleus to make the cement hydrate dense and improves the interfacial transition zone despite of small amount of replacement. From some conducted experiments, Zhang and Islam [14] and Jo et al. [15] reported better performance of concrete containing NS than that containing silica fume. Nano silica also improved the microstructure and mechanical properties of high calcium fly ash based geopolymer cured at ambient temperature [16].

Nanoclay (NC) is a new generation of processed clay for a wide range of high-performance cement nanocomposite [17,18]. As a kind of nano-pozzolanic material, nanoclay not only reduces the pore size and porosity of the cement matrix, but also improves the strength of cement matrix [19]. Furthermore, nanoclay particles enhance hardened properties of cement paste and mortar. Farzadnia et al. [20] reported that incorporation of 3% halloysite nanoclay into cement mortars increased the 28th day compressive

* Corresponding author.
E-mail address: j.low@curtin.edu.au (I.M. Low).

http://dx.doi.org/10.1016/j.compositesb.2015.03.074
1359-8368/

strength up to 24% compared to the control samples. However, little research is reported on the use of calcined nanoclay (CNC) as reinforcement in cement nanocomposite. In this paper, the effect of different amounts of nanoclay and calcined nanoclay on the mechanical and thermal properties of cement nanocomposite is studied. Due to calcination the amorphous contents of nanoclay is increased, which later reacted with $Ca(OH)_2$ of the cement hydration products and formed additional calcium-silica-hydrate (CSH) gel. The benefit of the use of CNC is the improvement of microstructure of the cement nanocomposite. The microstructures of cement nanocomposite were investigated using Quantitative X-ray Diffraction Analysis (QXDA) and High Resolution Transmission Electron Microscopy (HRTEM).

2. Experimental procedure

2.1. Materials

The nanoclay platelets (Cloisite 30B) used in this investigation is a natural montmorillonite modified with a quaternary ammonium salt, which was supplied by Southern Clay Products, USA. The specification and physical properties of Cloisite 30B are shown in Table 1. Ordinary Portland cement (ASTM Type I) was used in all mixes.

2.2. Thermal treatment of nanoclay

Calcined nanoclay (CNC) was prepared by heating the nanoclay at 800, 850 and 900 °C for 2 h in an electric furnace with a heating rate of 10 °C/min. The calcined nanoclay was then characterized by XRD, EDS and TEM in order to determine the amorphous phase of calcined nanoclay.

2.3. Sample preparation

2.3.1. Cement nanocomposite

Ordinary Portland cement (OPC) is partially substituted by nanoclay (NC) or calcined nanoclay (CNC) of 1, 2 and 3% by weight of OPC. The OPC and NC or CNC were first dry mixed for 5 min in a Hobart mixer at a low speed and then mixed for another 10 min at high speed until homogeneity was achieved. The binder is either nanoclay-cement dry powder or calcined nanoclay-cement dry powder. The cement nanocomposite paste was prepared through adding water with a water/binder ratio of 0.485. The cement nanocomposite containing 1, 2 and 3 wt% NC is termed as NCC1, NCC2 and NCC3, respectively. And also the cement nanocomposite containing 1, 2 and 3 wt% CNC is termed as CNCC1, CNCC2 and CNCC3, respectively. The cement paste (C) was considered as a control. The mix proportions are shown in Table 2.

2.3.2. Curing and specimens

Regarding each series, five cubes of size 50 × 50 × 50 mm and five prismatic plate specimens of 300 × 70 × 10 mm in dimension were cast. All specimens were demolded after 24 h of casting and kept under water for approximately 56 days. Five rectangular specimens of each series with dimensions 70 × 20 × 10 mm were cut from the fully cured prismatic plate for each mechanical and physical test. For compressive strength test, five cubes of size 50 × 50 × 50 mm were cast.

Table 1
Physical properties of the nanoclay platelets (Cloisite 30B).

Physical properties of the (Cloisite 30B)	
Colour	Off white
Density (g/cm^3)	1.98
d-spacing (001) (nm)	1.85
Aspect ratio	200-1000
Surface area (m^2/g)	750
Mean particle size (μm)	6

Table 2
Mix proportions of specimens.

Sample	Mix proportions (wt %)			
	Cement	NC	CNC	Water/binder
C	100	0	0	0.485
NCC1	99	1	0	0.485
NCC2	98	2	0	0.485
NCC3	97	3	0	0.485
CNCC1	99	0	1	0.485
CNCC2	98	0	2	0.485
CNCC3	97	0	3	0.485

2.4. Material characterisation

2.4.1. High Resolution Transmission Electron Microscopy (HRTEM)

High Resolution Transmission Electron Microscopy imaging was done using 3000F (JEOL company) operating at 300 kV equipped with a 4 × 4 k CCD camera (Gatan). Nanoclay and calcined nanoclay powders were dispersed in ethanol inside small glass containers by using ultrasonic device for 15 min. After that few drops of suspension were mounted onto copper grid and then kept to dry for 24 h at room temperature prior to examination.

2.4.2. The Quantitative X-ray Diffraction Analysis (QXDA)

The samples were measured on a D8 Advance Diffractometer (Bruker-AXS) using Cu Ka (λ = 1.5406 Å) radiation. The diffractometer were scanned from 7° to 70° (2θ) using a scanning rate of 0.5°/min. The Quantitative X-ray Diffraction Analysis (QXDA) with Rietveld refinement was done with Bruker *DIFFRAC^{plus}* TOPAS software associated with the International Centre for Diffraction Data PDF-4 2013 database. Corundum [Al_2O_3] was chosen to serve as an internal standard [2,21–23]. The samples for QXDA were prepared by mixing a dry weight of 3.0 g of cement paste or cement nanocomposite paste with 0.33 g of Corundum [Al_2O_3] as the internal standard [4,24].

2.4.3. Scanning electron microscopy (SEM)

Scanning electron microscopy imaging was obtained using a NEON 40ESB, ZEISS, equipped with energy dispersive spectroscopy (EDS). The SEM investigation of samples was carried out in detail on their microstructures and the fractured surfaces. Samples were coated with a thin layer of platinum before observation by SEM to avoid charging.

2.4.4. Thermogravimetric analysis (TGA)

The thermal stability of samples was studied by thermogravimetry analysis (TGA). A Mettler Toledo TGA 1 star system analyser was used for all measurements. Samples with 30 mg were placed in an alumina crucible and tests were carried out in Argon atmosphere with a heating rate of 10 °C/min from 25 to 1000 °C.

2.5. Physical properties

Measurements of bulk density and porosity were conducted to determine the quality of cement nanocomposite. The calculation for density was carried out by using the following equation:

$$\rho = \frac{m_d}{V} \tag{1}$$

where, ρ = density in (g/cm^3), m_d = mass of the dried sample (g) and V = volume of the test specimen (cm^3).

According to ASTM C-20 Standard [25], the apparent porosity P_S was calculated using the following equation:

$$P_S = \frac{m_s - m_d}{m_s - m_i} \times 100 \tag{2}$$

where m_i = mass of the sample saturated with and suspended in water, m_s = mass of the sample saturated in air.

For the water absorption test, the produced specimens were dried at a temperature of 80 °C until their mass became constant and then the mass was weighed (W_0). The specimens were then immersed in clean water at a temperature of 20 °C for 48 h. After the desired immersion period, the specimens were taken out and wiped quickly with wet cloth, and then the mass was weighed (W_1) immediately. The water absorption (W_A) was calculated by using the formula:

$$W_A = \frac{W_1 - W_0}{W_0} \times 100 \tag{3}$$

2.6. Mechanical properties

2.6.1. Compressive strength

Compressive strength of specimens was tested according to ASTM: C109 using a loading rate of 0.33 MPa/s. The cube samples of size 50 × 50 × 50 mm are cast. Five cubic specimens of each composition were used to measure the compressive strength.

2.6.2. Flexural strength and fracture toughness

Three-point bend tests were conducted using a LLOYD Material Testing Machine to evaluate the flexural strength and fracture toughness of the specimens. The support span used was 40 mm with a displacement rate of 0.5 mm/min. The flexural strength σ_F was evaluated using the following equation:

$$\sigma_F = \frac{3P_m S}{2BW^2} \tag{4}$$

where P_m is the maximum load, S is the span of the sample, W is the specimen depth and B is the specimen width.

In order to determine the fracture toughness, a sharp razor blade was used to initiate a sharp crack in the samples. The ratio of crack length to depth (a/W) was about 1/3. The fracture toughness was calculated using the following equation [4]:

$$K_{IC} = \frac{P_m S}{BW^{3/2}} f\left(\frac{a}{W}\right) \tag{5a}$$

where a is the crack length (mm) and $f(a/W)$ is the polynomial geometrical correction factor given by:

$$f\left(\frac{a}{W}\right) = \frac{3(a/W)^{1/2}\left[1.99 - (a/W)(1 - a/W) \times (2.15 - 3.93a/W + 2.7a^2/W^2)\right]}{2(1 + 2a/W)(1 - a/W)^{3/2}} \tag{5b}$$

Five specimens, measuring 70 × 20 × 10 mm, of each composition were used to measure the flexural strength and the fracture toughness.

2.6.3. Impact strength

The impact strength of the specimen was determined using a Zwick Charpy impact tester with 15 J pendulum hammer and 40 mm support span. Un-notched samples were used to compute the impact strength using the following formula:

$$\sigma_I = \frac{E}{A} \tag{6}$$

where E is the impact energy to break a sample with a ligament of area$A$. Five specimens, measuring 70 × 20 × 10 mm, of each composition were used to measure the impact strength.

2.6.4. Rockwell hardness

The hardness of the specimen was determined by the Rockwell hardness test, according to the specifications of ASTM E-18. Hardness of specimen was measured on an Avery Rockwell hardness tester using 1/8″ H scale steel ball indenter having a major loading capacity of 60 kg. Before measurement, the surfaces of test samples were ground using a Struers Pedimat polisher with 10 μm diamond polishing wheel. An average of five measurements from each specimen was used to measure the Rockwell hardness.

3. Results and discussion

3.1. Material characterisation

3.1.1. Effect of thermal treatment on nanoclay microstructure

3.1.1.1. XRD analysis of calcined nanoclay. Fig. 1 shows the XRD patterns of nanoclay and those calcined at 800, 850 and 900 °C for 2 h, respectively. XRD patterns of nanoclay show wide diffraction peaks which refer to Montmorillonite-18A [$Na_{0.3}(Al,Mg)_2Si_4O_{10}OH_2 \cdot 6H_2O$] (PDF000120219) and also exhibit crystalline phase at 2θ of 4.82° which indicate the presence of the ammonium salt. Patterns of calcined nanoclay at 800, 850 and 900 °C show that the ammonium salt peak completely disappeared at these temperatures. Also other nanoclay peaks gradually disappeared and transformed to amorphous state (calcined nanoclay) at 900 °C (see curve 'd' in Fig. 1). Results of XRD clearly show the transformation of crystalline phases of nanoclay to amorphous phases due to calcination [26].

3.1.1.2. Energy dispersive spectroscopy (EDS) analysis of calcined nanoclay. Fig. 2a and b shows typical EDS spectra of nanoclay and calcined nanoclay (at 900 °C). In Fig. 2a, ammonium salt in the nanoclay is identified by carbon and nitrogen elements (Fig. 3). The content of nitrogen element is very small, thus EDS cannot detect it but the carbon element is clearly detected at 2.5 KeV. However, in Fig. 2b, the carbon element disappeared because of combustion which yielded carbon dioxide during calcination. This result also confirms the decomposition of ammonium salt in calcined nanoclay which agrees with XRD results.

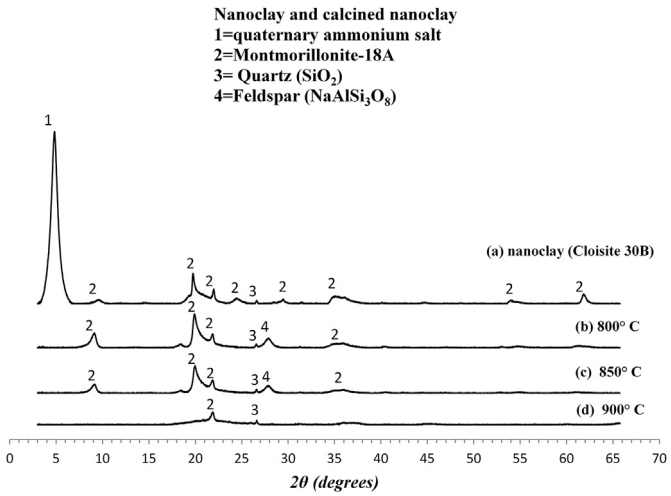

Fig. 1. X-ray diffraction patterns of nanoclay and calcined nanoclay.

3.1.1.3. High Resolution Transmission Electron Microscopy (HRTEM) of calcined nanoclay. HRTEM images of nanoclay (Cloisite 30B) at low and high magnification are shown in Fig. 4a–b. In the high magnification image (Fig. 4b), it can be seen clearly that the distances between the nanoclay platelets (i.e. layers) were about 1.85 nm and thus this is evidence that the d-spacing of (001) planes in nanoclay layers was 1.85 nm as shown in Table 1. The HRTEM images for calcined nanoclay (at 900 °C) at low and high magnification respectively are shown in Fig. 4c–d. In high magnification image (Fig. 4d), it can be seen that many platelets in calcined nanoclay were destroyed and some of them broke to small nanoparticles with approximate spherical shapes ranging 3–8 nm. This result also confirms the amorphous phase of calcined nanoclay which agrees with the XDR results above.

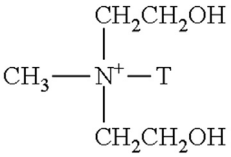

Where T is Tallow (~65% C18, ~30% C16, and ~5% C14)

Fig. 3. Chemical structure of quaternary ammonium salt.

3.1.2. Quantitative X-ray Diffraction Analysis (QXDA) of cement nanocomposite

The XRD patterns of cement paste, cement nanocomposite containing 1, 2 and 3 wt% CNC and cement nanocomposite containing 1 wt% NC are shown in Fig. 5a–e, that included Corundum [Al_2O_3] (PDF 000461212) phase as the internal standard. Table 3 shows the results of quantitative analysis with Rietveld refinement of cement paste and cement nanocomposite containing NC and CNC. Three important phases are noticed in this study: portlandite [$Ca(OH)_2$] (PDF 00-044-1481), tricalcium silicate [C_3S] (00-049-0442) and dicalcium silicate [C_2S] (PDF 00-033-0302). Moreover, four less important phases are also noticed: Ettringite [$Ca_6Al_2(SO_4)_3(OH)_{12}.26H_2O$] (PDF 000411451), Gypsum [$Ca(SO_4)(H_2O)_2$] (PDF 040154421), Quartz [SiO_2](PDF 000461045) and Calcite [$CaCO_3$](PDF 000050586) [2,21,23,27]. As can be seen in Table 3 and Fig. 5b, the addition of 1 wt% CNC reduced the amount of $Ca(OH)_2$ from 16.8 wt% to 12.1 wt%, about 28% reduction compared to cement paste. Also the intensities of major peaks of $Ca(OH)_2$ were significantly reduced compared to cement paste (Fig. 5b and a). Furthermore, the amorphous content was increased from 70.1 to 74.8 wt%, about 6.7% increase. This indicates that an obvious consumption of $Ca(OH)_2$ crystals mainly due to the effect of pozzolanic reaction in the presence of amorphous CNC and good dispersion of amorphous calcined nanoclay in the matrix, which leads to more calcium silicate

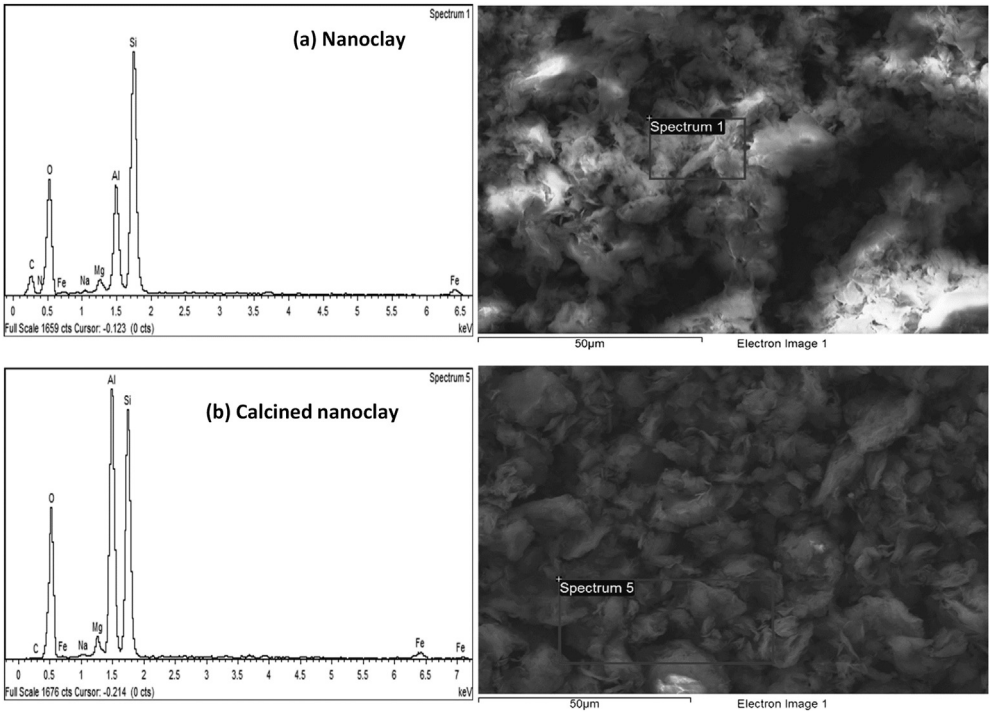

Fig. 2. EDS analysis with SEM images of: (a) nanoclay, (b) calcined nanoclay (at 900 °C).

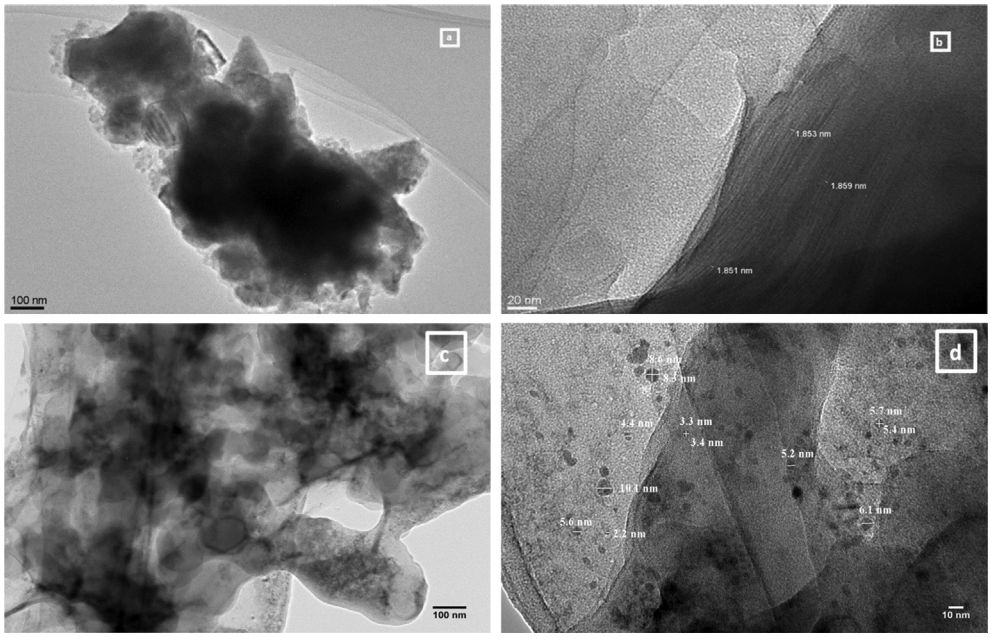

Fig. 4. TEM images of nanoclay and calcined nanoclay (at 900 °C) at: (a, c) low magnification, (b, d) high magnification.

hydrate gel (C–S–H) being produced. This explanation is also confirmed by an increase in the amount of unreacted C_3S (2.0 wt %) and C_2S (6.6 wt %), relative to the cement paste. Wei et al. [28] reported that pozzolanic reaction decelerates the hydration reaction of C_3S and C_2S during the curing time of 28–90 days. In this study, these unreacted phases could react with water later to produce more C–S–H gel after 56 days. Recently, Shaikh et al. [29] reported that the cement nanocomposite containing 2wt % nano-silica exhibited less calcium hydroxide but slightly more C_2S than the control cement paste.

On the other hand, as can be seen in Table 3 and Fig. 5e, the NCC1 cement nanocomposite shows lower amounts of C_3S and C_2S and also higher amount of $Ca(OH)_2$ compared to CNCC1 cement nanocomposite but slightly higher amounts of C_3S and C_2S and also lower amount of $Ca(OH)_2$ compared to CNCC3 cement nanocomposite. This result confirms that less pozzolanic reaction has occurred in NCC1 cement nanocomposite than CNCC1 cement nanocomposite. In contrast, as can be seen from Table 3 and Fig. 5d for cement nanocomposite containing 3 wt% CNC, the amount of $Ca(OH)_2$ was decreased from 16.8 wt% to 14.1 wt%, about 16% reduction compared to cement paste. Also the intensities of major peaks of $Ca(OH)_2$ were slightly decreased compared to cement paste (Fig. 5a and d). But this reduction of amount of $Ca(OH)_2$ is less than the reduction in cement nanocomposite containing 1 wt% CNC. Moreover, the amounts of C_3S (1.4 wt%) and C_2S (5.4 wt%) are also lower than cement nanocomposite containing 1 wt% CNC. This may be attributed to agglomerations of CNC at high contents which lead to relatively poor dispersion of CNC and hence relatively poor pozzolanic reaction [2,30]. Table 3 also shows that the calcite content varies in all samples. For example, the content of calcite

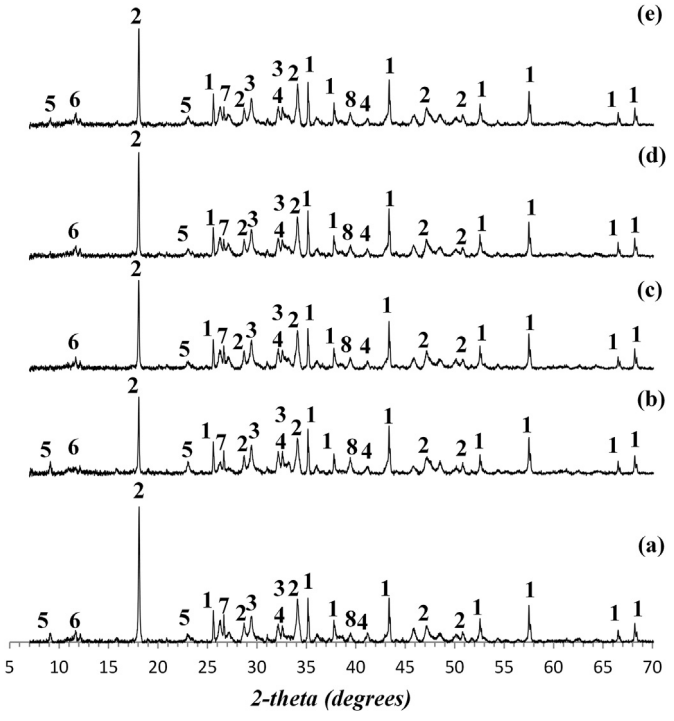

Fig. 5. XRD patterns of: (a) cement paste, cement nanocomposite containing: (b) 1 wt % CNC (CNCC1), (c) 2 wt% CNC (CNCC2), (d) 3 wt% CNC (CNCC3), (e) 1 wt% NC (NCC1). Numbers indicate to: 1 = Corundum [Al_2O_3] phase, 2 = Portlandite [$Ca(OH)_2$] phase, 3 = Tricalcium silicate [C_3S] phase, 4 = Dicalcium silicate [C_2S] phase, 5 = Ettringite phase, 6 = Gypsum phase, 7 = Quartz phase, 8 = Calcite phase.

Table 3
QXDA results for cement paste (C) and cement nanocomposite containing 1, 2 and 3 wt% CNC and 1 wt% NC.

Phase	Weight % (phase abundance)				
	C	CNCC1	CNCC2	CNCC3	NCC1
Portlandite [$Ca(OH)_2$]	16.8	12.1	13.2	14.1	13.8
Ettringite [$Ca_6Al_2(SO_4)_3(OH)_{12}\cdot 26H_2O$]	2.0	1.3	1.5	1.8	1.6
Tricalcium silicate [C_3S]	1.3	2.0	1.7	1.4	1.5
Dicalcium silicate [C_2S]	4.4	6.6	6.1	5.4	6.1
Gypsum [$Ca(SO_4)(H_2O)_2$]	0.7	0.4	0.6	0.4	0.4
Calcite [$CaCO_3$]	3.7	2.1	2.7	3.3	3.0
Quartz [SiO_2]	0.9	0.6	0.4	0.7	0.5
Amorphous content	70.1	74.8	73.7	72.8	73.0

decreased from 3.7 to 2.1 wt% in cement nanocomposite containing 1 wt% CNC. This indicates that little carbonation occurred over the 56 day curing period. Table 3 shows that Ettringite is slightly less in cement nanocomposite than cement paste. For example, it decreased from 2.0 to 1.3 wt% in cement nanocomposite containing 1 wt% CNC.

3.1.3. Calculation of $Ca(OH)_2$ content in cement nanocomposite by the combination of QXDA and TGA techniques

The $Ca(OH)_2$ content (CH) is calculated from the TGA curves using the following equation [31]:

$$CH(\%) = WL_{CH}(\%)\frac{MW_{CH}}{MW_{H_2O}} \quad (7)$$

where $WL_{CH}(\%)$ is corresponds to the weight loss attributable to $Ca(OH)_2$ decomposition, MW_{CH} is the molecular weight of CH (74.01 g/mol) and MW_{H_2O} is the molecular weight of H_2O (18 g/mol). The thermograms (TGA) of cement paste and cement nanocomposite containing CNC and NC are shown in Fig. 6. Table 4 summarises the CH content of above measured by QXDA and TGA techniques. Results in Table 4 indicate that TGA is at least as good as QXDA for quantifying the amount of calcium hydroxide [27]. It can be seen that there is good agreement between the two techniques, where both measured amounts are very close to each other [28]. However, the amounts of CH by TGA are slightly lower than the QXDA. This observation is in agreement with the work done by Scrivenera et al. [24] and Korpa et al. [32], in which they reported that this discrepancy could be attributed to the possible error sources of each method itself that were difficult to quantify. Nevertheless, inside the error margin there is a good correlation of the values assessed by both techniques employed [32]. And also the above consistency added a new evidence for reliability of the QXRD method to characterize quantitatively the hydration of cement systems [28]. The TGA and QXDA results in Table 4 also confirm the reactivity of 1 wt% CNC in reducing the CH content in cement nanocomposite. The CNC is mainly amorphous material and behaves as a highly reactive artificial pozzolan. The CH content by the TGA and QXDA in cement nanocomposite containing 1 wt% CNC was 10.7 and 12.1 wt%, respectively. It is also be seen that the CH content in cement nanocomposite containing 1 wt% CNC is reduced significantly when compared to cement paste and cement nanocomposite containing NC and CNC such as cement nanocomposite containing 1 wt% NC. This could be due to the reactivity of 1 wt% CNC in cement nanocomposite and the consumption of CH by the pozzolanic reaction.

Table 4
Calculation of $Ca(OH)_2$ content in cement paste and cement nanocomposite containing 1, 2 and 3 wt% CNC and 1 wt% NC by QXDA and TGA techniques.

Sample	TGA (wt %)	QXRD (wt %)	Difference (wt %)
C	15.5	16.8	1.3
CNCC1	10.7	12.1	1.4
CNCC2	12.1	13.2	1.1
CNCC3	13.0	14.1	1.1
NCC1	12.3	13.8	1.5

Table 5
Porosity, density and water absorption values for cement paste (C), (NCC) cement nanocomposite containing NC and (CNCC) cement nanocomposite containing CNC.

Sample	Porosity (%)	Density (g/cm^3)	Water absorption (%)
C	23.9	1.76	13.4
NCC1	18.7	1.87	10.2
NCC2	19.6	1.78	11.0
NCC3	19.9	1.76	11.3
CNCC1	16.5	1.93	8.9
CNCC2	17.6	1.91	9.6
CNCC3	18.9	1.85	10.3

3.2. Porosity, water absorption and density

The porosity, water absorption and density of cement paste and cement nanocomposite containing NC and CNC are shown in Table 5. It is noticed that the addition of CNC or NC decreases the porosity and water absorption of these cement nanocomposites when compared to control cement paste. In CNCC1 cement nanocomposite, the porosity and water absorption decreased by 31.2% and 34%, respectively compared to cement paste. This indicates that 1 wt% CNC has a filling effect in the porosity of cement nanocomposite. This result is in agreement with the work done by Jo et al. [15] where the porosity of cement mortar is decreased by the addition of nano-SiO_2 particles. Supit and Shaikh [33] reported that the addition of 2 wt% nano-silica significantly reduced the porosity of high volume fly ash (HVFA) concrete. Furthermore, In Table 5, the addition of 1 wt% CNC increased the density of control cement paste from 1.76 to 1.93 g/cm^3, about 9.7% increase. This improvement demonstrates that cement nanocomposite with 1 wt% CNC yields consolidated denser microstructure. However, further addition of CNC or NC leads to an increase in porosity and water absorption and a decrease in density. This could be attributed to the poor dispersion and agglomerations of the high CNC or NC contents which create more voids in the matrix [3,34].

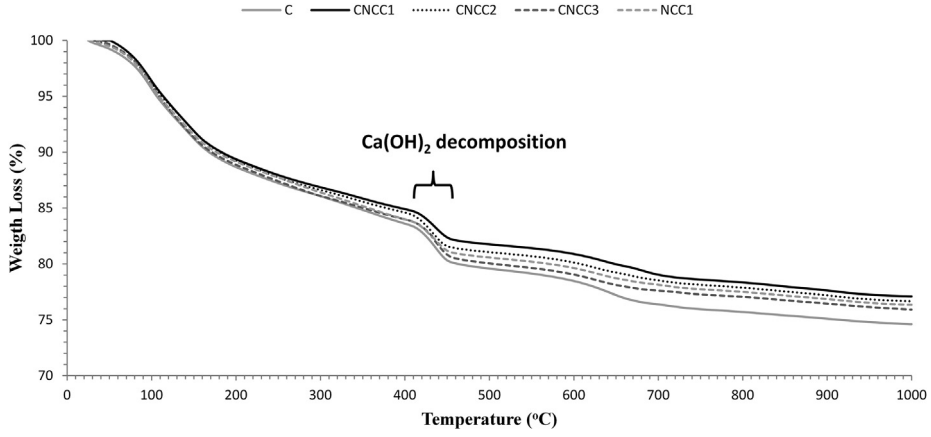

Fig. 6. TGA curves of cement paste (C) and cement nanocomposite: CNCC1, CNCC2, CNCC3 and NCC1.

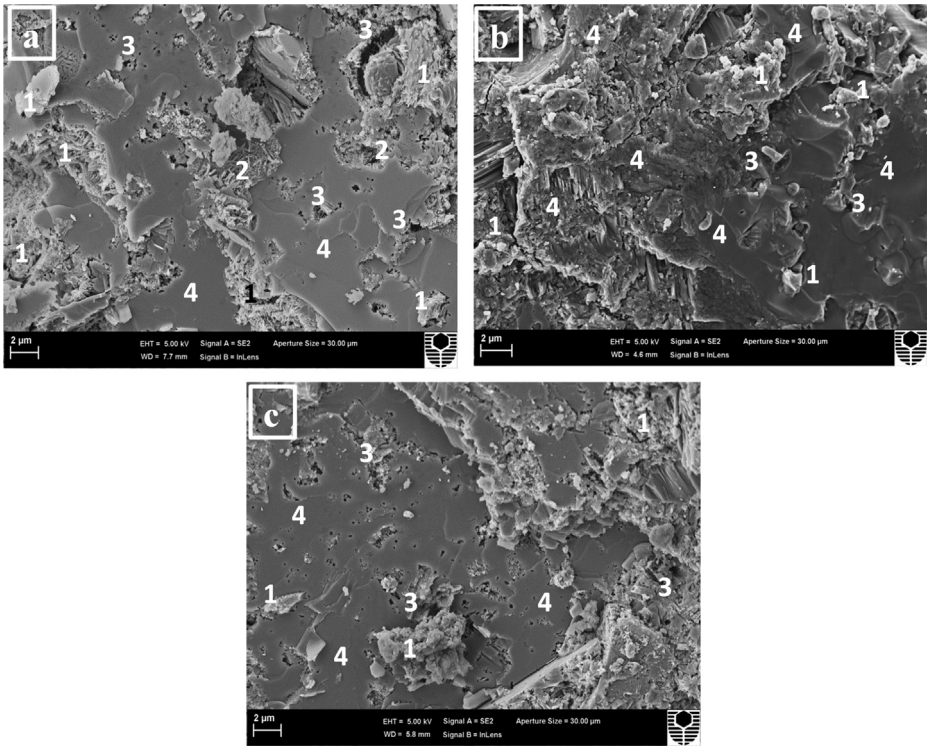

Fig. 7. SEM micrographs of: (a) cement paste, cement nanocomposite containing: (b) 1 wt% CNC, (c) 3 wt% CNC. Numbers indicate to: 1 = $[Ca(OH)_2]$ crystals, 2 = Ettringite, 3 = pores, 4 = C–S–H gel.

SEM examinations of the microstructure of cement paste, CNCC1 and CNCC3 cement nanocomposite are shown in Fig. 7a–c. For cement paste, Fig. 7a shows more $Ca(OH)_2$ crystals and Ettringite as well as more pores which revealed a weak structure. Fig. 7b shows the SEM micrograph of CNCC1, which is different from that of cement paste, the structure is dense and compact with few pores and more C–S–H gel. On the other hand, in Fig. 7c, the CNCC3 shows more pores than CNCC1which relatively weaken the structure.

3.3. Mechanical properties

3.3.1. Compressive strength

The compressive strength of the cement paste, cement nanocomposite containing NCC and CNCC are presented in Fig. 8. It can be noticed from results in Fig. 8 that the addition of NC and CNC to cement paste increases the compressive strength of all cement nanocomposite pastes. For instance, the cement nanocomposite containing 1 wt% CNC exhibited an enhancement in the compressive strength from 53.1 to 74.2 MPa or 40% increase, whereas in the cement nanocomposite containing 1 wt% NC, the compressive strength reached 69.8 MPa. The increase in compressive strength of cement nanocomposite containing 1 wt % CNC is due to amorphous state of CNC (i.e. small particle size) and extremely large surface area, in which the CNC reacts more quickly with free lime in the hydration reaction than NC and subsequently produced more secondary C–S–H gel and filled the capillary pores in the matrix efficiently [2,35]. Thus the microstructure of the matrix is densified by the nanoparticles. Chang [36] reported that the addition of 0.6 wt% nano-montmorillonite into cement paste increased compressive at age of 56 days from 46 to 52.1 MPa (i.e. 13.2% increases) compared to the cement paste. Li et al. [37] noticed 26% improvement in 28 days compressive strength of cement mortar containing 3% nano silica. Despite benefits of CNC and NC, it is important to note that the nanoparticles have a tendency to agglomerate when using at high content (i.e. more 3 wt% CNC) in the mixes [3,38]. This aggregation forms weak zones and consequently prevents the formation of homogenous hydrate microstructure. Therefore, the appropriate proportion of CNC content should be taken into account.

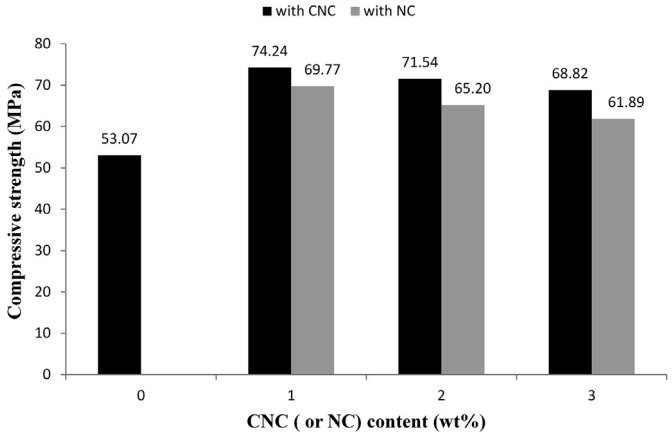

Fig. 8. Compressive strength as a function of calcined nanoclay (or nanoclay) content for cement paste and cement nanocomposite.

3.3.2. Flexural strength

Flexural strengths of cement paste, cement nanocomposite containing NC and CNC are shown in Fig. 9. Overall, the incorporation of CNC or NC into the cement matrix led to significant enhancement in the flexural strength of all cement nanocomposites. The flexural strength of cement nanocomposite containing 1, 2 and 3 wt% CNC is increased by 42.9%, 34.8% and 30.6%, respectively compared to cement paste. While the flexural strength

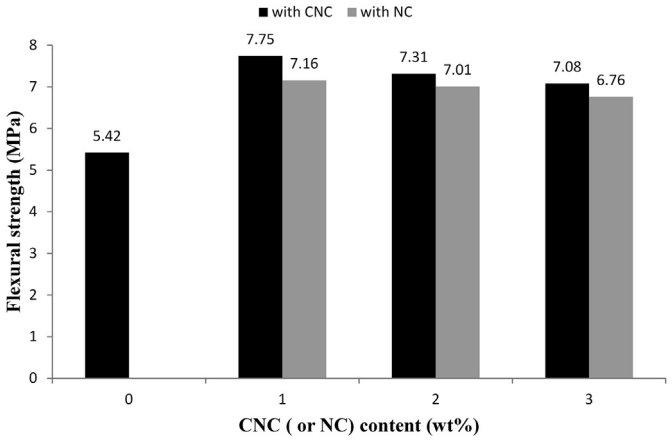

Fig. 9. Flexural strength as a function of calcined nanoclay (or nanoclay) content for cement paste and cement nanocomposite.

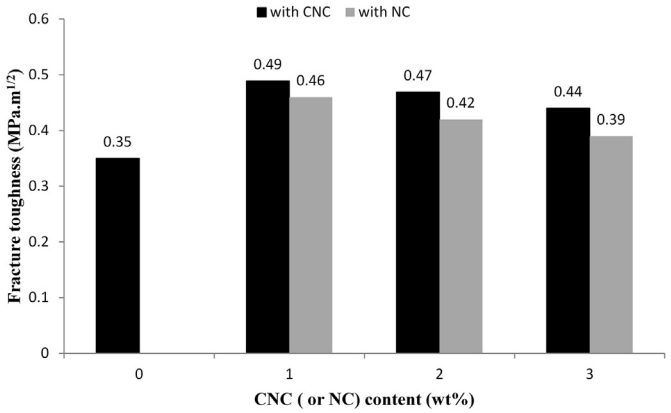

Fig. 10. Fracture toughness as a function of calcined nanoclay (or nanoclay) content for cement paste and cement nanocomposite.

of cement nanocomposite containing 1, 2 and 3 wt% NC is increased by 32.1%, 29.3% and 24.7% respectively compared to cement paste. This improvement clearly indicates the effectiveness of CNC in consuming calcium hydroxide (CH), supporting pozzolanic reaction and filling the micro pores in the matrix [2,38]. Thus the microstructure of cement nanocomposite is denser than the cement matrix, especially in the case of using 1 wt% CNC, which is evident from its higher flexural strength. Hosseini et al. [39] studied the effect of nanoclay (Cloisite15A) on the mechanical properties of cement mortar at 28 days with water/binder ratio of 0.4. They reported that addition of 1 wt% nanoclay improved the flexural strength from 7.0 to 9.1 MPa, about 30% increase. Qing et al. [13] studied the influence of 3 wt% nano-SiO_2 (NS) addition on properties of hardened cement paste. They observed that the flexural strength increased by about 72% compared to control cement matrix. They attributed this improvement to the pozzolanic and filler effects of nano-SiO_2 particles.

However, the addition of more than 1 wt% CNC caused a marked reduction in the flexural strength. This could be attributed to the relatively poor dispersion and agglomerations of the CNC in the cement matrix at higher CNC contents, which create weak zones, in the form of micro-voids which cause stress concentration [2,40]. Moreover, the addition of more CNC (i.e. 2 wt%) led to a significant reduction in the flexural strength due to an increase in porosity. Nevertheless the addition of CNC improved the flexural strength of cement nanocomposite. For example, in this study, although the flexural strength of cement nanocomposite with 3 wt% CNC decreased compared to cement nanocomposite with 1 wt% CNC but it is still higher than the control cement paste.

3.3.3. Fracture toughness

Fracture toughness of cement paste and cement nanocomposite containing NCC and CNCC are shown in Fig. 10. As shown in Fig. 10, the fracture toughness of cement nanocomposite containing 1, 2 and 3 wt% CNC were 0.49, 0.47 and 0.44 MPa $m^{1/2}$, respectively. It can be seen that the fracture toughness of CNCC1 cement nanocomposite is increased by 40% compared to cement paste. This is attributed to the fact that the CNC modified the matrix through pozzolanic reaction and reduced the $Ca(OH)_2$ content. Alamri and Low [41] reported that the addition of 1 wt% halloysite nanotubes (HNTs) into epoxy matrix significantly increased the fracture toughness from 0.85 to 1.33 MPa $m^{1/2}$ (i.e. by 56.5%) compared to epoxy matrix. However, facture toughness of CNCC cement nanocomposite gradually decreased when CNC contents are increased after the optimum content of 1 wt%. This is attributed to the poor dispersion of high content of CNC into the matrix, which leads to increase in porosity [4,42].

3.3.4. Impact strength

The impact strength is defined as the ability of the material to withstand impact loading [43]. The impact strengths of cement paste and cement nanocomposite containing NCC and CNCC are shown in Table 6. Generally, it can be seen that the impact strength of cement paste is significantly improved due to the addition of CNC or NC. The impact strength of NCC1 cement nanocomposite is 3.1 kJ/m^2, about 29.4% increase compared to the cement paste. While the impact strength of CNCC1 cement nanocomposite is 3.2 kJ/m^2, about 33.6% increase compared to cement paste. Alamri and Low [44] reported that the addition of 5 wt% nanoclay to epoxy matrix increased the impact strength from 5.6 to 7.8 kJ/m^2 about 39.3% increase compared to epoxy matrix. However, as CNC loading increased after the optimum content of 1 wt% the impact strength is decreased. For example, the impact strength of CNCC3 cement nanocomposite was 3.1 kJ/m^2, about 4% decrease compared to CNCC1 cement nanocomposite. This reduction in impact strength at higher CNC loading was due to the formation of CNC agglomerates and voids which led to weaken nanocomposite [3].

3.3.5. Rockwell hardness

The Rockwell hardness of cement paste and cement nanocomposite containing NCC and CNCC are shown in Table 6. Generally, the addition of CNC or NC into the cement matrix led to significant enhancement in the Rockwell hardness of all cement nanocomposites. As shown in Table 6 the Rockwell hardness of cement nanocomposite containing 1, 2 and 3 wt% CNC were 91.3, 89.0 and 86.3 HRH, respectively, which corresponds to about 31.1%, 27.7% and 23.9%, respectively increase compared to cement paste. While the Rockwell hardness of cement nanocomposite containing

Table 6
Impact strength and Rockwell hardness values for cement paste (C), (NCC) cement nanocomposite containing NC and (CNCC) cement nanocomposite containing CNC.

Sample	Impact strength (kJ/m^2)	Rockwell hardness (HRH)
C	2.38 ± 0.06	70 ± 1
NCC1	3.08 ± 0.15	87 ± 2
NCC2	3.01 ± 0.11	84 ± 1
NCC3	2.92 ± 0.08	83 ± 1
CNCC1	3.18 ± 0.05	91 ± 1
CNCC2	3.14 ± 0.08	89 ± 1
CNCC3	3.05 ± 0.14	86 ± 2

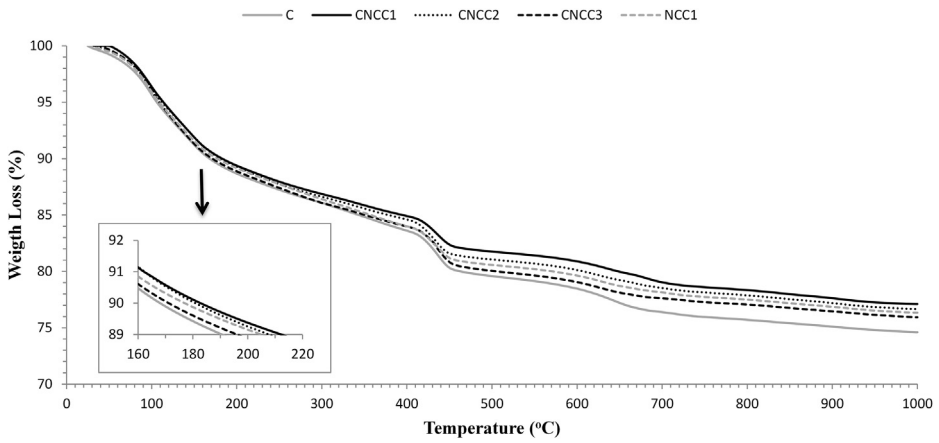

Fig. 11. Weight loss (%) curves by TGA of cement paste (C) and cement nanocomposite: CNCC1, CNCC2, CNCC3 and NCC1.

1, 2 and 3 wt% NC is increased by 25.3%, 21.0% and 18.6% respectively compared to the cement paste. This improvement demonstrates that the microstructure of cement nanocomposite is denser than the cement matrix, especially in the case of using 1 wt% CNC. That is because of the efficiency of CNC in promoting pozzolanic reaction and filling effect [3,45,46]. In an analogous research, Gupta et al. [47] reported that the hardness number (HRH) of the Fe−Al_2O_3 metal matrix nanocomposite was much higher in comparison to the cast iron specimen. However, the addition of high CNC or NC contents e.g. 3% did not show any improvement in the hardness when compared to 1 wt% CNC [4].

3.4. Thermal stability

Weight loss (%) curves of cement paste and cement nanocomposite containing CNCC and NCC1 are shown in Fig. 11. The char yields at different temperatures are summarized in Table 7. The TGA analysis shows three distinct stages of decomposition in these samples. The first stage of decomposition is between room temperature and 230 °C, which may be related to the decomposition of Ettringite and dehydration of C–S–H gel (loss of water). The second stage of decomposition is between 400 °C and 510 °C, which corresponds to $Ca(OH)_2$ decomposition. The third stage of decomposition is between 670 °C and 780 °C, which correspond to $CaCO_3$ decomposition [48,49]. In the first stage, generally all cement nanocomposites exhibited slightly better thermal stability than cement paste due to higher resistance of CNC or NC to decomposition [3,5]. Concerning the cement nanocomposite containing CNCC in second and third stage, the CNCC1 cement nanocomposite shows better thermal stability than CNCC2, CNCC3 and NCC1 cement nanocomposite due to dense and compact nanocomposite through consumption of calcium hydroxide and formation of secondary CSH gels during pozzolanic reaction [28]. In contrast, NCC1 cement nanocomposite shows lower thermal stability than CNCC2 cement nanocomposite but slightly higher than CNCC3 cement nanocomposite. This result confirms that slightly poor pozzolanic reaction has occurred and hence this NCC1 nanocomposite is less dense when compared to CNCC1 and CNCC2 cement nanocomposites. From Table 7 at 1000 °C, the char residue of cement paste, CNCC1, CNCC2 and CNCC3 cement nanocomposite was about 74.6, 77.1, 76.7 and 75.9 wt%, respectively. It can be seen that the CNCC1 cement nanocomposite performed better in thermal stability with higher char residue of about 3.3% and 1.5% more than cement paste and CNCC3 cement nanocomposite, respectively. In a similar study, Chen et al. [50] reported that addition of 10 wt% nano-TiO_2 into cement paste improved the thermal stability of cement nanocomposite considerably.

4. Cost-benefit analysis and applications

There is a huge optimism on the use of nanomaterials in construction and building applications although the nanoparticles are expensive and could limit their applications [1,51]. However, nanoparticles exhibit unique characteristics which result in new generation of concrete that is stronger and more durable [52]. With progress of manufacturing technologies the cost of nanoparticles is also expected to drop in future. Moreover, the nanoparticles are used in very small amount in the concrete or other cementitious nanocomposites. For example, in this study 1 wt% calcined nanoclay in cement nanocomposite led significant improvement in mechanical properties. From economic point of view, the addition of 1% calcined nanoclay in cement nanocomposite will not add any significant cost but improved the mechanical properties by about 40%. Shaikh and Supit [28] stated that although the use of nano-$CaCO_3$ was first considered as filler to partially replace cement or gypsum, some studies have shown advantages of using 1% nano-$CaCO_3$ nanoparticles in terms of compressive strength, accelerating

Table 7
Thermal properties of cement paste (C) and cement nanocomposite containing 1, 2 and 3 wt% CNC and cement nanocomposite containing 1 wt% NC.

Sample	Char yield (%) at different temperature (°C)									
	100	200	300	400	500	600	700	800	900	1000
C	95.82	88.82	86.03	83.57	79.57	78.44	76.37	75.69	75.09	74.61
CNCC1	96.19	89.32	86.83	84.88	81.75	80.86	79.01	78.33	77.61	77.10
CNCC2	96.02	89.20	86.59	84.57	81.04	80.09	78.51	77.86	77.18	76.67
CNCC3	95.82	88.82	86.03	83.96	80.03	79.02	77.60	77.05	76.45	75.93
NCC1	95.72	89.10	86.37	83.96	80.56	79.60	78.12	77.49	76.85	76.35

effect and economic benefits as compared to cement and other supplementary cementitious materials.

5. Conclusions

The influence of nanoclay (NC) and calcined nanoclay (CNC) on the microstructures, mechanical and thermal properties of cement nanocomposite has been presented. Results of the combination of QXDA and TGA techniques indicate that TGA is at least as good as QXDA for quantifying the amount of $Ca(OH)_2$. The optimum content of CNC was found to be 1 wt%. The cement nanocomposite containing 1 wt% CNC decreased the porosity (by 31.2%), water absorption (by 34%) and increased the density (by 9.7%), compressive strength (by 40%) flexural strength (by 42.9%), fracture toughness (by 40%), impact strength (by 33.6%) and Rockwell hardness (by 31.1%) as well as improved thermal stability (by 3.3%) compared to the control cement paste. The microstructural analysis such as QXDA and SEM showed that the addition of 1 wt% CNC in cement matrix enhanced the microstructure of cement nanocomposite through the filler and pozzolanic reaction effects. However, the addition of more NC or CNC (beyond 1 wt %) into cement nanocomposite adversely affected the mechanical and thermal properties. In fact, it could be recommended that much research is needed to overcome the agglomerations of NC or CNC and identify the best method of mixing which leads to good dispersion of CNC in the matrix.

Acknowledgements

The authors are grateful to Ms E. Miller from Applied Physics for assistance with SEM.

References

[1] Sanchez F, Sobolev K. Nanotechnology in concrete – a review. Constr Build Mater 2010;24(11):2060–71.
[2] Hakamy A, Shaikh FUA, Low IM. Characteristics of hemp fabric reinforced nanoclay–cement nanocomposites. Cem Concr Compos 2014;50:27–35.
[3] Hakamy A, Shaikh FUA, Low IM. Thermal and mechanical properties of hemp fabric-reinforced nanoclay–cement nanocomposites. J Mater Sci 2014;49(4):1684–94.
[4] Hakamy A, Shaikh FUA, Low IM. Microstructures and mechanical properties of hemp fabric reinforced organoclay–cement nanocomposites. Constr Build Mater 2013;49:298–307.
[5] Alhuthali A, Low IM, Dong C. Characterization of the water absorption, mechanical and thermal properties of recycled cellulose fibre reinforced vinylester eco-nanocomposites. Compos Part B 2012;43(7):2772–81.
[6] Nazari A, Riahi S. The effects of zinc oxide nanoparticles on flexural strength of self-compacting concrete. Compos Part B 2011;42(2):167–75.
[7] Morsy MS, Alsayed SH, Aqel M. Hybrid effect of carbon nanotube and nano-clay on physico-mechanical properties of cement mortar. Constr Build Mater 2011;25(1):145–9.
[8] Li H, Xiao H, Guan X, Wang Z, Yu L. Chloride diffusion in concrete containing nano-TiO_2 under coupled effect of scouring. Compos Part B 2014;56:698–704.
[9] Nazari A, Riahi S. The effects of ZrO_2 nanoparticles on properties of concrete using ground granulated blast furnace slag as binder. J Compos Mater 2012;46(9):1079–90.
[10] Moradpour R, Taheri-Nassaj E, Parhizkar T, Ghodsian M. The effects of nanoscale expansive agents on the mechanical properties of non-shrink cement-based composites: the influence of nano-MgO addition. Compos Part B 2013;55:193–202.
[11] Supit S, Shaikh FUA. Effect of nano-$CaCO_3$mon compressive strength development of high volume fly ash mortars and concretes. J Adv Concr Technol 2014;12(6):178–86.
[12] Hou P, Kawashima S, Kong D, Corr D, Qian J, Shah S. Modification effects of colloidal nano-SiO_2 on cement hydration and its gel property. Compos Part B 2013;45(1):440–8.
[13] Qing Y, Zenan Z, Deyu K, Rongshen C. Influence of Nano-SiO_2 addition on properties of hardened cement paste as compared with silica fume. Constr Build Mater 2007;21(3):539–45.
[14] Zhang MH, Islam J. Use of nano-silica to reduce setting time and increase early strength of concretes with high volume fly ash or slag. Constr Build Mater 2012;29:573–80.
[15] Jo BW, Kim CH, Lim JH. Characteristics of cement mortar with nano-silica particles. ACI Mater J 2007;104(4):404–7.
[16] Phoo-ngernkham T, Chindaprasirt P, Sata V, Hanjitsuwan S. The effect of adding nano-silica and nano-alumina on properties of high calcium fly ash geopolymer cured at ambient temperature. Mater Des 2014;55:58–65.
[17] Aly M, Hashmi MSJ, Olabi AG, Messeiry M, Hussain AI. Effect of nano clay particles on mechanical, thermal and physical behaviours of waste glass cement mortars. Mater Sci Eng A 2011;528(27):7991–8.
[18] Alamri H, Low IM, Alothman Z. Mechanical, thermal and microstructural characteristics of cellulose fibre reinforced epoxy/organoclay nanocomposites. Compos Part B 2012;43(7):2762–71.
[19] Wei J, Meyer C. Sisal fiber-reinforced cement composite with Portland cement substitution by a combination of metakaolin and nanoclay. J Mater Sci 2014;49(21):7604–19.
[20] Farzadnia N, Ali A, Demirboga R, Anwar M. Effect of halloysite nanoclay on mechanical properties, thermal behavior and microstructure of cement mortars. Cem Concr Res 2013;48:97–104.
[21] ASTM C-1365–06. Standard test method for determination of the proportion of phases in Portland cement and Portland-cement clinker using X-ray powder diffraction analysis. 2011.
[22] Taylor HFW. Cement chemistry. London: Academic Press Limited; 1990.
[23] Aldridge A. Accuracy and precision of phase analysis in Portland cement by Bogue, microscopic and X-ray diffraction methods. Cem Concr Res 1982;12(3):381–98.
[24] Scrivenera K, Fullmanna T, Galluccia E, Walentab G, Bermejob E. Quantitative study of Portland cement hydration by X-ray diffraction/Rietveld analysis and independent methods. Cem Concr Res 2004;34(9):1541–7.
[25] ASTM C-20. Standard test methods for apparent porosity, water absorption, apparent specific gravity, and bulk density of burned refractory brick and shapes by boiling water. 2010.
[26] He C, Makovicky E, Osbaeck B. Thermal treatment and pozzolanic activity of Na- and Ca-montmorillonite. Appl Clay Sci 1996;10(5):351–68.
[27] Soin A, Catalan L, Kinrade S. A combined QXRD/TG method to quantify the phase composition of hydrated Portland cements. Cem Concr Res 2013;48:17–24.
[28] Wei Y, Yao W, Xing X, Wu M. Quantitative evaluation of hydrated cement modified by silica fume using QXRD, 27Al MAS NMR, TG–DSC and selective dissolution techniques. Constr Build Mater 2012;36:925–32.
[29] Shaikh FUA, Supit SWM, Sarker PK. A study on the effect of nano silica on compressive strength of high volume fly ash mortars and concretes. Mater Des 2014;60:433–42.
[30] Najigivi A, Khaloo A, Iraji A, Abdul-Rashid S. Investigating the effects of using different types of SiO_2 nanoparticles on the mechanical properties of binary blended concrete. Compos Part B 2013;54:52–8.
[31] Shaikh FUA, Supit S. Mechanical and durability properties of high volume fly ash (HVFA) concrete containing calcium carbonate ($CaCO_3$) nanoparticles. Constr Build Mater 2014;70:309–21.
[32] Korpa A, Kowald T, Trettin R. Phase development in normal and ultra-high performance cementitious systems by quantitative X-ray analysis and thermoanalytical methods. Cem Concr Res 2009;39(2):69–76.
[33] Supit SWM, Shaikh FUA. Durability properties of high volume fly ash concrete containing nano-silica. Mater Struct 2014. http://dx.doi.org/10.1617/s115270140329-0.
[34] Senff L, Tobaldi D, Lucas S, Hotza D, Ferreira V, Labrincha J. Formulation of mortars with nano-SiO_2 and nano-TiO_2 for degradation of pollutants in buildings. Compos Part B 2013;44(1):40–7.
[35] Stefanidou M, Papayianni I. Influence of nano-SiO_2 on the Portland cement pastes. Compos Part B 2012;43(6):2706–10.
[36] Chang T, Shih J, Yang K, Hsiao T. Material properties of portland cement paste with nano-montmorillonite. J Mater Sci 2007;42(17):7478–87.
[37] Li H, Xiao H, Yuan J, Ou J. Microstructure of cement mortar with nano-particles. Compos Part B 2004;35(2):185–9.
[38] Shebl S, Allie L, Morsy M, Aglan H. Mechanical behavior of activated nano silicate filled cement binders. J Mater Sci 2009;44(6):1600–6.
[39] Hosseini P, Hosseinpourpia R, Pajum A, Khodavirdi M, Izadi H, Vaezi A. Effect of nano-particles and aminosilane interaction on the performances of cement-based composites: an experimental study. Constr Build Mater 2014;66:113–24.
[40] Givi A, Abdul-Rashid S, Aziz F, Salleh M. Experimental investigation of the size effects of SiO_2 nano-particles on the mechanical properties of binary blended concrete. Compos Part B 2010;41(8):673–7.
[41] Alamri H, Low IM. Microstructural, mechanical, and thermal characteristics of recycled cellulose fiber-halloysite-epoxy hybrid composites. Polym Compos 2012;33(4):589–600.
[42] Givi A, Abdul-Rashid S, Aziz F, Salleh M. The effects of lime solution on the properties of SiO_2 nanoparticles binary blended concrete. Compos Part B 2011;42(3):562–9.
[43] Zhou X, Ghaffar S, Dong W, Oladiran O, Fan M. Fracture and impact properties of short discrete jute-fiber reinforced cementitious composites. Mater Des 2013;49:35–47.
[44] Alamri H, Low IM. Effect of water absorption on the mechanical properties of nano-filler reinforced epoxy nanocomposites. Mater Des 2012;42:214–22.

[45] Yu M, George C, Cao Y, Wootton D, Zhou J. Microstructure, corrosion, and mechanical properties of compression-molded zinc-nanodiamond composites. J Mater Sci 2014;49(10):3629–41.
[46] Karimzadeh A, Ayatollahi M. Investigation of mechanical and tribological properties of bone cement by nano-indentation and nano-scratch experiments. Polym Test 2012;31(6):828–33.
[47] Gupta P, Kumar D, Parkash O, Jha A. Sintering and hardness behavior of Fe-Al_2O_3 metal matrix nanocomposites prepared by powder metallurgy. J Compos 2014;2014. http://dx.doi.org/10.1155/2014/145973. Article ID 145973.
[48] Lothenbach B, Winnefeld F, Alder C, Wieland E, Lunk P. Effect of temperature on the pore solution, microstructure and hydration products of Portland cement pastes. Cem Concr Res 2007;37(4):483–91.
[49] Djaknoun S, Ouedraogo E, Benyahia A. Characterisation of the behaviour of high performance mortar subjected to high temperatures. Constr Build Mater 2012;28(1):176–86.
[50] Chen J, Kou S, Poon C. Hydration and properties of nano-TiO_2 blended cement composites. Cem Concr Compos 2012;34(5):642–9.
[51] Pacheco-Torgal F, Jalali S. Nanotechnology: advantages and drawbacks in the field of construction and building materials. Constr Build Mater 2011;25(2):582–90.
[52] Singh T. A review of nanomaterials in civil engineering works. Inter J Struct Civ Eng Res 2014;3:31–5.

Corrigendum sheet

This corrigendum sheet shows the error bars for Figures 8, 9 and 10 for "**HAKAMY, A.,** SHAIKH, F.U.A. & LOW, I.M. 2015. Characteristics of nanoclay and calcined nanoclay-cement nanocomposites. *Composites Part B: Engineering*, 78, 174-184".

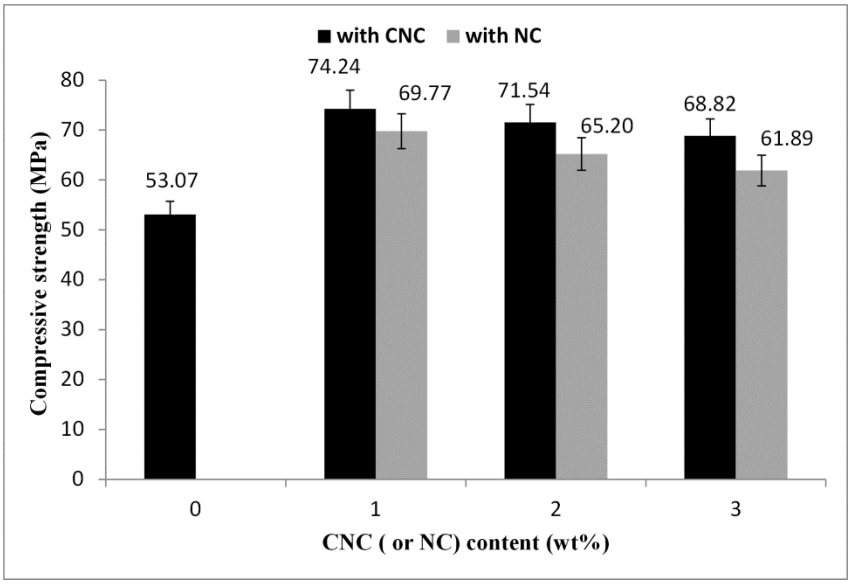

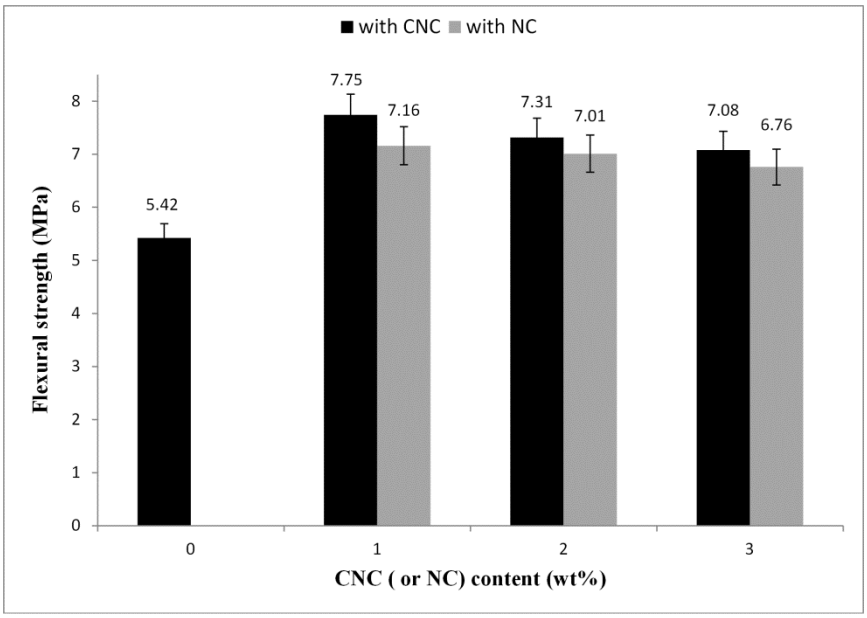

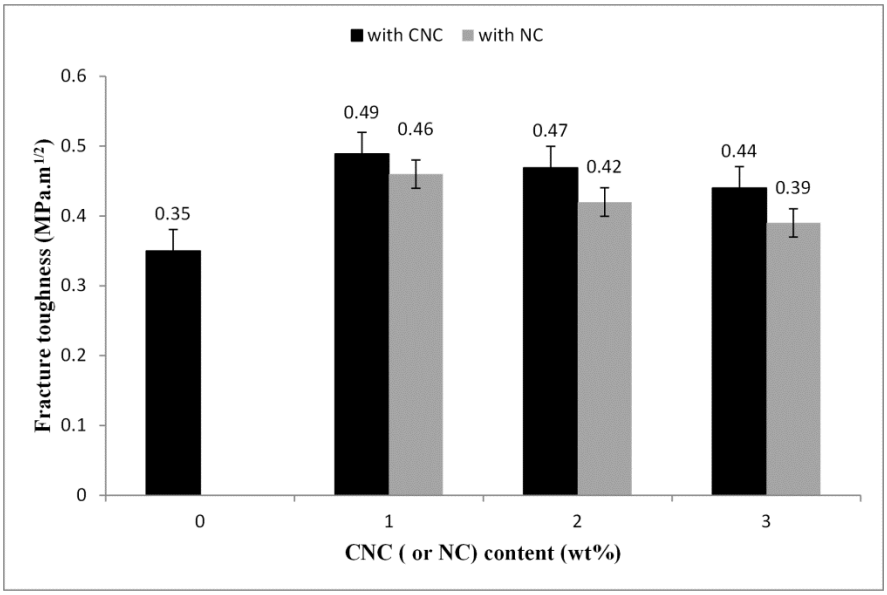
with CNC
with NC
Fracture toughness (MPa.m^1/2)
0.6
0.5
0.4
0.3
0.2
0.1
0
0.35
0.49
0.46
0.47
0.42
0.44
0.39
0
1
2
3
CNC (or NC) content (wt%)

3.5 Effect of calcined nanoclay on microstructural and mechanical properties of chemically treated hemp fabric reinforced cement nanocomposites.

HAKAMY, A., SHAIKH, F.U.A. & LOW, I.M. 2015. Effect of calcined nanoclay on microstructural and mechanical properties of chemically treated hemp fabric reinforced cement nanocomposites. *Construction & Building Materials*, 95, 882–891.

Construction and Building Materials 95 (2015) 882–891

Contents lists available at ScienceDirect

Construction and Building Materials

journal homepage: www.elsevier.com/locate/conbuildmat

Effect of calcined nanoclay on microstructural and mechanical properties of chemically treated hemp fabric-reinforced cement nanocomposites

A. Hakamy [a,b], F.U.A. Shaikh [c], I.M. Low [a,d,*]

[a] Department of Imaging & Applied Physics, Curtin University, GPO Box U1987, Perth, WA 6845, Australia
[b] Department of Physics, Umm Al-Qura University, P.O. Box 715, Makkah, Saudi Arabia
[c] Department of Civil Engineering, Curtin University, GPO Box U1987, Perth, WA 6845, Australia
[d] Department of Engineering, Curtin College, Bentley, WA 6102, Australia

HIGHLIGHTS

- Synthesis of treated hemp fabric reinforced nanoclay–cement nanocomposites.
- The optimum hemp fabric content was 6.9 wt% (i.e. 6 fabric layers).
- Treated hemp fabric reinforced cement composites exhibited the highest strength.
- Addition of 1 wt% calcined nanoclay imparted the optimum strength and toughness.

ARTICLE INFO

Article history:
Received 25 November 2014
Received in revised form 4 July 2015
Accepted 15 July 2015

Keywords:
Nanoclay
Hemp fabric
Cement
Mechanical properties
Microstructure

ABSTRACT

The influence of calcined nanoclay (CNC) and chemical treatment on the microstructure and mechanical properties of treated hemp fabric-reinforced cement nanocomposites has been investigated. The optimum hemp fabric content for these nanocomposites is 6.9 wt% (i.e. 6 fabric layers). Alkali-treated hemp fabric-reinforced cement composites exhibit the highest flexural strength when compared to their non-treated counterparts. In addition, mechanical properties are improved as a result of CNC addition. An optimum replacement of ordinary Portland cement with 1 wt% CNC is observed through reduced porosity and increased density, flexural strength and fracture toughness in treated hemp fabric-reinforced nanocomposite. It is shown that CNC behaves not only as a filler to improve the microstructure, but also as the activator to facilitate the pozzolanic reaction and thus improved the adhesion between the treated hemp fabric and the matrix.

1. Introduction

Nowadays, nanotechnology is one of the most active research areas in civil engineering and construction materials [1,2]. Nanoparticles are used in polymer, ceramic and construction materials in order to produce composites that exhibit superior physical and mechanical properties [3,4]. In the construction industry, several types of nanomaterials have been incorporated into concrete such as nano-SiO_2, nano-Al_2O_3, nano-Fe_2O_3, nano-ZnO_2, nano-$CaCO_3$, nano-TiO_2, carbon nanotubes and nano-metakaolin in order to improve the durability and mechanical properties of concrete and Portland cement matrix [5–7]. Qing et al. [8] reported that the addition of 5 wt% nano-SiO_2 into cement paste increased the compressive and flexural strength significantly. Nanoclay (NC) is a new generation of processed clay for a wide range of high-performance cement nanocomposite. Some examples of nanoclay are nano-halloysite, nano-cloisite 30B and nano-kaolin [2,9]. As a kind of nano-pozzolanic material, nanoclay not only reduces the pore size and porosity of the cement matrix, but also improves the strength of cement matrix through pozzolanic reactions [10]. Farzadnia et al. [11] reported that incorporation of 3 wt% halloysite nanoclay into cement mortars increased the 28-day compressive strength up to 24% increase compared to the control samples. Calcined nanoclay is prepared by heating nanoclay at elevated temperature to transform it into an amorphous state which then becomes highly reactive similar to artificial pozzolan such as silica fume, metakaolin, nano-SiO_2, and nano-metakaolin [5,12,13].

Recently, natural fibres are gaining increasing popularity to develop 'environmental-friendly construction materials' as alternative to synthetic fibres in fibre-reinforced concrete [14–16]. Natural and cellulose fibres have been used in polymer and cement matrices to improve their tensile/flexural strength and fracture

* Corresponding author at: Department of Imaging & Applied Physics, Curtin University, GPO Box U1987, Perth, WA 6845, Australia.
E-mail address: j.low@curtin.edu.au (I.M. Low).

http://dx.doi.org/10.1016/j.conbuildmat.2015.07.145
0950-0618/

resistance properties [17,18]. They are cheaper, biodegradable and lighter than synthetic fibres. Some examples of natural fibres are: sisal, flax, hemp, bamboo and others [19–21]. Some researchers have shown that pre-treatments of natural fibre surfaces either via pulping processes such as the Kraft process or some chemical agents such as alkalization, PEI (polyethylene imine), $Ca(OH)_2$ and $CaCl_2$ have slightly improved the interfacial bond strength between natural fibres and the matrix of the eco-composites. As a result, the mechanical properties of such materials are enhanced [22–24]. Troedec et al. [25] reported that the modification of hemp fibres with NaOH has improved the interfacial bonding between the fibres and the lime-based mineral matrix (mortar).

On the other hand, one of the most effective techniques to obtain a high performance cementitious composite is by reinforcement with textile fabric, which is impregnated with cement paste or mortar. Synthetic textile fabrics such as polyethylene (PE) and polypropylene (PP) have been used as reinforcement for cement composites, in which the fabrics are made of multi-filaments. When compared to continuous or short fibres, this system has superior filament-matrix bonding which improves the tensile and flexural strength [26–29]. The use of natural fibre sheets and fabrics is more prevalent in polymer matrix when compared to cement-based matrix [30].

However, the interfacial bonding between the natural fibre and the cement matrix is relatively weak and also the degradation of fibres in a high alkaline environment of cement can adversely affect the mechanical and durability properties of natural fibre reinforced cement composites [31]. Much research is clearly needed to overcome these problems [32]. However, little or no research has reported on the combined use of calcined nanoclay (CNC) and hemp fabrics as hybrid reinforcement in cement-composites. In this paper, we report the use of CNC in hemp fibre-reinforced cement composite in an attempt to overcome the above-mentioned disadvantages of hemp fibres in cementitious composites. The effect of CNC on the microstructural and mechanical properties of chemically-treated hemp fabric-reinforced cement composite is also studied.

2. Experimental procedure

2.1. Materials

The nanoclay (Cloisite 30B) used in this investigation is a natural montmorillonite (Ca, $Na)_{0.3}Al_2(Si, Al)_4O_{10}(OH)_2{\cdot}xH_2O$) modified with a quaternary ammonium salt which was supplied by Southern Clay Products, USA. The specification and physical properties of Cloisite 30B are outlined in Table 1. The hemp fabric was supplied by Hemp Wholesale Australia Pty. Kalamunda, Western Australia. The physical properties and characteristics of hemp fabric are shown in Table 2. The chemical composition of hemp fabric is given as 58.7 wt% of cellulose residue, 16.8 wt% of pectins, 14.2 wt% of hemicelluloses, 6 wt% of lignins and 4.3 wt% of waxes and fat. Ordinary Portland cement (ASTM Type I) was used in all mixes.

2.2. Thermal treatment of nanoclay

Calcined nanoclay (CNC) was prepared by heating the nanoclay at 800, 850 and 900 °C for 2 h in an electric furnace with a heating rate of 10 °C/min. The calcined nanoclay was then characterised by XRD and TEM in order to determine its phase composition and microstructure.

Table 1
Physical properties of the nanoclay platelets (Cloisite 30B).

Physical properties	
Colour	Off white
Density (g/cm^3)	1.98
d-spacing (001) (nm)	1.85
Aspect ratio	200–1000
Surface area (m^2/g)	750
Mean particle size (μm)	6

Table 2
Properties and characteristics of hemp fabric.

Fabric thickness (mm)	0.54
Fabric geometry	Woven (plain weave)
Yarn nature	Bundle
Fibre (Filament) size (mm)	0.04253
Number of filaments in a bundle	40
Bundle diameter (mm)	0.27
Opening size (mm)	0.3
Fabric Density (g/cm^3)	1.37
Modulus of elasticity (GPa)	38–58
Tensile strength (MPa)	591–857
Water absorption %	85.42

2.3. Chemical treatment of hemp fabric

The surface modification of hemp fibres was treated by immersing the fabric in 1.7 M NaOH solution (pH = 14) for 48 h at 25 °C, followed by neutralization with 1 vol% acetic acid. They were then washed several times with deionized water until the pH reached between 6.8 and 7.2. Finally the treated fabric was dried in an oven at 40 °C for 24 h.

2.4. Sample preparation

2.4.1. Untreated and treated hemp fabric-reinforced cement composites

The cement paste (C) was prepared through adding water (W) with W/C ratio of 0.485. The fabrication of untreated hemp fabric-reinforced cement composite (UHFRC) samples was done in two stages. In the first stage, the hemp fabric (295 mm in length and 65 mm in width) was first soaked into the cement matrix in order to achieve better penetration of matrix into the openings of the fabric. Then layers of pre-soaked hemp fabric were laid on a polished timber plate. The compacted layers of fabric were then left under a 30 kg weight (or 4.9 kPa compressive pressure) for 1 h to reduce the air bubbles and voids which might otherwise be trapped inside the samples. This step is essential to ensure better penetration of the cement matrix into the filaments of the hemp fabric and thus improves the interfacial bonding between the fibre and the matrix. In the second stage, a thin layer of cement matrix was first poured into the prismatic mould followed by the compacted pre-soaked hemp fabrics. Finally a thin layer of matrix was poured into the mould to form the upper layer and the samples were left to cure for 24 h at room temperature. Samples of un-treated hemp fabric-reinforced cement composites were fabricated with various contents of hemp fabric: 4.5 wt% (4 layers of fabric), 5.7 wt% (5 layers of fabric), 6.9 wt% (6 layers of fabric) and 8.1 wt% (7 layers of fabric). For the fabrication of treated hemp fabric-reinforced cement composite (6THFRC) samples, only 6 layers of treated hemp fabric were used because they have been shown to exhibit the best mechanical performance. The fabrication procedure of 6THFRC was similar to that of UHFRC described above.

2.4.2. Nanocomposites

The ordinary Portland cement (OPC) was partially substituted by calcined nanoclay (CNC) of 1%, 2% and 3% by weight of OPC. The OPC and CNC were first dry mixed for 5 min in a Hobart mixer at low speed and then mixed for another 10 min at high speed until a uniform mixture was achieved. The cement–nanocomposite paste was prepared through adding water with a water/binder (calcined nanoclay–cement) ratio of 0.485. The nanocomposite containing 1, 2 and 3 wt% CNC was termed as CNCC1, CNCC2 and CNCC3, respectively. The cement paste without CNC was considered as a control.

2.4.3. Treated hemp fabric-reinforced nanocomposites

Only 6 layers of treated hemp fabric were used to reinforce the nanocomposite matrix. The fabrication steps were similar to that of UHFRC described before. The treated hemp fabric-reinforced nanocomposite containing 1, 2 and 3 wt% calcined nanoclay was termed as 6THFR-CNCC1, 6THFR-CNCC2 and 6THFR-CNCC3, respectively. The total amount of treated hemp fabric in each specimen was about 6.9 wt%. The mix proportions are given in Table 3.

2.4.4. Curing and specimens

For each series, five prismatic plate specimens of length 300 mm, width 70 mm and depth 10 mm were cast. All specimens were demolded after 24 h of casting and kept under water for approximately 56 days. Five rectangular specimens of each series with dimensions of 70 mm (length) by 20 mm (width) by10 mm (depth) were cut for mechanical and physical tests.

Table 3
Mixing proportions of specimens.

Sample	Hemp fabric (HF)		Mix proportions (wt%)		
	Content (wt%)	Fabric layers	Cement	CNC	Water/binder
C	0	0	100	0	0.485
4UHFRC	4.5	4	100	0	0.485
5UHFRC	5.7	5	100	0	0.485
6UHFRC	6.9	6	100	0	0.485
7UHFRC	8.1	7	100	0	0.485
6THFRC	6.9	6	100	0	0.485
CNCC1	0	0	99	1	0.485
CNCC2	0	0	98	2	0.485
CNCC3	0	0	97	3	0.485
6THFR-CNCC1	6.9	6	99	1	0.485
6THFR-CNCC2	6.9	6	98	2	0.485
6THFR-CNCC3	6.9	6	97	3	0.485

2.5. Characterisation

2.5.1. High resolution transmission electron microscopy (HRTEM)

High resolution transmission electron microscopy imaging of powder specimens was done using 3000F (JEOL company) operating at 300 kV equipped with a 4 × 4 k CCD camera (Gatan). Nanoclay and calcined nanoclay powders were dispersed in ethanol inside small glass container by using ultrasonic device for 15 min. After that few drops of suspension were mounted onto copper grid and then kept to dry for 24 h at room temperature.

2.5.2. The Quantitative X-ray Diffraction Analysis (QXDA)

XRD patterns were obtained using Cu K_α (λ = 1.5406 Å) radiation with a Bruker D8 Advance diffractometer equipped with a LynxEye detector (1-dimensional detector, Bruker-AXS, Karlsruhe, Germany). The diffractometer was scanned from 7° to 70° (2θ) in step size of 0.015° and the counting time per step was 1.8 s. The Quantitative X-ray Diffraction Analysis (QXDA) with Rietveld refinement was done with Bruker *DIFFRAC^{plus}* TOPAS 4.2 software associated with the International Centre for Diffraction Data PDF-4 2013 database. The samples for QXDA were prepared by mixing a dry weight of 3.0 g of cement paste or nanocomposite paste with 0.33 g of corundum [Al_2O_3] as an internal standard [33–36].

2.5.3. Scanning electron microscopy (SEM)

Scanning electron microscopy was conducted using a NEON 40ESB, ZEISS to observe the microstructures and the fractured surfaces of samples. Specimens were coated with a thin layer of platinum before observation to avoid charging.

2.6. Physical properties

Prior to measuring the porosity and density, the samples were dried in an oven at 80 °C for 24 h to obtain the dried mass. The values of porosity and density were calculated according to ASTM C20 [37].

2.7. Mechanical properties

Five specimens, measuring 70 mm (length) × 20 mm (width) × 10 mm (depth) in each composition were used to measure the mechanical properties. Three-point bend tests were conducted using a LLOYD Material Testing Machine to evaluate the flexural strength of the composites. The support span used was 40 mm with a displacement rate of 0.5 mm/min. The flexural strength (σ_F) was evaluated using the following equation [16,26]

$$\sigma_F = \frac{3P_m S}{2BW^2} \quad (1)$$

where P_m is the maximum load, S is the span of the sample, W is the specimen depth and B is the specimen width.

In order to determine the fracture toughness, a sharp razor blade was used to initiate a sharp crack in the samples. The ratio of crack length to depth ($\frac{a}{W}$) was about 1/3 (i.e. about 0.33), in which the crack length was about 3.3 mm. The fracture toughness was calculated using the following equation [38,39]:

$$K_{IC} = \frac{p_m S}{BW^{3/2}} f\left(\frac{a}{W}\right) \quad (2a)$$

where a is the crack length (mm) and $f(\frac{a}{W})$ is the polynomial geometrical correction factor given by:

$$f\left(\frac{a}{W}\right) = \frac{3(a/W)^{1/2}[1.99 - (a/W)(1 - a/W) \times (2.15 - 3.93a/W + 2.7a^2/W^2)]}{2(1 + 2a/W)(1 - a/W)^{3/2}} \quad (2b)$$

3. Results and discussion

3.1. Characterisation

3.1.1. Effect of thermal treatment on nanoclay microstructure

3.1.1.1. XRD analysis of calcined nanoclay. Fig. 1(a–d) shows the XRD patterns of as-received nanoclay and calcined nanoclay at 800, 850 and 900 °C for 2 h, respectively. Four phases have been indexed in the diffraction pattern of nanoclay (Fig. 1a) with the major phase being Montmorillonite [$(Ca, Na)_{0.3}Al_2(Si, Al)_4O_{10}(OH)_2{\cdot}xH_2O$] (PDF 00052039), and minor phases of Cristobalite [SiO_2] (PDF 000391425), Quartz [SiO_2](PDF 000470718) and the quaternary ammonium salt (PDF 000571718). Montmorillonite has five major peaks in the XRD pattern that correspond to 2θ of 4.84°, 19.74°, 35.12°, 53.98° and 61.80°. Each of Cristobalite and Quartz has a peak that corresponds to 2θ of 21.99° and 26.61° respectively. The quaternary ammonium salt has four peaks that correspond to 2θ of 4.84°, 9.55°, 24.42° and 29.49°. Note that there was an overlap of peaks at 2θ of 4.84° for Montmorillonite and quaternary ammonium salt. However these peaks disappeared after calcination due to the decomposition of the latter in calcined nanoclay.

In Fig. 1(b and c), the diffraction peaks of calcined nanoclay at 800 and 850 °C are related to heated-Montmorillonite [$NaMgAlSi_4O_{11}$] (PDF 000070304). After calcination at 800 °C (Fig. 1b), the basal spacing of Montmorillonite collapsed from 1.85 nm to 0.97 nm (2θ of 4.84–9.13°) due to dehydration and dehydroxylation. The two new diffraction peaks that appeared at 2θ of 18.47° and 27.87° (Fig. 1b) correspond to the formation of $NaMgAlSi_4O_{11}$. The initial transformation process of nanoclay was mainly due to the dehydration and dehydroxylation of montmorillonite clay. After further calcination at 850 °C (Fig. 1c) the basal spacing of Montmorillonite collapsed further to 0.96 nm. Finally, the peaks belonging to $NaMgAlSi_4O_{11}$ disappeared completely at 900 °C due to the destruction of its platelets and the concomitant formation of an amorphous phase of alumino-silicate (Fig. 1d).

3.1.1.2. High resolution transmission electron microscopy (HRTEM) of calcined nanoclay. HRTEM images of nanoclay (Cloisite 30B) are shown in Fig. 2(a and b). The lower magnification image in Fig. 2a gives a general view of the nanoclay platelets. The high magnification image in Fig. 2b shows the layer structure of

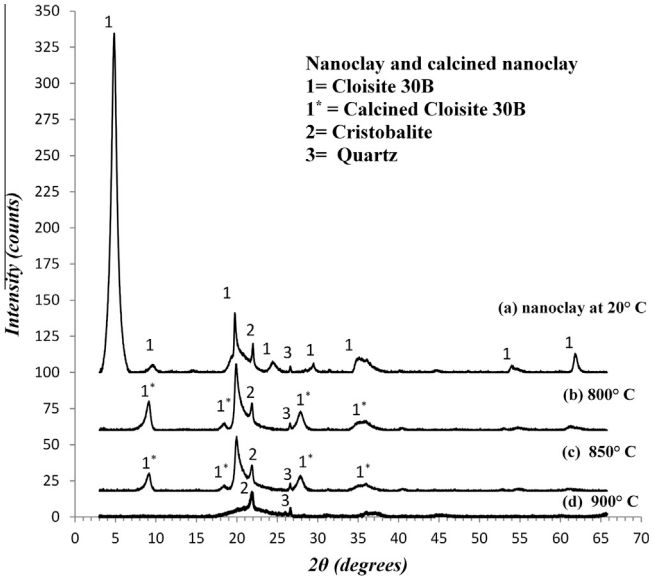

Fig. 1. X-ray diffraction patterns of nanoclay and calcined nanoclay.

platelets. It can be seen clearly that the distances between the nanoclay platelets were about 1.85 nm and thus this is evidence that the d-spacing of (001) planes in nanoclay was 1.85 nm as shown in Table 1 [12]. However, Fig. 2(c and d) shows the HRTEM images for calcined nanoclay (at 900 °C) at low and high magnification, respectively. At high magnification (Fig. 2d), it can be seen that many platelets in calcined nanoclay have been destroyed and broken into nanoparticles with semi-spherical shapes. The transformation of nanoclay platelets into amorphous alumino-silicate during calcination was due to: (a) dehydration and dehydroxylation of montmorillonite clay, (b) decomposition of quaternary ammonium salt, and (c) phase destruction of $NaMgAlSi_4O_{11}$. The natural montmorillonite clay [$(Ca, Na)_{0.3}Al_2(Si, Al)_4O_{10}(OH)_2{\cdot}xH_2O$] has a 2:1 layer crystal structure that consists of aluminium octahedrons within two silicon tetrahedron layers. Dehydration can cause the loss of interlayer H_2O at low temperature and dehydroxylation can lead to OH removal from the octahedral sheets at higher temperatures. He et al. [13] indicated that when montmorillonite nanoclay was calcined at 920 °C, it transformed to an amorphous phase of alumino-silicate. Similarly, Shebl et al. [5] reported that the calcination of montmorillonite nanoclay (Cloisite 30B) at 850 °C for 2 h led to transformation from crystalline nano alumino-silicate into amorphous nano alumino-silicate.

3.1.2. Effect of chemical treatment on hemp fabric

3.1.2.1. Surface morphology of hemp fabric. SEM micrographs of un-treated and NaOH-treated hemp fabrics are shown in Fig. 3(a and b). It is clearly seen that the un-treated fabric had some impurities on its surface (Fig. 3a), which were mostly waxes or fatty substances. However, after chemical treatment with NaOH solution (Fig. 3b), it can be seen that the fabric surface became more uniform due to the removal of these waxes or fatty substances [40–42].

3.1.2.2. Crystallinity index of hemp fabric. Fig. 4 shows the XRD patterns of un-treated and NaOH-treated hemp fabrics. The X-ray diffraction patterns of hemp fabric show a typical crystal lattice of native cellulose (cellulose I). The fibre crystallinity index (*CrI*) of hemp fabric was determined by using the equation of the Segal empirical method [43,44];

$$CrI = \frac{I_{002} - I_{am}}{I_{002}} \times 100 \quad (3)$$

where I_{002} is the maximum intensity of the (002) crystalline peak and I_{am} is the minimum intensity of the amorphous material between (101) and (002) peaks as shown in Fig. 4. The crystallinity index of un-treated and treated hemp fabric was found to be about 82.6% and 86.2%, respectively. It is clear that the NaOH treatment had increased the crystallinity index of hemp fabric as a result of the removal of hemicellulose, pectins, oils and waxes from the surface of hemp fabric [44]. Troedec et al. [41] reported that NaOH treatment is well-known to bleach and clean the surface of hemp fibres and to remove amorphous materials such as hemicellulose, pectins and impurities (fatty substances and waxes) from their surface. They observed that the cellulose crystallinity index of un-treated and NaOH treated hemp fibres was increased from 80% to 86%.

3.1.3. Quantitative X-ray Diffraction Analysis (QXDA) of nano-matrix

The XRD patterns of cement paste and nanocomposites containing 1, 2 and 3 wt% CNC are shown in Fig. 5(a–d), with Corundum [Al_2O_3] (PDF 000461212) as the internal standard. Table 4 shows the Rietveld quantitative phase analysis of cement paste and nanocomposites. Three important phases are noticed in this study: portlandite [$Ca(OH)_2$] (PDF 00-044-1481), tricalcium silicate [C_3S] (00-049-0442) and dicalcium silicate [C_2S] (PDF 00-033-0302). Moreover, four less important phases are also noticed: Ettringite [$Ca_6Al_2(SO_4)_3(OH)_{12}{\cdot}26H_2O$] (PDF 000411451), Gypsum [$Ca(SO_4)(H_2O)_2$] (PDF 040154421), Quartz [SiO_2](PDF 000461045) and Calcite [$CaCO_3$](PDF 000050586).

As can be seen from Table 4 and Fig. 5b, the addition of 1 wt% CNC reduced the amount of $Ca(OH)_2$ from 16.8 wt% to 12.1 wt%, about 28% reduction when compared to cement paste. Also the intensities of major peaks of $Ca(OH)_2$ were significantly reduced when compared to cement paste (Fig. 5b and a). Furthermore, the amorphous content increased from 70.1 wt% to 74.8 wt%, about 6.7% increase. This indicates an obvious consumption of $Ca(OH)_2$ crystals for the pozzolanic reaction due to the presence of CNC

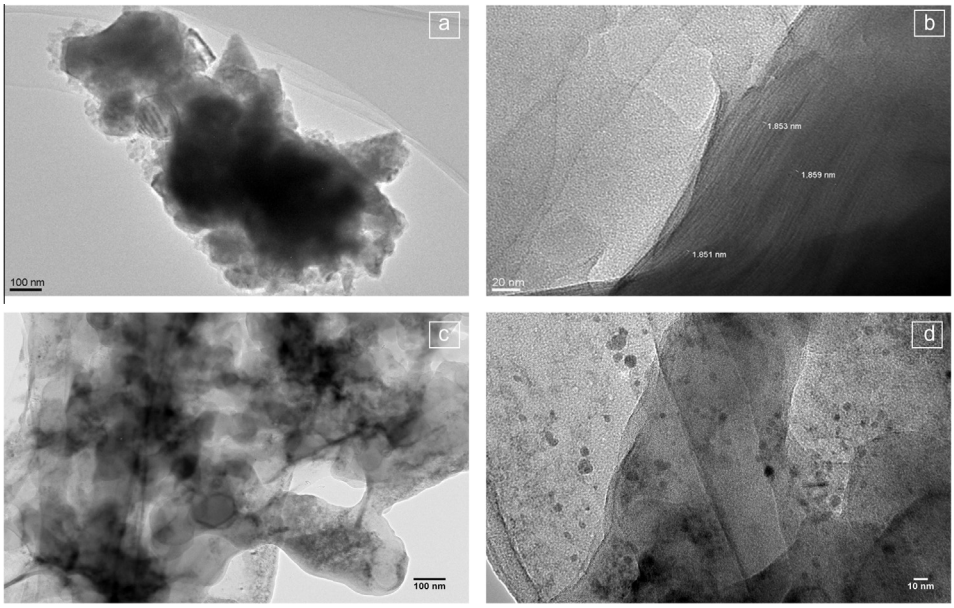

Fig. 2. TEM images of nanoclay and calcined nanoclay (at 900 °C) at low magnification (a and c), and high magnification (b and d).

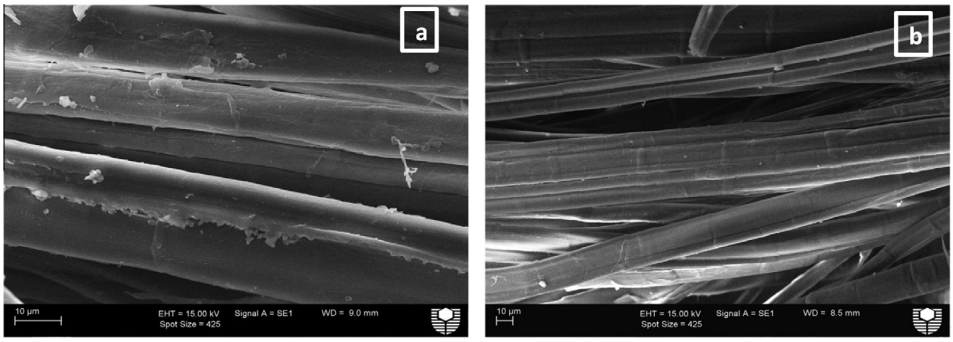

Fig. 3. SEM images showing the surface structure of: (a) untreated hemp fabric and (b) NaOH-treated hemp fabric.

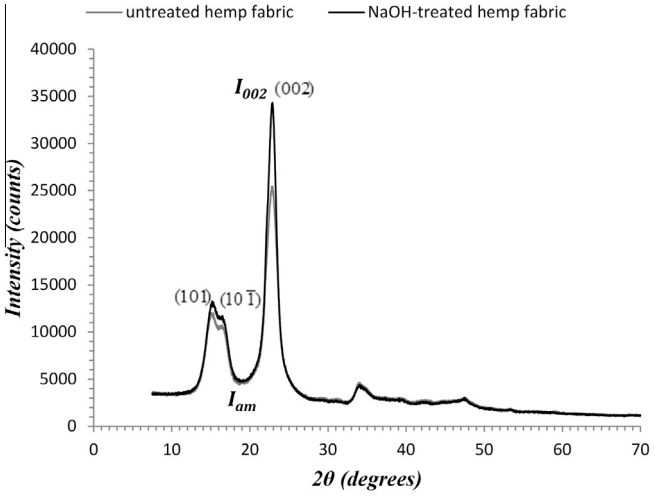

Fig. 4. X-ray diffraction patterns of untreated hemp fabric and NaOH-treated hemp fabric.

and good dispersion of calcined nanoclay in the matrix. As a result more amorphous calcium silicate hydrate gel (C–S–H) was produced. This explanation can be confirmed by the inspection of the amounts of unreacted C_3S (2.0 wt%) and C_2S (6.6 wt%), in which the amounts of unreacted C_3S and C_2S are slightly higher than the cement paste. Wei et al. [45] reported that pozzolanic reaction decelerates the hydration reaction of C_3S and C_2S during the curing time. In this study, these unreacted C_3S and C_2S could react with water later to produce more C–S–H gel after 56 days [36,46]. Recently, Shaikh et al. [47] reported that the quantitative XRD analysis after 28 days showed that the cement paste containing 2% nano-silica exhibited less calcium hydroxide but more C_2S than the control cement paste.

On the other hand, as can be seen from Table 4 and Fig. 5d for nanocomposites containing 3 wt% CNC, the amount of $Ca(OH)_2$ was reduced from 16.8 wt% to 14.1 wt%, about 16% reduction when compared to cement paste. Also the intensities of major peaks of $Ca(OH)_2$ are slightly decreased when compared to cement paste (Fig. 5 d and a). But this reduction of amount of $Ca(OH)_2$ is less than the reduction in nanocomposites containing 1 wt% CNC. Moreover, the amounts of C_3S (1.4 wt%) and C_2S (5.4 wt%) are also lower than nanocomposites containing 1 wt% CNC. This may be attributed to the agglomeration of CNC at high contents which led to relatively poor dispersion and hence relatively poor pozzolanic reaction [2,48].

In summary, it is important to note that the reduction of calcium hydroxide could be attributed to two reasons: (i) increased pozzolanic reaction from amorphous nanoparticles (i.e. CNC) that led to more C–S–H gel being produced, and (ii) reduction of the

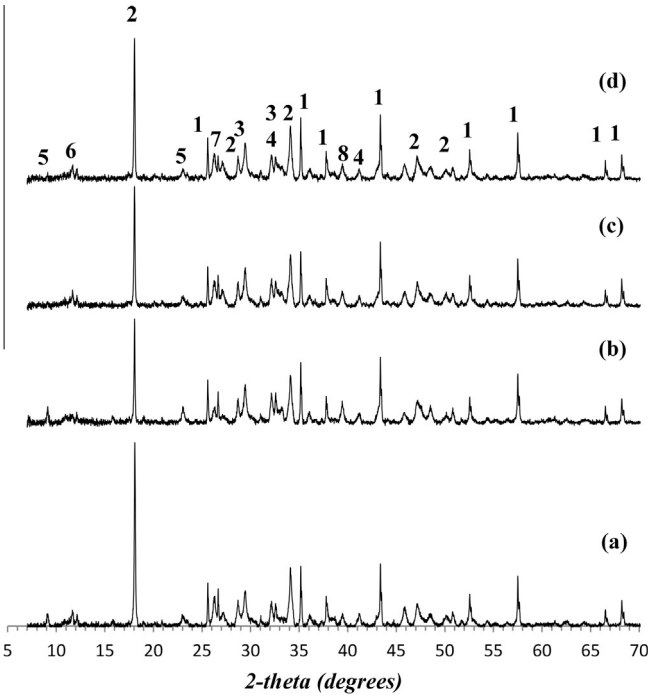

Fig. 5. XRD patterns of: (a) cement paste, nanocomposites containing various amounts of calcined nanoclay: (b) 1 wt% (CNCC1), (c) 2 wt% (CNCC2) and (d) 3 wt% (CNCC3). Legend: 1 = corundum [Al_2O_3], 2 = portlandite [$Ca(OH)_2$], 3 = tricalcium silicate [C_3S], 4 = dicalcium silicate [C_2S], 5 = ettringite, 6 = gypsum, 7 = quartz and 8 = calcite.

Table 4
QXDA results (Phase abundance) by Bruker *DIFFRAC*^{plus} TOPAS 4.2 software for cement paste and nanocomposites containing 1, 2 and 3 wt% calcined nanoclay. (Values in parentheses are the estimated standard deviation of the least significant figure.)

Weight% (Phase abundance)				
Phase	C	CNCC1	CNCC2	CNCC3
Portlandite [$Ca(OH)_2$]	16.8 (6)	12.1 (6)	13.2 (6)	14.1 (6)
Ettringite [$Ca_6Al_2(SO_4)_3(OH)_{12}{\cdot}26H_2O$]	2.0 (3)	1.3 (2)	1.5 (2)	1.8 (3)
Tricalcium silicate [C_3S]	1.3 (2)	2.0 (2)	1.7 (2)	1.4 (2)
Dicalcium silicate [C_2S]	4.4 (2)	6.6 (3)	6.1 (3)	5.4 (3)
Gypsum [$Ca(SO_4)(H_2O)_2$]	0.7 (1)	0.4 (1)	0.6 (1)	0.4 (1)
Calcite [$CaCO_3$]	3.7 (3)	2.1 (2)	2.7 (2)	3.3 (2)
Quartz [SiO_2]	0.9 (1)	0.6 (1)	0.4 (1)	0.7 (1)
Amorphous content	70.1 (8)	74.8 (7)	73.7 (7)	72.8 (8)
Rwp	5.28	5.22	5.29	5.17
Rexp	3.53	3.54	3.52	3.52
χ^2 (Rwp/Rexp)	1.50	1.47	1.50	1.47

Table 5
Porosity and density values for cement paste (C), untreated (UHFRC) composites and 6THFRC composites, nanocomposites (CNCC) and treated hemp fabric-reinforced calcined nanoclay–cement nanocomposites (6THFR-CNCC).

Sample	Porosity %	Density (g/cm^3)
C	23.9 ± 0.5	1.76 ± 0.02
4UHFRC	30.1 ± 0.7	1.61 ± 0.01
5UHFRC	31.2 ± 0.7	1.56 ± 0.03
6UHFRC	33.0 ± 0.4	1.53 ± 0.03
7UHFRC	34.2 ± 0.6	1.51 ± 0.01
6THFRC	32.1 ± 0.8	1.55 ± 0.01
CNCC1	16.5 ± 0.6	1.93 ± 0.01
CNCC2	17.6 ± 0.5	1.91 ± 0.02
CNCC3	18.9 ± 0.6	1.85 ± 0.02
6THFR-CNCC1	28.1 ± 0.5	1.62 ± 0.01
6THFR-CNCC2	29.4 ± 0.8	1.60 ± 0.01
6THFR-CNCC3	30.2 ± 0.7	1.57 ± 0.03

hydration reaction rate of the Portland cement components due to the pozzolanic reaction. As it was found in [45,47] and also in this study, the effect of enhanced pozzolanic reaction by amorphous nanoparticles was more dominant than the reduction of the hydration reaction rate, particularly at the optimum content of nanoparticles with good dispersion.

3.2. Porosity and density

Values of porosity and density of cement paste, un-treated hemp fabric-reinforced cement composites (UHFRC), 6THFRC composites, nanocomposites and treated hemp fabric-reinforced calcined nanoclay–cement nanocomposites (6THFR-CNCC) are shown in Table 5. As expected for all UHFRC composites, the porosity increased but density decreased with increasing hemp fabric content as compared to cement paste [30]. On the other hand, it can be seen also from Table 4 that the NaOH treatment of hemp fabric has slightly reduced the porosity and increased the density of 6THFRC composite when compared to 6UHFRC. For example, the porosity of 6THFRC composite was reduced from 33.0 to 32.0. This slight improvement could be attributed to reduced voids in the fibre–matrix interface region after NaOH treatment of hemp fabric.

Table 5 also shows that the addition of calcined nanoclay caused a decrease in porosity and an increase in density of nanocomposites and 6THFR-CNCC nanocomposites when compared to control cement paste and 6THFRC composites. For nanocomposites with 1 wt% of CNC, the porosity decreased by 31.2% and density increased by 9.7% when compared to cement paste. Moreover, in treated hemp fabric-reinforced nanocomposites containing 1 wt% of CNC, the porosity decreased by 12.4% and density increased by 4.5% when compared to 6THFRC composites. This indicates that CNC has both filling effect and pozzolanic activity in cement paste composites with or without 6 layers of treated hemp fabric, in which the nanocomposite matrix becomes a more dense microstructure due to filling of the micro-pores and densification by the enhanced pozzolanic activity [49]. Supit and Shaikh [50] reported that the addition of 2 wt% nano-silica significantly reduced the porosity of high volume fly ash (HVFA) concrete. However, the addition of more CNC led to increase in porosity and decrease in density. This could be attributed to the poor dispersion and agglomeration of CNC which created more voids in the matrix [2,49].

SEM examinations of the microstructure of control cement paste, nanocomposites containing 1 wt% and 3 wt% CNC are shown in Fig. 6(a–c). The SEM micrograph of control cement matrix (Fig. 6a) shows more Ca(OH)$_2$ crystals (portlandite), Ettringite and pores when compared to nanocomposites. Fig. 6b shows the SEM micrograph of nanocomposites containing 1 wt% CNC, where the microstructure appears denser with fewer pores and more C–S–H gels than the control cement matrix. On the other hand, the

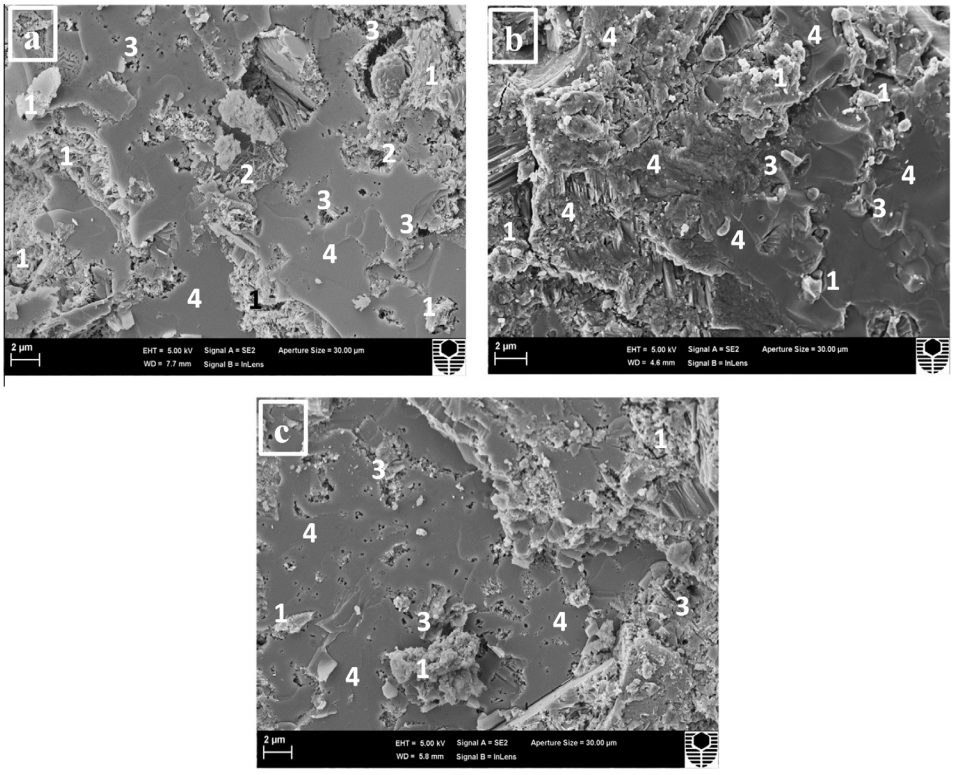

Fig. 6. SEM micrographs of: (a) cement paste, (b) nanocomposites containing 1 wt% calcined nanoclay and (c) nanocomposites containing 3 wt% calcined nanoclay. Legend: 1 = [Ca(OH)$_2$] crystals, 2 = ettringite, 3 = pores and 4 = C–S–H gel.

nanocomposite containing 3 wt% CNC (Fig. 6c) shows more pores than 1 wt% CNC nanocomposite. These SEM results confirm the reduction of portlandite crystals in nanocomposites when compared to cement matrix, thus in agreement with the quantitative X-ray diffraction results (QXDA) above.

3.3. Mechanical properties

3.3.1. Flexural strength of un-treated and treated hemp fabric-reinforced cement composites

Values of flexural strength for cement paste, un-treated hemp fabric-reinforced cement composite (UHFRC) and 6THFRC composites are shown in Fig. 7. It can be seen that the flexural strengths of all hemp fabric-reinforced cement composites have significantly improved when compared to cement paste. This enhancement in flexural properties can be attributed to the ability of hemp fabric to withstand the bending force. Peled and Bentur [26] studied the effect of High Density Polyethylene (HDP) with 8 fabric layers on the flexural strength of cement composites. They reported that the flexural strength of HDP fabric-reinforced cement composite was increased by about 173.7% when compared to control cement paste.

In this study, the flexural strength was increased with an increase in fibre content up to the optimum hemp fibre content, and then decreased after this limit. The optimum hemp fabric content was found to be 6.9 wt%, in which the flexural strength increased from 5.4 to 12.6 MPa, about 133% increase when compared to cement paste. However, beyond this optimum content of hemp fibre, the flexural strength of the UHFRC composites decreased due to the poor adhesion between the fibres and the matrix [51]. For example, the flexural strength of 7UHFRC composites with 8.1 wt% hemp fabric content decreased by about 11.5% when compared to 6UHFRC composites. In a similar work, Bentchikou et al. [52] studied recycled cellulose fibres-cement board with fibre fraction ranged from 0 to 16 wt%. They concluded that composite with the optimum fibre content (4 wt%) gave the maximum flexural strength. In addition, Fig. 7 also shows the effect of NaOH treatment of hemp fabric on the flexural strength of 6THFRC composites. It can be clearly seen that the flexural strength of 6THFRC composites has increased from 12.6 to 14.5 MPa, about 14.9% increase when compared to 6UHFRC composite. This improvement may be explained as follows: after NaOH treatment, most of waxes and fats were removed from the hemp fibre surface, and the surface became more uniform but rough. Thus, this could lead to good interfacial bonding between the matrix and the hemp

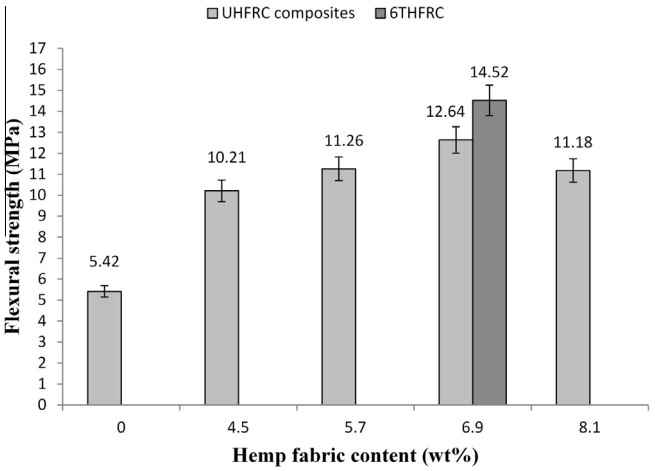

Fig. 7. Flexural strength as a function of hemp fabric content for cement paste, untreated hemp fabric-reinforced cement composites (UHFRC) and treated hemp fabric-reinforced composites (6THFRC).

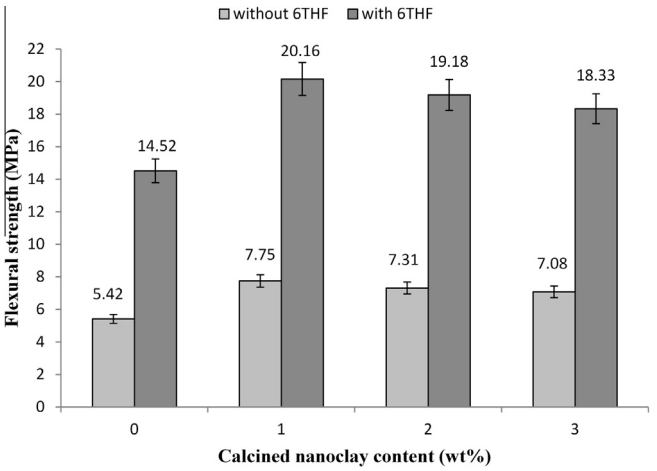

Fig. 8. Flexural strength as a function of calcined nanoclay content for cement paste and its nanocomposites with and without treated hemp fabric (6THF).

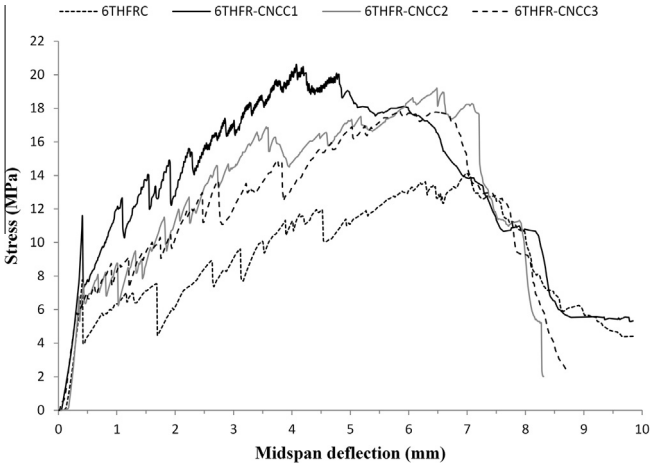

Fig. 9. Stress versus mid-span deflection curves for treated hemp fabric-reinforced cement composites and treated hemp fabric-reinforced nanocomposites.

Table 6
Fracture toughness values for cement paste (C), untreated (UHFRC) composites and 6THFRC composites, nanocomposites (CNCC) and treated hemp fabric-reinforced calcined nanoclay–cement nanocomposites (6THFR-CNCC).

Sample	Fracture toughness (MPa $m^{1/2}$)
C	0.35 ± 0.02
4UHFRC	1.07 ± 0.11
5UHFRC	1.26 ± 0.09
6UHFRC	1.41 ± 0.11
7UHFRC	1.23 ± 0.08
6THFRC	1.60 ± 0.10
CNCC1	0.49 ± 0.02
CNCC2	0.47 ± 0.03
CNCC3	0.44 ± 0.03
6THFR-CNCC1	2.21 ± 0.10
6THFR-CNCC2	2.14 ± 0.11
6THFR-CNCC3	2.04 ± 0.09

fibres which serves to enhance the load transfer process at the interface [53]. Sedan et al. [16] studied the untreated and treated hemp fibre reinforced cement composites with different fibre volume fractions of 7, 10, 16 and 20 vol% ($w/c = 0.5$). They reported that the flexural strength of NaOH treated hemp fibre reinforced cement composite with the optimum fibre content of 16 vol% reached up to 9.5 MPa.

3.3.2. Flexural strength of treated hemp fabric-reinforced cement nanocomposites

The flexural strengths of nanocomposites and treated hemp fabric reinforced-nanocomposites are shown in Fig. 8. Overall, the incorporation of CNC into the cement matrix has led to significant enhancement in the flexural strengths of all nanocomposites and treated hemp fabric reinforced nanocomposites. The flexural strength of nanocomposites containing 1, 2 and 3 wt% CNC increased by 42.9%, 34.8% and 30.6% respectively when compared to cement paste. In addition, the flexural strength of treated hemp fabric reinforced nanocomposites containing 1 wt% CNC (6THFR-CNCC1) increased from 14.5 to 20.2 MPa, about 38.8% increase when compared to treated hemp fabric-reinforced composites. This improvement clearly indicates the effectiveness of CNC in consuming calcium hydroxide (CH), supporting pozzolanic reaction, and filling the micro pores in the matrix. Thus the microstructure of nanocomposite matrix was denser than the cement matrix [54,55]. Consequently, the interfacial bonding of treated hemp fabric-nanocomposite matrix was mostly improved, especially in the case of using 1 wt% CNC, as evident from its higher flexural strength. An analogous research was done by Khorami and Ganjian [56] where they studied the bagasse fibre-reinforced cement matrix with fibre content of 4 wt%, and silica fume was used as 5% replacement for cement. They observed that the flexural strength increased by about 20% when compared to control bagasse fibre-reinforced cement matrix. They attributed this improvement to the Pozzolanic and filler effects of very fine silica fume particles, which led to enhancement of the bonding strength between the matrix and fibres. However, the addition of CNC with more than 1 wt% caused a marked decrease in flexural strength. This strength reduction could be attributed to relatively poor dispersion and agglomeration of the CNC in the cement matrix at higher CNC contents, which caused an increase in porosity and led to the poor adhesion between the fibres and the matrix [2,12,57]. Nevertheless the addition of CNC improved the flexural strength of treated hemp fabric reinforced cement composites. For example, in this study, although the flexural strength of composite with 3 wt% CNC was decreased when compared to composite with 1 wt% CNC but it was still higher than the control composite.

The stress-midspan deflection curves for treated hemp fabric reinforced cement composite and treated hemp fabric reinforced nanocomposites containing 1, 2 and 3 wt% CNC are shown in Fig. 9. The treated hemp fabric reinforced nanocomposite

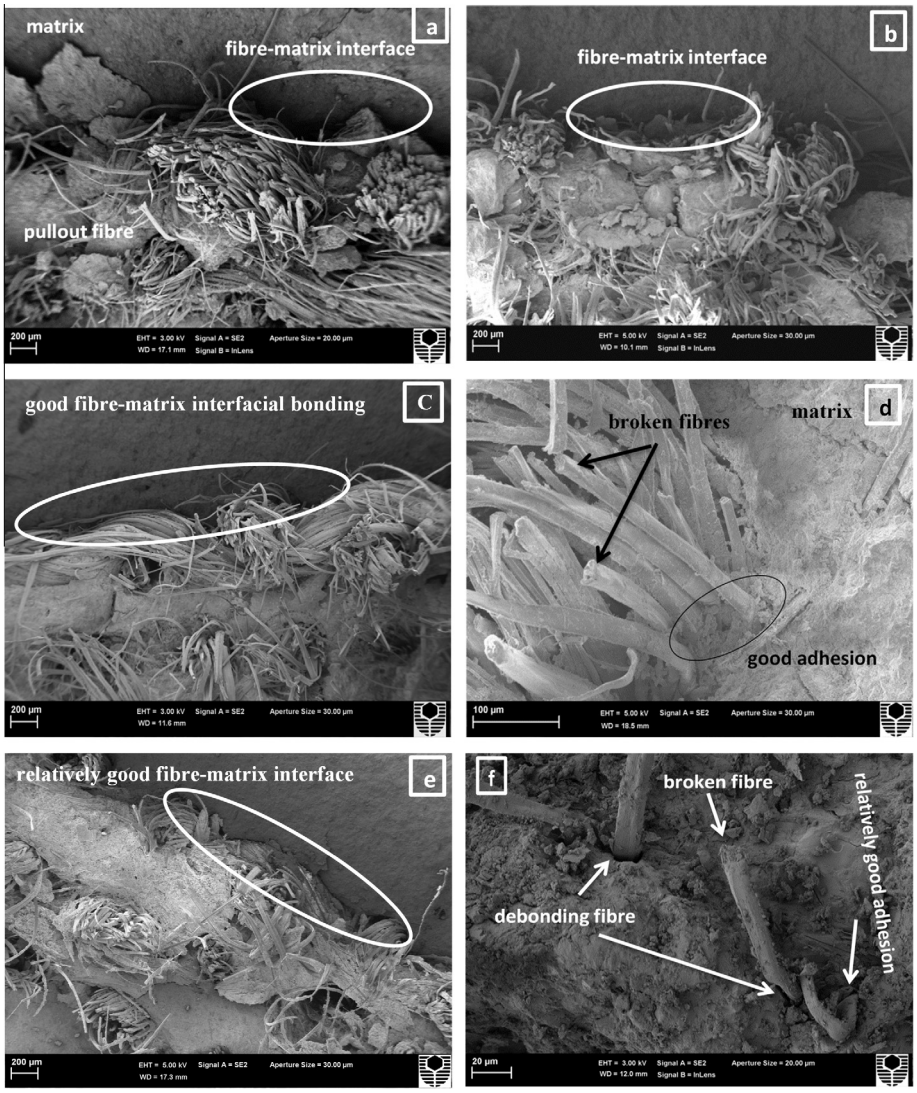

Fig. 10. SEM images showing the fracture surfaces of: (a) 6UHFRC composite, (b) 6THFRC composite, (c and d) 6THFR-CNCC1 nanocomposite, and (e and f) 6THFR-CNCC3 nanocomposite.

containing 1 wt% CNC shows the highest stress. This is due to high fibre–matrix interfacial bonding, which increases the maximum load-transfer capacity [2]. On the other hand, the treated hemp fabric reinforced nanocomposites containing 2 and 3 wt% CNC and treated hemp fabric reinforced cement composite show low flexural stress. This could be attributed to the increase in porosity which reduced the bond strength between the fibres and the matrix, and thus the load-transfer capacity.

3.3.3. Fracture toughness

Results of fracture toughness for cement paste, untreated hemp fabric-reinforced cement composites (UHFRC) and treated hemp fabric-reinforced composites (6THFRC) are shown in Table 6. Overall, these composites showed significant improvement in fracture toughness. This enhancement can be attributed to fracture resistance provided by the hemp fabric which resulted in increased energy dissipation from crack-deflection at the fibre–matrix interface, fibre-debonding, fibre-bridging, fibre pull-out and fibre-fracture [58,59]. As such, these composites are likely to exhibit crack-growth resistance or R-curve behaviour in their fracture resistance due to substantial fibre-bridging at the crack-wake. In UHFRC composites, the 6UHFRC composite achieved the highest fracture toughness with improvement reaching up to 303% when compared to cement paste. However, the increase of the fibre content beyond the optimum content led to a decrease in fracture toughness, as indicated by the lower fracture toughness for the 7UHFRC composites. After NaOH treatment, the 6THFRC composite exhibited 13.5% increase in fracture toughness. This result confirms that chemical treatment has improved the interfacial bond between the matrix and the treated hemp fibres. In a similar study, Li et al. [60] reported that the fracture toughness of treated sisal textile reinforced vinyl-ester composites increased by 31% when compared to untreated ones.

Values of fracture toughness for nanocomposites with and without treated hemp fabrics are also shown in Table 6. The addition of CNC into treated hemp fabric reinforced nanocomposites significantly increased the fracture toughness. The fracture toughness of treated hemp fabric reinforced nanocomposites containing 1, 2 and 3 wt% CNC was 2.21, 2.14 and 2.04 MPa $m^{1/2}$, respectively. It can again be seen that the fracture toughness of 6THFR-CNCC1 composite was increased by 38.1% which can be attributed to the fact that CNC modified the matrix through pozzolanic reaction and reduction of $Ca(OH)_2$ content. Thus, good interfacial bonding between the nanomatrix and treated hemp fibres was achieved. In a similar study, Alamri and Low [61] reported that the addition of 1 wt% halloysite nanotubes (HNTs) into recycled cellulose fibres (RCF)/epoxy matrix significantly increased the fracture toughness by 38.8%. However, when the CNC content increased over the optimum content of 1 wt%, the facture toughness of nanocomposites and treated-hemp fabric-reinforced nanocomposites gradually decreased. This can be attributed to the poor dispersion of CNC within the matrix, which leads to an increase in porosity and weakening of the interfacial bond between the fibres and the matrix.

3.3.4. Failure mechanisms

Fig. 10(a–f) shows the SEM micrographs of 6UHFRC composite, 6THFRC composites and treated hemp fabric-reinforced nanocomposites containing 1 and 3 wt% CNC. A variety of failure mechanisms such as fibre–matrix interfacial debonding, fibre pull-out, rupture fibre and matrix fracture are observed. SEM micrographs of 6UHFRC composite (Fig. 10a) shows relatively poor fibre–matrix interfaces with small gaps between the fabric layers and the cement matrix. In contrast, the 6THFRC composite (Fig. 10b) shows very small gaps between the fabrics and the matrix, which indicates better fibre–matrix interfacial bonding. The images of 6THFR-CNCC1 nanocomposite show good fibre–nanomatrix interfacial bonding (Fig. 10c) with ruptured fibres (Fig. 10d). Similarly, there was good adhesion between the fibre and the matrix in the 6THFR-CNCC3 nanocomposite as evidenced by broken fibres and debonding of fibres (Fig. 10e and f). Relatively good adhesion between the fibre and the matrix and fibre ruptures indicates that the fibre–matrix interface in this nanocomposite was better than the 6THFRC composite (Fig. 10e and b). In addition, these failure mechanisms of composites are in agreement with the stress versus mid-span deflection curves (Fig. 9). For example, 6THFR-CNCC1 nanocomposite shows the highest flexural stress (Fig. 9) which indicates better fibre–nanomatrix interfacial bonding as shown in (Fig. 10c).

4. Conclusions

The influence of calcined nanoclay (CNC) on microstructures and mechanical properties of treated hemp fabric-reinforced cement nanocomposite has been presented. The hemp fabric-reinforced composites were fabricated with fabric loadings of 4.5, 5.7, 6.9 and 8.1 wt%. The optimum content of hemp fabric was found to be 6.9 wt% (6 hemp fabric layers). The flexural strength and fracture toughness of NaOH treated hemp fabric (6THFRC) composite were improved by 14.9% and 13.5% respectively. The optimum content of CNC was found to be 1 wt%. For the treated hemp fabric-reinforced nanocomposites containing 1 wt% calcined nanoclay, the porosity was decreased by 12.4% and properties such as density, flexural strength and fracture toughness were increased by 4.5%, 38.8% and 38.1% respectively. The QXDA analysis showed that the addition of 1 wt% CNC in cement paste reduced the amount of $Ca(OH)_2$ and increased the amount of C–S–H gel. However, the flexural strength of treated hemp fabric-reinforced composites was adversely affected when excess CNC was added.

Acknowledgments

The authors gratefully acknowledge Ms E. Miller for her assistance with SEM imaging. We thank Dr. Cat Kealley of Curtin University for assistance with the work on Quantitative X-ray Diffraction Analysis (QXDA).

References

[1] F. Sanchez, K. Sobolev, Nanotechnology in concrete – a review, Constr. Build. Mater. 24 (2010) 2060–2071.
[2] A. Hakamy, F.U.A. Shaikh, I.M. Low, Microstructures and mechanical properties of hemp fabric reinforced organoclay–cement nanocomposites, Constr. Build. Mater. 49 (2013) 298–307.
[3] A. Alhuthali, I.M. Low, C. Dong, Characterization of the water absorption, mechanical and thermal properties of recycled cellulose fibre reinforced vinyl-ester eco-nanocomposites, Compos. Part B 43 (2012) 2772–2781.
[4] A. Nazari, S. Riahi, The effects of zinc oxide nanoparticles on flexural strength of self-compacting concrete, Compos. Part B 42 (2011) 167–175.
[5] S. Shebl, L. Allie, M. Morsy, H. Aglan, Mechanical behavior of activated nano silicate filled cement binders, J. Mater. Sci. 44 (2009) 1600–1606.
[6] A. Givi, S. Rashid, F. Aziz, M. Salleh, Investigations on the development of the permeability properties of binary blended concrete with nano-SiO_2 particles, J. Compos. Mater. 45 (2011) 1931–1938.
[7] S. Supit, S. Ahmad, Effect of nano-$CaCO_3$ on compressive strength development of high volume fly ash mortars and concretes, J. Adv. Concr. Technol. 12 (2014) 178–186.
[8] Y. Qing, Z. Zenan, K. Deyu, C. Rongshen, Influence of nano-SiO_2 addition on properties of hardened cement paste as compared with silica fume, Constr. Build. Mater. 21 (1) (2007) 539–545.
[9] M. Aly, M.S.J. Hashmi, A.G. Olabi, M. Messeiry, A.I. Hussain, Effect of nano-clay particles on mechanical, thermal and physical behaviours of waste glass cement mortars, Mater. Sci. Eng. A 528 (2011) 7991–7998.
[10] J. Wei, C. Meyer, Sisal fiber-reinforced cement composite with Portland cement substitution by a combination of metakaolin and nanoclay, J. Mater. Sci. 49 (2014) 7604–7619.
[11] N. Farzadnia, A. Ali, R. Demirboga, M. Anwar, Effect of halloysite nanoclay on mechanical properties, thermal behavior and microstructure of cement mortars, Cem. Concr. Res. 48 (2013) 97–104.

[12] S. Filippi, M. Paci, G. Polacco, N. Dintcheva, P. Magagnini, On the interlayer spacing collapse of Cloisite® 30B organoclay, Polym. Degrad. Stab. 96 (2011) 823–832.
[13] C. He, E. Makovicky, B. Osbaeck, Thermal treatment and pozzolanic activity of Na- and Ca-montmorillonite, Appl. Clay Sci. 10 (5) (1996) 351–368.
[14] F. Silva, B. Mobasher, Cracking mechanisms in durable sisal fiber reinforced cement composites, Cem. Concr. Compos. 31 (2009) 721–730.
[15] S. Islam, R. Hussain, M. Morshed, Fiber-reinforced concrete incorporating locally available natural fibers in normal-and high-strength concrete and a performance analysis with steel fiber-reinforced composite concrete, J. Compos. Mater. 46 (2012) 111–122.
[16] D. Sedan, C. Pagnoux, A. Smith, T. Chotard, Mechanical properties of hemp fibre reinforced cement: influence of the fibre/matrix interaction, J. Eur. Ceram. Soc. 28 (2008) 183–192.
[17] M. Ali, A. Liu, H. Sou, N. Chouw, Mechanical and dynamic properties of coconut fibre reinforced concrete, Constr. Build. Mater. 30 (2012) 814–825.
[18] A. Elsaid, M. Dawood, R. Seracino, C. Bobko, Mechanical properties of kenaf fiber reinforced concrete, Constr. Build. Mater. 25 (2011) 1991–2001.
[19] E. Awwada, M. Mabsout, B. Hamad, M. Farran, H. Khatib, Studies on fiber-reinforced concrete using industrial hemp fibers, Constr. Build. Mater. 35 (2012) 710–717.
[20] Z. Li, L. Wang, X. Wang, Compressive and flexural properties of hemp fiber reinforced concrete, Fibers Polym. 5 (2004) 187–197.
[21] Z. Li, X. Wang, L. Wang, Properties of hemp fibre reinforced concrete composites, Compos. Part A 37 (2006) 497–505.
[22] A. Rachini, M. Troedec, C. Peyratout, A. Smith, Comparison of the thermal degradation of natural, alkali-treated and silane-treated hemp fibers under air and an inert atmosphere, J. Appl. Polym. Sci. 112 (2009) 226–234.
[23] P. Blankenhorn, B. Blankenhorn, M. Silsbee, M. DiCola, Effects of fiber surface treatments on mechanical properties of wood fiber–cement composites, Cem. Concr. Res. 31 (2001) 1049–1055.
[24] P. Dalmay, A. Smith, T. Chotard, P. Sahay-Turner, V. Gloaguen, P. Krausz, Properties of cellulosic fibre reinforced plaster: influence of hemp or flax fibres on the properties of set gypsum, J. Mater. Sci. 45 (2010) 793–803.
[25] M. Troëdec, C. Peyratout, A. Smith, T. Chotard, Influence of various chemical treatments on the interactions between hemp fibres and a lime matrix, J. Eur. Ceram. Soc. 29 (2009) 1861–1868.
[26] A. Peled, A. Bentur, Fabric structure and its reinforcing efficiency in textile reinforced cement composites, Compos. Part A 34 (2003) 107–118.
[27] A. Peled, S. Sueki, B. Mobasher, Bonding in fabric–cement systems: effects of fabrication methods, Cem. Concr. Res. 36 (2006) 1661–1671.
[28] A. Peled, B. Mobasher, Tensile behavior of fabric cement-based composites: pultruded and cast, J. Mater. Civ. Eng. 19 (2007) 340–348.
[29] C. Soranakom, B. Mobasher, Geometrical and mechanical aspects of fabric bonding and pull out in cement composites, Mater. Struct. 42 (2009) 765–777.
[30] H. Alamri, I.M. Low, Z. Alothman, Mechanical, thermal and microstructural characteristics of cellulose fibre reinforced epoxy/organoclay nanocomposites, Compos. Part B 43 (2012) 2762–2771.
[31] D. Snoeck, N. De Belie, Mechanical and self-healing properties of cementitious composites reinforced with flax and cottonised flax, and compared with polyvinyl alcohol fibres, Biosyst. Eng. 111 (2012) 325–335.
[32] F. Pacheco-Torgal, S. Jalali, Cementitious building materials reinforced with vegetable fibres: a review, Constr. Build. Mater. 25 (2011) 575–581.
[33] ASTM C-1365-06, Standard test method for determination of the proportion of phases in Portland cement and Portland-cement clinker using X-ray powder diffraction analysis, 2011.
[34] H.F.W. Taylor, Cement Chemistry, Academic Press Limited, London, 1990.
[35] A. Aldridge, Accuracy and precision of phase analysis in Portland cement by Bogue, microscopic and X-ray diffraction methods, Cem. Concr. Res. 12 (1982) 381–398.
[36] K. Scrivenera, T. Fullmanna, E. Galluccia, G. Walentab, E. Bermejob, Quantitative study of Portland cement hydration by X-ray diffraction/Rietveld analysis and independent methods, Cem. Concr. Res. 34 (2004) 1541–1547.
[37] ASTM C-20, Standard test methods for apparent porosity, water absorption, apparent specific gravity, and bulk density of burned refractory brick and shapes by boiling water, 2010.
[38] H. Toutanji, B. Xu, J. Gilbert, T. Lavin, Properties of poly (vinyl alcohol) fiber reinforced high-performance organic aggregate cementitious material: converting brittle to plastic, Constr. Build. Mater. 24 (2010) 1–10.
[39] H. Savastano, A. Turner, C. Mercer, W. Soboyejo, Mechanical behavior of cement-based materials reinforced with sisal fibers, J. Mater. Sci. 41 (2006) 6938–6948.
[40] M. Troëdec, A. Rachini, C. Peyratout, S. Rossignol, E. Max, O. Kaftan, A. Fery, A. Smith, Influence of chemical treatments on adhesion properties of hemp fibres, J. Colloid Interface Sci. 356 (2011) 303–310.
[41] M. Troedec, D. Sedan, C. Peyratout, J. Bonnet, A. Smith, R. Guinebretiere, V. Gloaguen, P. Krausz, Influence of various chemical treatments on the composition and structure of hemp fibres, Compos. Part A 39 (2008) 514–522.
[42] A. Bismarck, I. Askargorta, J. Springer, Surface characterization of flax, hemp and cellulose fibers; surface properties and the water uptake behavior, Polym. Compos. 23 (2002) 872–894.
[43] D. Sedan, C. Pagnoux, T. Chotard, A. Smith, D. Lejolly, V. Gloaguen, Effect of calcium rich and alkaline solutions on the chemical behaviour of hemp fibres, J. Mater. Sci. 42 (2007) 9336–9342.
[44] M. Sawpan, K. Pickering, A. Fernyhough, Effect of various chemical treatments on the fibre structure and tensile properties of industrial hemp fibres, Compos. Part A 42 (2011) 888–895.
[45] Y. Wei, W. Yao, X. Xing, M. Wu, Quantitative evaluation of hydrated cement modified by silica fume using QXRD, 27Al MAS NMR, TG–DSC and selective dissolution techniques, Constr. Build. Mater. 36 (2012) 925–932.
[46] D. Govindarajan, R. Gopalakrishnan, Spectroscopic studies on Indian Portland cement hydrated with distilled water and sea water, Front. Sci. 1 (2011) 21–27.
[47] F.U.A. Shaikh, S.W.M. Supit, P.K. Sarker, A study on the effect of nano silica on compressive strength of high volume fly ash mortars and concretes, Mater. Des. 60 (2014) 433–442.
[48] A. Soin, L. Catalan, S. Kinrade, A combined QXRD/TG method to quantify the phase composition of hydrated Portland cements, Cem. Concr. Res. 48 (2013) 17–24.
[49] B. Jo, C. Kim, G. Tae, J. Park, Characteristics of cement mortar with nano-SiO_2 particles, Constr. Build. Mater. 21 (2007) 1351–1355.
[50] S.W.M. Supit, F.U.A. Shaikh, Durability properties of high volume fly ash concrete containing nano-silica, Mater. Struct. (2014), http://dx.doi.org/10.1617/s115270140329-0.
[51] A. Abdullah, S. Jamaludin, M. Noor, K. Hussin, Composite cement reinforced coconut fiber: physical and mechanical properties and fracture behavior, Aus. J. Basic Appl. Sci. 5 (2011) 1228–1240.
[52] M. Bentchikou, A. Guidoum, K. Scrivener, K. Silhadi, S. Hanini, Effect of recycled cellulose fibres on the properties of lightweight cement composite matrix, Constr. Build. Mater. 34 (2012) 451–456.
[53] D. Asprone, M. Durante, A. Prota, G. Manfredi, Potential of structural pozzolanic matrix–hemp fiber grid composites, Constr. Build. Mater. 25 (2011) 2867–2874.
[54] S. Shebl, L. Allie, M. Morsy, H. Aglan, Mechanical behavior of activated nano silicate filled cement binders, J. Mater. Sci. 44 (2009) 1600–1606.
[55] T. Chang, J. Shih, K. Yang, T. Hsiao, Material properties of Portland cement paste with nano-montmorillonite, J. Mater. Sci. 42 (2007) 7478–7487.
[56] M. Khorami, E. Ganjian, Comparing flexural behaviour of fibre-cement composites reinforced bagasse: wheat and eucalyptus, Constr. Build. Mater. 25 (2011) 3661–3667.
[57] H. Li, H. Xiao, J. Yuan, J. Ou, Microstructure of cement mortar with nano-particles, Compos. Part B 35 (2004) 185–189.
[58] S.F.U. Ahmed, H. Mihashi, Strain hardening behavior of lightweight hybrid polyvinyl alcohol (PVA) fiber reinforced cement composites, Mater. Struct. 44 (2011) 1179–1191.
[59] X. Zhou, S. Ghaffar, W. Dong, O. Oladiran, M. Fan, Fracture and impact properties of short discrete jute-fiber reinforced cementitious composites, Mater. Des. 49 (2013) 35–47.
[60] Y. Li, Y. Mai, L. Ye, Effects of fibre surface treatment on fracture-mechanical properties of sisal-fibre composites, Compos. Interface 12 (2005) 141–163.
[61] H. Alamri, I.M. Low, Microstructural, mechanical, and thermal characteristics of recycled cellulose fiber-halloysite-epoxy hybrid composites, Polym. Compos. 33 (2012) 589–600.

3.6 Thermal and mechanical properties of NaOH treated hemp fabric and calcined nanoclay-reinforced cement nanocomposites.

HAKAMY, A., SHAIKH, F.U.A. & LOW, I.M. 2015. Thermal and mechanical properties of NaOH treated hemp fabric and calcined nanoclay-reinforced cement nanocomposites. *Materials and Design,* 80, 70–81.

Materials and Design 80 (2015) 70–81

Contents lists available at ScienceDirect

Materials and Design

journal homepage: www.elsevier.com/locate/matdes

Thermal and mechanical properties of NaOH treated hemp fabric and calcined nanoclay-reinforced cement nanocomposites

A. Hakamy [a,b], F.U.A. Shaikh [c], I.M. Low [a,*]

[a] Department of Imaging & Applied Physics, Curtin University, GPO Box U1987, Perth, WA 6845, Australia
[b] Department of Physics, Umm Al-Qura University, P.O. Box 715, Makkah, Saudi Arabia
[c] Department of Civil Engineering, Curtin University, GPO Box U1987, Perth, WA 6845, Australia

ARTICLE INFO

Article history:
Received 2 December 2014
Revised 13 April 2015
Accepted 2 May 2015
Available online 4 May 2015

Keywords:
Nanoclay–cement composites
Hemp fabric
Mechanical properties
Microstructure

ABSTRACT

Cement nanocomposites reinforced with hemp fabrics and calcined nanoclay (CNC) have been fabricated and investigated. CNC is prepared by heating nanoclay (Cloisite 30B) at 900 °C for 2 h. The influences of CNC dispersion on the mechanical properties and thermal properties of these composites have been characterized in terms of porosity, density, water absorption, flexural strength, fracture toughness, impact strength and thermal stability. The microstructure is investigated using Quantitative X-ray Diffraction Analysis (QXDA) and High Resolution Transmission Electron Microscopy (HRTEM). The effects of alkali (NaOH) treatment of hemp fabric on the mechanical properties of hemp fabric-reinforced cement composites with different fabric contents of 4.5, 5.7, 6.9 and 8.1 wt% are also investigated. Results show that the optimum hemp fabric content is 6.9 wt% (i.e. 6 fabric layers). Results also indicated that physical, mechanical and thermal properties were enhanced due to the addition of CNC into the cement matrix and the optimum content of CNC was 1 wt%. The treated hemp fabric-reinforced nanocomposites containing 1 wt% CNC exhibited the highest flexural strength, fracture toughness, impact strength and thermal stability by virtue of good fibre–matrix interface. This environmentally friendly nanocomposite can be used for various construction applications such as ceilings and roofs.

1. Introduction

Nowadays, nanotechnology is one of the most active research areas in the civil engineering and construction materials [1–3]. Nanoparticles are used in polymer, ceramic and construction materials in order to produce composites that exhibit superior physical and mechanical properties [4,5]. In the construction industry, several types of nanomaterials have been incorporated into concretes such as nano-SiO_2, nano-Al_2O_3, nano-Fe_2O_3, nano-ZnO_2, nano-$CaCO_3$, nano-TiO_2, carbon nanotubes, nano-metakaolin and nano-ZrO_2 in order to improve the durability and mechanical properties of concrete and Portland cement matrix [6–9]. Supit and Shaikh [10] reported that the addition of 1% nano-$CaCO_3$ increased the compressive strength of mortar and concrete significantly.

Recently, natural fibres are gaining increasing popularity to develop 'environmental-friendly construction materials' as alternative to synthetic fibres in fibre-reinforced concrete [11–13]. These fibres are cheaper, biodegradable and lighter than their synthetic counterparts. Some examples of natural fibres are: Sisal, Flax, Hemp, Bamboo, Coir and others [14–16]. Some researchers have showed that pre-treatments of natural fibre surfaces via some chemical agents such as alkalization, PEI (polyethylene imine), $Ca(OH)_2$ and $CaCl_2$ have slightly improved the fibre–matrix interface of the eco-composites. As a result, the mechanical properties of such composites are enhanced [17,18]. Troėdec et al. [19] reported that the modification of hemp fibres with NaOH has reasonably improved the interfacial bonding between the fibres and the lime-based mineral matrix. On the other hand, one of the most effective techniques to obtain a high performance cementitious composite is by reinforcement with textile (fabrics), which are impregnated with cement matrix. Synthetic fabrics such as polyethylene (PE) and polypropylene (PP) have been used as reinforcement for cement composites. This system has superior filament-matrix bonding which improves the mechanical properties such as tensile and flexural strengths than continuous or short fibres [20–22]. In contrast, the use of natural fibre sheets and fabrics is more prevalent in polymer matrix when compared to cement-based matrix [23].

Despite the advantages of natural fibres and fabrics, there are still some obstacles which have limited their applications in cementitious composites. The interfacial bonding between the

* Corresponding author.
E-mail address: j.low@curtin.edu.au (I.M. Low).

http://dx.doi.org/10.1016/j.matdes.2015.05.003
0261-3069/

natural fibre and the cement matrix is relatively weak and also the degradation of fibres in a high alkaline environment of cement can adversely affect the mechanical and durability properties of natural fibre reinforced cement composites [24]. Pacheco-Torgal and Jalali [25] have recently recommended that much research is needed to overcome these problems.

However, in the construction industry, a combination of eco-composite materials and nanocomposites could lead to new eco-nanocomposites which possess superior physical and mechanical properties. Therefore, little or no research is reported on the combined use of calcined nanoclay (CNC) and treated hemp fabrics as reinforcement in cement nanocomposites. In this paper, the use of CNC in treated hemp fibre-reinforced cement composite overcomes the above disadvantages of hemp fibres in cementitious composites. Due to calcination the amorphous contents of nano clay is increased, which later reacted with $Ca(OH)_2$ of the cement hydration products and formed additional calcium-silica-hydrate (CSH) gel. The benefit of the use of CNC is two folds. Firstly, it reduces the alkalinity of the matrix through reducing the $Ca(OH)_2$. Secondly, the formation of additional CSH improves the microstructure of the matrix and contributes the bonding between the matrix and the hemp fabrics. The effect of CNC on the thermal and mechanical properties of treated hemp fabric-reinforced cement composite is also studied.

2. Experimental procedure

2.1. Materials

The nanoclay platelets (Cloisite 30B) used in this investigation is a natural montmorillonite modified with a quaternary ammonium salt, which was supplied by Southern Clay Products, USA. The specification and physical properties of Cloisite 30B are shown in Table 1. The woven hemp fabric of 0.54 mm thickness and 0.3 mm opening size between bundles was supplied by Hemp Wholesale Australia Pty, Kalamunda, Western Australia. The Hemp fabrics contain 58.7 wt% of cellulose residue, 16.8 wt% of pectins, 14.2 wt% of hemicelluloses, 6 wt% of lignins and 4.3 wt% of waxes and fat. Ordinary Portland cement (ASTM Type I) was used in all mixes.

2.2. Thermal treatment of nanoclay

Calcined nanoclay (CNC) was prepared by heating the nanoclay at 800, 850 and 900 °C for 2 h in an electric furnace with a heating rate of 10 °C/min. The calcined nanoclay was then characterized by XRD and TEM in order to determine the amorphous phase of calcined nanoclay at calcination temperature.

2.3. Chemical treatment of hemp fabric

In order to treat the surface of the fibres, the hemp fabrics were immersed in 1.7 M NaOH solution (pH = 14) for 48 h at 25 °C and then neutralized with 1% vol. acetic acid. They were then washed several times with deionized water until the pH reached about at 7. Finally the fabrics were dried in an oven at 40 °C for 24 h.

Table 1
Physical properties of the nanoclay platelets (Cloisite 30B).

Physical properties of the (Cloisite 30B)	
Colour	Off white
Density (10^3 kg/m^3)	1.98
d-spacing (001) (nm)	1.85
Aspect ratio	200–1000
Surface area (m^2/g)	750
Mean particle size (μm)	6

2.4. Sample preparation

2.4.1. Untreated and treated hemp fabric-reinforced cement composites

The cement paste was prepared through adding water with W/C ratio of 0.485. The fabrication of untreated hemp fabric-reinforced cement composite (UHFRC) specimens was done in two stages. In the first stage, the hemp fabrics (with dimension of 295 mm in length and 65 mm in width) were first soaked into the cement matrix in order to achieve a better penetration of matrix into the openings of the fabrics. Then the first pre-soaked hemp fabric was laid on polished timber mould, followed by another layer of pre-soaked hemp fabric, and so on, depending on the number of fabric layers. After that, the compacted fabrics were then left under 4.9 kPa compressive pressure (heavy weight 30 kg) for 1 h to reduce entrapped air inside the specimens. In the second stage, a thin layer of cement matrix was poured into the prismatic mould followed by the compacted pre-soaked hemp fabrics into the mould. Finally a thin layer of matrix was poured into the mould as upper layer and the specimens were left for 24 h to cure at room temperature. UHFRC composites are fabricated with different weight percentages of hemp fabrics of 4.5 wt% (4 layers of fabrics), 5.7 wt% (5 layers of fabrics), 6.9 wt% (6 layers of fabrics) and 8.1 wt% (7 layers of fabrics). For the fabrication of treated hemp fabric-reinforced cement composite (6THFRC) specimens, only 6 layers of treated hemp fabric was used because 6 layers of hemp fabric exhibited the best performance among all hemp fabric layers. The fabrication procedure of 6THFRC is similar to that of UHFRC described above.

2.4.2. Nanocomposites

Ordinary Portland cement (OPC) is partially substituted by calcined nanoclay (CNC) of 1%, 2% and 3% by weight of OPC. The OPC and CNC were first dry mixed for 5 min in a Hobart mixer (model A00) at a low speed (rpm 483) and then mixed for another 10 min at high speed (rpm 966) until a uniform mixture was achieved. The cement –nanocomposite paste was prepared through adding water with a water/binder (calcined nanoclay–cement) ratio of 0.485. The nanocomposite containing 1, 2 and 3 wt% CNC is termed as CNCC1, CNCC2 and CNCC3, respectively. The cement paste without CNC was considered as a control.

2.4.3. Treated hemp fabric-reinforced nanocomposites

Only 6 layers of treated hemp fabrics were used to reinforce the matrix. The fabrication steps are similar to that of UHFRC described before. The treated hemp fabric-reinforced nanocomposite containing 1, 2 and 3 wt% CNC is termed as 6THFR-CNCC1, 6THFR-CNCC2 and 6THFR-CNCC3, respectively. The total amount of treated hemp fabrics in each specimen was about 6.9 wt%. The mix proportions are shown in Table 2. The position through the depth of sample containing 6 layers of treated hemp fabric is shown in Fig. 1.

2.4.4. Curing and specimens

For each series, five prismatic plate specimens of 300 × 70 × 10 mm in dimension were cast. All specimens were demolded after 24 h of casting and kept under water for approximately 56 days. Five rectangular specimens of each series with dimensions 70 × 20 × 10 mm were cut from the fully cured prismatic plate for each mechanical and physical test.

Table 2
Mix proportions of specimens.

Sample	Hemp fabric (HF)		Mix proportions (wt%)		
	Content (wt%)	Fabric layers	Cement	CNC	Water/ binder
C	0	0	100	0	0.485
4UHFRC	4.5	4	100	0	0.485
5UHFRC	5.7	5	100	0	0.485
6UHFRC	6.9	6	100	0	0.485
7UHFRC	8.1	7	100	0	0.485
6THFRC	6.9	6	100	0	0.485
CNCC1	0	0	99	1	0.485
CNCC2	0	0	98	2	0.485
CNCC3	0	0	97	3	0.485
6THFR-CNCC1	6.9	6	99	1	0.485
6THFR-CNCC2	6.9	6	98	2	0.485
6THFR-CNCC3	6.9	6	97	3	0.485

2.5. Material characterization

2.5.1. High resolution transmission electron microscopy (HRTEM)

High Resolution Transmission electron microscopy imaging was done using 3000F (JEOL company) operating at 300 kV equipped with a 4 × 4 k CCD camera (Gatan). HRTEM was carried out at University of Western Australia.

2.5.2. The quantitative X-ray diffraction analysis (QXDA)

The samples were measured on a D8 Advance Diffractometer (Bruker-AXS) using Cu Kα (λ = 1.5406 Å) radiation. The diffractometer were scanned from 7° to 70° (2θ) using a scanning rate of 0.5°/min. The Quantitative X-ray Diffraction Analysis (QXDA) with Rietveld refinement was done with Bruker *DIFFRAC^{plus}* TOPAS software associated with the International Centre for Diffraction Data PDF-4 2013 database. Corundum [Al_2O_3] was chosen to serve as an internal standard [2,26–28]. The samples for QXDA were prepared by mixing a dry weight of 3.0 g of cement paste or nanocomposite paste with 0.33 g of Corundum [Al_2O_3] as the internal standard [4,29].

2.5.3. Scanning electron microscopy (SEM)

Scanning electron microscopy imaging was obtained using a NEON 40ESB, ZEISS. The SEM investigation was carried out in detail on microstructures and the fractured surfaces of samples.

2.5.4. Thermogravimetric analysis (TGA)

The thermal stability of samples was studied by thermogravimetry analysis (TGA). A Mettler Toledo TGA 1 star system analyser was used for all measurements. Samples with 30 mg were placed in an alumina crucible and tests were carried out in Argon atmosphere with a heating rate of 10 °C/min from 25 to 1000 °C.

2.6. Physical properties

Measurements of bulk density and porosity were conducted to determine the quality of nanocomposites. Five specimens, measuring 70 × 20 × 10 mm, in each composition were used to measure the physical properties. The calculation for density was carried out by using the following equation [30]:

$$\rho = \frac{m_d}{V} \tag{1}$$

where ρ = density in (kg/m^3), m_d = mass of the dried sample (kg) and V = volume of the test specimen (m^3).

The apparent porosity P_S was calculated using the following equation [30]:

$$P_S = \frac{m_s - m_d}{m_s - m_i} \times 100 \tag{2}$$

where m_i = mass of the sample saturated with and suspended in water, m_s = mass of the sample saturated in air.

For the water absorption test, the produced specimens were dried at a temperature of 80 °C until their mass became constant and then the mass was weighed (W_0). The specimens were then immersed in clean water at a temperature of 20 °C for 48 h. After the desired immersion period, the specimens were taken out and wiped quickly with wet cloth, and then the mass was weighed (W_1) immediately. The water absorption (W_A) was calculated by using the formula [31]:

$$W_A = \frac{W_1 - W_0}{W_0} \times 100 \tag{3}$$

2.7. Mechanical properties

Five specimens, measuring 70 × 20 × 10 mm, in each composition were used to measure the mechanical properties. The orientation of the hemp fabrics is horizontal to the direction of the applied force (Fig. 2). Three-point bend tests were conducted using a LLOYD Material Testing Machine to evaluate the flexural strength and fracture toughness of the composites. The support span used was 40 mm with a displacement rate of 0.5 mm/min. The flexural strength σ_F was evaluated using the following equation [12]:

$$\sigma_F = \frac{3P_m S}{2BW^2} \tag{4}$$

where P_m is the maximum load at crack extension, S is the span of the sample, W is the specimen depth and B is the specimen width.

In order to determine the fracture toughness, a sharp razor blade was used to initiate a sharp crack in the samples. The ratio of crack length to depth ($\frac{a}{W}$) was about 1/3. The fracture toughness was calculated using the following equation [32]:

$$K_{IC} = \frac{p_m S}{BW^{3/2}} f\left(\frac{a}{W}\right) \tag{5a}$$

where a is the crack length (mm) and $f\left(\frac{a}{W}\right)$ is the polynomial geometrical correction factor given by:

$$f\left(\frac{a}{W}\right) = \frac{3(a/W)^{1/2}\left[1.99 - (a/W)(1 - a/W) \times \left(2.15 - 3.93a/W + 2.7a^2/W^2\right)\right]}{2(1 + 2a/W)(1 - a/W)^{3/2}} \tag{5b}$$

The impact strength of the composite was determined using, Zwick Charpy impact tester with 15 J pendulum hammer and 40 mm support span. Un-notched sampled were used to compute the impact strength using the following formula [5]:

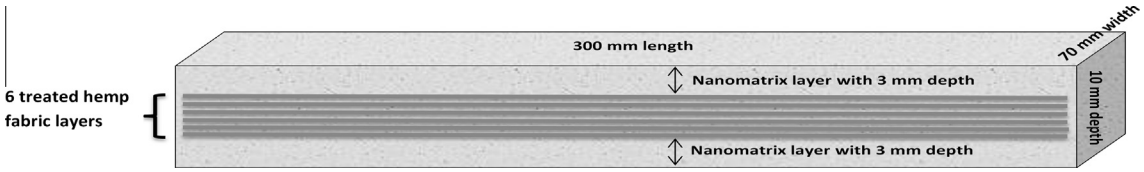

Fig. 1. Schematic representation of 6 treated hemp fabric layers position through the depth of sample.

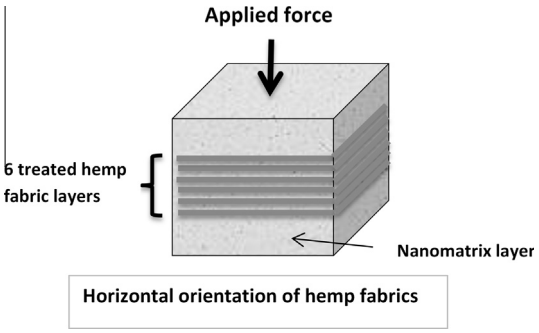

Fig. 2. Schematic representation of the horizontal orientation of hemp fabrics relative to the direction of the applied force.

$$\sigma_I = \frac{E}{A} \tag{6}$$

where E is the impact energy to break a sample with a ligament of area A.

3. Results and discussion

3.1. Effect of thermal treatment on nanoclay microstructure

(a) XRD analysis of calcined nanoclay

Fig. 3 shows the XRD patterns of nanoclay and those calcined at 800, 850 and 900 °C for 2 h, respectively. Curve shows the XRD patterns of nanoclay with wide diffraction peaks and exhibits crystalline phase at 2θ of 4.82° which indicates the presence of the ammonium salt and also it has other crystalline phases which refers to Montmorillonite-18A $[Na_{0.3}(Al,Mg)_2Si_4O_{10}OH_2{\cdot}6H_2O]$ (PDF000120219). Patterns of calcined nanoclay at 800, 850 and 900 °C show that the ammonium salt peak completely disappeared at these temperatures. Also other nanoclay peaks gradually disappeared and transferred to amorphous state (calcined nanoclay) at 900 °C (see curve 'd' in Fig. 3). This XRD analysis clearly shows the transformation of crystalline phases of nanoclay to amorphous phases due to calcination. Amorphous materials such as silica fume, flay ash, metakaolin, nano-SiO_2, nano-metakaolin and also this calcined nanoclay behave as a highly reactive pozzolan to support pozzolanic reaction and then produce more CSH gel in cement-composite [7]. Therefore by using one of these materials such as calcined nanoclay, the mechanical properties of cement-composites could be improved noticeably. He et al. [33] indicated that when montmorillonite clay calcined at 920 °C the clay phases disappeared completely and then clay transformed to amorphous phase, but further calcination after 920 °C leads to form another crystalline phase which called spinel. Shebl et al. [34] reported that the thermal activation of nano silicate (at 850 °C for 2 h) transformed its structure from crystalline silica into amorphous silica as a result of this the indirect tensile was strongly enhanced of the nano structured blended cement pastes.

(b) High Resolution Transmission Electron Microscopy (HRTEM) of calcined nanoclay

HRTEM images of nanoclay (Cloisite 30B) at low and high magnification are shown in Fig. 4a and b. In the high magnification image (Fig. 4b), it can be seen clearly that the distances between the nanoclay platelets (layers) were about 1.85 nm and thus this is evidence that the d-spacing of (001) planes in nanoclay layers were 1.85 nm as shown in Table 1. However, Fig. 4c and d show the HRTEM images for calcined nanoclay (at 900 °C) at low and high magnification, respectively. In high magnification image in Fig. 4d, it can be seen that many platelets in calcined nanoclay were destroyed and some of them broken to small nanoparticles with semi-spherical shapes. This result also confirms the amorphous phase of calcined nanoclay which agrees with XDR result above.

(c) Surface morphology of hemp fabric

SEM micrographs of un-treated and NaOH-treated hemp fabrics are shown in Fig. 5a–c, respectively. It is clearly seen that the untreated fabric had some impurities on its surface (Fig. 5a and b). Troëdec et al. [35] reported that these impurities are mostly waxes or fatty substances and also they indicated that NaOH treatment is well-known to bleach and clean the surface of plant fibres and to remove amorphous materials such as hemicelluloses and pectins from their surface. As can be seen from Fig. 5c, the NaOH treatment removed impurities, hemicelluloses and pectins from the fabric surfaces and thus surfaces become more homogeneous [36].

(d) TGA of hemp fabric

The thermograms (TGA) of untreated hemp fabric and treated hemp fabric are shown in Fig. 6. It can be seen from TGA curve that

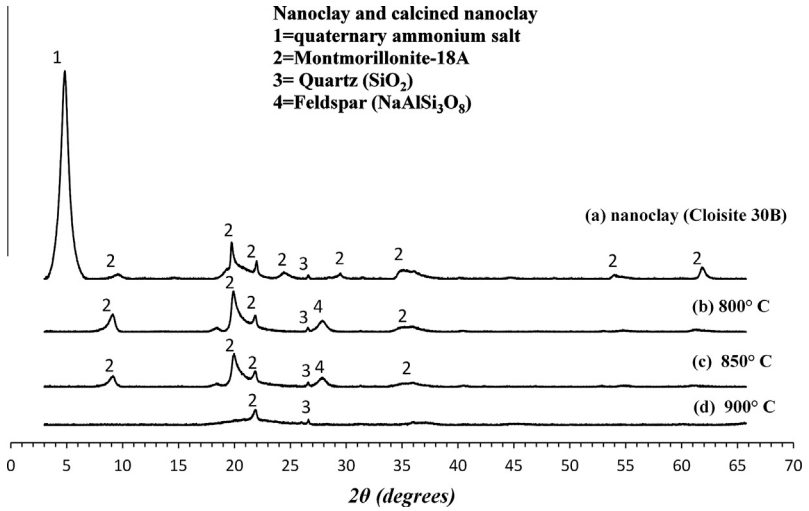

Fig. 3. X-ray diffraction patterns of nanoclay and calcined nanoclay.

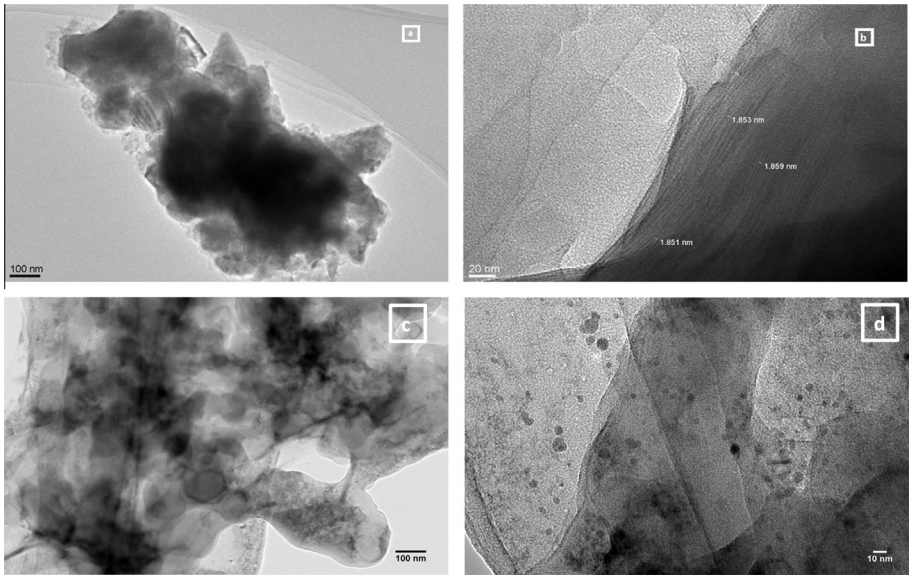

Fig. 4. TEM images of nanoclay and calcined nanoclay (at 900 °C) at: (a and c) low magnification, (b and d) high magnification.

the weight loss (%) between 285 and 390 °C is due to decomposition of cellulose [19]. Among all range 25–1000 °C, it can be seen that the treated hemp fabric shows slightly higher thermal stability than untreated. This indicates that the NaOH treatment increases the thermal stability of hemp fibres through removal of the most fats, waxes and amorphous materials [17,37].

(e) Quantitative X-ray Diffraction Analysis (QXDA) of nano-matrix

The XRD patterns of cement paste and nanocomposites containing 1, 2 and 3 wt% CNC are shown in Fig. 7, that including Corundum [Al_2O_3] (PDF 000461212) phase as the internal standard. Table 3 shows the quantitative analysis with Rietveld refinement of cement paste and nanocomposites. Three important phases are noticed in this study: portlandite [$Ca(OH)_2$] (PDF 00-044-1481), tricalcium silicate [C_3S] (00-049-0442) and dicalcium silicate [C_2S] (PDF 00-033-0302). Moreover, four less important phases are also noticed: Ettringite [$Ca_6Al_2(SO_4)_3(OH)_{12}{\cdot}26H_2O$] (PDF 000411451), Gypsum [$Ca(SO_4)(H_2O)_2$] (PDF 040154421), Quartz [SiO_2] (PDF 000461045) and Calcite [$CaCO_3$] (PDF 000050586) [2,26,29,38].

Generally, the addition of 1, 2 and 3 wt% CNC into the cement matrix has resulted in apparent change to the crystalline components of the samples. As can be seen from Table 3 and Fig. 7b, the addition of 1 wt% CNC reduced the amount of $Ca(OH)_2$ from 16.8 wt% to 12.1 wt%, about 28% reduction compared to cement paste. Also the intensities of major peaks of $Ca(OH)_2$ were significantly reduced compared to cement paste (Fig. 7b and a). Furthermore, the amorphous content was increased from 70.1 wt% to 74.8 wt%, about 6.7% increase. This indicates that an obvious consumption of $Ca(OH)_2$ crystals mainly due to the effect of pozzolanic reaction in the presence of CNC and good dispersion of calcined nanoclay in the matrix leads to more amorphous calcium silicate hydrate gel (C–S–H). This explanation is also confirmed by the inspection of amount of unreacted C_3S (2.0 wt%) and C_2S (6.6 wt%), in which the amount of unreacted C_3S and C_2S are slightly higher than the cement paste. Wei et al. [39] reported that pozzolanic reaction decelerates the hydration reaction of C_3S and C_2S during the curing time of 28–90 days. In this study, these unreacted phases could react with water later to produce more C–S–H gel after 56 days [29]. Recently, Shaikh et al. [40] reported that the cement paste containing 2% NS (nano-silica) exhibited less the amount of calcium hydroxide and slightly higher amount of C_2S than control cement paste.

On the other hand, as can be seen from Table 3 and Fig. 7d for nanocomposites containing 3 wt% CNC, the amount of $Ca(OH)_2$ was decreased from 16.8 wt% to 14.1 wt%, about 16% reduction compared to cement paste. Also the intensities of major peaks of $Ca(OH)_2$ were slightly decreased compared to cement paste (Fig. 7d and a). But this reduction of amount of $Ca(OH)_2$ is less than the reduction in nanocomposites containing 1 wt% CNC. Moreover, the amounts of C_3S (1.4 wt%) and C_2S (5.4 wt%) are also lower than nanocomposites containing 1 wt% CNC. This may be attributed to agglomerations of CNC at high contents which lead to relatively poor dispersion of CNC and hence relatively poor pozzolanic reaction [2,4].

3.2. Porosity, water absorption and density

The porosity, water absorption and density of cement paste, UHFRC composites, 6THFRC composites, nanocomposites and 6THFR-CNCC nanocomposites are shown in Table 4. As expected for all UHFRC composites the porosity and water absorption are increased and the density is decreased with increasing hemp fabric content as compared to cement paste. However, it can be seen that the NaOH treatment of hemp fabric has slightly reduced the porosity and water absorption and increased the density of 6THFRC composite when compared to 6UHFRC. This slight improvement could be attributed to reduced voids in the fibre–matrix interface region after NaOH treatment in 6THFRC composite [41]. Table 4 also shows that the addition of CNC decreases the porosity and water absorption of these composites when compared to control cement paste and 6THFRC composites. In 6THFR-CNCC1 composite, the porosity and water absorption decreased by 12.4% and 14%, respectively compared to 6THFRC composites. This indicates that CNC has filling effect in the porosity of cement paste composites with 6 treated hemp fabric [42]. Supit and Shaikh [43] reported that the addition of 2 wt% NS (nano-silica) significantly reduced the porosity of high volume fly ash (HVFA) concrete. Furthermore, In Table 4, the addition of 1 wt% CNC increased the density of control cement paste and 6THFRC composite by 9.7% and 4.5%, respectively. This improvement demonstrated that cement composites with 1 wt% CNC yields more consolidated

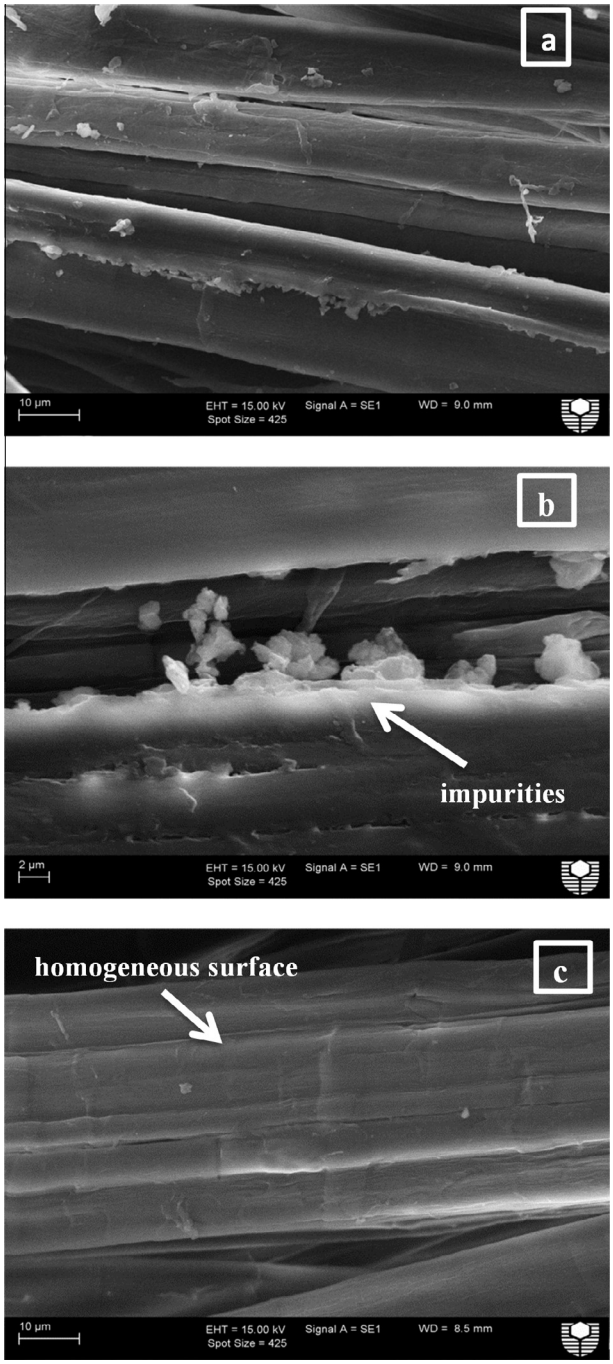

Fig. 5. SEM images of surface structure: (a and b) untreated hemp fabric, (c) NaOH-treated hemp fabric.

microstructure. However, the addition of more CNC leads to increase in porosity and water absorption and also decrease in density. This could be attributed to the poor dispersion and agglomerations of the CNC which create more voids in the matrix [3,42,43].

SEM examinations of the microstructure of cement paste, CNCC1and CNCC3 nanocomposites are shown in Fig. 8a–c. Fig. 8a shows more $Ca(OH)_2$ crystals and Ettringite as well as more pores which revealed weak structure. Fig. 8b shows the SEM micrograph of CNCC1, which is different from that of cement paste, the structure is dense and compact with few pores and more C–S–H gel. On the other hand, in Fig. 8c, the CNCC3 shows more pores than CNCC1which relatively weaken the structure.

3.3. Mechanical properties

In general, the horizontal orientation of hemp fabrics relative to the direction of the applied force could lead to better uniformity in load distribution among the compacted fabrics of hemp fabrics and then increase the ability (resistance) of hemp fibres to withstand applied load of the composites.

(a) Flexural strength

Flexural strength of cement paste, un-treated hemp fabric-reinforced cement composite (UHFRC), 6THFRC composites, nanocomposites (CNC) and treated hemp fabric reinforced-nanocomposites (6THFR-CNCC) are shown in Table 5. It can be seen that flexural strength is increased with increase in fabric content up to the optimum Hemp fabric content, and then decreased after this limit. The optimum Hemp fabric content was found to be 6.9 wt%, in which the flexural strength is increased from 5.42 to 12.64 MPa, about 133.2% increase compared to cement paste. However, beyond this optimum content of Hemp fibre, the flexural strength of the UHFRC composites decreased due to the poor adhesion between the fibres and the matrix [44]. In addition, Table 5 also shows the effect of the NaOH treatment of Hemp fabric on the flexural strength of 6THFRC composites. It can be clearly seen that the flexural strength of 6THFRC composites is increased from 12.64 to 14.52 MPa, about 14.9% increase compared to 6UHFRC composite. This improvement may be explained as follows: after NaOH treatment, the most of waxes, hemicelluloses and pectins are removed from the hemp fibre surface, and then the surface became more homogeneous. Thus, this could lead to the good interfacial bond between the matrix and the hemp fibres which also enhanced the load transfer process at the interface. For comparison with similar research, Asprone et al. [45] investigated composite system consisting of a thin pozzolanic mortar slab reinforced with different layers of hemp fibre grids after hemp fibre grids were coated by epoxy resin coating at 28 days. They observed that the flexural strength of epoxy coated hemp fibre grid-reinforced pozzolanic matrix with fibre content of 7 wt% (i.e. 6 layers) increased from 7.0 to 15.0 MPa compared to control mortar matrix. Whereas in this study, the flexural strength of treated hemp fibre reinforced cement composites (6THFRC) reached up to 14.52 MPa. Sedan et al. [12] studied the untreated and treated hemp fibre reinforced cement composite with different fibre volume fractions of 7, 10, 16 and 20 vol% (w/c = 0.5). They reported that the flexural strength of NaOH treated Hemp fibre reinforced cement composite with the optimum Hemp fibres content of 16 vol% reached up to 9.5 MPa.

Overall, the incorporation of CNC into the 6UHFRC composite led to significant enhancement in the flexural strength of all treated Hemp fabric reinforced nanocomposites. The flexural strength of 6THFR-CNCC1 is increased from 14.52 to 20.16 MPa, about 38.8% increase compared to 6UHFRC composite. This improvement clearly indicates the effectiveness of CNC in consuming calcium hydroxide (CH), supporting pozzolanic reaction and filling the micro pores in the matrix. Thus the microstructure of nanocomposite matrix is denser than the cement matrix [34,46]. Consequently, the treated hemp fabric-nanocomposite matrix interfacial bonding is mostly improved, especially in the case of using 1 wt% CNC, which is evident from the higher flexural strength value. For comparison with similar research, Wei and Meyer [47] studied the sisal fibre reinforced cement mortar nanocomposites with long and aligned layers of fibres (185 mm long) and content of 2 vol%, and also metakaolin and nanoclay were replaced by 29 wt% and 1 wt% respectively of cement weight. The water/binder ratio was 0.4 and composites were tested at 28 days. They reported that the flexural strength increased about 36.46% compared to sisal fibre-reinforced cement mortar. They

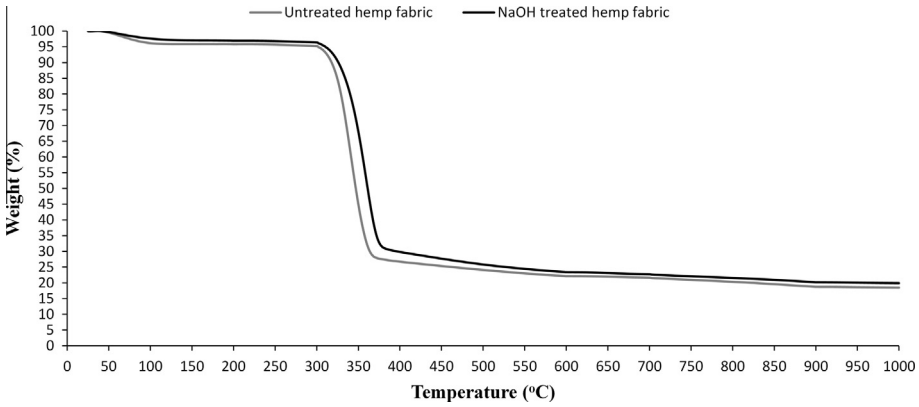

Fig. 6. TGA curves of untreated hemp fabric and NaOH-treated hemp fabric.

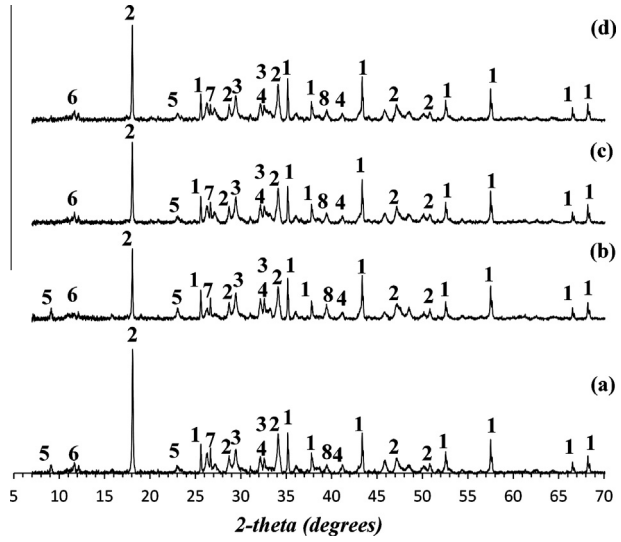

Fig. 7. XRD patterns of: (a) cement paste, nanocomposites containing various of calcined nanoclay, (b) 1 wt% (CNCC1), (c) 2 wt% (CNCC2), (d) 3 wt% (CNCC3). Numbers indicate to: 1 = Corundum [Al_2O_3] phase, 2 = Portlandite [$Ca(OH)_2$] phase, 3 = Tricalcium silicate [C_3S] phase, 4 = Dicalcium silicate [C_2S] phase, 5 = Ettringite phase, 6 = Gypsum phase, 7 = Quartz phase, 8 = Calcite phase.

attributed this enhancement to the efficiency of metakaolin and nanoclay through filler and pozzolanic effects, which led to improve the interfacial bond strength of sisal fibre in cement matrix. Hence, the improvement in flexural strength of 6THFR-CNCC1 nanocomposites observed in this study (38.8%) is slightly better than that observed by Wei and Meyer. Khorami and Ganjian [48] investigated the bagasse fibre-reinforced cement matrix with fibres content of 4 wt% and 5% silica fume. They observed that the flexural strength improved about 20% compared to control bagasse fibre-reinforced cement matrix because of the pozzolanic and filler effects of very fine silica fume particles, thus better fibre–matrix interface was achieved.

However, the addition of CNC more than 1 wt% caused a marked decrease in flexural strength. This could be attributed to the relatively poor dispersion and agglomerations of the CNC in the cement matrix at higher CNC contents, which create weak zones, in the form of micro-voids which cause stress concentration [2,49]. Moreover, the addition of more CNC (i.e. 2 wt%) led to a significant reduction in flexural strength due to an increase in porosity. Nevertheless the addition of CNC improved the flexural strength of treated hemp fabric reinforced cement composites. For example, in this study, although the flexural strength of composite with 3 wt% CNC decreased compared to composite with 1 wt% CNC but it is still higher than the 6UHFRC composite.

The load-midspan deflection curves of 6UHFRC composite and 6THFR-CNCC nanocomposites are shown in Fig. 9. The 6THFR-CNCC1 shows the highest flexural load among all. This is due to high fibre–matrix interface bonding, which increases the maximum load-transfer capacity [2]. On the other hand, the 6THFR-CNCC2, 6THFR-CNCC3 and 6UHFRC composites show low flexural load. This could be attributed to the increase in porosity which decreases the bond strength between the fibres and the matrix, and thus the load-transfer [3,4].

(b) Fracture toughness

Fracture toughness of cement paste, 6UHFRC composites, 6THFRC composites and nanocomposites with treated Hemp fabrics (6THF) are shown in Fig. 10. Overall, all these composites showed significant improvement in fracture toughness. This

Table 3
QXDA results for cement paste (C) and nanocomposites containing 1, 2 and 3 wt% CNC.

Weight % (phase abundance)				
Phase	C	CNCC1	CNCC2	CNCC3
Portlandite [$Ca(OH)_2$]	16.8	12.1	13.2	14.1
Ettringite [$Ca_6Al_2(SO_4)_3(OH)_{12}{\cdot}26H_2O$]	2.0	1.3	1.5	1.8
Tricalcium silicate [C_3S]	1.3	2.0	1.7	1.4
Dicalcium silicate [C_2S]	4.4	6.6	6.1	5.4
Gypsum [$Ca(SO_4)(H_2O)_2$]	0.7	0.4	0.6	0.4
Calcite [$CaCO_3$]	3.7	2.1	2.7	3.3
Quartz [SiO_2]	0.9	0.6	0.4	0.7
Amorphous content	70.1	74.8	73.7	72.8

Table 4
Porosity, density and water absorption values for cement paste (C), UHFRC composites, 6THFRC composites, (CNCC) nanocomposites and (6THFR-CNCC) nanocomposites.

Sample	Porosity (%)	Density (10^3 kg/m^3)	Water absorption (%)
C	24.0 ± 0.5	1.76 ± 0.02	13.4 ± 0.7
4UHFRC	30.1 ± 0.7	1.61 ± 0.01	18.7 ± 0.6
5UHFRC	31.6 ± 0.7	1.56 ± 0.03	20.3 ± 0.7
6UHFRC	33.0 ± 0.4	1.53 ± 0.03	21.6 ± 0.6
7UHFRC	34.2 ± 0.6	1.51 ± 0.01	22.7 ± 0.5
6THFRC	32.1 ± 0.8	1.55 ± 0.01	20.7 ± 0.7
CNCC1	16.5 ± 0.6	1.93 ± 0.01	8.9 ± 0.6
CNCC2	17.6 ± 0.5	1.91 ± 0.02	9.6 ± 0.8
CNCC3	18.9 ± 0.6	1.85 ± 0.02	10.3 ± 0.4
6THFR-CNCC1	28.1 ± 0.5	1.62 ± 0.01	17.8 ± 0.4
6THFR-CNCC2	29.4 ± 0.8	1.60 ± 0.01	19.0 ± 0.7
6THFR-CNCC3	30.2 ± 0.7	1.57 ± 0.03	19.8 ± 0.3

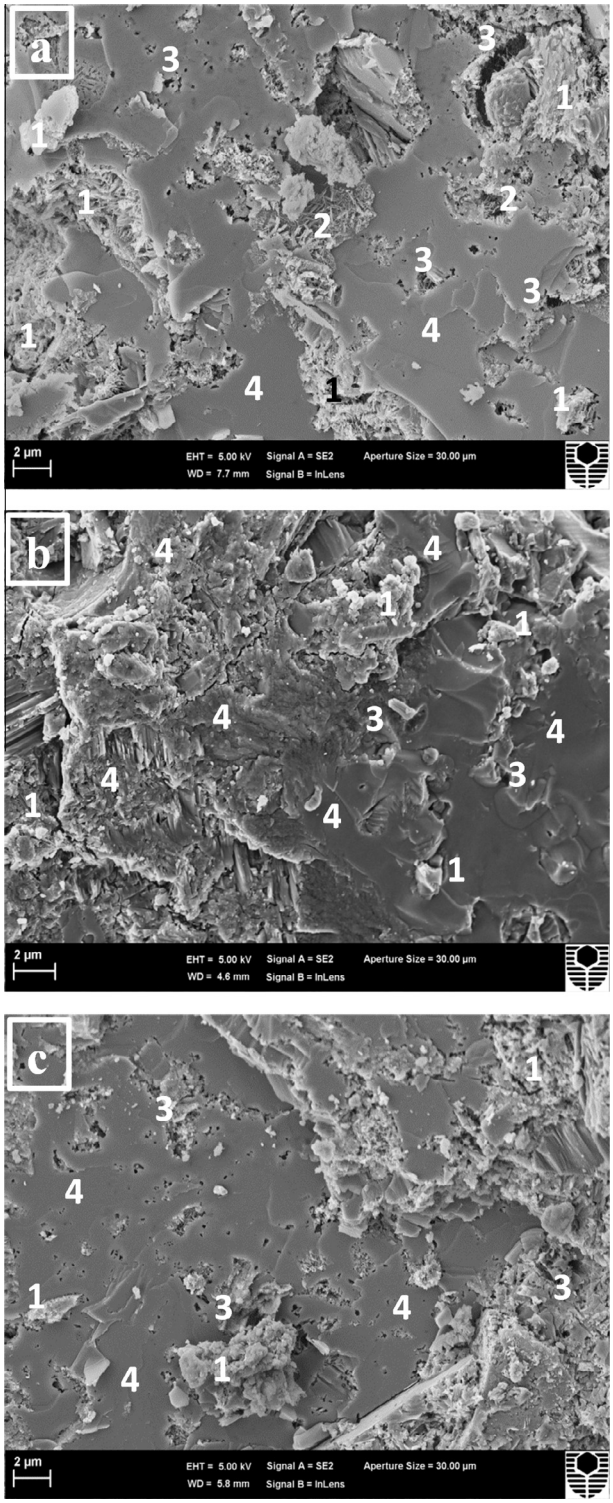

Fig. 8. SEM micrographs of: (a) cement paste, nanocomposites containing, (b) 1 wt% CNC, (c) 3 wt% CNC. Numbers indicate to: 1 = [$Ca(OH)_2$] crystals, 2 = Ettringite, 3 = pores, 4 = C–S–H gel.

enhancement is due to fracture resistance by Hemp fabrics which resulted in increased energy dissipation from crack-deflection at the fibre–matrix interface, fibre-debonding, fibre-bridging, fibre pull-out and fibre-fracture [50]. It can be seen clearly that the 6THFRC composite exhibited increase in the fracture toughness by 13.5% compared to 6UHFRC composite. This result confirms that the chemical treatment improved the interfacial bond between the matrix and the treated Hemp fibres. In a similar study, Li et al. [51] studied the effect of silane treatment on Sisal textile surface. They reported that the fracture toughness of treated Sisal textile reinforced vinyl-ester composites is increased by 31% compared to untreated ones.

As shown in Fig. 10 for 6THFR-CNCC nanocomposite, the fracture toughness of treated hemp fabric reinforced nanocomposites containing 1, 2 and 3 wt% CNC were 2.21, 2.14 and 2.04 MPa $m^{1/2}$, respectively. It can again be seen that the fracture toughness of 6THFR-CNCC1 nanocomposite is increased by 38.1% compared to 6THFRC composite. This is attributed to the fact that the CNC modified the matrix through pozzolanic reaction and reduced the $Ca(OH)_2$ content. Thus, good interfacial bond between the nanomatrix and the treated Hemp fibres was achieved, which reduced the loads transferred from the matrix to the fibres. Alamri and Low [52] reported that the addition of 1 wt% halloysite nanotubes (HNTs) into recycled cellulose fibres (RCF)/epoxy matrix significantly increased the fracture toughness by 38.8% compared to RCF-reinforced epoxy composites. However, facture toughness of 6THFR-CNCC nanocomposites gradually decreased when CNC content increase after the optimum content of 1 wt%. This is attributed to the poor dispersion of high content of CNC into the matrix, which leads to increase in porosity and weaken the fibre–matrix interface [4].

Fig. 11a–d shows the SEM micrographs of the fracture surface and fibre–matrix interface of 6THFR-CNCC1 and 6THFR-CNCC3 nanocomposite after fracture toughness test. A variety of toughening mechanisms such as fibre–matrix interface, fibre pull-out, rupture fibre and matrix fracture are observed. The examination of fracture surface of 6THFR-CNCC1 nanocomposite shows good fibre–matrix interfacial bonding (Fig. 11a and b), which revealed that good fibre–nanomatrix interfaces was achieved. However, SEM images of 6THFR-CNCC3 nanocomposite (Fig. 11 c and d) show relatively poor adhesion between the fibre and the matrix as well as debonding of fibre was observed. This result indicated relatively weak matrix in this nanocomposite than 6THFR-CNCC1 nanocomposite.

3.3.3. Impact strength

The impact strength is defined as the ability of the material to withstand impact loading [53]. Fig. 12 shows the impact strength of cement paste, 6UHFRC composites, 6THFRC composites and nanocomposites with treated hemp fabrics (6THF). Generally, it can be seen that the impact strength of cement paste is significantly improved due to reinforced by Hemp fabrics [50]. It can be seen clearly that after NaOH treatment, the impact strength of 6THFRC composite has slightly increased from 28.94 to 31.57 by about 9% compared to 6UHFRC composite. This result indicates that relatively good interfacial bonding between the Hemp fabric

Table 5
Flexural strength values for cement paste (C), UHFRC composites, 6THFRC composites, (CNCC) nanocomposites and 6THFR-CNCC nanocomposites.

Sample	Flexural strength (MPa)
C	5.4 ± 0.2
4UHFRC	10.2 ± 0.4
5UHFRC	11.3 ± 0.7
6UHFRC	12.6 ± 0.5
7UHFRC	11.2 ± 0.9
6THFRC	14.5 ± 0.3
CNCC1	7.8 ± 0.2
CNCC2	7.3 ± 0.2
CNCC3	7.1 ± 0.4
6THFR-CNCC1	20.2 ± 0.8
6THFR-CNCC2	19.2 ± 0.6
6THFR-CNCC3	18.3 ± 0.9

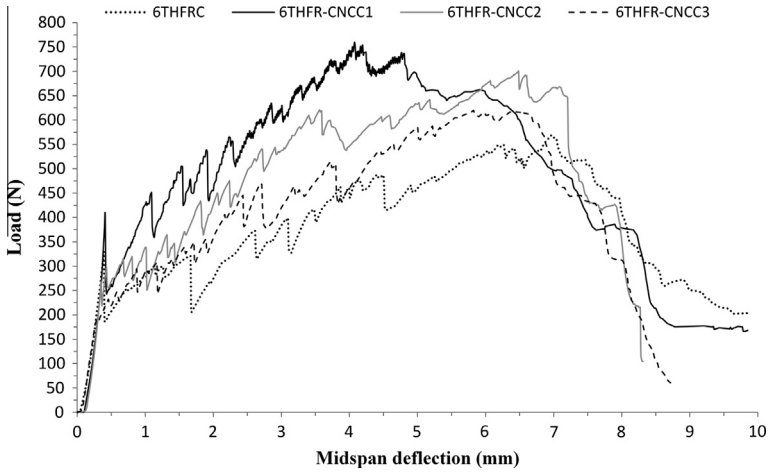

Fig. 9. Load versus mid-span deflection curves for 6THFRC composite and 6THFR-CNCC nanocomposites from flexural test.

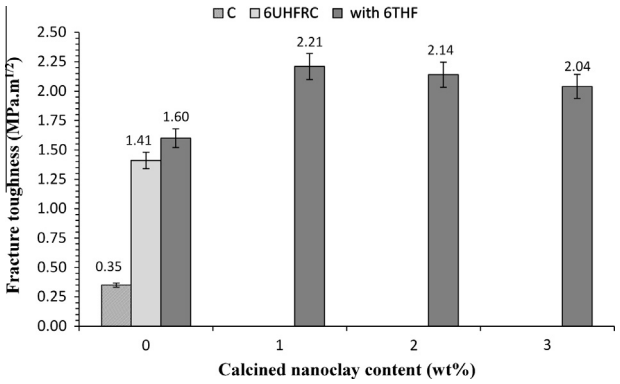

Fig. 10. Fracture toughness as a function of calcined nanoclay content for cement paste and 6UHFRC composite, 6THFRC composite and nanocomposites with treated hemp fabrics (6THF).

and the cement matrix was achieved due to NaOH treatment of Hemp fabric. As shown in Fig. 12, the presence of CNC enhanced the impact strength for treated hemp fabric-reinforced nanocomposites. The impact strength of 6THFR-CNCC1 was 37.56 kJ/m^2, about 19% increase compared to 6HFRC composite. This is due to good interfacial bonding between the fibres and the nanomatrix. Alhuthali et al. [5] reported that the addition of 3 wt% nanoclay into recycled cellulose fibres (RCF)/vinyl ester matrix increased the impact strength by 27% compared to RCF-reinforced vinyl ester composites. However, as CNC loading increased after the optimum content of 1 wt% the impact strength is decreased. For example, the impact strength of 6THFR-CNCC3 was 34.72 kJ/m^2, about 10% increase compared to 6HFRC composite, in which it is less than 6THFR-CNCC1. This reduction in impact strength at higher CNC loading was due to the formation of CNC agglomerates and voids which led to reduced fibre–nanomatrix adhesion [3].

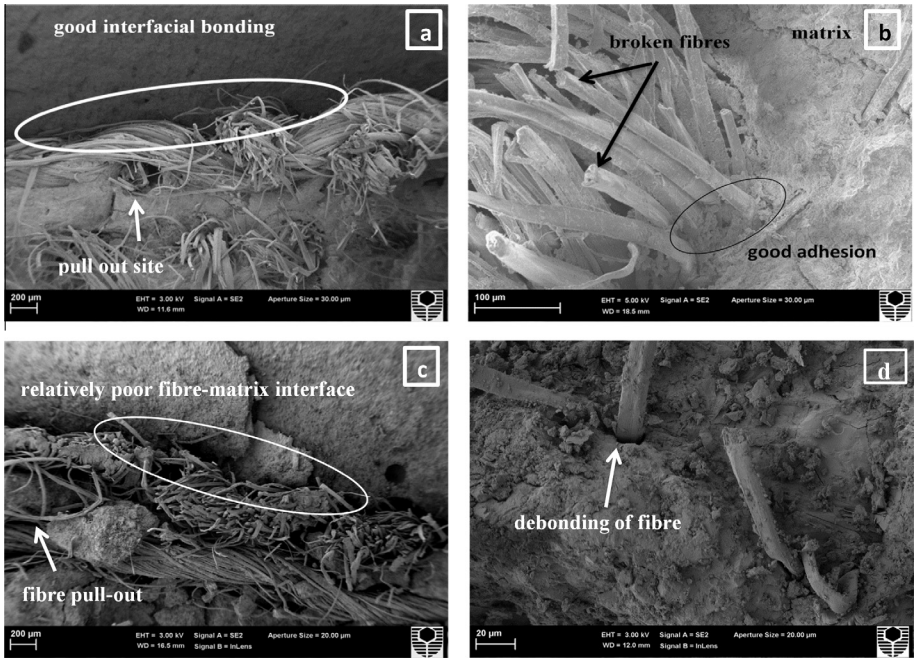

Fig. 11. SEM images of the fracture surfaces after fracture toughness test for: (a and b) 6THFR-CNCC1, (c and d) 6THFR-CNCC3.

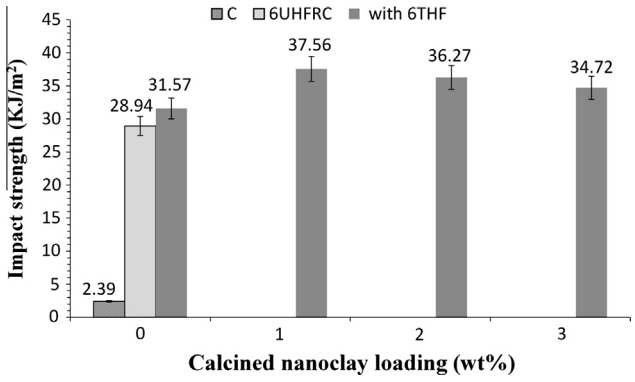

Fig. 12. Impact strength as a function of calcined nanoclay content for cement paste and 6UHFRC composite, 6THFRC composite and nanocomposites with treated hemp fabrics (6THF).

3.4. Thermal stability

The thermograms (TGA) of cement paste, 6UHFRC composites, 6THFRC composites and treated hemp fabric reinforced-nanocomposites (6THFR-CNCC) are shown in Fig. 13. The char yields at different temperatures are summarized in Table 6. The TGA analysis shows four distinct stages of decomposition in these samples. The first stage of decomposition is between room temperature and 230 °C, which may be related to the decomposition of Ettringite and dehydration of C–S–H gel (loss of water). The second stage of decomposition is between 285 °C and 390 °C, which corresponds to decomposition of cellulose of hemp fibre. The third stage of decomposition is between 400 °C and 510 °C, which corresponds to $Ca(OH)_2$ decomposition. The last stage of decomposition is between 670 °C and 780 °C, which correspond to $CaCO_3$ decomposition [54–56].

In the first stage, generally all composites with Hemp fabrics showed better thermal stability than cement paste due to resistance of Hemp fabrics to the decomposition. Furthermore, 6THFR-CNCC composite exhibited slightly better thermal stability than 6UHFRC composite, 6THFRC composites and cement paste due to resistance of calcined nanoclay to the decomposition [3,5]. The 6THFRC composite in the second, third and fourth stage showed higher thermal stability than 6UHFRC because of the efficiency of NaOH treatment. From Table 6 at 1000 °C, the char residue of 6UHFRC and 6THFRC composites was about 65.51 and 62.94 wt%, respectively. Hence, it can be said that the 6THFRC composite performed better in thermal stability with slightly higher char residue of about 4% more than 6UHFRC [57].

Concerning 6THFR-CNCC composites in second, third and fourth stage, the 6THFR-CNCC1 composites show better thermal stability than 6THFRC composites, 6THFR-CNCC2 composites and 6THFR-CNCC3 composites due to dense and compact nanomatrix through consumption of calcium hydroxide and formation of secondary CSH gels during pozzolanic reaction [38]. Whereas, 6THFR-CNCC3 composites show lower thermal stability than 6THFR-CNCC1 composites but higher than 6THFRC composites, in which this result confirms that slightly poor pozzolanic reaction has occurred and hence nanomatrix is less compacted. From Table 6 at 1000 °C, the char residue of 6THFRC composites, 6THFR-CNCC1 composites, 6THFR-CNCC2 composites and 6THFR-CNCC3 composites was about 65.51, 68.57, 67.48 and 66.49 wt% respectively. It can be seen that 6THFR-CNCC1 composites performed better in thermal stability with higher char residue of about 5% and 3% more than 6UHFRC and 6THFR-CNCC3 composites, respectively. In a similar study, Chen et al. [58] reported that addition of 10 wt% nano-

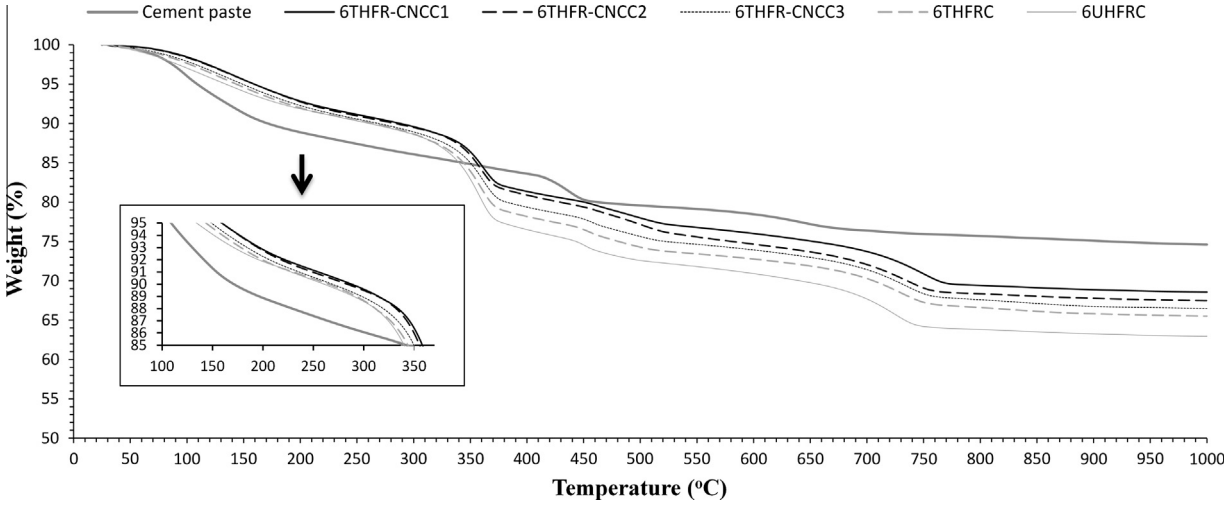

Fig. 13. TGA curves of cement paste and 6UHFRC composite, 6THFRC composite and nanocomposites with treated hemp fabrics (6THF).

Table 6
Thermal properties of cement paste (C), 6UHFRC, 6THFRC and 6THFR-CNCC nanocomposites.

Sample	Char yield (%) at different temperature (°C)									
	100	200	300	400	500	600	700	800	900	1000
C	95.82	88.82	86.03	83.57	79.57	78.44	76.37	75.69	75.09	74.61
6UHFRC	96.94	91.81	88.51	76.46	72.56	70.88	67.58	63.80	63.25	62.94
6THFRC	97.56	91.91	88.57	78.13	74.23	72.75	70.21	66.58	65.81	65.51
6THFR-CNCC1	98.38	92.76	89.53	81.32	77.93	75.99	73.66	69.40	68.86	68.57
6THFR-CNCC2	98.31	92.68	89.43	80.85	77.08	74.63	71.99	68.34	67.77	67.48
6THFR-CNCC3	97.81	92.20	88.85	79.32	75.58	73.90	71.34	67.58	66.73	66.49

TiO_2 into cement paste improved the thermal stability of nanocomposite considerably. However, overall in between 360 and 1000 °C, the 6THFR-CNCC1 composite showed lower thermal stability than cement paste but still better than other samples.

4. Conclusions

Based on all different analyses and discussing results in this study, a combination of eco-composite materials and nanocomposites has led to new eco-nanocomposites "NaOH treated hemp fabric reinforced cement nanocomposites", which has shown good microstructures, physical and mechanical properties. Cement eco-composites and nanocomposites reinforced with hemp fabrics and CNC have been fabricated and characterized. The optimum content of hemp fabric was 6.9 wt% (i.e., 6 hemp fabric layers) and the optimum content of CNC was 1 wt%. The mechanical and thermal properties of NaOH treated hemp fabric reinforced cement composites were noticeably improved when compared to the non-treated counterparts. In the 6THFR-CNCC1 nanocomposites, the porosity and water absorption declined by 12.4% and 14% respectively, as well as the density, flexural strength, fracture toughness, impact strength and thermal stability improved by 4.5%, 38.8%, 38.1%, 19% and 5% respectively compared to the 6THFRC composites. Indeed, particles agglomeration increased as CNC content increased which adversely reduced the mechanical properties of composites. It could be recommended that much research is required to overcome the CNC agglomerations. Construction applications of this eco-nanocomposite involve ceilings and roofing.

Acknowledgment

The authors are grateful to Ms. E. Miller from Applied Physics for assistance with SEM.

References

[1] F. Sanchez, K. Sobolev, Nanotechnology in concrete – a review, Constr. Build. Mater. 24 (2010) 2060–2071.
[2] A. Hakamy, F.U.A. Shaikh, I.M. Low, Characteristics of hemp fabric reinforced nanoclay–cement nanocomposites, Cem. Concr. Compos. 50 (2014) 27–35.
[3] A. Hakamy, F.U.A. Shaikh, I.M. Low, Thermal and mechanical properties of hemp fabric-reinforced nanoclay–cement nanocomposites, J. Mater. Sci. 49 (2014) 1684–1694.
[4] A. Hakamy, F.U.A. Shaikh, I.M. Low, Microstructures and mechanical properties of hemp fabric reinforced organoclay–cement nanocomposites, Constr. Build. Mater. 49 (2013) 298–307.
[5] A. Alhuthali, I.M. Low, C. Dong, Characterization of the water absorption, mechanical and thermal properties of recycled cellulose fibre reinforced vinyl-ester eco-nanocomposites, Composites Part B 43 (2012) 2772–2781.
[6] A. Nazari, S. Riahi, The effects of zinc oxide nanoparticles on flexural strength of self-compacting concrete, Composites Part B 42 (2011) 167–175.
[7] M.S. Morsy, S.H. Alsayed, M. Aqel, Hybrid effect of carbon nanotube and nano-clay on physico-mechanical properties of cement mortar, Constr. Build. Mater. 25 (2011) 145–149.
[8] A. Givi, S. Rashid, F. Aziz, M. Salleh, Investigations on the development of the permeability properties of binary blended concrete with nano-SiO_2 particles, J. Compos. Mater. 45 (2011) 1931–1938.
[9] A. Nazari, S. Riahi, The effects of ZrO_2 nanoparticles on properties of concrete using ground granulated blast furnace slag as binder, J. Compos. Mater. 46 (2012) 1079–1090.
[10] S. Supit, F.U.A. Shaikh, Effect of nano-$CaCO_3$ on compressive strength development of high volume fly ash mortars and concretes, J. Adv. Concr. Technol. 12 (2014) 178–186.
[11] F. Silva, B. Mobasher, Cracking mechanisms in durable sisal fiber reinforced cement composites, Cem. Concr. Compos. 31 (2009) 721–730.
[12] D. Sedan, C. Pagnoux, A. Smith, T. Chotard, Mechanical properties of hemp fibre reinforced cement: influence of the fibre/matrix interaction, J. Eur. Ceram. Soc. 28 (2008) 183–192.
[13] A. Elsaid, M. Dawood, R. Seracino, C. Bobko, Mechanical properties of kenaf fiber reinforced concrete, Constr. Build. Mater. 25 (2011) 1991–2001.
[14] E. Awwada, M. Mabsout, B. Hamad, M. Farran, H. Khatib, Studies on fiber-reinforced concrete using industrial hemp fibers, Constr. Build. Mater. 35 (2012) 710–717.
[15] Z. Li, L. Wang, X. Wang, Compressive and flexural properties of hemp fiber reinforced concrete, Fiber Polym. 5 (2004) 187–197.
[16] Z. Li, X. Wang, L. Wang, Properties of hemp fibre reinforced concrete composites, Composites Part A 37 (2006) 497–505.
[17] A. Rachini, M. Troedec, C. Peyratout, A. Smith, Comparison of the thermal degradation of natural, alkali-treated and silane-treated hemp fibers under air and an inert atmosphere, J. Appl. Polym. Sci. 112 (2009) 226–234.
[18] P. Blankenhorn, B. Blankenhorn, M. Silsbee, M. DiCola, Effects of fiber surface treatments on mechanical properties of wood fiber–cement composites, Cem. Concr. Res. 31 (2001) 1049–1055.
[19] M. Troëdec, C. Peyratout, A. Smith, T. Chotard, Influence of various chemical treatments on the interactions between hemp fibres and a lime matrix, J. Eur. Ceram. Soc. 29 (2009) 1861–1868.
[20] A. Peled, S. Sueki, B. Mobasher, Bonding in fabric–cement systems: effects of fabrication methods, Cem. Concr. Res. 36 (2006) 1661–1671.
[21] A. Peled, B. Mobasher, Tensile behavior of fabric cement-based composites: pultruded and cast, J. Mater. Civ. Eng. 19 (2007) 340–348.
[22] B. Mobasher, A. Peled, J. Pahilajani, Distributed cracking and stiffness degradation in fabric–cement composites, Mater. Struct. 39 (2006) 317–331.
[23] H. Alamri, I.M. Low, Z. Alothman, Mechanical, thermal and microstructural characteristics of cellulose fibre reinforced epoxy/organoclay nanocomposites, Composites Part B 43 (2012) 2762–2771.
[24] D. Snoeck, N. De Belie, Mechanical and self-healing properties of cementitious composites reinforced with flax and cottonised flax, and compared with polyvinyl alcohol fibres, Biosyst. Eng. 111 (2012) 325–335.
[25] F. Pacheco-Torgal, S. Jalali, Cementitious building materials reinforced with vegetable fibres: a review, Constr. Build. Mater. 25 (2011) 575–581.
[26] ASTM C-1365-06, Standard Test Method for Determination of the Proportion of Phases in Portland Cement and Portland-Cement Clinker Using X ray Powder Diffraction Analysis, 2011.
[27] H.F.W. Taylor, Cement Chemistry, Academic press limited, London, 1990.
[28] A. Aldridge, Accuracy and precision of phase analysis in Portland cement by Bogue, microscopic and X-ray diffraction methods, Cem. Concr. Res. 12 (1982) 381–398.
[29] K. Scrivenera, T. Fullmanna, E. Galluccia, G. Walentab, E. Bermejob, Quantitative study of Portland cement hydration by X-ray diffraction/rietveld analysis and independent methods, Cem. Concr. Res. 34 (2004) 1541–1547.
[30] ASTM C-20, Standard Test Methods for Apparent Porosity, Water Absorption, Apparent Specific Gravity, and Bulk Density of Burned Refractory Brick and Shapes by Boiling Water, 2010.
[31] F.U.A. Shaikh, Mechanical and durability properties of mortars modified with combined polymer and supplementary cementitious materials, J. Mater. Civ. Eng. 23 (2011) 1311–1319.
[32] ASTM E-399, Standard Fracture Toughness Specimens, ASTM international, 2013.
[33] C. He, E. Makovicky, B. Osbaeck, Thermal treatment and pozzolanic activity of Na- and Ca-montmorillonite, Appl. Clay Sci. 10 (5) (1996) 351–368.
[34] S. Shebl, L. Allie, M. Morsy, H. Aglan, Mechanical behavior of activated nano silicate filled cement binders, J. Mater. Sci. 44 (2009) 1600–1606.
[35] M. Troëdec, A. Rachini, C. Peyratout, S. Rossignol, E. Max, O. Kaftan, A. Fery, A. Smith, Influence of chemical treatments on adhesion properties of hemp fibres, J. Colloid Interface Sci. 356 (2011) 303–310.
[36] A. Bismarck, I. Askargorta, J. Springer, Surface characterization of flax, hemp and cellulose fibers; surface properties and the water uptake behavior, Polym. Compos. 23 (2002) 872–894.
[37] M. Troedec, D. Sedan, C. Peyratout, J. Bonnet, A. Smith, R. Guinebretiere, V. Gloaguen, P. Krausz, Influence of various chemical treatments on the composition and structure of hemp fibres, Composites Part A 39 (2008) 514–522.
[38] A. Soin, L. Catalan, S. Kinrade, A combined QXRD/TG method to quantify the phase composition of hydrated Portland cements, Cem. Concr. Res. 48 (2013) 17–24.
[39] Y. Wei, W. Yao, X. Xing, M. Wu, Quantitative evaluation of hydrated cement modified by silica fume using QXRD, 27Al MAS NMR, TG–DSC and selective dissolution techniques, Constr. Build. Mater. 36 (2012) 925–932.
[40] F.U.A. Shaikh, S.W.M. Supit, P.K. Sarker, A study on the effect of nano silica on compressive strength of high volume fly ash mortars and concretes, Mater. Des. 60 (2014) 433–442.
[41] G. Tonoli, U. Filho, H. Savastano, J. Bras, M. Belgacem, F. Rocco Lahr, Cellulose modified fibres in cement based composites, Composites Part A 40 (2009) 2046–2053.
[42] B. Jo, C. Kim, G. Tae, J. Park, Characteristics of cement mortar with nano-SiO_2 particles, Constr. Build. Mater. 21 (2007) 1351–1355.
[43] S.W.M. Supit, F.U.A. Shaikh, Durability properties of high volume fly ash concrete containing nano-silica, Mater. Struct. (2014), http://dx.doi.org/10.1617/s115270140329-0.
[44] M. Bentchikou, A. Guidoum, K. Scrivener, K. Silhadi, S. Hanini, Effect of recycled cellulose fibres on the properties of lightweight cement composite matrix, Constr. Build. Mater. 34 (2012) 451–456.
[45] D. Asprone, M. Durante, A. Prota, G. Manfredi, Potential of structural pozzolanic matrix–hemp fiber grid composites, Constr. Build. Mater. 25 (2011) 2867–2874.
[46] T. Chang, J. Shih, K. Yang, T. Hsiao, Material properties of Portland cement paste with nano-montmorillonite, J. Mater. Sci. 42 (2007) 7478–7487.
[47] J. Wei, C. Meyer, Sisal fiber-reinforced cement composite with Portland cement substitution by a combination of metakaolin and nanoclay, J. Mater. Sci. 49 (2014) 7604–7619.

[48] M. Khorami, E. Ganjian, Comparing flexural behaviour of fibre-cement composites reinforced bagasse: wheat and eucalyptus, Constr. Build. Mater. 25 (2011) 3661–3667.
[49] H. Li, H. Xiao, J. Yuan, J. Ou, Microstructure of cement mortar with nano-particles, Composites Part B 35 (2004) 185–189.
[50] X. Zhou, S. Ghaffar, W. Dong, O. Oladiran, M. Fan, Fracture and impact properties of short discrete jute-fiber reinforced cementitious composites, Mater. Des. 49 (2013) 35–47.
[51] Y. Li, Y. Mai, L. Ye, Effects of fibre surface treatment on fracture-mechanical properties of sisal-fibre composites, Compos. Interface 12 (2005) 141–163.
[52] H. Alamri, I.M. Low, Microstructural, mechanical, and thermal characteristics of recycled cellulose fiber-Halloysite-epoxy hybrid composites, Polym. Compos. 33 (2012) 589–600.
[53] H. Toutanji, B. Xu, J. Gilbert, T. Lavin, Properties of poly (vinyl alcohol) fiber reinforced high-performance organic aggregate cementitious material: converting brittle to plastic, Constr. Build. Mater. 24 (2010) 1–10.
[54] J. Filho, F. Silva, R. Filho, Degradation kinetics and aging mechanisms on sisal fiber cement composite systems, Cem. Concr. Compos. 40 (2013) 30–39.
[55] B. Lothenbach, F. Winnefeld, C. Alder, E. Wieland, P. Lunk, Effect of temperature on the pore solution, microstructure and hydration products of Portland cement pastes, Cem. Concr. Res. 37 (2007) 483–491.
[56] S. Djaknoun, E. Ouedraogo, A. Benyahia, Characterisation of the behaviour of high performance mortar subjected to high temperatures, Constr. Build. Mater. 28 (2012) 176–186.
[57] G. Beckermann, K. Pickering, Engineering and evaluation of hemp fibre reinforced polypropylene composites: fibre treatment and matrix modification, Composites Part A 39 (2008) 979–988.
[58] J. Chen, S. Kou, C. Poon, Hydration and properties of nano-TiO_2 blended cement composites, Cem. Concr. Compos. 34 (2012) 642–649.

3.7 Effect of calcined nanoclay on the durability of NaOH treated hemp fabric-reinforced cement nanocomposites.

HAKAMY, A., SHAIKH, F.U.A. & LOW, I.M. 2015. Effect of calcined nanoclay on the durability of NaOH treated hemp fabric-reinforced cement nanocomposites. *Materials and Design*, 92, 659-666.

Materials and Design 92 (2016) 659–666

Contents lists available at ScienceDirect

Materials and Design

journal homepage: www.elsevier.com/locate/matdes

Effect of calcined nanoclay on the durability of NaOH treated hemp fabric-reinforced cement nanocomposites

A. Hakamy [a,b], F.U.A. Shaikh [c], I.M. Low [a,*]

[a] Department of Imaging & Applied Physics, Curtin University, GPO Box U1987, Perth, WA 6845, Australia
[b] Department of Physics, Umm Al-Qura University, P.O. Box 715, Makkah, Saudi Arabia
[c] Department of Civil Engineering, Curtin University, GPO Box U1987, Perth, WA 6845, Australia

ARTICLE INFO

Article history:
Received 7 August 2015
Received in revised form 14 December 2015
Accepted 15 December 2015
Available online 17 December 2015

Keywords:
Nanoclay-cement composites
Hemp fabric
Durability
Microstructure

ABSTRACT

Cement nanocomposites reinforced with hemp fabrics and calcined nanoclay (CNC) have been fabricated and investigated. The treated hemp fabric-reinforced cement composites and nanocomposites were subjected to 3 wetting and drying cycles and then tested at 56 and 236 days. The influences of CNC dispersion on the durability of these composites have been characterized in terms of porosity, flexural strength, stress-midspan deflection curves and microstructural observation of hemp surface. The microstructure of matrix was investigated using X-ray Diffraction. Results indicated that the CNC effectively mitigated the degradation of hemp fibre. The durability and the degradation resistance of hemp fibre enhanced due to the addition of CNC into the cement matrix and the optimum content of CNC was 1 wt.%.

1. Introduction

Recently, natural fibres are gaining increasing popularity to develop 'environmental-friendly construction materials' as alternative to synthetic fibres in fibre-reinforced concrete [1,2]. These fibres are cheaper, biodegradable and lighter than their synthetic counterparts. Some examples of natural fibres are: Sisal, Flax, Hemp, Bamboo, Coir and others [3]. However, the long term durability of natural fibres in cement composites has been the major issue in which it has limited their applications in cementitious composites. These issues could be the degradation of fibres in a high alkaline environment of cement composites and also the interfacial bonding between the natural fibre and the cement matrix is relatively weak [4,5]. In order to improve the durability of fibre reinforced cement composites, there are two possible methods: (i) modification of fibre surfaces and (ii) modification of the cement matrix [6,7]. Regarding the first method, some researchers have showed that pre-treatments of natural fibre surfaces via some chemical agents such as alkalization, $Ca(OH)_2$ and Na_2CO_3 have slightly improved the fibre–matrix interface of the composites. As a result, the mechanical properties of such composites are enhanced [8,9]. Troedec et al. [10] reported that the modification of hemp fibres with NaOH has reasonably improved the interfacial bonding between the fibres and the lime-based mineral matrix. Regarding the second approach, it should be noted that the alkalinity (high pH value) of cement matrix come from two sources. The first source is minor compounds (alkalis) of cement clinker which are Na_2O and K_2O, in which these alkalis increase alkalinity of hydrated cement paste [11,12]. Some researchers reported that high alkali content can increase the early strength but reduce the long-term strength [13,11]. The Na_2O and K_2O can affect the strength through water-soluble K_2O or alkali-silica reaction (alkali reactive-aggregates) [14,15]. In contrast [12] reported that alkalis did not affect the compressive strength of concrete. The second source is the highest amount of calcium hydroxide that comes from hydration reaction and it is considered as the major portion of alkalinity of cement matrix and concrete. The calcium hydroxide has also been proven as an important factor leading to the degradation of natural fibres. However, in the second approach for modification of the cement matrix, calcium hydroxide in cement matrix can be reduced by using pozzolanic materials such as silica fume, fly ash, metakaolin and amorphous nanomaterials. Thus this approach could improve the interfacial bond, mechanical properties and durability of natural fibre-reinforced cement composites [16,17]. On the other hand, one of the most effective techniques to obtain a high performance cementitious composite is by reinforcement with textile (fabrics), which are impregnated with cement matrix. Synthetic fabrics such as polyethylene (PE) and polypropylene (PP) have been used as reinforcement for cement composites [18,19]. This system has superior filament-matrix bonding which improves the mechanical properties such as tensile and flexural strengths than

* Corresponding author at: Department of Imaging & Applied Physics, Curtin University, GPO Box U1987, Perth, WA 6845, Australia.
E-mail address: j.low@curtin.edu.au (I.M. Low).

http://dx.doi.org/10.1016/j.matdes.2015.12.097
0264-1275/

Table 1
Physical properties and chemical composition of the nanoclay [21,34].

Properties/compositions	
Physical properties	
Colour	Off white
Density (g/cm^3)	1.98
d-Spacing (001) (nm)	1.85
Aspect ratio	200–1000
Surface area (m^2/g)	750
Mean particle size (μm)	6
Chemical composition	
SiO_2	62.10
Al_2O_3	21.10
Fe_2O_3	4.57
CaO	0.06
MgO	2.24
Na_2O	0.38
K_2O	0.06
TiO_2	0.13
MnO	0.01
BaO	0.01
Cr_2O_3	0.01
P_2O_5	0.05
LOI (loss on ignition)	7.40

continuous or short fibres [20]. In contrast, the use of natural fibre sheets and fabrics is more prevalent in polymer matrix when compared to cement-based matrix [21,22].

Nowadays, nanotechnology is one of the most active research areas in the civil engineering and construction materials [23,24]. In the construction industry, several types of nanomaterials have been incorporated into concretes such as nano-SiO_2, nano-Al_2O_3, nano-Fe_2O_3, nano-ZnO_2, nano-$CaCO_3$, nano-TiO_2, carbon nanotubes, nano-metakaolin and nano-ZrO_2 in order to improve the durability and mechanical properties of concrete and Portland cement matrix [25–30]. Supit and Shaikh [31] reported that the addition of 1% nano-$CaCO_3$ increased the compressive strength of mortar and concrete significantly. Nanoclay (NC) is a new generation of processed clay for a wide range of high-performance cement nanocomposite. Some examples of nanoclay are nano-halloysite, nano-cloisite 30B and nano-kaolin [32]. As a kind of nano-pozzolanic material, nanoclay not only reduces the pore size and porosity of the cement matrix, but also improves the strength of cement matrix through pozzolanic reactions. Farzadnia et al. [33] reported that the incorporation of 3% halloysite nanoclay into cement mortars increased the 28-day compressive strength up to 24% compared to the control samples. Calcined nanoclay is prepared by heating nanoclay at certain temperature for certain period of time in order to transform nanoclay to amorphous state in which the calcined nanoclay can behave as a highly reactive artificial pozzolan such as silica fume, metakaolin, nano-SiO_2, and nano-metakaolin [29]. An interesting study on using nanoparticles and natural fibres as reinforcements in cement nanocomposites was obtained by Aly et al. [34]. They studied the durability of flax fibre reinforced cement mortar containing 2.5 wt.% nanoclay and 20 wt.% ground waste glass powder at 28 days and after 50 wet/dry cycles (378 days). They reported that the flax fibre reinforced nanocomposites after accelerating ageing cycles showed small reduction (19%) in the flexural strength when compared to its initial strength at 28 days due to the small degradation of flax fibre. The authors concluded that the presence of nanoclay reduced the degradation of flax fibres in such composites.

In this paper, in order to improve the durability of hemp fibre reinforced cement composites, the combination of both methods (modification of fibre surfaces and the cement matrix) are used. The effect of calcined nanoclay (CNC) on the durability properties of treated hemp fabric-reinforced cement composite is studied. The durability of the treated hemp fabric-reinforced cement composites and nanocomposites is discussed based on the porosity and flexural strength obtained at 56 days and 236 days.

2. Experimental procedure

2.1. Materials

The nanoclay platelets (Cloisite 30B) used in this investigation is a natural montmorillonite modified with a quaternary ammonium salt, which was supplied by Southern Clay Products, USA. Physical properties and chemical composition of the nanoclay are shown in Table 1 [21,35]. The woven hemp fabric of 0.54 mm thickness and 0.3 mm opening size between bundles was supplied by Hemp Wholesale Australia Pty, Kalamunda, Western Australia. The chemical composition of hemp fabrics is: 58.7 wt.% of cellulose residue, 16.8 wt.% of pectins, 14.2 wt.% of hemicelluloses, 6 wt.% of lignins and 4.3 wt.% of waxes and fat. Ordinary Portland cement (ASTM Type I) was used in all mixes. Amorphous calcined nanoclay (CNC) was prepared by heating the nanoclay at 900 °C for 2 h, details of that can be found in previous work [26]. In order to treat the surface of the fibres, the hemp fabrics were chemically treated by 1.7 M NaOH solution (pH = 14) for 48 h, details of this treatment can also be found in the previous work of the authors [26].

2.2. Sample preparation

2.2.1. Nanocomposites

The ordinary Portland cement (OPC) is partially substituted by calcined nanoclay (CNC) at 1, 2 and 3% by weight of OPC. The OPC and CNC were first dry mixed for 15 min in Hobart mixer. The binder is CNC-cement powder. The cement nanocomposite matrix was prepared with a water/binder ratio of 0.485.

2.2.2. Treated hemp fabric-reinforced nanocomposites

Firstly, six layers of treated hemp fabrics were first soaked into the nanocomposite matrix and then laid on polished timber plate by hand. After that, the compacted fabrics were left under heavy weight (30 kg) for 1 h to reduce air bubbles and voids inside the specimens. Secondly, a thin layer of nanocomposite matrix was poured into the prismatic mould followed by the compacted pre-soaked hemp fabrics into the mould. Finally a thin layer of matrix was poured into the mould as upper layer and the specimens were left for 24 h to cure at room temperature. The position through the depth of specimen containing 6 treated hemp fabrics is shown in Fig. 1. The total amount of treated hemp fabrics in each specimen was about 6.9 wt.%. The mix proportions are given in Table 2.

2.2.3. Curing and specimens

For each series, five prismatic plate specimens of 300 × 70 × 10 mm (length × width × depth) in dimension were cast. In first 24 h of casting, samples were cured in moist condition at 20 ± 2 °C and 80% relative humidity and also they were sealed by plastic sheets to prevent evaporation of water from their top surfaces in prismatic mould. All specimens were demolded after 24 h of casting and kept under water for approximately 56 days. For durability test, the period of the wetting and drying cycles was determined as 30 days under water followed by 30 days of drying in air for one cycle and it was performed for 3 cycles, after that the samples tested at 236 days counting from the casting day. Five rectangular specimens of each series with dimensions 70 × 20 × 10 mm (length × width × depth) were cut from the fully cured prismatic plate for each mechanical and physical test at 56 and 236 days.

2.3. Material characterization

2.3.1. The X-ray diffraction (XRD)

XRD patterns were obtained using CuK_α (λ = 1.5406 Å) radiation with a Bruker D8 Advance diffractometer equipped with a LynxEye detector (1-dimensional detector, Bruker-AXS, Karlsruhe, Germany). The

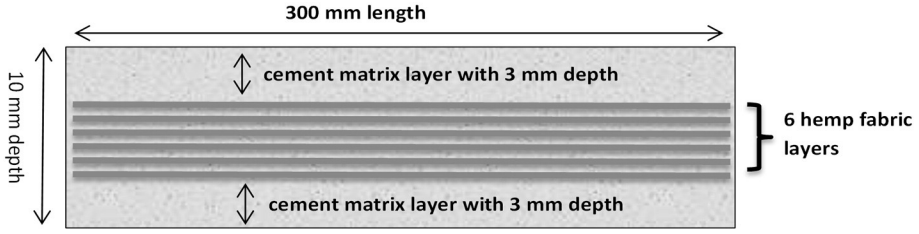

Fig. 1. Schematic representation of cross section of 6 treated hemp fabric layers position through the depth of sample.

diffractometer was scanned from 7° to 70° (2θ) in step size of 0.015° and the counting time per step was 1.8 s.

2.3.2. Scanning electron microscopy (SEM)

Scanning electron microscopy imaging was obtained using a NEON 40ESB, ZEISS. The SEM investigation was carried out in detail on microstructures and the fractured surfaces of samples.

2.4. Apparent porosity test

Five specimens, measuring 70 × 20 × 10 mm, in each composition were used to measure the apparent porosity. Prior to measuring the apparent porosity, the samples were dried in an oven at 80 °C for 24 h to obtain the dried mass. The apparent porosity was calculated according to ASTM C20 [36].

2.5. Flexural strength test

Five specimens, measuring 70 × 20 × 10 mm, in each composition were used to measure the flexural strength. Three-point bend tests were conducted using a LLOYD Material Testing Machine to evaluate the flexural strength of the composites. The support span used was 40 mm with a displacement rate of 0.5 mm/min. The flexural strength $\sigma_F$was evaluated using the following equation:

$$\sigma_F = \frac{3P_m S}{2BW^2}$$

where P_m is the maximum load at crack extension, $S$is the span of the sample, $W$is the specimen depth and$B$ is the specimen width.

3. Results and discussion

3.1. Porosity of nanocomposites

The porosity of cement paste and nanocomposites was shown in Table 3. Overall, it can be seen that the porosity of C, CNCC1, CNCC2 and CNCC3 decreased slightly in periods of between 56 and 236 days. Firstly, it is known that after 90 days curing, the compressive strength of control concrete or cement paste increase slightly with increasing ages as a result of reduction in porosity due to further hydration reaction. Secondly, in nanocomposites, slight reduction in porosity with increasing ages can be attributed to both hydration reaction and pozzolanic reaction as well as filling effect. For example, in CNCC1 cement nanocomposite, the porosity at 56 days is decreased by 31.2% compared to cement paste, however at 236 days it decreased slightly from 16.5 to 15.1% by about 8% decrease. This indicated that nanocomposites containing 1, 2 and 3 wt.% CNC had both filling and pozzolanic effects in the porosity of cement paste composites as well as to further hydration reaction (in between 56 and 236 days), in which the nanocomposite matrix becomes more a consolidated microstructure due to filling of the micro pores and densification by the enhanced pozzolanic activity and further hydration reaction [37]. This result is in agreement with the work done by Supit and Shaikh [38] reported that the addition of 2 wt.% nano-silica significantly reduced the porosity of high volume fly ash (HVFA) concrete after 90 days. However, the addition of more CNC leads to increase in porosity. This could be attributed to the poor dispersion and agglomerations of the CNC which create more voids in the matrix [39].

The XRD patterns of cement paste and nanocomposites containing 1, 2 and 3 wt.% CNC after 236 days are shown in Fig. 2(a–d). It can be seen from Figs. 2(b–d) that the addition of 1, 2, 3 wt.% CNC reduced the intensities of major peaks of $Ca(OH)_2$ when compared to cement paste (Fig. 2a). For example intensity of $Ca(OH)_2$ at 2θ of 18.01° for CNCC1 (Fig. 2b) is decreased by 13.9% compared to cement paste (Fig. 2a). This indicated an obvious consumption of $Ca(OH)_2$ in the pozzolanic reaction due to the presence of CNC and good dispersion of calcined nanoclay in the matrix which produce more amorphous calcium silicate hydrate gel (C–S–H). The formation of more C–S–H gel in CNCC1 nanocomposites can be also confirmed by the inspection of the increase in intensity peaks corresponding to 2θ of 31° (as mentioned by Hosino et al. [40]) in the close-up of Fig. 2 where peak for C_3S at 2θ of 29.4° is also reduced. Moreover, it can also be seen in the same close-up figure that the $Ca(OH)_2$ peak at 2θ of 28.7° is also lower in CNCC1 nanocomposite than the cement paste due to pozzolanic reaction. In the same close-up figure the XRD for CNCC1 at 56 days (as reported by our previous work, Hakamy et al. [26]) is also plotted. By comparing the peaks for CNCC1 at 56 and 236 days it can also be seen that the XRD peak of CNCC1 at 236 days at 2θ of 31° is slightly higher than at 56 days indicating the formation of more C–S–H and consumption of CH after 236 days. The reduction of C_3S peak of CNCC1 at 236 days at 2θ of 29.4° compared to the same at 56 days and cement paste is another indication of

Table 2
Mix proportions of specimens.

Sample	Hemp fabric (HF)		Mix proportions (wt.%)		
	Content (wt.%)	Fabric layers	Cement	CNC	Water/binder
C	0	0	100	0	0.485
CNCC1	0	0	99	1	0.485
CNCC2	0	0	98	2	0.485
CNCC3	0	0	97	3	0.485
6THFRC	6.9	6	100	0	0.485
6THFR-CNCC1	6.9	6	99	1	0.485
6THFR-CNCC2	6.9	6	98	2	0.485
6THFR-CNCC3	6.9	6	97	3	0.485

Table 3
Porosity (%) values for cement paste (C), (CNCC) nanocomposites, 6THFRC composites and (6THFR-CNCC) nanocomposites at 56 and 236 days.

Sample	Porosity (%) at 56 days	Porosity (%) at 236 days
C	23.9 ± 0.5	22.3 ± 0.7
CNCC1	16.5 ± 0.6	15.1 ± 0.3
CNCC2	17.6 ± 0.5	16.2 ± 0.5
CNCC3	18.9 ± 0.6	17.3 ± 0.7
6THFRC	32.1 ± 0.8	36.3 ± 0.7
6THFR-CNCC1	28.1 ± 0.5	30.5 ± 0.9
6THFR-CNCC2	29.4 ± 0.8	31.8 ± 0.9
6THFR-CNCC3	30.2 ± 0.7	33.1 ± 1.0

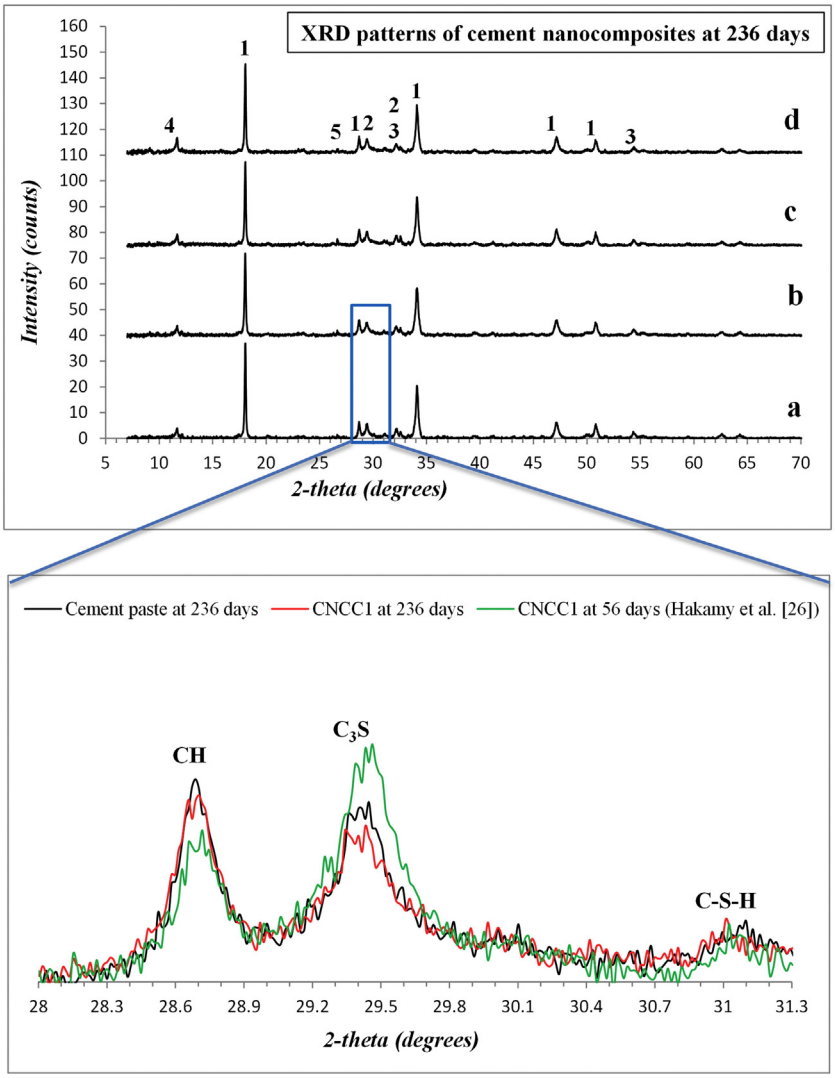

Fig. 2. XRD patterns of: (a) cement paste, nanocomposites containing various calcined nanoclay: (b) 1 wt.% (CNCC1), (c) 2 wt.% (CNCC2), and (d) 3 wt.% (CNCC3). Numbers indicate to phases of: 1 = Portlandite [$Ca(OH)_2$], 2 = Tricalcium silicate [C_3S], 3 = Dicalcium silicate [C_2S], 4 = Gypsum, 5 = Quartz.

pozzolanic and hydration reaction [41]. Shaikh et al. [42] reported in their XRD results that after 28 days the cement paste containing 2% nano-silica exhibited less calcium hydroxide peaks than the control cement paste.

On the other hand, as can be seen from Fig. 2d for nanocomposites containing 3 wt.% CNC, the intensities of major peaks of $Ca(OH)_2$ were slightly decreased when compared to cement paste (Fig.2d and a). For instance, the intensity of $Ca(OH)_2$ at 2θ of 18.01° for CNCC3 (Fig. 2d) decreased by 6.9% compared to cement paste (Fig. 2a). This may be attributed to agglomerations of CNC at high contents which led to relatively poor dispersion of CNC and hence relatively poor pozzolanic reaction. This agglomeration can be explained as follows; nanoparticles, due to their small size, have high inter-particle van der Waal's forces causing them to lose the desirable specific surface area to volume ratio [38]. Therefore, due to their higher van der Waal's forces, the 3 wt.% CNC agglomerate more than other 1 wt.% CNC and 2 wt.% CNC. As a result of this, the efficiency of 3 wt.% CNC (or nanoparticles) in consuming Ca $(OH)_2$ could be less due to the reduction of total surface areas that contribute in pozzolanic reaction. Shaikh et al. [42] also stated that nanoparticles agglomerate more than other micro-pozzolanic materials (e.g. silica fume, metakaolin) due to their higher van der Waal's forces. In summary, it is important to note that the reduction of the porosity could be attributed to two reasons: (i) filling effect of CNC due to its good dispersion, (ii) the pozzolanic reaction by amorphous nanoparticles (i.e. CNC) that lead more C-S-H gel being produced.

3.2. Porosity of treated hemp fabric-reinforced nanocomposites

The effect of wetting and drying cycles on the porosity of 6THFRC composites and 6THFR-CNCC nanocomposites was also shown in Table 3. Generally the porosity increased significantly after 3 wetting and drying cycles (at 236 days). The porosity of 6THFRC composites increased from 32.1 to 36.3% by about 13% increase. This was due to increase in voids in between fibres and matrix, whereas in 6THFR-CNCC1 nanocomposite, the porosity is increased by 8.5% at 56 days. This indicates that CNC relatively reduced the voids between the hemp fibre and the cement matrix containing CNC after 3 wet/dry cycles and thus fibre–matrix interfacial bounding was slightly maintained. Roma et al. [43] reported that in the period from 28 to 155 days, a tendency of increase in the permeable void volume was observed for the sisal fibres reinforced cement composite containing silica fume. It could be a consequence of the fast degradation of sisal fibres in the alkaline environment of Portland cement or even due to the detachment of the cellulose fibre during wet–dry cycles attributed to its shrinkage into the cement matrix.

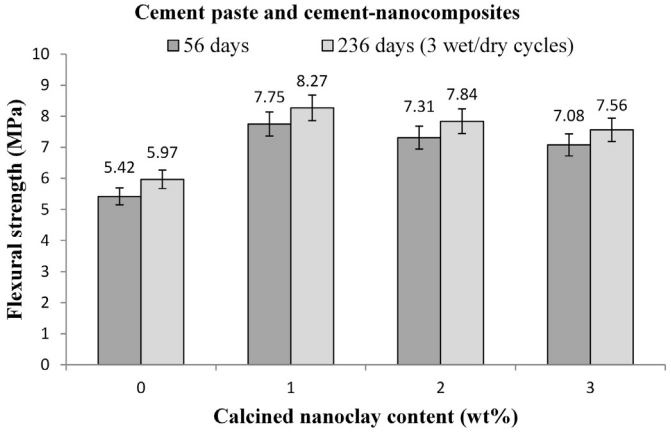

Fig. 3. Flexural strength as a function of calcined nanoclay content for cement paste and nanocomposites at 56 and 236 days.

3.3. Flexural strength of nanocomposites

The effect of 3 wet/dry cycles on the flexural strength of cement paste and nanocomposites (CNC) is shown in Fig. 3. Overall, the incorporation of CNC into the cement composite led to significant enhancement in the flexural strength at all ages. At 56 days, the flexural strength of cement nanocomposite containing 1, 2 and 3 wt.% CNC was increased by 42.9%, 34.8% and 30.6%, respectively compared to cement paste. This improvement clearly indicates the effectiveness of CNC in consuming calcium hydroxide (CH), supporting pozzolanic reaction and filling the micro pores in the matrix [44,45]. Thus the microstructure of cement nanocomposite is denser than the cement matrix, especially in the case of using 1 wt.% CNC, which is evident from its higher flexural strength. However, after 3 wet/dry cycles at 236 days, the flexural strength of nanocomposites increased slightly compared to their values at 56 days. For example, the flexural strength of CNCC1 nanocomposite increased from 7.75 to 8.27 MPa by about 7% increase. Rong et al. [46] studied the effects of 3% nano-SiO_2 particles on the durability of concrete containing 35% fly ash at 28 and 90 days, they reported about 11% improvement in flexural strength at 90 days compared to 28 days. Mohamed [47] also reported that flexural strength of concrete containing 1% nano-SiO_2 improved from 12.08 to 13.27 by 10% after 90 days compared to its strength at 28 days.

SEM images of the microstructure at 236 days of cement paste and the cement nanocomposite containing 1 wt.% CNC (CNCC1) are shown in Fig. 4a–b. For cement paste matrix, Fig. 4a demonstrates more Ca $(OH)_2$ crystals and Ettringite as well as more pores which revealed a weak microstructure. On the other hand, Fig. 4b displays the SEM micrograph of CNCC1 nanocomposite matrix, which is different from that of cement matrix, the microstructure is denser and more compact with fewer pores and more C–S–H gel.

3.4. Flexural strength of treated hemp fabric-reinforced nanocomposites

The effect of wetting and drying cycles on the flexural strength of 6THFRC composites and treated hemp fabric reinforced-nanocomposites (6THFR-CNCC) are shown in Fig. 5. Generally all composite showed reduction in the flexural strength after 3 wetting and drying cycles (at 236 days). This was attributed to some partial degradation of hemp fibre in cement matrix that led to slightly deteriorate fibre–matrix bonding and also the mineralization of the fibres in which fibre became more brittle. The incorporation of CNC into the 6THFRC composite led to significant enhancement in the flexural strength of all treated Hemp fabric reinforced nanocomposites. At 56 days, the flexural strength of 6THFR-CNCC1 increased from 14.52 to 20.16 MPa, about 38.8% increase compared to 6THFRC composite. However, after 3 wet/dry cycles (at 236 days) the flexural strength of 6THFRC composite dropped to 26.2% of the initial strength at 56 days, whereas the flexural strength of 6THFR-CNCC1 nanocomposites reduced by about 17.4% compared to its value at 56 days. Moreover, the flexural strength of 6THFR-CNCC2 and 6THFR-CNCC3 nanocomposites reduced by about 18.3% and 19.7% compared to their values at 56 days. Based on this result, it can be concluded that the reduction in the flexural strength for 6THFR-CNCC3 nanocomposites was less than the reduction of 6THFRC composite after 3 wet/dry cycles (at 236 days). This improvement is explained as follows: the degradation of natural fibres in Portland cement matrix is due to the high alkaline environment (especially calcium hydroxide solution) which dissolves the lignin and hemicellulose parts, thus weakening the fibre structure [1,2,17]. In order to improve the durability of natural fibre in cement paste, the matrix could be modified in which calcium-hydroxide (CH) must be mostly consumed or reduced. In this study, the CNC effectively prevented the hemp fabric degradation by reducing the CH in the matrix through pozzolanic reaction. Thus, the degradation of hemp fibres in nanocomposite was mostly prevented and the treated hemp fabric-nanocomposite matrix interfacial bonding was mostly improved especially in the case of 1 wt.% CNC. Other two reasons of this improvement were the effectiveness of CNC in filling the micro pores in the matrix which led to denser microstructure of nanocomposite matrix than the cement matrix and also the pre-treatment of hemp fibre by NaOH solution. Filho et al. [48] investigated the durability of sisal fibre-reinforced mortar with 50% metakaolin (PC-MK) and without metakaolin (PC) at 28 days and after 25 wet/dry cycles. They observed that the flexural strength of PC and PC-MK composites decreased by 63% and 23%, respectively compared to their control composites at 28 days. They reported that 50% metakaolin replacement significantly prevented the sisal fibres from the degradation in cement matrix. However, the addition of CNC more than 1 wt.% caused a marked decrease in flexural

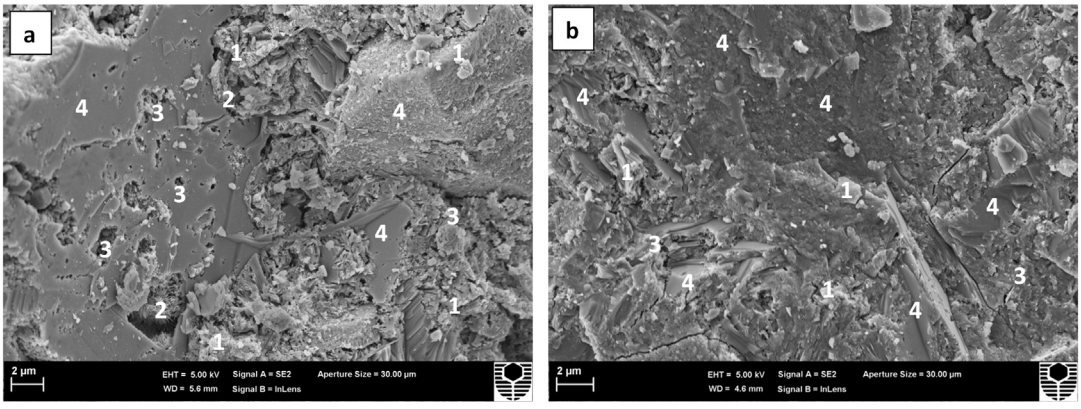

Fig. 4. SEM micrographs at 236 days of: (a) cement paste, (b) nanocomposites containing 1 wt.% CNC. Numbers indicate to: 1 = $[Ca(OH)_2]$ crystals, 2 = Ettringite, 3 = pores, 4 = C-S-H gel.

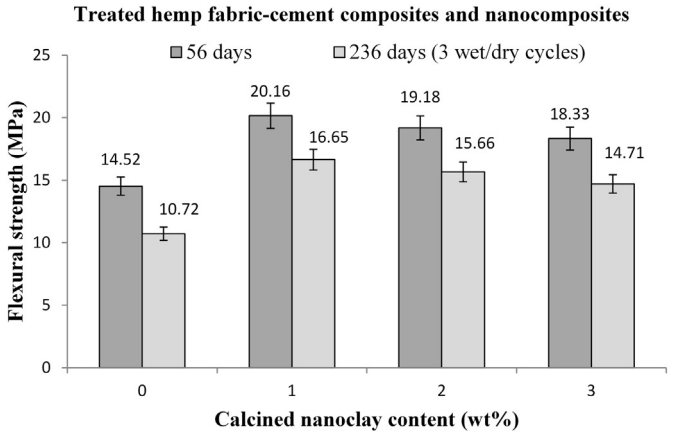

Fig. 5. Flexural strength as a function of calcined nanoclay content for 6THFRC composite and 6THFR-CNCC nanocomposites at 56 and 236 days.

strength. This could be attributed to the relatively poor dispersion and agglomerations of the CNC in the cement matrix at higher CNC contents, which created weak zones and then increased the porosity.

Figs. 6(a–b) show the effect of wetting and drying cycles on the stress-midspan deflection behaviour of 6THFRC composites and 6THFR-CNCC1nanocomposites. The ductile behaviour can be observed in both treated composites with and without CNC, with higher flexural strength (about 40% increases) and better post-peak ductility in the composite containing CNC. It was observed that ductile behaviour and bending stress are slightly reduced due to accelerated ageing. This reduction was attributed to the lignin and hemicellulose deterioration of hemp fibre in matrix by Ca^{2+} ions attack and embrittlement (brittleness) of hemp fibres due to fibre cell wall mineralization in cement matrix [2,17]. Moreover, alternating wet and dry conditioning increased the porosity and interface fatigue that led to decrease the bond strength between the fibres and the matrix, and thus the load-transfer. However, the 6THFR-CNCC1 nanocomposite (Fig.6b) presented better ductile behaviour and bending stress than 6THFRC composites (Fig.6a) after 236 days. This enhancement could be due to high fibre–matrix interfacial bonding, which increases the maximum load-transfer capacity.

3.5. Microstructural analysis

Figs.7(a–d) show the fibre–matrix interfacial bonding of 6THFRC composite and 6THFR-CNCC1 nanocomposite at 56 days and after 3 wet/dry cycles (at 236 days). At 56 days, the microstructural characteristic of the fracture surface of 6THFRC composite (Fig. 7a) showed relatively good fibre–matrix interfaces with small gaps between the fabric layers and the cement matrix. However, after 3 wet/dry cycles (at 236 days) the interface zone between the fabrics and the matrix is increased (Fig.7b), which indicated obvious deterioration of fibre–matrix interfacial bonding. Regarding the 6THFR-CNCC1 nanocomposite at 56 days, the SEM image showed better fibre–nanomatrix interfacial bonding (Fig. 7c) when compared to the 6THFRC composite (Fig.7a). However, after 3 wet/dry cycles (at 236 days) the interface zone between the fabrics and the matrix containing CNC slightly increased (Fig.7d), which indicated very small signs of degradation of fibre–matrix interface in nano-matrix. This confirmed that the CNC considerably reduced the deterioration of fibre–matrix interfacial bonding. The same phenomena was observed by Wei and Meyer [49], according to their SEM images where they reported that the use of metakaolin in cement composite reduced the deterioration of interface zone between natural fibre and matrix after accelerating ageing (30 wet/drying cycles).

SEM micrographs of raw NaOH treated hemp fibre and the hemp fibres extracted from 6THFRC composite and 6THFR-CNCC1 nanocomposite after 3 wet/dry cycles (at 236 days) are shown in Figs.8(a–d). It can be seen that the fibre surface of raw NaOH treated hemp fibre was more uniform (Fig.8a), whereas in 6THFRC composite (Figs.8b–c), the micrographs revealed some degradation on the fibre surface during accelerating ageing. Sedan et al. [9] reported that the CH content (Ca^{2+} ions) of cement matrix contributed to the degradation of hemp fibre rapidly. Regarding 6THFR-CNCC1 nanocomposite (Fig.8d), there was slight change in the fibre surface after 236 days, which indicated that CNC slightly prevented the degradation of hemp fibre surface.

4. Cost and applications

Natural fibres/fabrics are increasingly being utilized due to low density, low cost, renewability, recyclability and availability [1,2]. On the other hand, nanoparticles are expensive which could limit their applications [23,25]. Singh [50] stated that the nanomaterials have many unique characteristics which will definitely result in high strength and durable concrete, but the cost of nanomaterial is still very expensive due to novelty technology. Perhaps the nanomaterial cost will come down over time as manufacturing technologies upgrade their production efficiency [24]. However, nanomaterials are used in very small amounts in the concrete or other cementitious composites. Shaikh and Supit [51] stated that although the use of nano-$CaCO_3$ was first considered as filler to partially replace cement, some studies have shown advantages of using 1% nano-$CaCO_3$ nanoparticles in terms of compressive strength and economic benefits as compared to cement and other supplementary cementitious materials.

Among all types of nanomaterials that can be used in construction and building materials, nanoclay is considered as one of inexpensive nanomaterials. In this study the use of (very small amounts) only 1% calcined nanoclay in CNCC1 and 6THFR-CNCC1 nanocomposite led to significant improvement in mechanical properties and durability. From

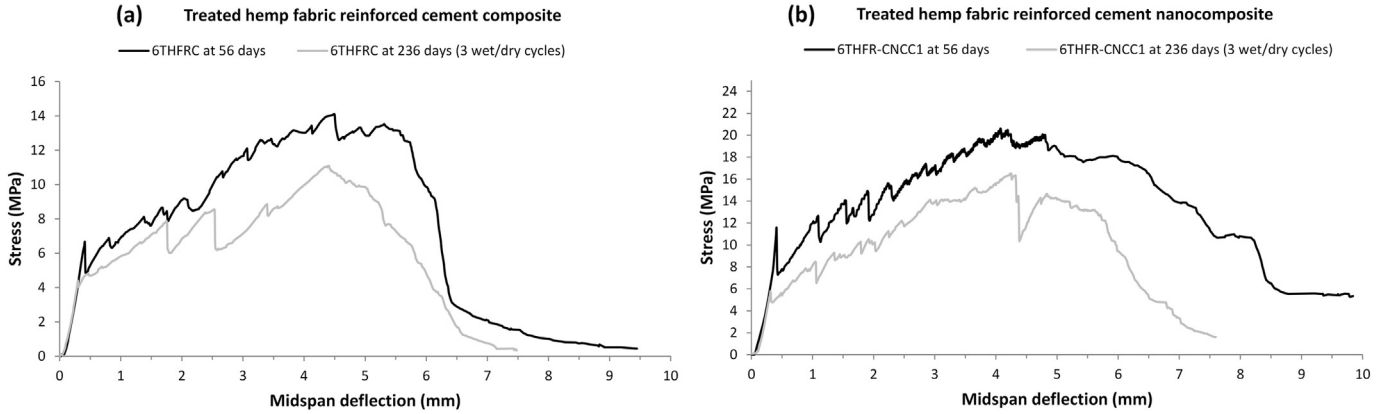

Fig. 6. Stress versus mid-span deflection curves for 6THFRC composite and 6THFR-CNCC1 nanocomposites at 56 and after 3 wet/dry cycles (236 days).

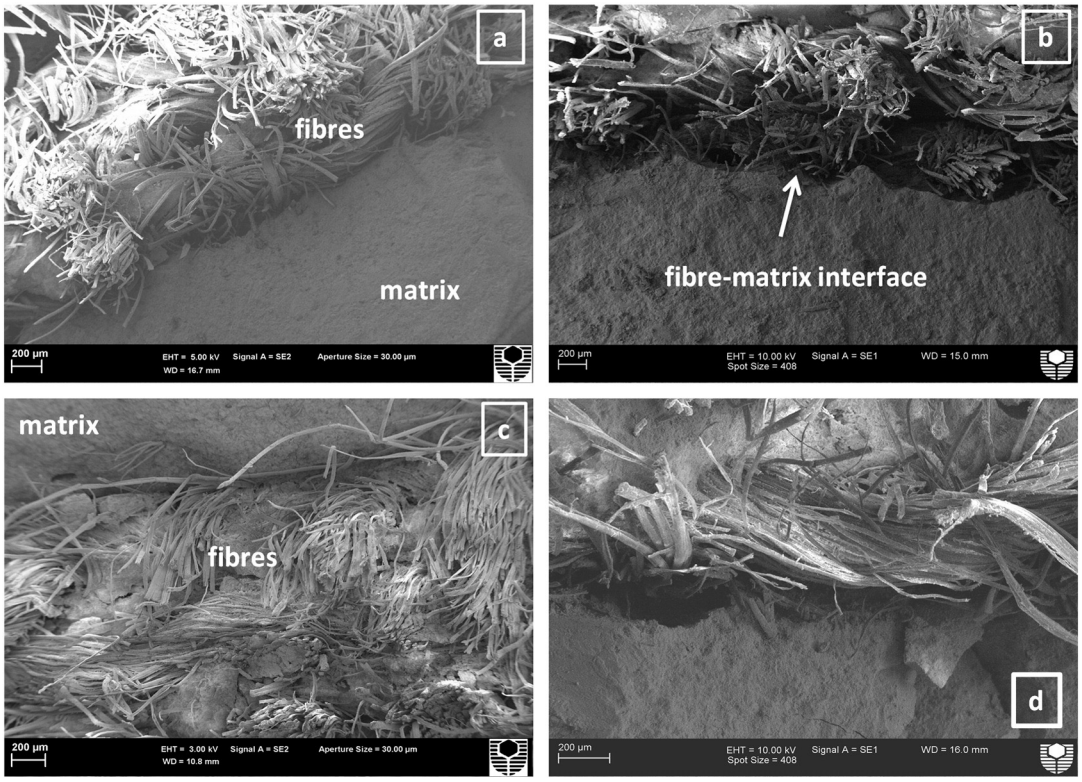

Fig. 7. SEM images of: 6THFRC composite (a) at 56 days, (b) after 3 wet/dry cycles (236 days) and 6THFR-CNCC1 nanocomposites (c) at 56 days, (d) after 3 wet/dry cycles (236 days).

economic point of view, the addition of 1% calcined nanoclay in cement paste or treated hemp fabric reinforced cement composite will not add any significant cost but improved the durability significantly after 236 days (3 wet/dry cycles).

Regarding the issue of durability/cost ratio, this study has found that (see Fig 5), after 236 days (3 wet/dry cycles), the 6THFR-CNCC1 nanocomposite showed higher flexural strength (by 55% increase) than control 6THFR composite. This means that the addition of 1% calcined

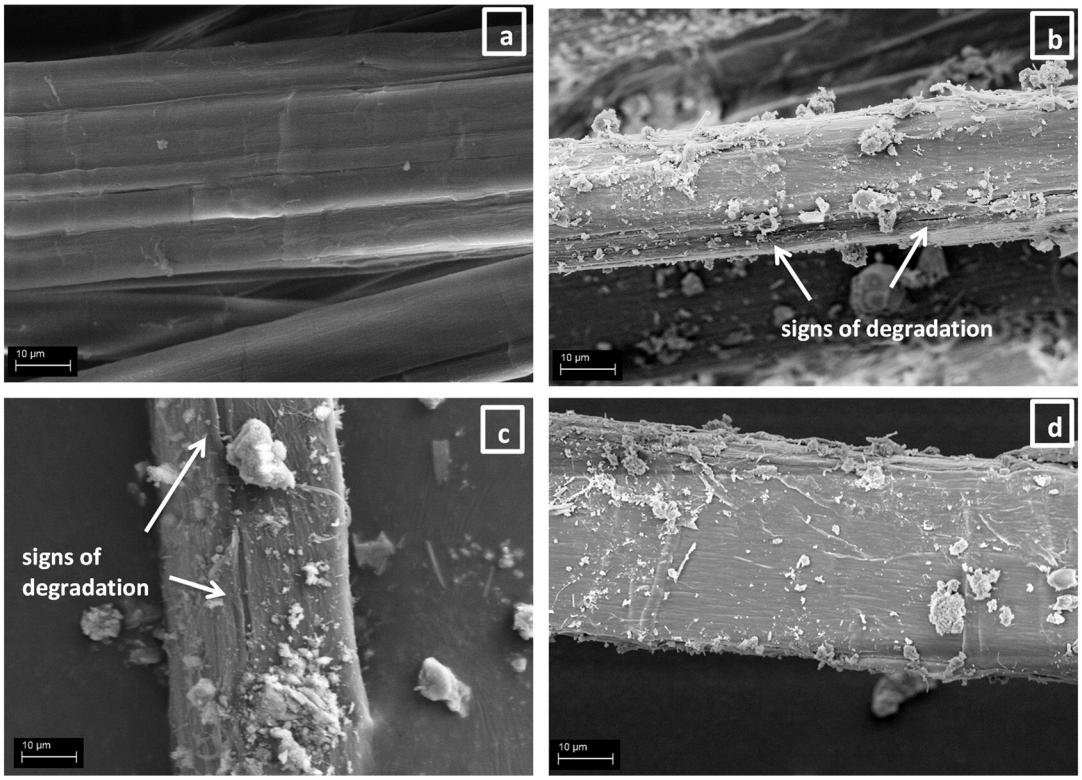

Fig. 8. SEM images of: (a) raw NaOH treated hemp fibre and the hemp fibres extracted from: (b, c) 6THFRC composite, (d) 6THFR-CNCC1 nanocomposite after 3 wet/dry cycles (236 days).

nanoclay will not add significant cost but can increase the life (durability) of treated hemp fabric reinforced cement composites by 1.55 times over their counterparts without calcined nanoclay. The benefit of developing the long-term durability of natural fibre in such fibre-nanocomposite will overcome the few cost. The developed treated hemp fabric reinforced nanocomposites can also be widely employed as an alternative to synthetic fibres in some applications including concrete tiles, roofing sheets, sandwich panels, on-ground floors, ceilings and structural laminate.

5. Conclusions

Cement composites and nanocomposites reinforced with hemp fabrics and calcined nano-clay (CNC) have been fabricated and characterized. The effect of CNC on the durability of treated hemp fabric reinforced cement nanocomposites and the degradation of hemp fibres are reported. The optimum content of CNC was 1 wt.%. After 236 days (3 wet/dry cycles), the flexural strength of 6THFRC composites decreased by 26.2% whereas flexural strength of 6THFR-CNCC1 nanocomposites decreased by 17.4%. SEM micrographs indicated that hemp fibre in 6THFRC composites undergo more degradation that in 6THFR-CNCC1 nanocomposites. Based on all results, the addition of CNC has great potential to improve the durability of treated hemp fabric reinforced cement nanocomposites during wet/dry cycles, particularly at 1% CNC. Indeed, particles agglomeration increased as CNC content increased which adversely affected the mechanical properties of the composites. It is recommended that more research is required to overcome the CNC agglomerations.

Acknowledgments

The authors are grateful to Ms. E. Miller for her assistance with SEM imaging.

References

[1] M. Ardanuy, J. Claramunt, R. Filho, Cellulosic fibre reinforced cement-based composites: a review of recent research, Constr. Build. Mater. 79 (2015) 115–128.
[2] F. Pacheco-Torgal, S. Jalali, Cementitious building materials reinforced with vegetable fibres: a review, Constr. Build. Mater. 25 (2011) 575–581.
[3] Z. Li, X. Wang, L. Wang, Properties of hemp fibre reinforced concrete composites, Compos. Part A 37 (2006) 497–505.
[4] B. Mohr, J. Biernacki, K. Kurtis, Microstructural and chemical effects of wet/dry cycling on pulp fibre–cement composites, Cem. Concr. Res. 36 (2006) 1240–1251.
[5] A. Almeida, G. Tonoli, S. Santos, H. Savastano, Improved durability of vegetable fibre reinforced cement composite subject to accelerated carbonation at early age, Cem. Concr. Compos. 42 (2013) 49–58.
[6] P. Soroushian, J. Won, M. Hassan, Durability characteristics of CO_2-cured cellulose fibre reinforced cement composites, Constr. Build. Mater. 34 (2012) 44–53.
[7] R. Filho, K. Ghavami, G. England, K. Scrivener, Development of vegetable fibre–mortar composites of improved durability, Cem. Concr. Compos. 25 (2003) 185–196.
[8] J. Wei, C. Meyer, Improving degradation resistance of sisal fibre in concrete through fibre surface treatment, Appl. Surf. Sci. 289 (2014) 511–523.
[9] D. Sedan, C. Pagnoux, A. Smith, T. Chotard, Mechanical properties of hemp fibre reinforced cement: influence of the fibre/matrix interaction, J. Eur. Ceram. Soc. 28 (2008) 183–192.
[10] M. Troėdec, C. Peyratout, A. Smith, T. Chotard, Influence of various chemical treatments on the interactions between hemp fibres and a lime matrix, J. Eur. Ceram. Soc. 29 (2009) 1861–1868.
[11] N. Smaoui, M. Berube, B. Fournier, B. Bissonnette, B. Durand, Effects of alkali addition on the mechanical properties and durability of concrete, Cem. Concr. Res. 35 (2005) 203–212.
[12] I. Odler, R. Wonnemann, Effect of alkalies on Portland cement hydration: I. Alkali oxides incorporated into the crystalline lattice of clinker minerals, Cem. Concr. Res. 13 (1983) 477–482.
[13] I. Jawed, J. Skalny, Alkalies in cement: a review: II. Effects of alkalies on hydration and performance of Portland cement, Cem. Concr. Res. 8 (1987) 37–52.
[14] A.M. Neville, Properties of Concrete, fifth ed. England, Pearson Education Limited, 2011.
[15] K. Kurtis, P. Monteiro, Chemical additives to control expansion of alkali-silica reaction gel: proposed mechanisms of control, J. Mater. Sci. 38 (2003) 2027–2036.
[16] B. Mohr, H. Nanko, K. Kurtis, Durability of kraft pulp fibre–cement composites to wet/dry cycling, Cem. Concr. Compos. 27 (2005) 435–448.
[17] B.Mohr, J.Biernacki, K.Kurtis, Supplementary cementitious materials for mitigating degradation of kraft pulp fibre-cement composites, Cem. Concr. Res. 37 (2007) 1531–1543.
[18] A. Peled, S. Sueki, B. Mobasher, Bonding in fabric–cement systems: effects of fabrication methods, Cem. Concr. Res. 36 (2006) 1661–1671.
[19] A. Peled, B. Mobasher, Tensile behavior of fabric cement-based composites: pultruded and cast, J. Mater. Civ. Eng. 19 (2007) 340–348.
[20] B. Mobasher, A. Peled, J. Pahilajani, Distributed cracking and stiffness degradation in fabric-cement composites, Mater. Struct. 39 (2006) 317–331.
[21] H. Alamri, I.M. Low, Z. Alothman, Mechanical, thermal and microstructural characteristics of cellulose fibre reinforced epoxy/organoclay nanocomposites, Compos. Part B 43 (2012) 2762–2771.
[22] A. Alhuthali, I.M. Low, C. Dong, Characterization of the water absorption, mechanical and thermal properties of recycled cellulose fibre reinforced vinyl-ester eco-nanocomposites, Compos. Part B 43 (7) (2012) 2772–2781.
[23] F. Pacheco-Torgal, S. Jalali, Nanotechnology: advantages and drawbacks in the field of construction and building materials, Constr. Build. Mater. 25 (2011) 582–590.
[24] M.J. Hanus, A.T. Harris, Nanotechnology innovations for the construction industry, Prog. Mater. Sci. 58 (2013) 1056–1102.
[25] F. Sanchez, K. Sobolev, Nanotechnology in concrete — a review, Constr. Build. Mater. 24 (2010) 2060–2071.
[26] A. Hakamy, F.U.A. Shaikh, I.M. Low, Thermal and mechanical properties of NaOH treated hemp fabric and calcined nanoclay-reinforced cement nanocomposites, Mater. Des. 80 (2015) 70–81.
[27] A. Nazari, S. Riahi, The effects of zinc oxide nanoparticles on flexural strength of self-compacting concrete, Compos. Part B 42 (2011) 167–175.
[28] H. Li, H. Xiao, X. Guan, Z. Wang, L. Yu, Chloride diffusion in concrete containing nano-TiO_2 under coupled effect of scouring, Compos. Part B 56 (2014) 698–704.
[29] M.S. Morsy, S.H. Alsayed, M. Aqel, Hybrid effect of carbon nanotube and nano-clay on physico-mechanical properties of cement mortar, Constr. Build. Mater. 25 (2011) 145–149.
[30] P. Hou, S. Kawashima, D. Kong, D. Corr, J. Qian, S. Shah, Modification effects of colloidal nano-SiO_2 on cement hydration and its gel property, Compos. Part B 45 (1) (2013) 440–448.
[31] S. Supit, F.U.A. Shaikh, Effect of nano-$CaCO_3$ on compressive strength development of high volume fly ash mortars and concretes, J. Adv. Concr. Technology 12 (2014) 178–186.
[32] A. Hakamy, F.U.A. Shaikh, I.M. Low, Characteristics of nanoclay and calcined nanoclay-cement nanocomposites, Compos. Part B 78 (2015) 174–184.
[33] N. Farzadnia, A. Ali, R. Demirboga, M. Anwar, Effect of halloysite nanoclay on mechanical properties, thermal behavior and microstructure of cement mortars, Cem. Concr. Res. 48 (2013) 97–104.
[34] M. Aly, M. Hashmi, A. Olabi, M. Messeiry, A. Hussain, E. Abadir, Effect of nano-clay and waste glass powder on the properties of flax fibre reinforced mortar, J. Eng. Appl. Sci. 6 (2011) 19–28.
[35] A. Botana, M. Mollo, P. Eisenberg, R. Sanchez, Effect of modified montmorillonite on biodegradable PHB nanocomposites, Appl. Clay Sci. 47 (2010) 263–270.
[36] ASTM C-20, Standard test methods for apparent porosity, water absorption, apparent specific gravity, and bulk density of burned refractory brick and shapes by boiling water, 2010.
[37] M. Stefanidou, I. Papayianni, Influence of nano-SiO_2 on the Portland cement pastes, Compos. Part B 43 (6) (2012) 2706–2710.
[38] S.W.M. Supit, F.U.A. Shaikh, Durability properties of high volume fly ash concrete containing nano-silica, Mater. Struct. 47 (2014) 1545–1559.
[39] B. Jo, C. Kim, G. Tae, J. Park, Characteristics of cement mortar with nano-SiO_2 particles, Constr. Build. Mater. 21 (2007) 1351–1355.
[40] S. Hoshino, K. Yamada, H. Hirao, XRD/Rietveld analysis of the hydration and strength development of slag and limestone blended cement, J. Adv. Concr. Technol. 4 (2006) 357–367.
[41] Y. Wei, W. Yao, X. Xing, M. Wu, Quantitative evaluation of hydrated cement modified by silica fume using QXRD, 27Al MAS NMR, TG–DSC and selective dissolution techniques, Constr. Build. Mater. 36 (2012) 925–932.
[42] F.U.A. Shaikh, S.W.M. Supit, P.K. Sarker, A study on the effect of nano silica on compressive strength of high volume fly ash mortars and concretes, Mater. Des. 60 (2014) 433–442.
[43] L. Roma, L. Martello, H. Savastano, Evaluation of mechanical, physical and thermal performance of cement-based tiles reinforced with vegetable fibres, Constr. Build. Mater. 22 (2008) 668–674.
[44] S. Shebl, L. Allie, M. Morsy, H. Aglan, Mechanical behavior of activated nano silicate filled cement binders, J. Mater. Sci. 44 (2009) 1600–1606.
[45] H. Li, H. Xiao, J. Yuan, J. Ou, Microstructure of cement mortar with nano-particles, Compos. Part B 35 (2) (2004) 185–189.
[46] Z. Rong, W. Sun, H. Xiao, G. Jiang, Effects of nano-SiO_2 particles on the mechanical and microstructural properties of ultra-high performance cementitious composites, Cem. Concr. Compos. 56 (2015) 25–31.
[47] A. Mohamed, Influence of nano materials on flexural behavior and compressive strength of concrete, HBRC Journal (2015) http://dx.doi.org/10.1016/j.hbrcj.2014.11.006 (article in press).
[48] J. Filho, F. Silva, R. Filho, Degradation kinetics and aging mechanisms on sisal fibre cement composite systems, Cem. Concr. Compos. 40 (2013) 30–39.
[49] J. Wei, C. Meyer, Degradation mechanisms of natural fibre in the matrix of cement composites, Cem. Concr. Res. 73 (2015) 1–16.
[50] T. Singh, A review of nanomaterials in civil engineering works, Inter. J. Struct. Civ. Eng. Res. 3 (2014) 31–35.
[51] F.U.A. Shaikh, S. Supit, Mechanical and durability properties of high volume fly ash (HVFA) concrete containing calcium carbonate ($CaCO_3$) nanoparticles, Constr. Build. Mater. 70 (2014) 309–321.

4 CONCLUSIONS AND FUTURE WORK

4.1 Conclusions

This study consists of seven consecutive parts. Therefore, each section is dependent on the results of previous sections.

4.1.1 Nanoclay-cement nanocomposites

Ordinary Portland cement (OPC) was partially substituted by nanoclay with 1, 2 and 3% by weight of OPC to fabricate a series of nanoclay-cement nanocomposites. Dry mixing method of the binder (OPC and nanoclay powder) was used and the samples were tested at 56 days. The microstructures of nanocomposites were investigated using X-ray Diffraction (XRD), Quantitative X-ray Diffraction Analysis (QXDA), synchrotron radiation diffraction (SRD) and scanning electron microscopy (SEM). The effect of nanoclay on physical and mechanical properties of nanoclay-cement nanocomposite has been investigated. The thermal stability of samples was determined using thermogravimetric analysis (TGA).

The results generally indicated that the optimum content of nanoclay was found to be 1 wt%. Based on the XRD and SRD results, the addition of nanoclay reduced the intensities of major peaks of $Ca(OH)_2$ crystals comparing to the control cement paste. Also from QXDA, the addition of 1 wt% nanoclay reduced the amount of $Ca(OH)_2$ from 19.5 wt% to 15.7 wt%, about 19.5% reduction compared to cement paste. Also the intensities of major peaks of $Ca(OH)_2$ were significantly reduced compared to cement paste. Furthermore, the amorphous content was increased slightly from 67.4 wt% to 70 wt%, about 3.7% increase. This indicates that an obvious consumption of $Ca(OH)_2$ crystals mainly due to the effect of pozzolanic reaction in the presence of nanoclay and good dispersion of nanoclay in the matrix leads to produce more amorphous calcium silicate hydrate gel (C-S-H). In addition, SEM images of the microstructure of cement paste, nanocomposites containing 1 wt% and 3 wt% nanoclay were also presented. SEM images of cement paste showed more $Ca(OH)_2$ crystals and Ettringite as well as more pores which revealed a weak structure. It was found that the SEM micrograph of nanocomposites containing 1 wt% nanoclay was

different from that of cement paste, the structure was denser and compact with few pores due to the filler effect of 1 wt% nanoclay and more CSH gel due to pozzolanic effect. On the other hand, the SEM micrograph of nanocomposites containing 3 wt% nanoclay showed more pores and micro-cracks which led to weaken the structure of this nanocomposite when compared to nanocomposites containing 1 wt% nanoclay.

Regarding the physical and mechanical properties and thermal stability, in general, the incorporation of nanoclay in cement matrix led to a modest enhancement in physical and mechanical properties of all nanocomposites. Moreover, it was found that the nanocomposites with 1wt% of nanoclay achieve the highest improvement in all properties. The cement nanocomposite containing 1 wt% nanoclay decreased the porosity (by 20.6%) and water absorption (by 23.5%) and increased the density (by 4%), compressive strength (by 31%), flexural strength (by 32%), fracture toughness (by 31%), impact strength (by 29%) and Rockwell hardness (by 24%) as well as improved thermal stability (by 2.3%) compared to the control cement paste.

This improvement can be attributed to pozzolanic and filler effects of 1 wt% nanoclay in which this nanocomposite had more consolidated microstructure than others. However, the addition of more nanoclay (beyond 1 wt %) into cement nanocomposite adversely affected the mechanical and thermal properties. This could be attributed to the poor dispersion and agglomerations of the high nanoclay contents which created more voids in the matrix.

4.1.2 Hemp fabric-reinforced nanoclay-cement nanocomposites (small depth specimens - 10 mm)

Hemp fabric-reinforced nanoclay-cement nanocomposites were fabricated with two layers of hemp fabrics and different contents of nanoclay (1, 2 and 3 wt %). The total amount of hemp fabric in each specimen was about 2.5 wt%. In sample preparation and curing stage, three prismatic plate specimens of length 300 mm × width 70 mm × depth 10 mm were cast and after 56 days several specimens of each series with dimensions 70 mm ×20 mm ×10 mm were cut from the fully cured prismatic plate for each test. The influence of nanoclay on physical, mechanical and thermal properties of hemp fabric-reinforced cement composite as well as hemp fibre-matrix interface was investigated. SEM

micrographs of fracture surfaces and hemp fibre-matrix interface were presented. The thermal stability of samples was determined using thermogravimetric analysis (TGA).

Generally, the results indicated that the addition of nanoclay into hemp fabric-reinforced nanocomposite improved the physical, mechanical and thermal properties. Moreover, the hemp fabric-reinforced nanocomposites containing 1wt% nanoclay achieved the highest improvements than others. It was found that the incorporation of 1 wt% nanoclay into the hemp fibre-reinforced nanocomposites decreased the porosity (by 16%) and water absorption (by 18%) as well as increased the density (by 3%), flexural strength (by 28.5%), fracture toughness (by 24.6%), impact strength (by 23%) and also improved the thermal stability (by 19%), when compared to the control hemp fibre-reinforced cement composite.

SEM micrographs of fracture surfaces of hemp fibre-reinforced nanocomposites containing 1wt% nanoclay showed good fibre-matrix interface as well as the presence of hydration products on the fibre surface indicating better fibre/matrix interface bond. However, poor adhesion between fibres and matrix was observed in hemp fibre reinforced cement composite. In hemp fibre reinforced -nanocomposite containing 3 wt% nanoclay, macro-cracking was observed in the matrix which revealed relatively weak matrix and also debonding of fibre occurred.

This improvement in physical and mechanical properties as well as fibre-matrix interface of hemp fibre-reinforced nanocomposites containing 1 wt% nanoclay was attributed to the fact that the nanoclay modified the microstructure of matrix through pozzolanic reaction and pore-filling effect. Thus, good interfacial bonding between the nanomatrix and the hemp fibres was achieved. However, the addition of more nanoclay (> than 1 wt%) into the hemp fibre-reinforced cement composites adversely affected the thermal, physical and mechanical properties as well as fibre-matrix interface.

4.1.3 Hemp fabric-reinforced nanoclay-cement nanocomposites (large depth specimens - 40 mm)

Eight layers of hemp fabrics were used to prepare hemp fabric reinforced nanoclay nanocomposites, in which their positions were placed above and down the centre of the nanocomposite sample over the depth of the specimen. The total amount of hemp fabric in

each specimen was about 2.4 wt% and different contents of nanoclay (1, 2 and 3 wt %) were used. Based on ASTM C348–08 standard, four prismatic plate specimens of 160 × 40 × 40 mm (length×width×depth) in dimension were cast for each test and samples were tested at 56 days. The effect of nanoclay on physical and mechanical properties of hemp fabric-reinforced cement composites as well as hemp fibre-matrix interface was investigated.

The results showed that the optimum content of nanoclay is 1 wt%. The hemp fibre-reinforced nanocomposites containing 1 wt% nanoclay decreased the porosity (15.5%) and also increased the density (5.3%), flexural strength (26.2%) and fracture toughness (24.9%) compared to the hemp fibre-reinforced cement composite. SEM micrographs of hemp fibre-reinforced nanocomposite containing 1 wt% nanoclay also supported its improvement as compared to other samples in terms of better fibre-matrix interface. This improvement was due to the efficiency of pozzolanic reaction and filler effects of 1 wt% nanoclay to improve the microstructure and achieve high fibre-matrix interface bonding, which increases the maximum load-transfer capacity. However, no such significant improvement was observed when nanoclay content exceeds the optimum content. This could be attributed to the increase in porosity which decreased the bonding between fibres and matrix, and thus the attendant load-transfer. In other words, pores act as defects as well as stress-raisers to weaken the material.

4.1.4 Calcined nanoclay-cement nanocomposites

Calcined nanoclay-cement nanocomposites were studied and the results were compared with the previous work of nanoclay-cement nanocomposites. Prior to preparation of samples, thermal treatment of nanoclay was carried out. Calcined nanoclay (CNC) was prepared by heating the nanoclay (NC) at 800, 850 and 900°C for 2 h and then it was characterized by XRD, energy dispersive spectroscopy (EDS) and High Resolution Transmission Electron Microscopy (HRTEM) in order to determine its amorphous phase. OPC was partially substituted by calcined nanoclay of 1, 2 and 3% by weight of OPC and dry mixing method of binder was used. Estimation of $Ca(OH)_2$ content in the cement nanocomposite was studied by the combination of QXDA and thermogravimetry analysis

(TGA) techniques. The influence of calcined nanoclay on the physical, mechanical and thermal properties of cement nano-composites was presented.

Based on the results of XRD, EDS and HRTEM, nanoclay transformed to amorphous state (calcined nanoclay) at 900 °C. Moreover, at high magnification by HRTEM, it was found that many platelets in calcined nanoclay were destroyed and some of them broke to small nanoparticles with approximate spherical shapes ranging 3-8 nm. Overall, the results showed that the microstructures, physical, mechanical and thermal properties of the cement nanocomposites were improved as a result of CNC addition. The optimum content of CNC was 1 wt%.

Regarding characterisation of microstructure for nanocomposites, the results of XRD patterns and QXDA indicated that the addition of 1 wt% CNC reduced the amount of $Ca(OH)_2$ from 16.8 wt% to 12.1 wt%, about 28% reduction compared to cement paste. Also the intensities of major peaks of $Ca(OH)_2$ were significantly reduced compared to cement paste. Furthermore, the amorphous content of C-S-H gel was increased from 70.1 to 74.8 wt%, about 6.7% increase. This improvement in microstructure can be explained as follows: the CNC was mainly amorphous nanomaterial and behaved as a highly reactive artificial pozzolan and thus it could consume more CH through the pozzolanic reaction. As a result the CH content in cement nanocomposite containing 1 wt% CNC was reduced significantly when compared to cement paste and other cement nanocomposites containing NC and CNC such as cement nanocomposite containing 1 wt% NC. SEM examinations of the microstructure of cement paste, 1 wt% CNC nanocomposites and 3 wt% CNC nanocomposites confirmed the effectiveness of 1 wt% CNC. SEM micrograph of 1 wt% CNC nanocomposite showed that its microstructure was denser and more compact with fewer pores, less CH and more C-S-H gel when compared to cement paste and 3 wt% CNC nanocomposites.

Regarding the estimation of $Ca(OH)_2$ content in the cement nanocomposite by the combination of QXDA and TGA techniques, the results of the combination of QXDA and TGA techniques indicated that TGA was at least as good as QXDA for quantifying the amount of $Ca(OH)_2$, where both measured amounts were very close to each other.

Regarding the physical, mechanical and thermal properties of cement nanocomposites, overall, the addition of CNC into the cement matrix led to significant enhancement in these properties when compared to cement nanocomposites containing NC or cement paste. The cement nanocomposite containing 1 wt% CNC decreased the porosity (by 31.2%) and water absorption (by 34%) and increased the density (by 9.7%), compressive strength (by 40%) flexural strength (by 42.9%), fracture toughness (by 40%), impact strength (by 33.6%) and Rockwell hardness (by 31.1%) as well as improved thermal stability (by 3.3%) compared to the control cement paste. This improvement was due to the effective filler and pozzolanic reaction effects and good dispersion of 1 wt% CNC. In fact, it could be recommended that more research is needed to overcome the agglomerations of NC or CNC and to identify the best method of mixing to achieve good dispersion of CNC in the matrix.

4.1.5 Un-treated and NaOH treated hemp fabric-reinforced cement composites

A series of untreated and treated hemp fabric-reinforced cement composites were fabricated and investigated in this part. Prior to preparation of samples, chemical pre-treatment of hemp fabric surface was carried out by immersing the fabrics in 1.7 M NaOH solution (pH=14) for 48 hours at 25° C, followed by neutralization, washing and drying. The fibre surface was then characterized by SEM, XRD and TGA. Samples of un-treated hemp fabric-reinforced cement composites (UHFRC) were fabricated with various contents of hemp fabric: 4.5 wt% (4 layers of fabric), 5.7 wt% (5 layers of fabric), 6.9 wt% (6 layers of fabric) and 8.1 wt% (7 layers of fabric). As six un-treated hemp fabrics achieved good mechanical performance, only 6 layers of treated hemp fabric were used to fabricate treated hemp fabric-reinforced cement composite (6THFRC). In sample preparation and curing stage, three prismatic plate specimens of 300×70×10 mm (length×width×depth) in dimension were cast and after 56 days several specimens of each series with dimensions 70×20×10 mm (length×width×depth) were cut from the fully cured prismatic plate for each test. The influence of untreated hemp fabric contents and chemical treatment on the mechanical properties and fibre-matrix interfaces of untreated and treated hemp fabric-reinforced cement nanocomposites were investigated.

Based on the results from SEM, XRD and TGA of hemp fibre surface, it was found that the NaOH treatment effectively bleached and cleaned the surface of hemp fibres and removed the amorphous materials such as hemicellulose, pectins and impurities (fatty substances and waxes) from their surface. Thus the fabric surface became more uniform with slightly higher crystallinity index and thermal stability when compared to un-treated hemp fabric surface.

Regarding the flexural strength and fracture toughness of un-treated hemp fabric-reinforced cement composites (UHFRC), overall, the flexural strength and fracture toughness increased with an increase in fibre content up to the optimum hemp fibre content, and then decreased after this limit. Results indicated that the optimum hemp fabric content among these composites was 6.9 wt% (i.e. 6 fabric layers) for 6UHFRC composite. In 6UHFRC composite, the flexural strength and fracture toughness are improved by about 133% and 303%, respectively compared to the cement paste. However, beyond this optimum content of hemp fibre, the flexural strength and fracture toughness of the UHFRC composites are decreased. This could be attributed to the increase in porosity which reduced adhesion between the fibres and the matrix, and thus decreased the load transfer.

Results also showed the effect of NaOH treatment of hemp fabric on the flexural strength and fracture toughness of 6THFRC composites. It was found that the flexural strength of 6THFRC composite increased from 12.6 to 14.5 MPa, about 14.9% increase when compared to 6UHFRC composite. Moreover, the 6THFRC composite exhibited 13.5% increase in fracture toughness.

SEM micrographs of 6UHFRC composite showed relatively poor fibre-matrix interfaces with small gaps between the fabric layers and the cement matrix. In contrast, the 6THFRC composite showed very small gaps between the fabrics and the matrix, which indicated better fibre-matrix interfacial bonding. This improvement could be explained as follows: after NaOH treatment, most of waxes and fats were removed from the hemp fibre surface, and the surface became more uniform but rough. Thus, this led to good interfacial bonding between the matrix and the hemp fibres which served to enhance the load transfer process at the interface.

4.1.6 NaOH treated hemp fabric reinforced calcined nanoclay-cement nanocomposites

Based on the results from previous works, the NaOH treated hemp fabric-reinforced calcined nanoclay-cement nanocomposites were fabricated with six layers of treated hemp fabrics and different contents of calcined nanoclay (1, 2 and 3 wt %). Total amount of treated hemp fabric in each specimen was about 6.9 wt%. The influence of calcined nanoclay on the physical, mechanical and thermal properties as well as fibre-matrix interface of NaOH treated hemp fabric-reinforced calcined nanoclay cement nanocomposites was studied and samples were tested after 56 days.

Results indicated that the physical, mechanical and thermal properties enhanced due to the addition of CNC into the 6THFRC composites and the optimum content of CNC was 1 wt%. The treated hemp fabric-reinforced nanocomposites containing 1 wt% CNC (6THFR-CNCC1) exhibited the highest flexural strength, fracture toughness, impact strength and thermal stability than their counterparts and good fibre-matrix interface. In other words, for 6THFR-CNCC1 nanocomposites, it was found that the porosity and water absorption decreased by 12.4% and 14%, respectively, as well as the density, flexural strength, fracture toughness, impact strength and thermal stability improved by 4.5%, 38.8%, 38.1%, 19% and 5%, respectively compared to the 6THFRC composites. SEM micrographs of 6THFR-CNCC1 nanocomposite showed better fibre-nanomatrix interfacial bonding with ruptured fibres when compared to 6THFRC composites or even the treated hemp fabric-reinforced nanocomposites containing 3 wt% CNC (6THFR-CNCC3).

This improvement clearly indicated the effectiveness of CNC in consuming calcium hydroxide (CH), thus facilitating the pozzolanic reaction, and pore-filling in the matrix. As a result, the microstructure of nanocomposite matrix was denser than the cement matrix. Consequently, the interfacial bonding of treated hemp fabric-nanocomposite matrix was mostly improved, especially in the case of using 1 wt% CNC, as evident from its higher strength and toughness values. It could be seen that CNC behaves not only as a filler to improve the microstructure, but also as the activator to facilitate the pozzolanic reaction and thus improved the adhesion between the treated hemp fabric and the matrix.

However, the mechanical properties of treated hemp fabric-reinforced composites were adversely affected when CNC content increased beyond the optimum content of 1 wt%. This was attributed to the poor dispersion of high content of CNC into the matrix, which led to increase in porosity and weaken the fibre-matrix interface.

4.1.7 Durability of NaOH treated hemp fabric reinforced calcined nanoclay-cement nanocomposites subjected to wet/dry cycles

Based on the results from previous works, cement nanocomposites reinforced with 6 treated hemp fabrics and calcined nanoclay (CNC) were fabricated and their durability investigated. The treated hemp fabric-reinforced cement composites and nanocomposites were subjected to 3 wetting and drying cycles and then tested at 56 and 236 days. The influences of CNC dispersion on the durability of these composites were characterized in terms of porosity, flexural strength, stress-midspan deflection curves and microstructural observation of hemp surface. The effect of CNC on the degradation of hemp fibres was also studied.

Regarding the durability of calcined nanoclay-cement nanocomposites, the results indicated that the porosity and flexural strength improved slightly in periods of between 56 and 236 days. For example, the flexural strength of CNCC1 nanocomposite increased by about 7%. This improvement could be attributed to further hydration reaction and pozzolanic reaction as well as pore-filling effect.

Regarding NaOH treated hemp fabric reinforced calcined nanoclay-cement nanocomposites, the results also indicated that the durability and the degradation resistance of hemp fibre enhanced due to the addition of CNC into the cement matrix and the optimum content of CNC was 1 wt%. After 236 days (3 wet/dry cycles), the flexural strength of 6THFRC composites decreased about 26.2% compared to its initial strength at 56 days. Whereas the flexural strength of 6THFR-CNCC1 nanocomposites decreased by about 17.4% compared to its value at 56 days.

The SEM micrographs after 3 wet/dry cycles (at 236 days) indicated that there were very small signs of degradation of fibre-matrix interface for 6THFR-CNCC1 nanocomposites when compared to 6THFRC composites. Moreover, the SEM images of the hemp fibres

extracted from 6THFRC composites showed that they underwent more degradation than the hemp fibres extracted from 6THFR-CNCC1 nanocomposites.

Based on all results, the addition of CNC had great potential to improve the durability of treated hemp fabric reinforced cement nanocomposites during wet/dry cycles, particularly at 1 wt% CNC. This improvement was explained as follows: the degradation of natural fibres in Portland cement matrix is due to the high alkaline environment (especially calcium hydroxide solution) which dissolves the lignin and hemicellulose parts, thus weakening the fibre structure. In order to improve the durability of natural fibre in cement paste, the matrix could be modified in which calcium-hydroxide (CH) must be mostly consumed or reduced. In this study, the CNC effectively prevented the hemp fabric degradation by reducing the CH in the matrix through pozzolanic reaction. Thus, the degradation of hemp fibres in nanocomposite was mostly prevented and the treated hemp fabric-nanocomposite matrix interfacial bonding was mostly improved especially in the case of 1 wt% CNC. Other two reasons of this improvement were the effectiveness of CNC in filling the micro pores in the matrix which led to denser microstructure of nanocomposite matrix than the cement matrix and also the pre-treatment of hemp fibre by NaOH solution.

4.2 Recommendations for Future Work

The primary objectives of this research have been achieved. The effect of nanoparticles (nanoclay and calcined nanoclay) and hemp fabrics (untreated and NaOH treated) on the microstructure, physical, mechanical and thermal properties as well as durability of cement nanocomposites, untreated and NaOH treated hemp fabric-reinforced cement nanocomposites were investigated and discussed. The research results provided a fundamental knowledge on the mechanism and performance of a new class of treated hemp fabric-reinforced cement nanocomposites. Despite the significant improvement in mechanical properties for both cement nanocomposites and NaOH treated hemp fabric-reinforced cement nanocomposites, the agglomeration of nanoparticles at high content is still a major issue. For future work, there is a need to continue research and development in this field of materials science. Thus, the following recommendations have been formulated to help guide future study:

1. This project concentrated on cement paste as a matrix. The ideas of using calcined nanoclay and treated natural fibres from this research can be developed and applied for other material systems such as cement mortar, concrete, and natural fibre reinforced concrete.

2. In this research, it was found that the addition of more nanoclay and calcined nanoclay (beyond 1 wt %) into cement nanocomposite matrix adversely affected the mechanical and thermal properties of cement nanocomposites, untreated and NaOH treated hemp fabric-reinforced cement nanocomposites. In fact, it could be recommended that much research is needed to overcome the problems of nanoclay agglomerations and also to identify the best method of mixing to achieve good dispersion of nanoclay and calcined nanoclay at high contents in the matrix.

3. Because the main issue of using natural fibres in cement composites is long term durability of natural fibre reinforced concrete, it is recommended that more research is required to overcome natural fibre degradation. Consequently this can help to develop environmental friendly building materials.

4. In this experimental work, the durability of NaOH treated hemp fabric reinforced calcined nanoclay-cement nanocomposites was investigated under wet/dry cycles condition at 236 days (about 8 months). Other durability conditions such as freeze-thaw cycle and testing after long durations such as 1-5 years are needed to validate the findings of this study.

5. Advanced computer models are required to investigate the influence of nanostructures, such as shape and size distribution, orientation, aspect ratio, degree of spatial and interfaces on the physical and mechanical properties of cement nanocomposites, untreated and treated hemp fabric-reinforced cement nanocomposites. Multi-scale mechanics models and numerical methods should

be developed for better understanding of the enhanced mechanisms of such building nanomaterials.

6. From the outcome the experimental results and analyses, the challenge for further research on the use of nanomaterials for building construction and their compatibility in environmental issues and cost are still necessary.

5. APPENDICES

5.1 APPENDIX A

Statements of Contributions of Others

5.1.1 Appendix A-1: Statements of Contribution of Others for "Microstructures and mechanical properties of hemp fabric reinforced organoclay cement nanocomposites".

Statement of Contribution of Others for "Microstructures and mechanical properties of hemp fabric reinforced organoclay cement nanocomposites".

13th January 2016

To Whom It May Concern

I, Prof. I.M. Low, contributed by project supervision and manuscript editing of the paper/publication entitled

HAKAMY, A., SHAIKH, F.U.A. & LOW, I.M. 2013. Microstructures and mechanical properties of hemp fabric reinforced organoclay–cement nanocomposites. *Construction & Building Materials,* 49, 298–307.

Undertaken with Ahmad Hakamy

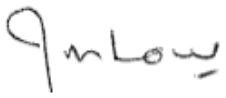

(Signature of Co-Author)

I. M. Low

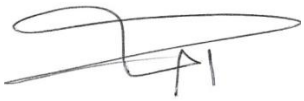

(Signature of First Author)

Ahmad Hakamy

Statement of Contribution of Others for "Microstructures and mechanical properties of hemp fabric reinforced organoclay cement nanocomposites".

13th January 2016

To Whom It May Concern

I, Dr. Faiz U.A. Shaikh, contributed by project supervision and manuscript editing of the paper/publication entitled

HAKAMY, A., SHAIKH, F.U.A. & LOW, I.M. 2013. Microstructures and mechanical properties of hemp fabric reinforced organoclay–cement nanocomposites. *Construction & Building Materials,* 49, 298–307.

Undertaken with Ahmad Hakamy

(Signature of Co-Author)

Faiz U.A. Shaikh

(Signature of First Author)

Ahmad Hakamy

5.1.2 Appendix A-2: Statements of Contribution of Others for “Thermal and mechanical properties of hemp fabric-reinforced nanoclay–cement nanocomposites”.

Statement of Contribution of Others for "Thermal and mechanical properties of hemp fabric-reinforced nanoclay–cement nanocomposites".

13th January 2016

To Whom It May Concern

I, Prof. I.M. Low, contributed by project supervision and manuscript editing of the paper/publication entitled

HAKAMY, A., SHAIKH, F.U.A. & LOW, I.M. 2014. Thermal and mechanical properties of hemp fabric-reinforced nanoclay–cement nanocomposites. *Journal of Materials Science,* 49, 1684–1694.

Undertaken with Ahmad Hakamy

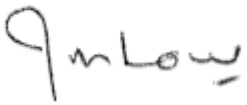

(Signature of Co-Author)

I. M. Low

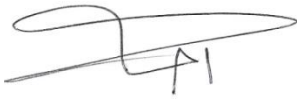

(Signature of First Author)

Ahmad Hakamy

Statement of Contribution of Others for "Thermal and mechanical properties of hemp fabric-reinforced nanoclay–cement nanocomposites".

13th January 2016

To Whom It May Concern

I, Dr. Faiz U.A. Shaikh, contributed by project supervision and manuscript editing of the paper/publication entitled

HAKAMY, A., SHAIKH, F.U.A. & LOW, I.M. 2014. Thermal and mechanical properties of hemp fabric-reinforced nanoclay–cement nanocomposites. *Journal of Materials Science,* 49, 1684–1694.

Undertaken with Ahmad Hakamy

(Signature of Co-Author)

Faiz U.A. Shaikh

(Signature of First Author)

Ahmad Hakamy

5.1.3 Appendix A-3: Statements of Contribution of Others for “Characteristics of hemp fabric reinforced nanoclay–cement nanocomposites”.

Statement of Contribution of Others for "Characteristics of hemp fabric reinforced nanoclay–cement nanocomposites".

13th January 2016

To Whom It May Concern

I, Prof. I.M. Low, contributed by project supervision and manuscript editing of the paper/publication entitled

HAKAMY, A., SHAIKH, F.U.A. & LOW, I.M. 2014. Characteristics of hemp fabric reinforced nanoclay–cement nanocomposites. *Cement & Concrete Composites,* 50, 27–35.

Undertaken with Ahmad Hakamy

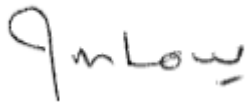

(Signature of Co-Author)

I. M. Low

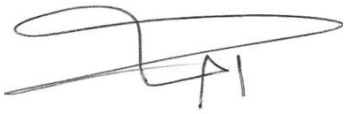

(Signature of First Author)

Ahmad Hakamy

Statement of Contribution of Others for "Characteristics of hemp fabric reinforced nanoclay–cement nanocomposites".

13th January 2016

To Whom It May Concern

I, Dr. Faiz U.A. Shaikh, contributed by project supervision and manuscript editing of the paper/publication entitled

HAKAMY, A., SHAIKH, F.U.A. & LOW, I.M. 2014. Characteristics of hemp fabric reinforced nanoclay–cement nanocomposites. *Cement & Concrete Composites,* 50, 27–35.

Undertaken with Ahmad Hakamy

(Signature of Co-Author)

Faiz U.A. Shaikh

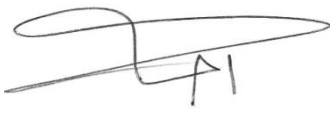

(Signature of First Author)

Ahmad Hakamy

5.1.4 Appendix A-4: Statements of Contribution of Others for “Characteristics of nanoclay and calcined nanoclay-cement nanocomposites”.

Statement of Contribution of Others for "Characteristics of nanoclay and calcined nanoclay-cement nanocomposites".

13th January 2016

To Whom It May Concern

I, Prof. I.M. Low, contributed by project supervision and manuscript editing of the paper/publication entitled

HAKAMY, A., SHAIKH, F.U.A. & LOW, I.M. 2015. Characteristics of nanoclay and calcined nanoclay-cement nanocomposites. *Composites Part B: Engineering,* 78, 174-184.

Undertaken with Ahmad Hakamy

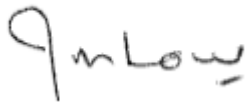

(Signature of Co-Author)

I. M. Low

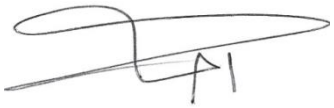

(Signature of First Author)

Ahmad Hakamy

Statement of Contribution of Others for "Characteristics of nanoclay and calcined nanoclay-cement nanocomposites".

13th January 2016

To Whom It May Concern

I, Dr. Faiz U.A. Shaikh, contributed by project supervision and manuscript editing of the paper/publication entitled

HAKAMY, A., SHAIKH, F.U.A. & LOW, I.M. 2015. Characteristics of nanoclay and calcined nanoclay-cement nanocomposites. *Composites Part B: Engineering*, 78, 174-184.

Undertaken with Ahmad Hakamy

(Signature of Co-Author)

Faiz U.A. Shaikh

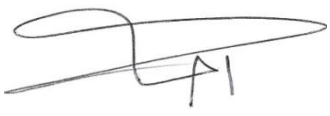

(Signature of First Author)

Ahmad Hakamy

5.1.5 Appendix A-5: Statements of Contribution of Others for “Effect of calcined nanoclay on microstructural and mechanical properties of chemically treated hemp fabric reinforced cement nanocomposites”.

Statement of Contribution of Others for "Effect of calcined nanoclay on microstructural and mechanical properties of chemically treated hemp fabric reinforced cement nanocomposites".

13th January 2016

To Whom It May Concern

I, Prof. I.M. Low, contributed by project supervision and manuscript editing of the paper/publication entitled

HAKAMY, A., SHAIKH, F.U.A. & LOW, I.M. 2015. Effect of calcined nanoclay on microstructural and mechanical properties of chemically treated hemp fabric reinforced cement nanocomposites. *Construction & Building Materials,* 95, 882–891.

Undertaken with Ahmad Hakamy

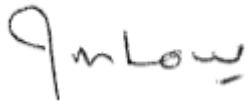

(Signature of Co-Author)

I. M. Low

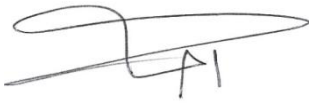

(Signature of First Author)

Ahmad Hakamy

Statement of Contribution of Others for "Effect of calcined nanoclay on microstructural and mechanical properties of chemically treated hemp fabric reinforced cement nanocomposites".

13th January 2016

To Whom It May Concern

I, Dr. Faiz U.A. Shaikh, contributed by project supervision and manuscript editing of the paper/publication entitled

HAKAMY, A., SHAIKH, F.U.A. & LOW, I.M. 2015. Effect of calcined nanoclay on microstructural and mechanical properties of chemically treated hemp fabric reinforced cement nanocomposites. *Construction & Building Materials,* 95, 882–891.

Undertaken with Ahmad Hakamy

(Signature of Co-Author)

Faiz U.A. Shaikh

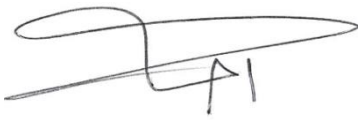

(Signature of First Author)

Ahmad Hakamy

5.1.6 Appendix A-6: Statements of Contribution of Others for “Thermal and mechanical properties of NaOH treated hemp fabric and calcined nanoclay-reinforced cement nanocomposites”.

Statement of Contribution of Others for "Thermal and mechanical properties of NaOH treated hemp fabric and calcined nanoclay-reinforced cement nanocomposites".

13th January 2016

To Whom It May Concern

I, Prof. I.M. Low, contributed by project supervision and manuscript editing of the paper/publication entitled

HAKAMY, A., SHAIKH, F.U.A. & LOW, I.M. 2015. Thermal and mechanical properties of NaOH treated hemp fabric and calcined nanoclay-reinforced cement nanocomposites. *Materials and Design,* 80, 70–81.

Undertaken with Ahmad Hakamy

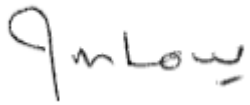

(Signature of Co-Author)

I. M. Low

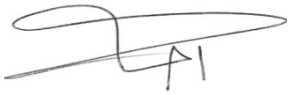

(Signature of First Author)

Ahmad Hakamy

Statement of Contribution of Others for "Thermal and mechanical properties of NaOH treated hemp fabric and calcined nanoclay-reinforced cement nanocomposites".

13th January 2016

To Whom It May Concern

I, Dr. Faiz U.A. Shaikh, contributed by project supervision and manuscript editing of the paper/publication entitled

HAKAMY, A., SHAIKH, F.U.A. & LOW, I.M. 2015. Thermal and mechanical properties of NaOH treated hemp fabric and calcined nanoclay-reinforced cement nanocomposites. *Materials and Design,* 80, 70–81.

Undertaken with Ahmad Hakamy

(Signature of Co-Author)

Faiz U.A. Shaikh

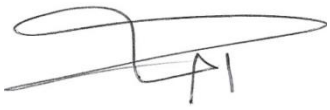

(Signature of First Author)

Ahmad Hakamy

5.1.7 Appendix A-7: Statements of Contribution of Others for “Effect of calcined nanoclay on the durability of NaOH treated hemp fabric-reinforced cement nanocomposites”.

Statement of Contribution of Others for "Effect of calcined nanoclay on the durability of NaOH treated hemp fabric-reinforced cement nanocomposites".

13th January 2016

To Whom It May Concern

I, Prof. I.M. Low, contributed by project supervision and manuscript editing of the paper/publication entitled

HAKAMY, A., SHAIKH, F.U.A. & LOW, I.M. 2016. Effect of calcined nanoclay on the durability of NaOH treated hemp fabric-reinforced cement nanocomposites. *Materials and Design*, 92, 659-666.

Undertaken with Ahmad Hakamy

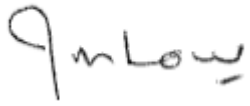

(Signature of Co-Author)

I. M. Low

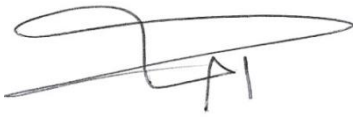

(Signature of First Author)

Ahmad Hakamy

Statement of Contribution of Others for "Effect of calcined nanoclay on the durability of NaOH treated hemp fabric-reinforced cement nanocomposites".

13th January 2016

To Whom It May Concern

I, Dr. Faiz U.A. Shaikh, contributed by project supervision and manuscript editing of the paper/publication entitled

HAKAMY, A., SHAIKH, F.U.A. & LOW, I.M. 2016. Effect of calcined nanoclay on the durability of NaOH treated hemp fabric-reinforced cement nanocomposites. *Materials and Design*, 92, 659-666.

Undertaken with Ahmad Hakamy

(Signature of Co-Author)

Faiz U.A. Shaikh

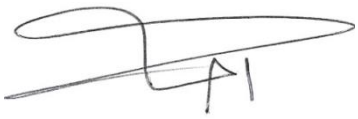

(Signature of First Author)

Ahmad Hakamy

5.2 APPENDIX B

Copyright Forms

5.2.1 Appendix B-1: Elsevier Journal Articles

Copyright information relating to;

HAKAMY, A., SHAIKH, F.U.A. & LOW, I.M. 2013. Microstructures and mechanical properties of hemp fabric reinforced organoclay–cement nanocomposites. *Construction & Building Materials,* 49, 298–307.

ELSEVIER LICENSE
TERMS AND CONDITIONS

Dec 18, 2015

This is a License Agreement between Ahmad Hakamy ("You") and Elsevier ("Elsevier") provided by Copyright Clearance Center ("CCC"). The license consists of your order details, the terms and conditions provided by Elsevier, and the payment terms and conditions.

All payments must be made in full to CCC. For payment instructions, please see information listed at the bottom of this form.

Supplier	Elsevier Limited The Boulevard,Langford Lane Kidlington,Oxford,OX5 1GB,UK
Registered Company Number	1982084
Customer name	Ahmad Hakamy
Customer address	Department of Imaging & Applied Physics Perth, GPO Box U1987
License number	3771860515108
License date	Dec 18, 2015
Licensed content publisher	Elsevier
Licensed content publication	Construction and Building Materials
Licensed content title	Microstructures and mechanical properties of hemp fabric reinforced organoclay–cement nanocomposites
Licensed content author	A. Hakamy,FUA Shaikh,I.M. Low
Licensed content date	December 2013
Licensed content volume number	49
Licensed content issue number	n/a
Number of pages	10
Start Page	298
End Page	307
Type of Use	reuse in a thesis/dissertation
Portion	full article
Format	electronic
Are you the author of this Elsevier article?	Yes
Will you be translating?	No
Title of your thesis/dissertation	Microstructural Design of High Performance Natural Fibre -Nanoclay-Cement Nanocomposites
Expected completion date	Jan 2016

5.2.2 Appendix B-2: Elsevier Journal Articles

Copyright information relating to;

HAKAMY, A., SHAIKH, F.U.A. & LOW, I.M. 2014. Characteristics of hemp fabric reinforced nanoclay–cement nanocomposites. *Cement & Concrete Composites*, 50, 27–35.

ELSEVIER LICENSE
TERMS AND CONDITIONS

Dec 18, 2015

This is a License Agreement between Ahmad Hakamy ("You") and Elsevier ("Elsevier") provided by Copyright Clearance Center ("CCC"). The license consists of your order details, the terms and conditions provided by Elsevier, and the payment terms and conditions.

All payments must be made in full to CCC. For payment instructions, please see information listed at the bottom of this form.

Supplier	Elsevier Limited The Boulevard,Langford Lane Kidlington,Oxford,OX5 1GB,UK
Registered Company Number	1982084
Customer name	Ahmad Hakamy
Customer address	Department of Imaging & Applied Physics Perth, GPO Box U1987
License number	3771871235099
License date	Dec 18, 2015
Licensed content publisher	Elsevier
Licensed content publication	Cement and Concrete Composites
Licensed content title	Characteristics of hemp fabric reinforced nanoclay–cement nanocomposites
Licensed content author	A. Hakamy,F.U.A. Shaikh,I.M. Low
Licensed content date	July 2014
Licensed content volume number	50
Licensed content issue number	n/a
Number of pages	9
Start Page	27
End Page	35
Type of Use	reuse in a thesis/dissertation
Portion	full article
Format	electronic
Are you the author of this Elsevier article?	Yes
Will you be translating?	No
Title of your thesis/dissertation	Microstructural Design of High Performance Natural Fibre -Nanoclay-Cement Nanocomposites
Expected completion date	Jan 2016

5.2.3 Appendix B-3: Elsevier Journal Articles

Copyright information relating to;

HAKAMY, A., SHAIKH, F.U.A. & LOW, I.M. 2015. Characteristics of nanoclay and calcined nanoclay-cement nanocomposites. *Composites Part B: Engineering*, 78, 174-184.

ELSEVIER LICENSE
TERMS AND CONDITIONS

Dec 18, 2015

This is a License Agreement between Ahmad Hakamy ("You") and Elsevier ("Elsevier") provided by Copyright Clearance Center ("CCC"). The license consists of your order details, the terms and conditions provided by Elsevier, and the payment terms and conditions.

All payments must be made in full to CCC. For payment instructions, please see information listed at the bottom of this form.

Supplier	Elsevier Limited The Boulevard,Langford Lane Kidlington,Oxford,OX5 1GB,UK
Registered Company Number	1982084
Customer name	Ahmad Hakamy
Customer address	Department of Imaging & Applied Physics Perth, GPO Box U1987
License number	3771871388188
License date	Dec 18, 2015
Licensed content publisher	Elsevier
Licensed content publication	Composites Part B: Engineering
Licensed content title	Characteristics of nanoclay and calcined nanoclay-cement nanocomposites
Licensed content author	A. Hakamy,F.U.A. Shaikh,I.M. Low
Licensed content date	1 September 2015
Licensed content volume number	78
Licensed content issue number	n/a
Number of pages	11
Start Page	174
End Page	184
Type of Use	reuse in a thesis/dissertation
Intended publisher of new work	other
Portion	full article
Format	electronic
Are you the author of this Elsevier article?	Yes
Will you be translating?	No
Title of your thesis/dissertation	Microstructural Design of High Performance Natural Fibre -Nanoclay-Cement Nanocomposites

5.2.4 Appendix B-4: Elsevier Journal Articles

Copyright information relating to;

HAKAMY, A., SHAIKH, F.U.A. & LOW, I.M. 2015. Effect of calcined nanoclay on microstructural and mechanical properties of chemically treated hemp fabric reinforced cement nanocomposites. *Construction & Building Materials*, 95, 882–891.

ELSEVIER LICENSE
TERMS AND CONDITIONS

Dec 18, 2015

This is a License Agreement between Ahmad Hakamy ("You") and Elsevier ("Elsevier") provided by Copyright Clearance Center ("CCC"). The license consists of your order details, the terms and conditions provided by Elsevier, and the payment terms and conditions.

All payments must be made in full to CCC. For payment instructions, please see information listed at the bottom of this form.

Supplier	Elsevier Limited The Boulevard,Langford Lane Kidlington,Oxford,OX5 1GB,UK
Registered Company Number	1982084
Customer name	Ahmad Hakamy
Customer address	Department of Imaging & Applied Physics Perth, GPO Box U1987
License number	3771871500024
License date	Dec 18, 2015
Licensed content publisher	Elsevier
Licensed content publication	Construction and Building Materials
Licensed content title	Effect of calcined nanoclay on microstructural and mechanical properties of chemically treated hemp fabric-reinforced cement nanocomposites
Licensed content author	A. Hakamy,F.U.A. Shaikh,I.M. Low
Licensed content date	1 October 2015
Licensed content volume number	95
Licensed content issue number	n/a
Number of pages	10
Start Page	882
End Page	891
Type of Use	reuse in a thesis/dissertation
Intended publisher of new work	other
Portion	full article
Format	electronic
Are you the author of this Elsevier article?	Yes
Will you be translating?	No
Title of your	Microstructural Design of High Performance Natural Fibre -Nanoclay-

5.2.5 Appendix B-5: Elsevier Journal Articles

Copyright information relating to;

HAKAMY, A., SHAIKH, F.U.A. & LOW, I.M. 2015. Thermal and mechanical properties of NaOH treated hemp fabric and calcined nanoclay-reinforced cement nanocomposites. *Materials and Design*, 80, 70–81.

ELSEVIER LICENSE
TERMS AND CONDITIONS

Dec 19, 2015

This is a License Agreement between Ahmad Hakamy ("You") and Elsevier ("Elsevier") provided by Copyright Clearance Center ("CCC"). The license consists of your order details, the terms and conditions provided by Elsevier, and the payment terms and conditions.

All payments must be made in full to CCC. For payment instructions, please see information listed at the bottom of this form.

Supplier	Elsevier Limited The Boulevard,Langford Lane Kidlington,Oxford,OX5 1GB,UK
Registered Company Number	1982084
Customer name	Ahmad Hakamy
Customer address	Department of Imaging & Applied Physics Perth, GPO Box U1987
License number	3772370899603
License date	Dec 19, 2015
Licensed content publisher	Elsevier
Licensed content publication	Materials & Design
Licensed content title	Thermal and mechanical properties of NaOH treated hemp fabric and calcined nanoclay-reinforced cement nanocomposites
Licensed content author	A. Hakamy,F.U.A. Shaikh,I.M. Low
Licensed content date	5 September 2015
Licensed content volume number	80
Licensed content issue number	n/a
Number of pages	12
Start Page	70
End Page	81
Type of Use	reuse in a thesis/dissertation
Portion	full article
Format	electronic
Are you the author of this Elsevier article?	Yes
Will you be translating?	No
Title of your thesis/dissertation	Microstructural Design of High Performance Natural Fibre -Nanoclay-Cement Nanocomposites
Expected completion date	Jan 2016

5.2.6 Appendix B-6: Elsevier Journal Articles

Copyright information relating to;

HAKAMY, A., SHAIKH, F.U.A. & LOW, I.M. 2015. Effect of calcined nanoclay on the durability of NaOH treated hemp fabric-reinforced cement nanocomposites. *Materials and Design*, 92, 659-666.

RE: License Agreement with Elsevier for Copyright Forms Elsevier Journal Articles

Samantray, Banita (ELS-CHN) <b.samantray@reedelsevier.com>

Mon 4/01/2016 7:27 AM

To: Ahmad Magbul M Hakamy <a.hakami3@postgrad.curtin.edu.au>;

Dear Dr. Hakamy

My previous email to you guides you regarding your usage of material from *"Effect of calcined nanoclay on the durability of NaOH treated hemp fabric-reinforced cement nanocomposites"*.

Please note that as one of the Authors of this article, you retain the right to include the journal article, in full or in part, in a thesis or dissertation. You do not require permission to do so.

Hence you do not have to open the Rightslink page for securing permission for this article.

Hope this email clarifies your doubt.

Regards

Banita Samantray
Global Rights Department

Elsevier
(A division of Reed Elsevier India Pvt. Ltd.)

Ascendas International Tech Park | Crest Building – 12th Floor | Taramani Road | Taramani | Chennai 600 113 | India
Tel: +91 44 42994667 | Fax: +91 44 42994701
E-mail: b.samantray@reedelsevier.com | url: www.elsevier.com

From: Ahmad Magbul M Hakamy [mailto:a.hakami3@postgrad.curtin.edu.au]
Sent: Monday, January 04, 2016 12:53 PM
To: Samantray, Banita (ELS-CHN)
Subject: Re: License Agreement with Elsevier for Copyright Forms Elsevier Journal Articles

Dear Dr. Samantray

Thanks for your email

But my problem that I could not open Rightslink link (it is close window) for my recent paper as in attachment 1 & 2,
Could you please help me to access to Rightslink link ? and then to get form similar to that in attachment 3

5.2.7 Appendix B-7: Springer Journal Articles

Copyright information relating to;

HAKAMY, A., SHAIKH, F.U.A. & LOW, I.M. 2014. Thermal and mechanical properties of hemp fabric-reinforced nanoclay–cement nanocomposites. *Journal of Materials Science*, 49, 1684–1694.

SPRINGER LICENSE
TERMS AND CONDITIONS

Dec 19, 2015

This is a License Agreement between Ahmad Hakamy ("You") and Springer ("Springer") provided by Copyright Clearance Center ("CCC"). The license consists of your order details, the terms and conditions provided by Springer, and the payment terms and conditions.

All payments must be made in full to CCC. For payment instructions, please see information listed at the bottom of this form.

License Number	3772371486800
License date	Dec 19, 2015
Licensed content publisher	Springer
Licensed content publication	Journal of Materials Science (full set)
Licensed content title	Thermal and mechanical properties of hemp fabric-reinforced nanoclay–cement nanocomposites
Licensed content author	A. Hakamy
Licensed content date	Jan 1, 2013
Volume number	49
Issue number	4
Type of Use	Thesis/Dissertation
Portion	Full text
Number of copies	1
Author of this Springer article	Yes and you are the sole author of the new work
Order reference number	None
Title of your thesis / dissertation	Microstructural Design of High Performance Natural Fibre -Nanoclay-Cement Nanocomposites
Expected completion date	Jan 2016
Estimated size(pages)	300
Total	0.00 USD
Terms and Conditions	

Introduction
The publisher for this copyrighted material is Springer. By clicking "accept" in connection with completing this licensing transaction, you agree that the following terms and conditions apply to this transaction (along with the Billing and Payment terms and conditions established by Copyright Clearance Center, Inc. ("CCC"), at the time that you opened your Rightslink account and that are available at any time at http://myaccount.copyright.com).
Limited License
With reference to your request to reuse material on which Springer controls the copyright, permission is granted for the use indicated in your enquiry under the following conditions:
- Licenses are for one-time use only with a maximum distribution equal to the number stated

6. BIBLIOGRAPHY

ABDEL ALEEM, S., HEIKAL, M. & MORSI, W. M. 2014. Hydration characteristic, thermal expansion and microstructure of cement containing nano-silica. *Construction and Building Materials,* 59**,** 151-160.

ABDEL GAWAD, A., ESAWI, A. M. K. & RAMADAN, A. R. 2010. Structure and properties of nylon 6–clay nanocomposites: effect of temperature and reprocessing. *Journal of Materials Science,* 45**,** 6677-6684.

ABDULLAH, A., JAMALUDIN, S. B., NOOR, M. M. & HUSSIN, K. 2011. Composite cement reinforced coconut fiber: Physical and Mechanical Properties and Fracture Behavior. *Australian Journal of Basic and Applied Sciences,* 5**,** 1228-1240.

AHMED, S. F. U., MAALEJ, M. & PARAMASIVAM, P. 2007. Flexural responses of hybrid steel–polyethylene fiber reinforced cement composites containing high volume fly ash. *Construction and Building Materials,* 21**,** 1088-1097.

AKIL, H. M., OMAR, M. F., MAZUKI, A. A. M., SAFIEE, S., ISHAK, Z. A. M. & ABU BAKAR, A. 2011. Kenaf fiber reinforced composites: A review. *Materials & Design,* 32**,** 4107-4121.

AL-MISHHADANI, S. A., IBRAHEM, A. M. & NAJI, Z. H. 2013. The effect of nano metakaolin material on some properties of concrete. *Diyala Journal of Engineering Sciences,* 6**,** 50-61.

AL-SALAMI, A. E., MORSY, M. S., TAHA, S. & SHOUKRY, H. 2013. Physico-mechanical characteristics of blended white cement pastes containing thermally activated ultrafine nano clays. *Construction and Building Materials,* 47**,** 138-145.

ALAMRI, H., LOW, I. M. & ALOTHMAN, Z. 2012. Mechanical, thermal and microstructural characteristics of cellulose fibre reinforced epoxy/organoclay nanocomposites. *Composites Part B: Engineering,* 43**,** 2762-2771.

ALHUTHALI, A., LOW, I. M. & DONG, C. 2012. Characterisation of the water absorption, mechanical and thermal properties of recycled cellulose fibre reinforced vinyl-ester eco-nanocomposites. *Composites Part B: Engineering,* 43**,** 2772-2781.

ALI, M., LIU, A., SOU, H. & CHOUW, N. 2012. Mechanical and dynamic properties of coconut fibre reinforced concrete. *Construction and Building Materials,* 30**,** 814-825.

ALIX, S., PHILIPPE, E., BESSADOK, A., LEBRUN, L., MORVAN, C. & MARAIS, S. 2009. Effect of chemical treatments on water sorption and mechanical properties of flax fibres. *Bioresour Technol,* 100**,** 4742-9.

ALMEIDA, A. E. F. S., TONOLI, G. H. D., SANTOS, S. F. & SAVASTANO, H. 2013. Improved durability of vegetable fiber reinforced cement composite subject to accelerated carbonation at early age. *Cement and Concrete Composites,* 42**,** 49-58.

ALY, M., HASHMI, M. S. J., OLABI, A. G., MESSEIRY, M., ABADIR, E. F. & HUSSAIN, A. I. 2012. Effect of colloidal nano-silica on the mechanical and physical behaviour of waste-glass cement mortar. *Materials & Design,* 33**,** 127-135.

ALY, M., HASHMI, M. S. J., OLABI, A. G., MESSEIRY, M. & HUSSAIN, A. I. 2011a. Effect of nano clay particles on mechanical, thermal and physical behaviours of waste-glass cement mortars. *Materials Science and Engineering: A,* 528**,** 7991-7998.

ALY, M., HASHMI, M. S. J., OLABI, A. G., MESSEIRY, M., HUSSAIN, A. I. & ABADIR, E. F. 2011b. Effect of nano-clay and waste glass powder on the properties of flax fibre reinforced mortar. *Journal of Engineering and Applied Sciences,* 6**,** 19-28.

AMIRI, R.-S. N., QAZVINI, N. T. & SANJANI, N. S. 2009. Water Expandable Polystyrene-Organoclay Nanocomposites: Role of Clay and Its Dispersion State. *Journal of Macromolecular Science, Part B,* 48**,** 955-966.

ANTONOVIČ, V., PUNDIENE, I., STONYS, R., ČESNIENE, J. & KERIENE, J. 2010. A review of the possible applications of nanotechnology in refractory concrete. *Journal of Civil Engineering and Management,* 16**,** 595-602.

ARDANUY, M., CLARAMUNT, J. & TOLEDO FILHO, R. D. 2015. Cellulosic fiber reinforced cement-based composites: A review of recent research. *Construction and Building Materials,* 79**,** 115-128.

ASASUTJARIT, C., HIRUNLABH, J., KHEDARI, J., CHAROENVAI, S., ZEGHMATI, B. & SHIN, U. C. 2007. Development of coconut coir-based lightweight cement board. *Construction and Building Materials,* 21**,** 277-288.

ASPRONE, D., DURANTE, M., PROTA, A. & MANFREDI, G. 2011. Potential of structural pozzolanic matrix–hemp fiber grid composites. *Construction and Building Materials,* 25**,** 2867-2874.

AWWAD, E., MABSOUT, M., HAMAD, B., FARRAN, M. T. & KHATIB, H. 2012. Studies on fiber-reinforced concrete using industrial hemp fibers. *Construction and Building Materials,* 35**,** 710-717.

AZIZ, S. H. & ANSELL, M. P. 2004. The effect of alkalization and fibre alignment on the mechanical and thermal properties of kenaf and hemp bast fibre composites: Part 1 – polyester resin matrix. *Composites Science and Technology,* 64**,** 1219-1230.

BALAGURU, P. N. & SHAH, S. P. 1992. *Fiber-reinforced cement composites,* USA, McGraw-Hill, Inc.

BARBHUIYA, S., CHOW, P. & MEMON, S. 2015. Microstructure, hydration and nanomechanical properties of concrete containing metakaolin. *Construction and Building Materials,* 95**,** 696-702.

BECKERMANN, G. W. & PICKERING, K. L. 2008. Engineering and evaluation of hemp fibre reinforced polypropylene composites: Fibre treatment and matrix modification. *Composites Part A: Applied Science and Manufacturing,* 39**,** 979-988.

BENDAPUDI, S. C. K. 2011. Contribution of fly ash to the properties of mortar and concrete. *International Journal of Earth Sciences and Engineering,* 4**,** 1017-1023.

BENTCHIKOU, M., GUIDOUM, A., SCRIVENER, K., SILHADI, K. & HANINI, S. 2012. Effect of recycled cellulose fibres on the properties of lightweight cement composite matrix. *Construction and Building Materials,* 34**,** 451-456.

BENTUR, A. & MINDESS, S. 2007. *Fibre Reinforced Cementitious Composites,* New York, Taylor & Francis

BENTUR, A., YARDıMCı, M. Y. & TIROSH, R. 2013. Preservation of telescopic bonding upon aging of bundled glass filaments by treatments with nano-particles. *Cement and Concrete Research,* 47**,** 69-77.

BEZERRA, E. M., JOAQUIM, A. P., SAVASTANO, H., JOHN, V. M. & AGOPYAN, V. 2006. The effect of different mineral additions and synthetic fiber contents on properties of cement based composites. *Cement and Concrete Composites,* 28**,** 555-563.

BISMARCK, A., ARANBERRI-ASKARGORTA, I. & SPRINGER, J. 2002. Surface Characterization of Flax, Hemp and Cellulose Fibers; Surface Properties and the Water Uptake Behavior. *POLYMER COMPOSITES,* 23**,** 872-894.

BLANKENHORN, P. R., BLANKENHORN, B. D., SILSBEE, M. R. & DICOLA, M. 2001. Effects of fiber surface treatments on mechanical properties of wood fiber–cement composites. *Cement and Concrete Research* 31**,** 1049-1055.

BOTANA, A., MOLLO, M., EISENBERG, P. & TORRES SANCHEZ, R. M. 2010. Effect of modified montmorillonite on biodegradable PHB nanocomposites. *Applied Clay Science,* 47**,** 263-270.

CALLISTER, W. D. 2007. *Materials science and engineering an introduction,* New York, John Wiley & Sons, Inc.

CAMILETTI, J., SOLIMAN, A. M. & NEHDI, M. L. 2012. Effects of nano- and micro-limestone addition on early-age properties of ultra-high-performance concrete. *Materials and Structures,* 46**,** 881-898.

CAMPILLO, I., GUERRERO, A., DOLADO, J. S., PORRO, A., IBÁÑEZ, J. A. & GOÑI, S. 2007. Improvement of initial mechanical strength by nanoalumina in belite cements. *Materials Letters,* 61**,** 1889-1892.

CHAIPANICH, A., NOCHAIYA, T., WONGKEO, W. & TORKITTIKUL, P. 2010. Compressive strength and microstructure of carbon nanotubes–fly ash cement composites. *Materials Science and Engineering: A,* 527**,** 1063-1067.

CHANG, T.-P., SHIH, J.-Y., YANG, K.-M. & HSIAO, T.-C. 2007. Material properties of portland cement paste with nano-montmorillonite. *Journal of Materials Science,* 42**,** 7478-7487.

CHEN, J., KOU, S.-C. & POON, C.-S. 2012. Hydration and properties of nano-TiO_2 blended cement composites. *Cement and Concrete Composites,* 34**,** 642-649.

CHOUDALAKIS, G. & GOTSIS, A. D. 2009. Permeability of polymer/clay nanocomposites: A review. *European Polymer Journal,* 45**,** 967-984.

COUTTS, R. S. P. 2005. A review of Australian research into natural fibre cement composites. *Cement and Concrete Composites,* 27**,** 518-526.

CWIRZEN, A., HABERMEHL-CWIRZEN, K., NASIBULIN, A. G., KAUPINEN, E. I., MUDIMELA, P. R. & PENTTALA, V. 2009. SEM/AFM studies of cementitious binder modified by MWCNT and nano-sized Fe needles. *Materials Characterization,* 60**,** 735-740.

DE GUTIÉRREZ, R. M., DÍAZ, L. N. & DELVASTO, S. 2005. Effect of pozzolans on the performance of fiber-reinforced mortars. *Cement and Concrete Composites,* 27**,** 593-598.

DE ROSA, I. M., SANTULLI, C. & SARASINI, F. 2010. Mechanical and thermal characterization of epoxy composites reinforced with random and quasi-

unidirectional untreated Phormium tenax leaf fibers. *Materials & Design,* 31**,** 2397-2405.
DEMIR, H., ATIKLER, U., BALKÖSE, D. & TıHMıNLıOĞLU, F. 2006. The effect of fiber surface treatments on the tensile and water sorption properties of polypropylene–luffa fiber composites. *Composites Part A: Applied Science and Manufacturing,* 37**,** 447-456.
ELSAID, A., DAWOOD, M., SERACINO, R. & BOBKO, C. 2011. Mechanical properties of kenaf fiber reinforced concrete. *Construction and Building Materials,* 25**,** 1991-2001.
FARZADNIA, N., ABANG ALI, A. A., DEMIRBOGA, R. & ANWAR, M. P. 2013. Effect of halloysite nanoclay on mechanical properties, thermal behavior and microstructure of cement mortars. *Cement and Concrete Research,* 48**,** 97-104.
FERNANDEZ, R., MARTIRENA, F. & SCRIVENER, K. L. 2011. The origin of the pozzolanic activity of calcined clay minerals: A comparison between kaolinite, illite and montmorillonite. *Cement and Concrete Research,* 41**,** 113-122.
FILIPPI, S., PACI, M., POLACCO, G., DINTCHEVA, N. T. & MAGAGNINI, P. 2011. On the interlayer spacing collapse of Cloisite® 30B organoclay. *Polymer Degradation and Stability,* 96**,** 823-832.
FLATT, R. J., ROUSSEL, N. & CHEESEMAN, C. R. 2012. Concrete: An eco material that needs to be improved. *Journal of the European Ceramic Society,* 32**,** 2787-2798.
GARG, N. & SKIBSTED, J. 2014. Thermal Activation of a Pure Montmorillonite Clay and Its Reactivity in Cementitious Systems. *The Journal of Physical Chemistry C,* 118**,** 11464-11477.
GHASEMI, A. M. R., PARHIZKAR, T. & RAMEZANIANPOUR, A. A. 2010. Influence of colloidal nano-SiO_2 addition as silica fume replacement material in properties of concrete. *Second Inernational Conference on Sustaiable Construction Materials and Technologies.* Ancona, Italy.
GIVI, A. N., RASHID, S. A., AZIZ, F. N. A. & SALLEH, M. A. M. 2010. Investigations on the development of the permeability properties of binary blended concrete with nano-SiO_2 particles. *Journal of Composite Materials,* 45**,** 1931-1938.
GOVINDARAJAN, D. & GOPALAKRISHNAN, R. 2012. Spectroscopic Studies on Indian Portland Cement hydrated with distilled water and sea water. *Frontiers in Science,* 1**,** 21-27.
HAMZAOUI, R., GUESSASMA, S., MECHERI, B., ESHTIAGHI, A. M. & BENNABI, A. 2014. Microstructure and mechanical performance of modified mortar using hemp fibres and carbon nanotubes. *Materials & Design,* 56**,** 60-68.
HAN, B., SUN, S., DING, S., ZHANG, L., YU, X. & OU, J. 2015. Review of nanocarbon-engineered multifunctional cementitious composites. *Composites Part A: Applied Science and Manufacturing,* 70**,** 69-81.
HANUS, M. J. & HARRIS, A. T. 2013. Nanotechnology innovations for the construction industry. *Progress in Materials Science,* 58**,** 1056-1102.
HE, C., MAKOVICKY, E. & OSBAECK, B. 1996. Thermal treatment and pozzolanic activity of Na and Ca-montmorillonite. *Applied Clay Science,* 10**,** 351-368.

HE, X. & SHI, X. 2008. Chloride permeability and microstructure of Portland cement mortars incorporating nanomaterials. *Transportation Research Record: Journal of the Transportation Research Board,* 2070**,** 13-21.
HEIKAL, M., ABD EL ALEEM, S. & MORSI, W. M. 2013. Characteristics of blended cements containing nano-silica. *HBRC Journal,* 9**,** 243-255.
HOSSEINI, P., HOSSEINPOURPIA, R., PAJUM, A., KHODAVIRDI, M. M., IZADI, H. & VAEZI, A. 2014a. Effect of nano-particles and aminosilane interaction on the performances of cement-based composites: An experimental study. *Construction and Building Materials,* 66**,** 113-124.
HOSSEINI, S. B., HEDJAZI, S., JAMALIRAD, L. & SUKHTESARAIE, A. 2014b. Effect of nano-SiO_2 on physical and mechanical properties of fiber reinforced composites (FRCs). *Journal of the Indian Academy of Wood Science,* 11**,** 116-121.
HOU, P., KAWASHIMA, S., KONG, D., CORR, D. J., QIAN, J. & SHAH, S. P. 2013. Modification effects of colloidal nanoSiO_2 on cement hydration and its gel property. *Composites Part B: Engineering,* 45**,** 440-448.
HU, Y., LUO, D., LI, P., LI, Q. & SUN, G. 2014. Fracture toughness enhancement of cement paste with multi-walled carbon nanotubes. *Construction and Building Materials,* 70**,** 332-338.
HUSSAIN, F., HOJJATI, M., OKAMOTO, M. & GORGA, R. E. 2006. Review article: Polymer-matrix nanocomposites, processing, manufacturing, and application: An overview. *Journal of Composite Materials,* 40**,** 1511-1575.
ISLAM, S. M., HUSSAIN, R. R. & MORSHED, M. A. Z. 2011. Fiber-reinforced concrete incorporating locally available natural fibers in normal- and high-strength concrete and a performance analysis with steel fiber-reinforced composite concrete. *Journal of Composite Materials,* 46**,** 111-122.
JARABO, R., FUENTE, E., MONTE, M. C., SAVASTANO, H., MUTJÉ, P. & NEGRO, C. 2012. Use of cellulose fibers from hemp core in fiber-cement production. Effect on flocculation, retention, drainage and product properties. *Industrial Crops and Products,* 39**,** 89-96.
JO, B.-W., KIM, C.-H., TAE, G.-H. & PARK, J.-B. 2007. Characteristics of cement mortar with nano-SiO_2 particles. *Construction and Building Materials,* 21**,** 1351-1355.
JO, B.-W., PARK, S.-K. & KIM, D.-K. 2008. Mechanical properties of nano-MMT reinforced polymer composite and polymer concrete. *Construction and Building Materials,* 22**,** 14-20.
JOHN, M. & THOMAS, S. 2008. Biofibres and biocomposites. *Carbohydrate Polymers,* 71**,** 343-364.
JUÁREZ, C., DURÁN, A., VALDEZ, P. & FAJARDO, G. 2007. Performance of "Agave lecheguilla" natural fiber in portland cement composites exposed to severe environment conditions. *Building and Environment,* 42**,** 1151-1157.
JUENGER, M. C. G. & SIDDIQUE, R. 2015. Recent advances in understanding the role of supplementary cementitious materials in concrete. *Cement and Concrete Research,* 78**,** 71-80.
KAWASHIMA, S., HOU, P., CORR, D. J. & SHAH, S. P. 2013. Modification of cement-based materials with nanoparticles. *Cement and Concrete Composites,* 36**,** 8-15.

KHORAMI, M. & GANJIAN, E. 2011. Comparing flexural behaviour of fibre–cement composites reinforced bagasse: Wheat and eucalyptus. *Construction and Building Materials,* 25**,** 3661-3667.

KILIARIS, P. & PAPASPYRIDES, C. D. 2010. Polymer/layered silicate (clay) nanocomposites: An overview of flame retardancy. *Progress in Polymer Science,* 35**,** 902-958.

KIM, H. K., NAM, I. W. & LEE, H. K. 2014. Enhanced effect of carbon nanotube on mechanical and electrical properties of cement composites by incorporation of silica fume. *Composite Structures,* 107**,** 60-69.

KONSTA-GDOUTOS, M. S., METAXA, Z. S. & SHAH, S. P. 2010. Multi-scale mechanical and fracture characteristics and early-age strain capacity of high performance carbon nanotube/cement nanocomposites. *Cement and Concrete Composites,* 32**,** 110-115.

KRIKER, A., BALI, A., DEBICKI, G., BOUZIANE, M. & CHABANNET, M. 2008. Durability of date palm fibres and their use as reinforcement in hot dry climates. *Cement and Concrete Composites,* 30**,** 639-648.

KUO, W.-Y., HUANG, J.-S. & LIN, C.-H. 2006. Effects of organo-modified montmorillonite on strengths and permeability of cement mortars. *Cement and Concrete Research,* 36**,** 886-895.

KWAN, W. H., RAMLI, M. & CHEAH, C. B. 2014. Flexural strength and impact resistance study of fibre reinforced concrete in simulated aggressive environment. *Construction and Building Materials,* 63**,** 62-71.

LE TROEDEC, M., DALMAY, P., PATAPY, C., PEYRATOUT, C., SMITH, A. & CHOTARD, T. 2011a. Mechanical properties of hemp-lime reinforced mortars: influence of the chemical treatment of fibers. *Journal of Composite Materials,* 45**,** 2347-2357.

LE TROËDEC, M., PEYRATOUT, C. S., SMITH, A. & CHOTARD, T. 2009. Influence of various chemical treatments on the interactions between hemp fibres and a lime matrix. *Journal of the European Ceramic Society,* 29**,** 1861-1868.

LE TROEDEC, M., RACHINI, A., PEYRATOUT, C., ROSSIGNOL, S., MAX, E., KAFTAN, O., FERY, A. & SMITH, A. 2011b. Influence of chemical treatments on adhesion properties of hemp fibres. *Journal of Colloid and Interface Science,* 356**,** 303-10.

LE TROEDEC, M., SEDAN, D., PEYRATOUT, C., BONNET, J. P., SMITH, A., GUINEBRETIERE, R., GLOAGUEN, V. & KRAUSZ, P. 2008. Influence of various chemical treatments on the composition and structure of hemp fibres. *Composites Part A: Applied Science and Manufacturing,* 39**,** 514-522.

LEE, S.-J. & WON, J.-P. 2015. Interfacial phenomena in structural polymeric nano-clay synthetic fiber reinforced cementitious composites. *Composite Structures,* 133**,** 62-69.

LI, G. 2004. Properties of high-volume fly ash concrete incorporating nano-SiO_2. *Cement and Concrete Research,* 34**,** 1043-1049.

LI, G. Y., WANG, P. M. & ZHAO, X. 2005. Mechanical behavior and microstructure of cement composites incorporating surface-treated multi-walled carbon nanotubes. *Carbon,* 43**,** 1239-1245.

LI, G. Y., WANG, P. M. & ZHAO, X. 2007a. Pressure-sensitive properties and microstructure of carbon nanotube reinforced cement composites. *Cement and Concrete Composites,* 29**,** 377-382.
LI, H., XIAO, H.-G. & OU, J.-P. 2004a. A study on mechanical and pressure-sensitive properties of cement mortar with nanophase materials. *Cement and Concrete Research,* 34**,** 435-438.
LI, H., XIAO, H.-G., YUAN, J. & OU, J. 2004b. Microstructure of cement mortar with nano-particles. *Composites Part B: Engineering,* 35**,** 185-189.
LI, H., ZHANG, M.-H. & OU, J.-P. 2006a. Abrasion resistance of concrete containing nano-particles for pavement. *Wear,* 260**,** 1262-1266.
LI, H., ZHANG, M.-H. & OU, J.-P. 2007b. Flexural fatigue performance of concrete containing nano-particles for pavement. *International Journal of Fatigue,* 29**,** 1292-1301.
LI, W., HUANG, Z., CAO, F., SUN, Z. & SHAH, S. P. 2015a. Effects of nano-silica and nano-limestone on flowability and mechanical properties of ultra-high-performance concrete matrix. *Construction and Building Materials,* 95**,** 366-374.
LI, W., HUANG, Z., ZU, T., SHI, C., DUAN, W. H. & SHAH, S. P. 2015b. Influence of nanolimestone on the hydration, mechanical strength, and autogenous shrinkage of ultrahigh-performance concrete. *Journal of Materials in Civil Engineering,* doi: 10.1061/(asce)mt.1943-5533.0001327.
LI, X., TABIL, L. G. & PANIGRAHI, S. 2007c. Chemical treatments of natural fiber for use in natural fiber-reinforced composites: A Review. *Journal of Polymers and the Environment,* 15**,** 25-33.
LI , Y., MAI, Y.-W. & YE, L. 2000. Australia-Sisal fibre and its composites: a review of recent developments. *Composites Science and Technology,* 60**,** 2037-2055.
LI, Z., WANG, H., HE, S., LU, Y. & WANG, M. 2006b. Investigations on the preparation and mechanical properties of the nano-alumina reinforced cement composite. *Materials Letters,* 60**,** 356-359.
LI, Z., WANG, L. & WANG, X. 2004c. Compressive and Flexural Properties of Hemp Fiber Reinforced Concrete. *Fibers and Polymers,* 5**,** 187-197.
LI, Z., WANG, X. & WANG, L. 2006c. Properties of hemp fibre reinforced concrete composites. *Composites Part A: Applied Science and Manufacturing,* 37**,** 497-505.
LIU, X., CHEN, L., LIU, A. & WANG, X. 2012. Effect of Nano-$CaCO_3$ on Properties of Cement Paste. *Energy Procedia,* 16**,** 991-996.
LOW, I. M., SOMERS, J., KHO, H. S., DAVIES, I. J. & LATELLA, B. A. 2006. Fabrication and Properties of Recycled Cellulose Fibre-Reinforced Epoxy Composites. *Composite Interfaces,* 16**,** 659-669.
MAHESWARAN, S., BHUVANESHWARI, B., PALANI, G. S., NAGESH, R. I. & KALAISELVAM, S. 2013. An Overview on the Influence of Nano Silica in Concrete and a Research Initiative. *Research Journal of Recent Sciences,* 2**,** 17-24.
MAKAR, J. M., BEAUDOIN, J. J., TORRES, F., CHAN, G. W. & TRISCHUK, K. 2012. Effect of n-CaCO3 and metakaolin on hydrated Portland cement. *Advances in Cement Research,* 24**,** 211-219.
MAKAR, J. M., MARGESON, J. C. & LUH, J. 2005. Carbon nanotube cement composites - early results and potential applications. *3rd International Conference*

on Construction Materials: Performance, Innovations and Structural Implications. Vancouver, Canada.

MAMULOVA KUTLAKOVA, K., TOKARSKY, J., KOVAR, P., VOJTESKOVA, S., KOVAROVA, A., SMETANA, B., KUKUTSCHOVA, J., CAPKOVA, P. & MATEJKA, V. 2011. Preparation and characterization of photoactive composite kaolinite/TiO_2. *J Hazard Mater,* 188**,** 212-20.

MANSUR, M. A. & AZIZF, M. A. 1982. A study of jute fibre reinforced Cement composites. *The International Journal of Cement Composites and Lightweight Concrete,* 4**,** 75-82.

MATĚJKA, V., MATĚJKOVÁ, P., KOVÁŘ, P., VLČEK, J., PŘIKRYL, J., ČERVENKA, P., LACNÝ, Z. & KUKUTSCHOVÁ, J. 2012. Metakaolinite/TiO2 composite: Photoactive admixture for building materials based on Portland cement binder. *Construction and Building Materials,* 35**,** 38-44.

MELO FILHO, J. D. A., SILVA, F. D. A. & TOLEDO FILHO, R. D. 2013. Degradation kinetics and aging mechanisms on sisal fiber cement composite systems. *Cement and Concrete Composites,* 40**,** 30-39.

MENDES, T. M., HOTZA, D. & REPETTE, W. L. 2015. Nanoparticles in cement based materials: a review. *Reviews on Advanced Materials Science,* 40**,** 89-96.

MENG, T., YU, Y., QIAN, X., ZHAN, S. & QIAN, K. 2012. Effect of nano-TiO_2 on the mechanical properties of cement mortar. *Construction and Building Materials,* 29**,** 241-245.

MISNON, M. I., ISLAM, M. M., EPAARACHCHI, J. A. & LAU, K. T. 2015. Analyses of woven hemp fabric characteristics for composite reinforcement. *Materials & Design,* 66**,** 82-92.

MITTAL, A., KATAHIRA, R., HIMMEL, M. E. & JOHNSON, D. K. 2011. Effects of alkaline or liquid-ammonia treatment on crystalline cellulose: changes in crystalline structure and effects on enzymatic digestibility. *Biotechnol Biofuels,* 4**,** 41.

MOBASHER, B., PELED, A. & PAHILAJANI, J. 2006. Distributed cracking and stiffness degradation in fabric-cement composites. *Materials and Structures,* 39**,** 317-331.

MOHR, B. J., BIERNACKI, J. J. & KURTIS, K. E. 2006. Microstructural and chemical effects of wet/dry cycling on pulp fiber–cement composites. *Cement and Concrete Research,* 36**,** 1240-1251.

MOHR, B. J., BIERNACKI, J. J. & KURTIS, K. E. 2007. Supplementary cementitious materials for mitigating degradation of kraft pulp fiber-cement composites. *Cement and Concrete Research,* 37**,** 1531-1543.

MOHR, B. J., NANKO, H. & KURTIS, K. E. 2005a. Durability of kraft pulp fiber–cement composites to wet/dry cycling. *Cement and Concrete Composites,* 27**,** 435-448.

MOHR, B. J., NANKO, H. & KURTIS, K. E. 2005b. Durability of thermomechanical pulp fiber-cement composites to wet/dry cycling. *Cement and Concrete Research,* 35**,** 1646-1649.

MORSY, M. S. & AGLAN, H. A. 2007. Development and characterization of nanostructured-perlite-cementitious surface compounds. *Journal of Materials Science,* 42**,** 10188-10195.

MORSY, M. S., AGLAN, H. A. & ABD EL RAZEK, M. M. 2009. Nanostructured zonolite–cementitious surface compounds for thermal insulation. *Construction and Building Materials,* 23**,** 515-521.
MORSY, M. S., ALSAYED, S. H. & AQEL, M. 2010. Effect of nano-clay on mechanical properties. *International Journal of Civil & Environmental Engineering,* 10**,** 23-27.
MUSSO, S., TULLIANI, J.-M., FERRO, G. & TAGLIAFERRO, A. 2009. Influence of carbon nanotubes structure on the mechanical behavior of cement composites. *Composites Science and Technology,* 69**,** 1985-1990.
MWAIKAMBO, L. Y. 2009. Tensile properties of alkalised jute fibres. *BioResources,* 4**,** 566-588.
MWAIKAMBO, L. Y. & ANSELL, M. P. 2002. Chemical modification of hemp, sisal, jute, and kapok fibers by alkalization. *Journal of Applied Polymer Science,* 84**,** 2222-2234.
NAZARI, A. 2010. The effects of curing medium on flexural strength and water permeability of concrete incorporating TiO_2 nanoparticles. *Materials and Structures,* 44**,** 773-786.
NAZARI, A. & RIAHI, S. 2010a. Assessment of the effects of Fe_2O_3 nanoparticles on water permeability, workability, and setting time of concrete. *Journal of Composite Materials,* 45**,** 923-930.
NAZARI, A. & RIAHI, S. 2010b. Microstructural, thermal, physical and mechanical behavior of the self compacting concrete containing SiO_2 nanoparticles. *Materials Science and Engineering: A,* 527**,** 7663-7672.
NAZARI, A. & RIAHI, S. 2011a. The effects of zinc dioxide nanoparticles on flexural strength of self-compacting concrete. *Composites Part B: Engineering,* 42**,** 167-175.
NAZARI, A. & RIAHI, S. 2011b. Splitting tensile strength of concrete using ground granulated blast furnace slag and SiO_2 nanoparticles as binder. *Energy and Buildings,* 43**,** 864-872.
NAZARI, A. & RIAHI, S. 2011c. TiO_2 nanoparticles' effects on properties of concrete using ground granulated blast furnace slag as binder. *Science China Technological Sciences,* 54**,** 3109-3118.
NAZARI, A. & RIAHI, S. 2012. The effects of ZrO_2 nanoparticles on properties of concrete using ground granulated blast furnace slag as binder. *Journal of Composite Materials,* 46**,** 1079-1090.
NAZARI, A., RIAHI, S., RIAHI, S., SHAMEKHI, S. F. & KHADEMNO, A. 2010a. Benefits of Fe2O3 nanoparticles in concrete mixing matrix. *Journal of American Science,* 6**,** 102-105.
NAZARI, A., RIAHI, S., RIAHI, S., SHAMEKHI, S. F. & KHADEMNO, A. 2010b. Influence of Al_2O_3 nanoparticles on the compressive strength and workability of blended concrete. *Journal of American Science,* 6**,** 6-9.
NEVILLE, A. M. 2011. *Properties of Concrete,* England, Pearson Education Limited.
NIK, A. S. & OMRAN, O. L. 2013. Estimation of compressive strength of self-compacted concrete with fibers consisting nano-SiO_2 using ultrasonic pulse velocity. *Construction and Building Materials,* 44**,** 654-662.

NOCHAIYA, T. & CHAIPANICH, A. 2011. Behavior of multi-walled carbon nanotubes on the porosity and microstructure of cement-based materials. *Applied Surface Science,* 257**,** 1941-1945.

OUAJAI, S. & SHANKS, R. A. 2005. Composition, structure and thermal degradation of hemp cellulose after chemical treatments. *Polymer Degradation and Stability,* 89**,** 327-335.

PACHECO-TORGAL, F. & JALALI, S. 2011a. Cementitious building materials reinforced with vegetable fibres: A review. *Construction and Building Materials,* 25**,** 575-581.

PACHECO-TORGAL, F. & JALALI, S. 2011b. Nanotechnology: Advantages and drawbacks in the field of construction and building materials. *Construction and Building Materials,* 25**,** 582-590.

PALUVAI, N. R., MOHANTY, S. & NAYAK, S. 2015. Mechanical and thermal properties of sisal fiber reinforced acrylated epoxidized castor oil toughened diglycidyl ether of bisphenol A epoxy nanocomposites. *Journal of Reinforced Plastics and Composites,* 34**,** 1476-1490.

PARVEEN, S., RANA, S. & FANGUEIRO, R. 2013. A Review on Nanomaterial Dispersion, Microstructure, and Mechanical Properties of Carbon Nanotube and Nanofiber Reinforced Cementitious Composites. *Journal of Nanomaterials,* 2013**,** 1-19.

PARVEEN, S., RANA, S., FANGUEIRO, R. & PAIVA, M. C. 2015. Microstructure and mechanical properties of carbon nanotube reinforced cementitious composites developed using a novel dispersion technique. *Cement and Concrete Research,* 73**,** 215-227.

PAVLIDOU, S. & PAPASPYRIDES, C. D. 2008. A review on polymer–layered silicate nanocomposites. *Progress in Polymer Science,* 33**,** 1119-1198.

PELED, A. & BENTUR, A. 2000. Geometrical characteristics and efficiency of textile fabrics. *Cement and Concrete Research,* 30**,** 781-790.

PELED, A., SUEKI, S. & MOBASHER, B. 2006. Bonding in fabric–cement systems: Effects of fabrication methods. *Cement and Concrete Research,* 36**,** 1661-1671.

QING, Y., ZENAN, Z., DEYU, K. & RONGSHEN, C. 2007. Influence of nano-SiO_2 addition on properties of hardened cement paste as compared with silica fume. *Construction and Building Materials,* 21**,** 539-545.

QUANJI, Z., LOMBOY, G. R. & WANG, K. 2014. Influence of nano-sized highly purified magnesium alumino silicate clay on thixotropic behavior of fresh cement pastes. *Construction and Building Materials,* 69**,** 295-300.

RACHINI, A., LE TROEDEC, M., PEYRATOUT, C. & SMITH, A. 2009. Comparison of the thermal degradation of natural, alkali-treated and silane-treated hemp fibers under air and an inert atmosphere. *Journal of Applied Polymer Science,* 112**,** 226-234.

RAKI, L., BEAUDOIN, J., ALIZADEH, R., MAKAR, J. & SATO, T. 2010. Cement and Concrete Nanoscience and Nanotechnology. *Materials,* 3**,** 918-942.

RAMAKRISHNA, G. & SUNDARARAJAN, T. 2005. Studies on the durability of natural fibres and the effect of corroded fibres on the strength of mortar. *Cement and Concrete Composites,* 27**,** 575-582.

RAMAKRISHNA, G., SUNDARARAJAN, T. & KOTHANDARAMAN, S. 2010. Evaluation of durability of natural fibre reinforced cement mortar composite- a new approach. *Journal of Engineering and Applied Sciences,* 5**,** 44-51.

RASHAD, A. M. 2013. A synopsis about the effect of nano-Al_2O_3, nano-Fe_2O_3, nano-Fe_3O_4 and nano-clay on some properties of cementitious materials – A short guide for Civil Engineer. *Materials & Design,* 52**,** 143-157.

RATHI, V. R. & MODHERA, C. D. 2014. Experimental study on effect of Colloidal Nano SiO_2 and Fly Ash addition on properties of cement mortar. *International Journal of Advanced Structures and Geotechnical Engineering,* 3**,** 261-264.

RAY, D., SARKAR, B. K., RANA, A. K. & BOSE, N. R. 2001. Effect of alkali treated jute fibres on composite properties. *Bulletin of Materials Science,* 24**,** 129-135.

RAZAK, H. A. & FERDIANSYAH, T. 2005. Toughness Characteristics of Arenga pinnata fibre Concrete. *Journal of Natural Fibers,* 2**,** 89-103.

ROMA, L. C., MARTELLO, L. S. & SAVASTANO, H. 2008. Evaluation of mechanical, physical and thermal performance of cement-based tiles reinforced with vegetable fibers. *Construction and Building Materials,* 22**,** 668-674.

RONG, Z., SUN, W., XIAO, H. & JIANG, G. 2015. Effects of nano-SiO_2 particles on the mechanical and microstructural properties of ultra-high performance cementitious composites. *Cement and Concrete Composites,* 56**,** 25-31.

SABA, N., TAHIR, P. & JAWAID, M. 2014. A Review on Potentiality of nano filler/natural fiber filled polymer hybrid composites. *Polymers,* 6**,** 2247-2273.

SABIR, B. B., WILD, S. & BAI, J. 2001. Metakaolin and calcined clays as pozzolans for concrete: a review. *Cement & Concrete Composites,* 23**,** 441-454.

SALEMI, N. & BEHFARNIA, K. 2013. Effect of nano-particles on durability of fiber-reinforced concrete pavement. *Construction and Building Materials,* 48**,** 934-941.

SANCHEZ, F. & SOBOLEV, K. 2010. Nanotechnology in concrete – A review. *Construction and Building Materials,* 24**,** 2060-2071.

SANTOS, S. F., TONOLI, G. H. D., MEJIA, J. E. B., FIORELLI, J. & SAVASTANO JR, H. 2015. Non-conventional cement-based composites reinforced with vegetable fibers: A review of strategies to improve durability. *Materiales de Construcción,* 65**,** doi.org/10.3989/mc.2015.05514

SATO, T. & BEAUDOIN, J. J. 2010. Effect of nano-$CaCO_3$ on hydration of cement containing supplementary cementitious materials. *Advances in Cement Research,* 23**,** 1-29.

SAVASTANO, H., SANTOS, S. F., RADONJIC, M. & SOBOYEJO, W. O. 2009. Fracture and fatigue of natural fiber-reinforced cementitious composites. *Cement and Concrete Composites,* 31**,** 232-243.

SAVASTANO, H., WARDEN, P. G. & COUTTS, R. S. P. 2003. Mechanically pulped sisal as reinforcement in cementitious matrices. *Cement & Concrete Composites,* 25**,** 311-319.

SAWPAN, M. A., PICKERING, K. L. & FERNYHOUGH, A. 2011. Effect of various chemical treatments on the fibre structure and tensile properties of industrial hemp fibres. *Composites Part A: Applied Science and Manufacturing,* 42**,** 888-895.

SCHNEIDER, M., ROMER, M., TSCHUDIN, M. & BOLIO, H. 2011. Sustainable cement production—present and future. *Cement and Concrete Research,* 41**,** 642-650.

SCRIVENER, K. L., FÜLLMANN, T., GALLUCCI, E., WALENTA, G. & BERMEJO, E. 2004. Quantitative study of Portland cement hydration by X-ray diffraction/Rietveld analysis and independent methods. *Cement and Concrete Research,* 34**,** 1541-1547.

SEDAN, D., PAGNOUX, C., CHOTARD, T., SMITH, A., LEJOLLY, D., GLOAGUEN, V. & KRAUSZ, P. 2007. Effect of calcium rich and alkaline solutions on the chemical behaviour of hemp fibres. *Journal of Materials Science,* 42**,** 9336-9342.

SEDAN, D., PAGNOUX, C., SMITH, A. & CHOTARD, T. 2008. Mechanical properties of hemp fibre reinforced cement: Influence of the fibre/matrix interaction. *Journal of the European Ceramic Society,* 28**,** 183-192.

SENFF, L., TOBALDI, D. M., LUCAS, S., HOTZA, D., FERREIRA, V. M. & LABRINCHA, J. A. 2013. Formulation of mortars with nano-SiO_2 and nano-TiO_2 for degradation of pollutants in buildings. *Composites Part B: Engineering,* 44**,** 40-47.

SHAHZAD, A. 2011. Hemp fiber and its composites - a review. *Journal of Composite Materials,* 46**,** 973-986.

SHAIKH, F. U. A. 2013. Review of mechanical properties of short fibre reinforced geopolymer composites. *Construction and Building Materials,* 43**,** 37-49.

SHAIKH, F. U. A. & SUPIT, S. W. M. 2014. Mechanical and durability properties of high volume fly ash (HVFA) concrete containing calcium carbonate ($CaCO_3$) nanoparticles. *Construction and Building Materials,* 70**,** 309-321.

SHAIKH, F. U. A., SUPIT, S. W. M. & SARKER, P. K. 2014. A study on the effect of nano silica on compressive strength of high volume fly ash mortars and concretes. *Materials & Design,* 60**,** 433-442.

SHEBL, S. S., ALLIE, L., MORSY, M. S. & AGLAN, H. A. 2009. Mechanical behavior of activated nano silicate filled cement binders. *Journal of Materials Science,* 44**,** 1600-1606.

SHEKARI, A. H. & RAZZAGHI, M. S. 2011. Influence of Nano Particles on Durability and Mechanical Properties of High Performance Concrete. *Procedia Engineering,* 14**,** 3036-3041.

SHIH, J.-Y., CHANG, T.-P. & HSIAO, T.-C. 2006. Effect of nanosilica on characterization of Portland cement composite. *Materials Science and Engineering: A,* 424**,** 266-274.

SIDDIQUE, R. & KLAUS, J. 2009. Influence of metakaolin on the properties of mortar and concrete: A review. *Applied Clay Science,* 43**,** 392-400.

SIDDIQUE, R. & MEHTA, A. 2014. Effect of carbon nanotubes on properties of cement mortars. *Construction and Building Materials,* 50**,** 116-129.

SILVA, F. D. A., MOBASHER, B. & FILHO, R. D. T. 2009. Cracking mechanisms in durable sisal fiber reinforced cement composites. *Cement and Concrete Composites,* 31**,** 721-730.

SILVA, F. D. A., MOBASHER, B., SORANAKOM, C. & FILHO, R. D. T. 2011. Effect of fiber shape and morphology on interfacial bond and cracking behaviors of sisal fiber cement based composites. *Cement and Concrete Composites,* 33**,** 814-823.

SILVA, F. D. A., ZHU, D., MOBASHER, B., SORANAKOM, C. & TOLEDO FILHO, R. D. 2010. High speed tensile behavior of sisal fiber cement composites. *Materials Science and Engineering: A,* 527**,** 544-552.

SINGH, L. P., AGARWAL, S. K., BHATTACHARYYA, S. K., SHARMA, U. & AHALAWAT, S. 2011. Preparation of silica nanoparticles and its beneficial role in cementitious materials. *Nanomaterials and Nanotechnology,* 1**,** 44-51.

SINGH, L. P., GOEL, A., BHATTACHHARYYA, S. K., AHALAWAT, S., SHARMA, U. & MISHRA, G. 2015. Effect of morphology and dispersibility of silica nanoparticles on the mechanical behaviour of cement mortar. *International Journal of Concrete Structures and Materials,* 9**,** 207-217.

SINGH, L. P., KARADE, S. R., BHATTACHARYYA, S. K., YOUSUF, M. M. & AHALAWAT, S. 2013. Beneficial role of nanosilica in cement based materials – A review. *Construction and Building Materials,* 47**,** 1069-1077.

SINGH, T. 2014. A review of nanomaterials in civil engineering works. *International Journal of Structural and Civil Engineering Research,* 3**,** 1-7.

SINHA RAY, S. & OKAMOTO, M. 2003. Polymer/layered silicate nanocomposites: a review from preparation to processing. *Progress in Polymer Science,* 28**,** 1539-1641.

SNOECK, D. & DE BELIE, N. 2012. Mechanical and self-healing properties of cementitious composites reinforced with flax and cottonised flax, and compared with polyvinyl alcohol fibres. *Biosystems Engineering,* 111**,** 325-335.

SOBOLKINA, A., MECHTCHERINE, V., KHAVRUS, V., MAIER, D., MENDE, M., RITSCHEL, M. & LEONHARDT, A. 2012. Dispersion of carbon nanotubes and its influence on the mechanical properties of the cement matrix. *Cement and Concrete Composites,* 34**,** 1104-1113.

SOIN, A. V., CATALAN, L. J. J. & KINRADE, S. D. 2013. A combined QXRD/TG method to quantify the phase composition of hydrated Portland cements. *Cement and Concrete Research,* 48**,** 17-24.

SORANAKOM, C. & MOBASHER, B. 2008. Geometrical and mechanical aspects of fabric bonding and pullout in cement composites. *Materials and Structures,* 42**,** 765-777.

SOROUSHIAN, P. & HASSAN, M. 2012. Evaluation of cement-bonded strawboard against alternative cement-based siding products. *Construction and Building Materials,* 34**,** 77-82.

SOROUSHIAN, P., WON, J.-P. & HASSAN, M. 2012. Durability characteristics of CO2-cured cellulose fiber reinforced cement composites. *Construction and Building Materials,* 34**,** 44-53.

STEFANIDOU, M. & PAPAYIANNI, I. 2012. Influence of nano-SiO_2 on the Portland cement pastes. *Composites Part B: Engineering,* 43**,** 2706-2710.

SUPIT, S. W. M. & SHAIKH, F. U. A. 2014a. Durability properties of high volume fly ash concrete containing nano-silica. *Materials and Structures,* 48**,** 2431-2445.

SUPIT, S. W. M. & SHAIKH, F. U. A. 2014b. Effect of Nano-$CaCO_3$ on Compressive Strength Development of High Volume Fly Ash Mortars and Concretes. *Journal of Advanced Concrete Technology,* 12**,** 178-186.

TAYLOR, H. F. W. 1990. *Cement Chemistry,* London, Academic Press Limited.

THELAKKADAN, A. S., COLETTI, G., GUASTAVINO, F. & FINA, A. 2012. Effect of clay dispersion methods on the mechano-dynamical and electrical properties of epoxy–organoclay nanocomposites. *Polymer Bulletin,* 70**,** 489-506.

THOSTENSON, E., LI, C. & CHOU, T. 2005. Nanocomposites in context. *Composites Science and Technology,* 65**,** 491-516.
TIRONI, A., TREZZA, M. A., SCIAN, A. N. & IRASSAR, E. F. 2013. Assessment of pozzolanic activity of different calcined clays. *Cement and Concrete Composites,* 37**,** 319-327.
TOLEDO FILHO, R. D., GHAVAMI, K., ENGLAND, G. L. & SCRIVENER, K. 2003. Development of vegetable fibre–mortar composites of improved durability. *Cement & Concrete Composites,* 25**,** 185-196.
TOLEDO FILHO, R. D., SCRIVENER, K., ENGLAND, G. L. & GHAVAMI, K. 2000. Durability of alkali-sensitive sisal and coconut fibres in cement mortar composites. *Cement & Concrete Composites* 22**,** 127-143.
TOLEDO FILHO, R. D., SILVA, F. D. A., FAIRBAIRN, E. M. R. & MELO FILHO, J. D. A. 2009. Durability of compression molded sisal fiber reinforced mortar laminates. *Construction and Building Materials,* 23**,** 2409-2420.
TONOLI, G. H. D., RODRIGUES FILHO, U. P., SAVASTANO, H., BRAS, J., BELGACEM, M. N. & ROCCO LAHR, F. A. 2009. Cellulose modified fibres in cement based composites. *Composites Part A: Applied Science and Manufacturing,* 40**,** 2046-2053.
TOUTANJI, H., DELATTE, N., AGGOUN, S., DUVAL, R. & DANSON, A. 2004. Effect of supplementary cementitious materials on the compressive strength and durability of short-term cured concrete. *Cement and Concrete Research,* 34**,** 311-319.
TSERKI, V., ZAFEIROPOULOS, N. E., SIMON, F. & PANAYIOTOU, C. 2005. A study of the effect of acetylation and propionylation surface treatments on natural fibres. *Composites Part A: Applied Science and Manufacturing,* 36**,** 1110-1118.
VILAY, V., MARIATTI, M., MAT TAIB, R. & TODO, M. 2008. Effect of fiber surface treatment and fiber loading on the properties of bagasse fiber–reinforced unsaturated polyester composites. *Composites Science and Technology,* 68**,** 631-638.
WALKER, R., PAVIA, S. & MITCHELL, R. 2014. Mechanical properties and durability of hemp-lime concretes. *Construction and Building Materials,* 61**,** 340-348.
WANG, J. & QIN, S. 2007. Study on the thermal and mechanical properties of epoxy–nanoclay composites: The effect of ultrasonic stirring time. *Materials Letters,* 61**,** 4222-4224.
WEI, J. & MEYER, C. 2014a. Degradation rate of natural fiber in cement composites exposed to various accelerated aging environment conditions. *Corrosion Science,* 88**,** 118-132.
WEI, J. & MEYER, C. 2014b. Improving degradation resistance of sisal fiber in concrete through fiber surface treatment. *Applied Surface Science,* 289**,** 511-523.
WEI, J. & MEYER, C. 2014c. Sisal fiber-reinforced cement composite with Portland cement substitution by a combination of metakaolin and nanoclay. *Journal of Materials Science,* 49**,** 7604-7619.
WEI, J. & MEYER, C. 2015. Degradation mechanisms of natural fiber in the matrix of cement composites. *Cement and Concrete Research,* 73**,** 1-16.
WEI, Y., YAO, W., XING, X. & WU, M. 2012. Quantitative evaluation of hydrated cement modified by silica fume using QXRD, ^{27}Al MAS NMR, TG–DSC and

selective dissolution techniques. *Construction and Building Materials,* 36**,** 925-932.
XU, S., LIU, J. & LI, Q. 2015. Mechanical properties and microstructure of multi-walled carbon nanotube-reinforced cement paste. *Construction and Building Materials,* 76**,** 16-23.
XU, Z., ZHANG, M. & MIN, F. 2011. Investigation for reaction mechanism of nano-silica-modified cement-based composite materials. *Integrated Ferroelectrics,* 129**,** 160-168.
YAN, L., CHOUW, N. & YUAN, X. 2012. Improving the mechanical properties of natural fibre fabric reinforced epoxy composites by alkali treatment. *Journal of Reinforced Plastics and Composites,* 31**,** 425-437.
YAZDI, N. A., AREFI, M. R., MOLLAAHMADI, E. & NEJAND, B. A. 2011. To study the effect of adding Fe_2O_3 nanoparticles on the morphology properties and microstructure of cement mortar. *Life Science Journal,* 8**,** 550-554.
YIM, H. J., KIM, J. H. & SHAH, S. P. 2014. Ultrasonic monitoring of the setting of cement-based materials: Frequency dependence. *Construction and Building Materials,* 65**,** 518-525.
ZHANG, M.-H. & LI, H. 2011. Pore structure and chloride permeability of concrete containing nano-particles for pavement. *Construction and Building Materials,* 25**,** 608-616.
ZHANG, P., ZHAO, Y.-N., LI, Q.-F., ZHANG, T.-H. & WANG, P. 2014. Mechanical properties of fly ash concrete composite reinforced with nano-SiO_2 and steel fibre. *Current Science,* 106**,** 1529-1537.
ZHOU, X., GHAFFAR, S. H., DONG, W., OLADIRAN, O. & FAN, M. 2013. Fracture and impact properties of short discrete jute fibre-reinforced cementitious composites. *Materials & Design,* 49**,** 35-47.
ZOU, B., CHEN, S. J., KORAYEM, A. H., COLLINS, F., WANG, C. M. & DUAN, W. H. 2015. Effect of ultrasonication energy on engineering properties of carbon nanotube reinforced cement pastes. *Carbon,* 85**,** 212-220.

"Every reasonable effort has been made to acknowledge the owners of copyright material. I would be pleased to hear from any copyright owner who has been omitted or incorrectly acknowledgement"

Ahmad Hakamy

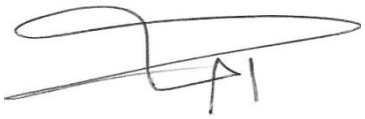

Signature

Date: 13th January 2016